Adding Complexity to Models of *Candida albicans* Human Colonization: Natural Isolates and Polymicrobial Interactions

by

Faith Anderson Davis

A dissertation submitted in partial fulfillment
of the requirements for the degree of
Doctor of Philosophy
(Microbiology and Immunology)
in the University of Michigan
2025

Doctoral Committee:

Assistant Professor Teresa O'Meara, Chair
Professor Gary Huffnagle
Associate Professor Nicole Koropatkin
Professor Eric Martens
Professor Mary O'Riordan

Faith Anderson Davis

faithma@umich.edu

ORCID iD: 0000-0001-8456-621X

© Faith Anderson Davis 2025

Dedication

This dissertation is dedicated to my incredible husband, Sam, who on our third date, promised to follow me wherever I went to graduate school. And so, he did. To my parents, who always encouraged my ambitions and whose belief in me never wavered. And to all the women who came before me and paved the way in medical mycology.

Acknowledgements

My passion for microbiology originated at Auburn University; I credit Dr. Paul Cobine for lighting that first spark. Dr. Sang-Jin Suh and Dr. Mark Liles continued to nurture and develop my curiosity and challenge me intellectually. Dr. Elizabeth Schwartz gave me my first opportunity to do research, solidifying for me that I wanted to pursue my own career in research. I owe so much to Dr. Keah Higgins and Dr. Haley Hallowell for guiding me in lab, assisting with my graduate school applications, and endlessly encouraging me.

More than anyone else, I will forever be grateful to my mentor, Dr. Teresa O'Meara, for her unwavering support through these past six years. I didn't know anything about fungi before I sat down across from Teresa, in a loud room full of incoming students and faculty pitching their research labs. I saw Teresa's passion for her science, and I saw someone who I knew would be an excellent mentor and advocate for her mentees. A lot of people had opinions about if I should join a brand-new PI's lab, but I have no doubts that it was the perfect decision for me. I had the most incredible opportunity to watch this lab grow and evolve and have a small part in it. I never doubted at any turn that Teresa believed in me, even when I didn't believe in myself. She never missed a chance to tell me she was proud of me and that external validation was instrumental in growing my own confidence. I always knew that Teresa cared deeply about my development as a scientist, but I also knew that more than that, she cared about me as a person.

At Michigan, I had the incredible privilege of having a number of strong women to look up to and rely on. Thank you to Dr. Beth Moore, Dr. Mary O'Riordan, and Dr. Nicole Koropatkin for being excellent role models and sources of encouragement.

Finally, I wouldn't have made it through this journey without the support of my friends, both new and old. It is a beautiful thing to have people in your corner, loving you and cheering you on always.

Table of Contents

Dedication ii

Acknowledgements iii

List of Tables ix

List of Figures x

Abstract xii

Chapter 1 Introduction 1

1.1 *Candida albicans* 1

1.2 Changing shape: the yeast to hyphal transition 1

1.3 From commensal to pathogen 3

1.4 The fungal cell wall: composition and function 4

1.4.1 β-glucan in antifungal immunity 5

1.4.2 The cell wall as a target of antifungal drugs 6

1.4.3 Cell wall remodeling 8

1.4.4 Molecular regulation of cell wall remodeling 10

1.5 Fungal-bacterial interactions 11

1.6 The power of natural genetic diversity 13

1.6.1 Natural diversity in *C. albicans* 15

1.7 Brief summary and chapter outline 17

Chapter 2 Germination of a Field: Women in *Candida albicans* Research 18

2.1 Abstract 18

2.2 Introduction 18

2.3 *C. albicans* Morphogenesis 19

2.4 *C. albicans* Treatment and Drug Resistance 23

2.5 Polymicrobial Interactions 26

2.6 In Vivo Pathogenesis Models 28

2.7 Host Immune Responses 29

2.8 Conclusions 31

Chapter 3 *Candida albicans* Selection for Human Commensalism Results in Substantial Within-Host Diversity Without Decreasing Fitness for Invasive Disease 33

3.1 Abstract 33

3.2 Introduction 34

3.3 Results 35

3.3.1 Phenotypic characterization of commensal *C. albicans* strains 35

3.3.2 Genomic variability 40

3.3.3 Deep phenotyping of commensal isolates 47

3.3.4 Limited diversity exploitation 52

3.3.5 Virulence 54

3.4 Conclusions 56

3.5 Methods 59

3.5.1 Human subjects and sample collection 59

3.5.2 Reference strains 59

3.5.3 Media and culture conditions 59

3.5.4 Growth curve analysis 59

3.5.5 Filamentation analysis 60

3.5.6 Agar invasion analysis 60

3.5.7 High molecular weight genomic DNA extraction and sequencing 60

3.5.8 Sequence variation analysis 61

3.5.9 Bootstrapping 62

3.5.10 Structural variant analysis from TELL-seq 62

3.5.11 CHEF gel electrophoresis 63

3.5.12 Biofilm formation 63

3.5.13 Mammalian cell culture 63

3.5.14 Phagocytosis 64

3.5.15 Macrophage filamentation assay 64

3.5.16 Cell death assay 65

3.5.17 ZMS1 strain construction 65

3.5.18 *Galleria mellonella* infections 66

Chapter 4 *Candida* albicans Remodels its Cell Wall in Response to Bacteria, Impacting Immune Recognition and Antifungal Sensitivity 71

4.1 Abstract 71

4.2 Introduction 72

4.3 Results 74

4.3.1 *Candida albicans* undergoes global cell wall remodeling during co-culture with *Escherichia coli* 74

4.3.2 *E. coli*-induced fungal cell wall remodeling impacts innate and adaptive immune responses and is relevant *in vivo* 78

4.3.3 Solid-State NMR analysis of the fungal cell wall 79

4.3.4 Fungal cell wall remodeling in response to bacteria is broadly conserved 81

4.3.5 The HOG pathway is required for fungal cell wall remodeling in response to bacterial co-culture 84

4.3.6 Bacterial-induced fungal cell wall remodeling is mediated by a secreted metabolite 87

4.3.7 Bacterial-mediated fungal cell wall remodeling modulates antifungal resistance 90

4.4 Discussion 91

4.5 Methods 93
4.5.1 Strains and culture conditions 93
4.5.2 Fungal-bacterial co-culture 93
4.5.3 Transmission electron microscopy 94
4.5.4 Flow cytometric quantification of cell wall components 94
4.5.5 Fluorescence microscopy 95
4.5.6 HEK-blue reporter cells 95
4.5.7 Quantification of IgA binding 95
4.5.8 Germ free mouse colonization 96
4.5.9 Staining intestinal contents 96
4.5.10 Solid-state NMR 97
4.5.11 RNA extraction 97
4.5.12 *E. coli*-conditioned YPD 98
4.5.13 Determination of media osmolality 98
4.5.14 Bioassay-guided fractionation 98
4.5.15 MIC assays 99
Chapter 5 Discussion 103
5.1 Overview 103
5.2 Unanswered questions and future directions 104
5.2.1 Demographic information and longitudinal sampling 104
5.2.2 Limited diversity exploitation 104
5.2.3 Potential transmission events 105
5.2.4 Investigating *ROB1* in commensal isolates 106
5.2.5 The role of *Bacteroides* in fungal cell wall remodeling 106
5.2.6 Bacterial-mediated fungal cell wall remodeling in the context of gastrointestinal colonization 108

5.3 Future perspectives: incorporating host-relevant conditions and considering limitations of current models 109

Bibliography 113

List of Tables

Table 3-1: Growth media used in this chapter. 68

Table 3-2: Plasmids used in this chapter. 69

Table 3-3: Oligonucleotides used in this chapter. 70

Table 4-1: Tested concentrations of organic fractions from Fig 4-14H 88

Table 4-2: Fungal strains used in this chapter. 101

Table 4-3: Bacterial strains used in this chapter. 102

List of Figures

Figure 3-1: Characterization of isolates from healthy donors reveals extensive phenotypic heterogeneity. 37

Figure 3-2: Comparisons of growth rate between samples and nutrient source. 39

Figure 3-3: The newly sequenced *C. albicans* commensal isolates include representatives from multiple clades. 41

Figure 3-4: Cladogram of the SNP tree (branch lengths all equal to 1) with the backbone colored by bootstrap support values. 42

Figure 3-5: *C. albicans* commensal isolates display extensive structural variation. 44

Figure 3-6: Structural variation. 46

Figure 3-7: Deep phenotyping reveals heterogeneity in *in vitro* and host phenotypes. 48

Figure 3-8: Biofilm formation. 49

Figure 3-9: Comparison between filamentation in macrophages and agar invasion. 51

Figure 3-10: UMAP embedding. 52

Figure 3-11: SNV limited diversity exploitation analysis of donor 814 commensal isolates reveals role for Zms1 in regulating agar invasion. 53

Figure 3-12: Commensal isolates retain pathogenic potential. 55

Figure 3-13: Virulence in *G. mellonella*. 56

Figure 4-1*:E. coli* grows under co-culture conditions. 74

Figure 4-2: *C. albicans* cells are viable after 24 hours of co-culture with *E. coli*. 74

Figure 4-3: *Candida albicans* undergoes cell wall remodeling during co-culture with *Escherichia coli* with an impact on immune recognition. 75

Figure 4-4 :TEM preparation did not preserve the inner fungal cell wall. 76

Figure 4-5: Relationship between cell size and cell wall contents. 77

Figure 4-6: Flow cytometry gating strategy and comparison of cell size. 77

Figure 4-7: Human fecal IgA binding to *C. albicans* grown in monoculture or co-culture with *E. coli.* 78

Figure 4-8: Composition of rigid and mobile polysaccharides probed by high-resolution ssNMR. 80

Figure 4-9: Representative dynamic gradients of polysaccharides in the cell wall. 81

Figure 4-10: Cell wall remodeling in response to bacteria is broadly conserved. 82

Figure 4-11: Cell wall mannan content of different *Candida* species. 83

Figure 4-12: Cell wall mannan during bacterial co-culture 84

Figure 4-13: Mutants in the high osmolarity glycerol cascade are defective at remodeling in response to *E. coli* co-culture. 85

Figure 4-14: *E. coli*-induced fungal cell wall remodeling is mediated by a secreted metabolite. 87

Figure 4-15: *E. coli*-conditioned YPD delays growth of *C. albicans*. 88

Figure 4-16: Bacterial-induced fungal cell wall remodeling alters antifungal resistance. ... 90

Figure 5-1: *C. albicans* displays increased mannan content following co-culture with *B. thetaiotaomicron.* 107

Figure 5-2: *B. thetaiotaomicron* mutants induce fungal cell wall remodeling, regardless of mannan-degradation abilities. 107

Abstract

The fungus *Candida albicans* represents a commensal colonizer of human mucosal surfaces and an opportunistic pathogen capable of causing both superficial mucosal and life-threatening disseminated infections. *C. albicans* is remarkably versatile and readily adapts to diverse environment conditions, allowing it to colonize multiple host niches. To adapt to changing environmental conditions, *C. albicans* may undergo a morphological transition, alters its metabolism, or actively remodel its multilayered cell wall. As life-threatening invasive infections arise from populations already colonizing the gastrointestinal tract, it is important to characterize *C. albicans*' role as both a commensal and pathogen, to inform how the shift to pathogenesis occurs.

The majority of research in *C. albicans* has been performed in the standard reference strain, SC5314, but *C. albicans* isolates display incredible genotypic and phenotypic diversity that can be leveraged to uncover new facets of fungal biology. We collected over 900 commensal *C. albicans* isolates from healthy donors to characterize within-host diversity and identify adaptations associated with commensalism. We demonstrated that healthy people can be simultaneously colonized by multiple, distinct lineages of *C. albicans*. These commensal isolates displayed wide variation in their phenotypic properties but consistently retained their ability to filament, a trait that is often associated with pathogenicity. Importantly, despite originating from healthy donors, all our commensal isolates maintained a high pathogenic potential. We did not identify any phenotypes that separated isolates by sample site or genetic clade, emphasizing the highly adaptive nature of *C. albicans*. Finally, we demonstrated that closely related isolates with divergent phenotypes can be leveraged to identify causative mutations through comparative genomics. This work emphasizes the versatility of *C. albicans* and highlights the value of characterizing natural diversity.

The fungal cell wall is an essential organelle that mediates interactions with host immune cells and represents a major target of antifungals. Due to its important roles, the fungal cell wall is highly responsive to its environment and undergoes active remodeling in response to changing

environmental conditions. Alterations in cell wall composition can allow *C. albicans* to evade immune detection or better tolerate antifungal drugs. Although bacteria are known to have profound impacts on fungal biology and virulence, little work has investigated how bacteria may influence the fungal cell wall and any downstream consequences on fungal virulence. We determined that bacterial co-culture induces cell wall remodeling in multiple genetic backgrounds of *C. albicans*, as well as some related *Candida* species. Critically, bacterial-mediated fungal cell wall remodeling alters antifungal sensitivity and immune recognition of *C. albicans*. We demonstrate that this interaction is relevant *in vivo*, as the addition of a single bacterial species to *C. albicans* colonizing the murine gastrointestinal tract was sufficient to change the cell wall. These findings underscore the importance of considering bacterial influences on *C. albicans* biology and virulence.

Overall, this dissertation demonstrates the power of incorporating host-relevant conditions when conducting research. Characterizing natural isolates of *C. albicans*, both commensal and clinical, from human hosts provides deeper insight into fundamental aspects of fungal biology. Considering the impact of and including bacteria in models of *C. albicans* colonization and disease increases the relevancy of our experimental results and more accurately replicates the reality of human colonization and disease. Ultimately, carefully incorporating further complexity in our studies improves our understanding of the intricate relationships between fungus and host.

Chapter 1 Introduction

1.1 *Candida albicans*

Candida albicans is a fungus that commonly exists as a commensal colonizer of human mucosal surfaces including the mouth, gastrointestinal tract, and vagina. It is estimated that between 40-80% of people from industrialized nations are colonized with *C. albicans*, and this fungus is rarely isolated from environmental reservoirs outside of their mammalian hosts[1–5]. Colonization with *C. albicans* is influenced by host's immune status, diet, lifestyle, and other environmental factors[4,6–8]. Although *C. albicans* is often considered a harmless commensal colonizer and generally does not cause disease in healthy hosts, it is also the leading cause of hospital acquired fungal infections. This fungus can cause a range of diseases, from superficial mucosal infections, like oral thrush or vaginal yeast infections, to life-threatening disseminated infections. Invasive *C. albicans* infections have a mortality rate up to 40%, due in part to increasing antifungal resistance[9,10]. In 2022, the World Health Organization included *C. albicans* in the critical group of the first ever fungal priority pathogens list[11]. Due to its medical significance and prevalence as a mucosal colonizer, it is important for researchers to characterize *C. albicans* as both a commensal and a pathogen, to ultimately achieve a deeper understanding of how it causes disease and for the development of antifungal therapies.

1.2 Changing shape: the yeast to hyphal transition

A hallmark of *C. albicans* is its unique ability to transition between the round yeast and elongated hyphal forms in response to a variety of host-associated cues. As this feature is not widely shared amongst *Candida* species, visual identification of this phenotype served as a simple and rapid method to identify *C. albicans* for early researchers and has been a significant focus of research in the field[12]. Historically, the yeast form was considered the "commensal" morphology, while hyphae were considered the "pathogenic" morphology. However, multiple lines of evidence have since emerged to indicate that both morphologies play distinct and important roles in the context of pathogenesis, and it is instead the ability to transition between

morphologies that is critical for full virulence[13–16]. Indeed, several studies have demonstrated that virulence does not perfectly correlate with morphology, as avirulent mutants can be filamentation-competent, yeast-locked, or hyphal-locked[13–16]. Furthermore, yeast-locked mutants can retain full virulence[18–20]. Similarly, filamentation is not required for the induction of macrophage cell death or pro-inflammatory cytokine production, as was previously believed[21]. Together, these studies demonstrate that although the yeast to hyphal transition is important, the ability to form hyphae is neither necessary nor sufficient for full virulence.

Numerous host-related cues that induce the yeast to hyphal transition and the corresponding signaling pathways have been identified and characterized. These include human body temperature of 37°C, hypoxia, elevated CO_2 levels, host serum, and alkaline pH, among others[21,22]. Conversely, several microbial derived molecules, including quorum-sensing molecules from both fungi and bacteria, have been shown to inhibit filamentation[22–27]. The molecular regulation of the yeast to hyphal transition has been extensively investigated, and many regulatory circuits and transcription factors involved in morphogenesis have been identified and characterized. Multiple central signaling cascades, including the high osmolarity glycerol (HOG) pathway, the protein kinase A (PKA) pathway, the Cek1 pathway, and the Rim101 pathway, are known to regulate yeast to hyphal transition, and each of these cascades may respond to different inducing cues through distinct upstream signaling components[21,28]. Similarly, dozens of transcription factors are involved in morphological switching; from these, major positive and negative regulators have been identified[29]. The transcription factors Efg1, Ume6, Brg1, Tec1, and Cph1 are among the most well-characterized positive regulators of filamentation, while the most extensively characterized negative regulators of filamentation are Tup1 and Nrg1[21,28,30].

As morphogenesis is intimately linked with, but ultimately neither necessary nor sufficient for, virulence, this implies that critical virulence factors are deployed in concert with the morphological transition but are induced through independent mechanisms that can be decoupled. In line with this idea, the proteome, secretome, cell wall composition, and gene expression of hyphae are distinct from that of yeast[31–37]. These differences are further amplified based on the hyphal-inducing cue[31,36]. This extensive remodeling of the entire molecular landscape contributes to the altered adhesive profile, antifungal sensitivities, and immune recognition observed between yeast and hyphae[32,38,39]. Some specific hyphal-associated virulence

factors will be explored in the next section. Overall, the shift from yeast to hyphae induces major changes in nearly all aspects of fungal biology, and careful investigation into these changes allows for identification of important *C. albicans* virulence factors.

1.3 From commensal to pathogen

While *C. albicans* is an important fungal pathogen, it primarily exists as a commensal colonizer. Characterizing the commensal role of *C. albicans* is a critical first step to understand how the shift to pathogen occurs. Investigation into fungal factors that regulate colonization has revealed morphogenesis, metabolic flexibility and nutrient acquisition, cell wall remodeling, and adherence to be important in *C. albicans* gastrointestinal colonization[40,41]. These traits are also fundamental to the highly adaptive nature of *C. albicans* that allows for colonization of incredibly diverse host niches and are therefore also important for virulence. As a commensal colonizer, *C. albicans* can provide beneficial effects to the host, such as providing protective immunity against invasive *C. albicans* and *C. auris* infections, as well as against bacterial pathogens like *Clostridioides difficile* and *Staphylococcus aureus*[42–46]. These protections are mediated by trained innate immunity, antifungal IgG, and expansion of Th17 cells[42–46].

The transition from commensal to pathogen is complex and multifactorial and depends on fungal, host, and environmental factors. First, we will explore fungal factors that are critical for virulence. As described above, the yeast to hyphal transition was once thought to be required for *C. albicans* to cause disease, but decoupling of filamentation with associated phenotypes has allowed for the identification of specific fungal factors important for virulence. A virulence factor of particular interest to researchers is candidalysin, a fungal peptide toxin encoded by *ECE1*[49]. This toxin is highly expressed in the hyphal form of *C. albicans* and mediates epithelial damage during infection[50,51]. The ability to form biofilms on biotic and abiotic surfaces is another important virulence factor for *C. albicans* that requires both yeast and hyphal morphologies. Biofilm formation is a multistep process and is controlled by an extensive network of transcriptional regulators, many of which also regulate morphogenesis[50,51]. Biofilms contribute to virulence by allowing dispersal of yeast cells from the mature biofilm and increasing resistance to antifungals[52,53]. Additional virulence factors include adhesins, invasins, and secreted hydrolases, which play roles in mediating attachment, penetration, and damage of host cells.

Immunocompromise is an important risk for *C. albicans* infection that can manifest through both primary and acquired immunodeficiencies. As *C. albicans* causes a multitude of infections, linking defects in particular branches of the immune response with increased susceptibility to specific infection types can provide insight into the pathways most important for controlling different manifestations of fungal disease. For example, individuals suffering from chronic mucocutaneous candidiasis typically have impaired IL-17 immunity, implicating this branch of immunity as a critical player in mucosal antifungal defense[54–57]. In fact, a number of primary and acquired immunodeficiencies that confer susceptibility to fungal infections have been linked to defects in IL-17 immunity. These include mutations in pattern recognition receptors, adaptor proteins, and transcription factors involved in IL-17 signaling, as well as patients dealing with HIV/AIDs[54,58–62]. Therefore, host-related immunodeficiencies, especially those that impair IL-17 immunity, are an important risk factor for mucosal fungal infections.

Invasive candidiasis, which encompasses deep tissue infections and bloodstream infections, termed candidemia, is the most prevalent fungal disease in hospitalized patients[63]. Candidemia is among the most common causes of nosocomial bloodstream infections and is of particular concern in intensive care units[64,65]. These infections can reach a mortality rate of 40%, in part due to rising antifungal resistance[64,65]. *C. albicans* is the leading cause of invasive candidiasis, although the incidence of non-albicans *Candida* infections is rising[66]. As invasive candidiasis infections arise primarily in hospitalized patients, there are a number of health-care-associated risk factors to consider in addition to the host's immune status. Importantly, invasive *C. albicans* infections are thought to arise from an existing gastrointestinal population; therefore, colonization with *C. albicans* is a risk factor for invasive candidiasis[67–70]. Prolonged hospital stays, major abdominal surgery, presence of an indwelling central venous catheter, and broad-spectrum antibiotic treatment represent major health-care-associated risk factors for developing invasive candidiasis[71–75]. Abdominal surgery and indwelling medical devices can cause damage to the epithelial barrier, allowing *C. albicans* to disseminate throughout the body. The mechanisms by which antibiotic treatment can allow for fungal overgrowth and subsequent disease will be explored in a later section.

1.4 The fungal cell wall: composition and function

The *Candida albicans* cell wall is a dynamic and essential organelle that provides the cell with structural support, protects from environmental stresses, and mediates interactions with the

surrounding environment. The *C. albicans* cell wall is organized into two layers and is composed of three main polysaccharides. The inner cell wall layer consists primarily of chitin and β-glucan. Chitin accounts for only 1-2% of the fungal cell wall by dry weight, but plays a critical role in providing structural integrity and mediating septum formation and cell separation[76,77]. Chitin has often been depicted as a continuous skeleton directly adjacent to the cell membrane; however, due to this polysaccharide's rigid nature, this distribution would render cells inflexible. Instead, recent models that combined transmission electron microscopy and visualization with a chitin-binding reporter have demonstrated that chitin is distributed throughout the inner cell wall layer and not as its own distinct layer neighboring the cell membrane[78]. This distribution allows chitin to provide support without restricting cellular elasticity[78]. The predominant component of the fungal cell wall is β-glucan, which accounts for up to 60% of the cell wall by dry weight[76]. This β-glucan can be further divided into β-1,3- and β-1,6-glucan, which constitute approximately 40% and 20% of the cell wall, respectively. β-1,3-glucan is an essential cell wall component that forms long single and triple helices that contribute to cellular elasticity, while β-1,6-glucan consists of relatively short moieties that link GPI-anchored proteins to β-1,3-glucan or chitin[78,79]. The outer cell wall layer is composed of mannan fibrils covalently linked to cell wall proteins, also termed mannoproteins, which constitutes the remaining ~40% of the fungal cell wall. Cell wall mannan consists of the short, linear O-linked mannans and the long and highly branched N-linked mannans. As the outermost cell wall layer, mannan plays an important role in adhesion, biofilm formation, and cell-to-cell interactions.

The importance of the fungal cell wall is underscored by the essentiality of genes involved in synthesis of chitin and β-1,3-glucan. *Chs1* encodes a major chitin synthase that is essential for cell viability; disruption of *Chs1* leads to cell separation defects[77,80]. *Fks1* encodes an essential β-1,3-glucan synthase and is a major antifungal drug target[81]. Although not all cell wall synthesis genes are essential, deletion of many of these genes results in increased susceptibility to cell wall damage, changes in immune recognition, and attenuated virulence, highlighting how critical this organelle is for environmental adaptation and pathogenesis[82–87].

1.4.1 β-glucan in antifungal immunity

All of the fungal cell wall polysaccharides serve as pathogen-associated molecular patterns (PAMPs) that are recognized by immune receptors to induce different immune responses. The recognition of fungal β-1,3-glucan by the C-type lectin receptor (CLR), Dectin-1, is considered a

particularly important PAMP-PRR interaction and has been extensively studied. Mice lacking Dectin-1 are more susceptible to systemic *C. albicans* infection but have no difference in gastrointestinal colonization levels[88,89]. However, another group demonstrated that increased susceptibility to systemic infection in Dectin-1 deficient mice is dependent on the fungal strain background[90]. In humans, early-stop codons in Dectin-1 and its downstream adaptor, CARD9, are associated with recurrent mucocutaneous fungal infections[90]. Importantly, these same genetic variants were not associated with increased risk of candidemia, highlighting that in humans, this signaling pathway is specifically involved in mucosal fungal immunity[91].

The role of Dectin-1 in macrophage recognition of *C. albicans* has been the most thoroughly studied, although Dectin-1 is also expressed on other immune cells, including neutrophils, dendritic cells, and γδ T cells[92–94]. Dectin-1 recognition of *C. albicans* β-1,3-glucan by macrophages mediates phagocytosis and cytokine production. Accordingly, changes in β-1,3-glucan surface exposure are tightly correlated with the rates of phagocytic uptake and cytokine production[32,95–100]. Phagocytosis by innate immune cells is a critical first step in controlling fungal infections through pathogen elimination, and fungal cell death can occur through multiple mechanisms within the phagosome[101].

In addition to mediating phagocytosis, Dectin-1 recognition of β-glucan is required for the development of innate immunological memory that provides protection against subsequent infections through epigenetic reprogramming of monocytes, also termed trained immunity[44,45,102]. Dectin-1-dependent fungal sensing and cytokine production promotes differentiation of CD4+ T cells into non-pathogenic T_H17 cells, which are crucial for clearing fungal infections[45,103,104]. Therefore, Dectin-1 plays significant roles in antifungal immunity by performing classic innate immune functions, contributing to the development of trained immunity, and instructing $CD4^+$ T cell differentiation.

1.4.2 The cell wall as a target of antifungal drugs

The development of antifungal drugs is difficult because fungi, like their mammalian hosts, are eukaryotic, making host toxicity a major concern. Therefore, to minimize potential host toxicity, antifungal drugs targets must be poorly conserved between fungi and their host, or ideally, entirely unique to fungi. The components of the fungal cell wall and cell membrane, as well as the enzymes that synthesize them, are an excellent target for antifungal drug development as these structures and enzymes are not present or are poorly conserved between fungi and humans.

Indeed, the three classes of antifungals currently approved for clinical use target components of the fungal cell wall or cell membrane.

The most commonly used class of antifungals are the azoles, like fluconazole, which were first introduced in the 1980s. Azoles target Erg11, a key enzyme involved in the biosynthesis of ergosterol, an essential component of the fungal cell membrane which is functionally equivalent to mammalian cholesterol. Disruption of ergosterol biosynthesis leads to accumulation of toxic sterol intermediates and exertion of membrane stress[105,106]. *C. albicans* may gain resistance to azoles through several mechanisms including upregulation of efflux pumps, overexpression of Erg11, or mutations in *ERG11*[107–111]. Resistance to azoles is a significant problem in *Candida* species, although *C. albicans* shows one of the lowest rates of fluconazole resistance, estimated to be less than 4%[107,112,113]. Alarmingly, the emergent fungal pathogen *Candida auris* is often multidrug resistant and displays rates of azole resistance around 90%, although this rate varies based on genetic clade[114–116]. Although azoles have limited host toxicity, an issue of concern is their interference with metabolism of other drugs. Despite concerns of growing antifungal resistance, the azoles remain in frequent use due to their limited host toxicity and availability in both oral and intravenous formulations.

The oldest class of antifungal drugs, introduced in the 1950s, are the polyenes. Amphotericin B is the most commonly used polyene, and it has broad spectrum activity across multiple clinically important fungal species[117]. Similar to the azoles, polyenes also target the essential membrane component ergosterol, but through a distinct mechanism. Amphotericin B forms large extracellular aggregates that function as a 'sterol sponge', extracting ergosterol from the membrane to cause fungal death[118]. Resistance to amphotericin B is rare, in part due to its unique mechanism of action, which targets the cell membrane directly, instead of a particular enzyme; additionally, as amphotericin B functions extracellularly, drug efflux is not a viable resistance mechanism. When resistance to amphotericin B is observed, it is frequently due to mutations in the ergosterol biosynthesis pathway[119]. However, such mutations have significant fitness costs, including hypersensitivity to host-associated stresses, defects in filamentation and tissue invasion, and ultimately avirulence[119]. Despite the broad spectrum activity of the polyenes and low rates of antifungal resistance, they are considered the last line of defense against life-threatening fungal infections due to their level of host toxicity, attributed to a weak affinity for cholesterol[121–123].

The most recently introduced class of antifungal are the echinocandins, which have been in use since the early 2000s. The echinocandins are fungicidal and function by binding to Fks1, the essential β-1,3-glucan synthase, thus blocking biosynthesis of this polysaccharide and disrupting cell wall integrity[122–124]. Echinocandins, including caspofungin, are favored due to their potent activity against *Candida* and *Aspergillus* and low host toxicity. Conversely, echinocandins use is limited as they are administered intravenously. Despite their relatively recent introduction into clinical use, emerging resistance to echinocandins has been reported, commonly mediated through mutations in *FKS1* hotspots[125]. Recently, additional mechanisms of echinocandin resistance have been explored, independent of direct alterations to *FKS1*. In particular, aneuploidy of chromosome 5 has emerged as a viable resistance mechanism to differentially regulate genes involved in caspofungin susceptibility[126]. Furthermore, *C. albicans* isolates that display aneuploidy-mediated caspofungin resistance frequently acquire cross-resistance to micafungin and anidulafungin, unlike the caspofungin-resistance isolates that have no ploidy changes[125,127,128]. Aneuploidy-mediated resistance to caspofungin is correlated with changes in fungal cell wall composition, specifically an increase in cell wall chitin[129]. Elevated chitin synthesis is an established and reversible mechanism to increase caspofungin tolerance by strengthening the fungal cell wall and thus limiting cell wall damage[129,130]. Despite evidence of emerging resistance through several mechanisms, echinocandins are considered the first line of treatment for invasive candidiasis[131].

1.4.3 Cell wall remodeling

As *C. albicans* colonizes diverse body sites with wide variations in environmental conditions, fungal cells must be able to sense and properly adapt to each niche. Key mechanisms of environmental adaptation in *C. albicans* include morphogenesis, metabolic alterations, and remodeling the cell wall, and these adaptations prepare *C. albicans* for niche-specific stresses and modulation of immune recognition[21,28,132,133]. Numerous host-associated cues that induce fungal cell wall remodeling have been identified, including changes in oxygen levels, environmental pH, carbon source, and nutrient availability[96–98,134–136]. Cell wall remodeling can manifest as changes in the total content, structure, and surface exposure of cell wall polysaccharides, and these changes have important downstream impacts on adhesion, susceptibility to antifungals, and the immune response[137–142]. Cell wall composition can even differ between microenvironments within the same niche; *C. albicans* isolated from different

murine gastrointestinal compartments show differences in cell wall composition[143]. The highly adaptable nature of *C. albicans* allows for its successful colonization of diverse niches.

Fungal cell wall remodeling has been extensively studied in relation to innate immune recognition, with a particular focus on recognition of β-1,3-glucan in the inner cell wall by the CLR, Dectin-1. Changing cell surface exposure of β-1,3-glucan will directly alter recognition of *C. albicans* and subsequent phagocytosis and cytokine production[96,97,134,135,144]. *C. albicans* uses the outer cell wall mannan layer and glucanase activity to reduce β-1,3-glucan exposure. A current model is that the cell wall mannan layer acts as a physical shield to "mask" β-1,3-glucan, and loss of cell wall mannan results in increased recognition by macrophages and decreased virulence[18,142,145–147]. However, changes in the total amount of cell wall mannan do not directly correlate to changes in β-1,3-glucan exposure[134,136]. In addition to other methods employed to reduce β-1,3-glucan exposure, this suggests that the structure of the mannan fibrils, not just the quantity, is important for β-glucan masking.

C. albicans deploys the endo-glucanase, Eng1, and the exo-glucanase, Xog1, to "shave" exposed β-1,3-glucan from the cell surface. Both glucanases have been shown to contribute to lactate-induced β-1,3-glucan masking, although differences in experimental conditions have made it difficult to definitively determine if one glucanase plays a more significant role than the other[137,144,148,149]. In addition to its role in lactate-induced β-1,3-glucan masking, *ENG1* is downregulated in response to fluconazole, caspofungin, and N-acetylglucosamine (GlcNAc) treatment and this downregulation was associated with increased β-1,3-glucan exposure under these treatment conditions[144,150]. In the murine gastrointestinal tract, *XOG1* expression is higher in the cecum and large intestine compared to the small intestine, *XOG1* expression correlates with β-1,3-glucan exposure in these compartments, with the small intestine showing the highest levels of β-1,3-glucan exposure[143]. Although Xog1 and Eng1 regulate β-1,3-glucan exposure and consequently cytokine production, phagocytic rate, antifungal susceptibility, and adhesion, their contribution to fungal virulence remains unclear and outcomes vary based on the infection model[137–139,144,148].

Overall, active cell wall remodeling, and altering β-1,3-glucan exposure in particular, represents an important mechanism of environmental adaptation for *C. albicans*. β-1,3-glucan exposure is tightly regulated to allow for evasion of innate immune surveillance.

1.4.4 Molecular regulation of cell wall remodeling

Many well-studied and fundamental signaling pathways have been implicated in the fungal cell wall remodeling response to different inducing cues. The PKA pathway, which is involved in the regulation of cell growth, filamentation, biofilm development, and antifungal susceptibility[151], is required for β-glucan masking in response to hypoxia, iron limitation, and lactate[95,96,134]. Despite the shared involvement of the PKA pathway, the molecular response to each inducing cue is different. For example, β-glucan masking in response to hypoxia also depends on mitochondrial signaling, lactate-induced β-glucan masking is mediated by the Gpr1 receptor and requires non-canonical activation of the transcription factor Crz1, and β-glucan masking induced by iron limitation does not dependent on the adenylyl cyclase, Cyr1, a canonical player in the PKA pathway[95,96,134]. Similarly, the highly-conserved mitogen activated protein kinase (MAPK) signaling cascades, including the HOG pathway, the PKC pathway, and the Cek1 pathway, are involved in regulating β-glucan unmasking in response to particular and sometimes overlapping stimuli[133]. The involvement of the MAPK cascades in β-glucan unmasking is in addition to their roles in mediating the yeast-to-hyphae transition and responding to osmotic stress, oxidative stress, and cell wall damage[133]. Despite the involvement of these major, well-characterized signaling pathways in fungal cell wall remodeling, the molecular response to each environmental stimuli is incredibly unique and requires coordination with additional pathways, activation of different transcription factors, and often involves non-canonical signaling.

There is significant molecular crosstalk between core cell wall integrity and stress responsive pathways in *C. albicans* to coordinately regulate cell wall synthesis and remodeling based on the activating stress. An excellent example of the complex regulation and crosstalk involved in regulating cell wall remodeling can be found in the response to the antifungal drug, caspofungin. In response to caspofungin-mediated cell wall stress, multiple well-defined signaling pathways work in parallel to increase chitin content and β-1,3-glucan exposure, consequently reducing susceptibility to the antifungal[129,130,152]. Increased chitin synthesis requires coordinated regulation by the PKC and HOG signaling cascades, as well as the calcineurin signaling pathway, although to a lesser extent[129,153]. The PKC and calcineurin pathways are also involved in unmasking β-1,3-glucan in response to caspofungin treatment[152,154]. Despite the prominent involvement of the calcineurin pathway in responding to caspofungin, Crz1, the

canonical transcription factor for this pathway is not involved in caspofungin-mediated β-1,3-glucan unmasking[154]. Instead, the transcription factors Cas5, Rlm1, and Sko1, as well as the Psk1 kinase, are all involved in the transcriptional response to caspofungin-mediated cell wall damage[155–159]. Although several signaling pathways and transcription factors have been implicated in the transcriptional and cell wall remodeling response to caspofungin, there is not yet an integrated model to concisely incorporate each of the known players.

In addition to the coordination and crosstalk of signaling pathways in cell wall remodeling, these pathways and transcription factors are frequently involved in the response to multiple stresses through disparate signaling mechanisms. For example, in addition to its role in regulating β-1,3-glucan unmasking following caspofungin treatment, the calcineurin pathway regulates an opposing phenotype, β-1,3-glucan masking, in response to high levels of exogenous calcium[154]. This response to calcium is dependent on the Crz1 transcription factor, unlike the remodeling in response to caspofungin[154]. Conversely, Crz1 also regulates β-1,3-glucan masking in response to lactate, although this regulation is not dependent on the calcineurin pathway and instead involves a non-canonical signaling pathway[71,160–166]. Finally, the transcription factor Sko1 relies on indirect activation through Rlm1 and Psk1 for responding to caspofungin-mediated damage, while Sko1 is phosphorylated by Hog1 in response to osmotic stress[155,157,158,160]. Therefore, the molecular response to any given inducing stress is highly specific and complexly regulated.

1.5 Fungal-bacterial interactions

Human mucosal surfaces are home to trillions of microbes, including bacteria, archaea, viruses, and of course, fungi. These microbial communities are dynamic and are constantly exerting influences on each other, their environmental niche, and the host. Defining how bacteria shape *C. albicans* biology is a critical component of characterizing *C. albicans* as both a commensal and a pathogen. The influence of bacteria on *C. albicans* virulence is apparent as antibiotic treatment is a known risk factor for developing invasive candidiasis and *C. albicans* is frequently isolated from polymicrobial infections, which have higher mortality rates than monomicrobial infections[71,161–167]. In addition to this clinical evidence that bacteria modulate *C. albicans* virulence, numerous *in vitro* studies have demonstrated that bacteria can influence filamentation, growth rate, biofilm formation, and other aspects of *C. albicans* biology.

As discussed above, treatment with broad-spectrum antibiotics is a risk factor for developing invasive *C. albicans* infections that has been acknowledged since the 1960s; however, it is not fully understood how antibiotic treatment increases risk for *C. albicans* infections[71,163–167]. Generally, it is believed that an intact bacterial microbiota prevents fungal overgrowth through competition for nutrients or through the production of antifungal compounds. Longitudinal studies investigating changes to the gut mycobiota in adults before, during, and after antibiotic treatment reveal that fungal burden, including *C. albicans* levels, is increased following antibiotic treatment[168,169]. Changes in fungal load persisted long-term, even after bacterial communities had recovered, and the treatment regimen and relative activity of antibiotics had differential impacts on *C. albicans* abundance[168,169]. Antibiotic treatment in infants also resulted in increased absence of *Candida*[170]. Therefore, disruption of gastrointestinal bacteria through antibiotic treatment has significant and long-term consequences on *C. albicans* abundance.

While we have evidence from human studies that antibiotic treatment allows for fungal overgrowth, mouse models have provided insights into several mechanisms by which gastrointestinal bacteria modulate colonization and infection by *C. albicans*. Anaerobic bacteria have been shown to be key mediators of colonization resistance against *C. albicans*, as antibiotics targeting anaerobic bacteria were the most effective at allowing stable fungal colonization of the murine gut[171]. In this case, anaerobic bacteria induced production of the antimicrobial peptide, CRAMP (LL-37 in humans), which was responsible for preventing *C. albicans* gastrointestinal colonization[171]. Other studies have implicated antibiotic-induced changes in the gastrointestinal metabolome, including decreased levels of short chain fatty acids (SCFAs), in permitting *C. albicans* gastrointestinal colonization[172–174]. Finally, the release of bacterial peptidoglycan subunits induced by β-lactam antibiotic treatment was revealed to promote *C. albicans* hyphal growth and contribute to systemic dissemination[175]. Intriguingly, the presence of *C. albicans* in antibiotic-treated mice alters the reassembly of the bacterial community during recovery. Specifically, *C. albicans* suppressed the recovery of *Lactobacillus* populations and promoted the recovery of *Bacteroidetes* populations[176–178]. These studies demonstrate that alterations in the gastrointestinal bacterial community through antibiotic treatment have major impacts on the environmental niche that allow *C. albicans* to establish

colonization and permits invasive infection and *C. albicans* subsequently impacts the reassembly of the bacterial microbiota following antibiotic treatment.

As discussed above, *C. albicans* is a common cause of nosocomial invasive infections, which encompasses bloodstream infections (BSIs) and intra-abdominal infections (IAIs). These invasive infections are frequently polymicrobial in nature, and polymicrobial invasive infections involving fungi have higher mortality rates than those that only involve bacteria[179–183]. Bacteria that are frequently isolated alongside *C. albicans* from polymicrobial invasive infections include *Staphylococcus aureus, Klebsiella pneumoniae, Acinetobacter baumannii*, and *Enterococcus faecalis*[180,184]. Polymicrobial infections involving *C. albicans* and *S. aureus* have been extensively studied and mouse models support the notion that co-infection with these pathogens results in synergistic lethality, whereas monomicrobial infections are nonlethal[185,186]. Mixed species biofilms on indwelling medical devices are thought to play an important role in the development of polymicrobial infections. *C. albicans* and *S. aureus* form robust polymicrobial biofilms, in which *S. aureus* binds to fungal hyphae in a manner dependent on the fungal adhesin, Als3[187–189]. These mixed species biofilms provide *S. aureus* with enhanced resistance to antimicrobials, but no impacts on antifungal resistance have been reported[190,191].

Although several bacteria have been reported to synergize with *C. albicans*, antagonistic relationships have also been reported. *Lactobacillus* species have been reported to have largely antagonistic interactions with *C. albicans*, inhibiting filamentation, biofilm formation, and attenuating virulence[27,192–195]. Similarly, *P. aeruginosa* can attach to and kill *C. albicans* hyphae, inhibit filamentation and biofilm formation, and alter fungal metabolism, and these interactions are primarily mediated by secreted bacterial metabolites, including quorum sensing molecules and phenazine toxins[23,196–200]. Although many antagonistic interactions have been reported between *C. albicans* and *P. aeruginosa in vitro*, in some models, co-infection with these pathogens resulted in synergistic lethality[201,202]. These results highlight the complexity of fungal-bacterial interactions and the importance of investigating multiple infection models.

1.6 The power of natural genetic diversity

In research, it is common for experimental systems to rely on models that were first established decades prior and have become the standard of a research field. When studying organisms, both macroscopic and microscopic, this often takes the form of using a single genetic background, or "wildtype", in the majority of studies for a given species. The use of a universal wildtype across

an entire field is important and useful for a number of reasons, as it removes a significant source of variation both within and between laboratory groups. This allows for molecular mechanisms to be investigated and related to one another while minimizing the impacts of genetic variation. Furthermore, it allows for results to be replicated, validated, and incorporated by researchers separated both geographically and across time. Another rationale for establishing a primary genetic background is that it establishes a universal standard reference for the sake of comparison, in terms of both genotype and phenotype. Therefore, adopting a standard genetic background makes research more accessible, results easier to share, and allows fields to be more collaborative. However, the use of laboratory wildtypes also has several drawbacks that must be acknowledged and carefully considered.

First, it is important to acknowledge how or why a particular wildtype was chosen. Often, a wildtype is chosen because it is easy to work with in a laboratory setting, but the same traits that make a wildtype well-suited for research can also make it a poor representative of its species as a whole. For example, *Saccharomyces cerevisiae* has served as a powerful model for studying fundamental eukaryotic biology and has been leveraged extensively in genetics research. The *S. cerevisiae* reference strain, S288c, was initially derived through genetic crosses to be used as a tool for genetic and biochemical studies[203]. S288c is maintained a stable haploid, whereas over 98% of natural *S. cerevisiae* isolates are diploid or polyploid, and this wildtype strain has also been demonstrated to be an outlier in terms of its growth rate and metabolic capacity, among other traits[204,205]. Therefore, although S288c is a powerful research tool, it behaves very differently than natural *S. cerevisiae* isolates.

Once introduced to the laboratory environment, a wild isolate can become better suited for this artificial environment over time, either through deliberate selection by researchers or natural evolution[206–209]. Over time, inter-laboratory evolution can contribute to phenotypic differences and epistatic effects that may confound the reproducibility of research between laboratory groups[206–209]. Additionally, studies in *Escherichia coli* have demonstrated that mutations acquired through laboratory evolution are distinct from those that occur through natural selection, emphasizing that the selective pressures applied during evolution experiments do not accurately replicate the selective pressures experienced in natural environments[210].

Finally, conclusions drawn from a single genetic background cannot necessarily be attributed to all members of the species. Knowledge gained from a wildtype, especially in

regards to processes that are considered fundamental, is frequently assumed to apply to all members of the species. However, gene essentiality studies in *S. cerevisiae* and *E. coli* demonstrate that essentiality is not universal and is instead highly dependent on genetic background[211–214]. Instead, incorporating genomic and phenotypic data from a large number of diverse isolates allows for finer resolution of intraspecies variation, including gene function, molecular mechanisms, and population structures that cannot be elucidated through work in a single genetic background[211–216]. This emphasizes that once a foundational understanding of an organism's basic biological functions has been achieved through work within the wildtype, genetic variation represents a powerful tool to expand the breadth and depth of our knowledge within a species. Altogether, it is clear that relying on a single genetic background has advantages in terms of communicating and incorporating results between research groups, but the significant drawbacks in focusing heavily on one 'representative' strain must be acknowledged.

1.6.1 Natural diversity in *C. albicans*

For *C. albicans*, SC5314 is the standard reference strain used in the majority of studies. SC5314 was isolated from a patient with a generalized *Candida* infection by Margarita Silva-Hutner at Columbia University, it has been used in academic research since at least 1968, and its genome was sequenced in 2004[217–219]. Studying SC5314 has provided the field with a strong foundation of knowledge about *C. albicans* biology. However, as described above, using a single genetic background has significant drawbacks, and it is clear that *C. albicans* displays remarkably genotypic and phenotypic diversity that is not captured through characterizing SC5314 alone. Nearly 300 *C. albicans* genomes have been sequenced to date, and these sequenced isolates contain a heterozygous SNP every ~200-250 base pairs[220]. *C. albicans* has 17 recognized genetic clades, as defined by multilocus sequence typing (MLST) and SC5314 belongs to Clade 1, which is the most frequently isolated clade[221,222]. Of these, five clades account for the majority of clinical isolates and some clades display geographic specificity[221–225].

In recent years, there has been increased interest in comprehensively characterizing *C. albicans* strains beyond SC5314. In 2015, Hirakawa *et al.* performed initial genotypic and phenotypic analyses on 21 clinical isolates of *C. albicans* that were representative of multiple clades, anatomical origins, and geographic regions[226]. Work from this group and subsequent studies have demonstrated substantial genotypic and phenotypic variation within this set,

including one isolate that was unable to filament due to a nonsense mutation in *EFG1*[226]. These isolates display genomic variation from SC5314 in the form of single nucleotide polymorphisms (SNPs), copy number variation, aneuploidy, chromosomal inversions, and loss of heterozygosity[226]. Furthermore, there was substantial diversity in phenotypes, including the ability to filament in response to solid and liquid cues, sensitivity to cell wall stressors, biofilm formation, response to iron limitation, and interactions with innate immune cells[226–229]. Finally, transcriptional rewiring is evident within this set, especially in regards to filamentation and biofilm regulatory networks[227,230,231]. This body of work investigating a small set of clinical isolates provides indisputable evidence that *C. albicans* is a remarkably diverse species and significant knowledge can be gained by collecting and characterizing natural isolates.

Characterization of *C. albicans* isolates beyond SC5314 has consistently demonstrated that these isolates can provide insights into fungal biology that cannot be captured using SC5314 alone. For example, *ECE1*, the gene that encodes the fungal peptide toxin, candidalysin, has several sequence variants that differ in their capacity to cause damage to epithelial cells, calcium flux, and cytokine secretion[232]. This sequence variation translates to differential pathogenicity, particularly during murine models of vulvovaginal candidiasis[232,233]. As discussed above, SC5314 cannot stably colonize the murine gastrointestinal tract without the use of antibiotics, but the depletion or lack of a robust gut microbiota can confound experimental results[234]. In contrast to SC5314, the strains 529L, an oral isolate, and CHN1, a lung isolate, are able to stably colonize the murine gastrointestinal tract without antibiotic intervention and each of these isolates outcompetes SC5314 in direct fitness comparisons[235]. The difference in colonization stability was attributed in part to SC5314's higher sensitivity to the antimicrobial peptide, CRAMP[235]. Another powerful application of *C. albicans* natural clinical isolates is to identify evolution and mechanisms of antifungal drug resistance[110,236–243]. Although drug resistance can be acquired and studied through evolution in the laboratory, there are several cases of resistance-conferring mutations that have been identified in the lab but not in clinical isolates[244–246]. Conversely, analyzing antifungal resistance in clinical isolates can reveal novel resistance mechanisms that do not arise during artificial evolution in the lab[110,238,240–243]. Taken together, this emphasizes that the selective pressures experienced by *C. albicans* in the laboratory environment and in the host are distinct and will therefore result in distinct mechanisms of resistance. These are but a handful of studies that demonstrate significant diversity amongst natural *C. albicans* isolates and how

this diversity can be leveraged to expand our knowledge of *C. albicans* biology, evolution, and pathogenicity.

In characterizing strains beyond the reference strain, it has been consistently demonstrated that SC5314 is an outlier in its highly filamentous nature, ability to invade solid agar, and form robust biofilms[247–250]. This striking phenotype, which has been of great interest to researchers for many years, can be attributed to SC5314 harboring a rare *ROB1* allele that is not present in 223 other *C. albicans* genomes[248]. SC5314 is heterozygous at the *ROB1* locus and the anomalous allele, which differs by a single nucleotide, is sufficient to drive high levels of filamentation and invasion and robust biofilm formation[248]. Critically, this implies that SC5314's impressive filamentation profile, which has been extensively characterized and has long been considered fundamental for virulence, may be relatively rare amongst *C. albicans* isolates. These results are concerning considering the significant emphasis that has been placed on this phenotype and is an excellent example of why extrapolating results from a single genetic background to an entire species can be detrimental.

1.7 Brief summary and chapter outline

The goal of this work was to expand the current knowledge of *C. albicans* biology by investigating natural genetic variation and considering how bacteria alter the fungal cell wall. In Chapter 2, I honor the historic contributions of women in *C. albicans* research by outlining five major areas of ongoing research and highlighting the women who pioneered important discoveries in these areas. In Chapter 3, I investigate natural genotypic and phenotypic amongst commensal *C. albicans* isolates. In Chapter 4, I characterize how bacteria alter the composition of the fungal cell wall and the downstream implications on immune recognition and antifungal resistance. Finally, in Chapter 5, I address the remaining questions from my work, propose future experimental directions, and reflect on the importance of considering host-relevant environmental conditions.

Chapter 2 Germination of a Field: Women in *Candida albicans* Research

The contents of this chapter have been published[251] as: Anderson FM, Polvi EJ, Veri AO, O'Meara TR; **Germination of a Field: Women in *Candida albicans* Research**; *Current Clinical Microbiology Reports* 2021. Amanda Veri drafted the morphogenesis section and collaborated on revisions. Elizabeth Polvi drafted the treatments and drug resistance section and collaborated on revisions. Teresa O'Meara drafted the host immune responses section, assisted with the pathogenesis models section, and collaborated on revisions.

2.1 Abstract

Candida albicans is a common human fungal pathogen that was first described in the 1930s and is currently one of the major causes of invasive fungal infections, especially in immunocompromised patients. Since its first identification and association with disease, *C. albicans* has been the subject of intense research investigations. In this review, we focus on the trailblazing women who made instrumental discoveries about some of the key research questions that we are still working on answering today. We highlight five major areas of *C. albicans* research: morphogenesis, drug resistance, polymicrobial interactions, in vivo pathogenesis, and host immune responses. In each section, we discuss early findings by women researchers as well as current, cutting-edge research being performed by women leaders in the field. In many cases, some of the "common knowledge" in *C. albicans* biology was first described by women, and we hope to re-emphasize their contributions to the work that is still being carried out today.

2.2 Introduction

Women have been significant contributors to medical mycology research since the beginning of this field of research. In 1923, Berkhout first described the genus *Candida* in her doctoral thesis[252]. In 1931, Benham's doctoral thesis described a pathogenic yeast that caused thrush and other diseases in humans, and her work helped to start the field of medical mycology and the study *of Candida albicans*[253]. In the almost 100 years since its discovery, scientists have unraveled many of the complexities of *C. albicans* biology and virulence. *C. albicans* is an

opportunistic pathogen, which exists as a benign member of the mucosal microbiota that can cause acute and invasive infections when immune function is compromised or after invasive clinical intervention or trauma[254]. The success of *C. albicans* as a pathogen has been attributed to its arsenal of virulence traits, including its ability to undergo morphogenetic switches and its rapid emergence of drug resistance. Using numerous animal models, scientists have interrogated the host-pathogen interactions of *C. albicans* including the effects on the host immune response, the delicate balance between commensalism and dis- ease, and the interactions with other commensal and pathogenic microbes. Our understanding of *C. albicans* as a pathogen is built off of the many discoveries from countless scientists around the globe, including many instrumental women scientists.

In this review, we intend to introduce the fundamental principles of *C. albicans* biology by featuring some of the women who have contributed to the field throughout history. Through historical PubMed searches, we identified early findings that were instrumental to the field, and we focused on discoveries published with woman first or last authors. To identify women authors, we attempted to confirm their identity through secondary sources such as university profiles, Wikipedia pages, and obituaries. We acknowledge that our methods are flawed as in many cases we assumed the researcher's sex by their given name, which is not indicative of a person's gender identity. The women highlighted in this review represent only a fraction of those who have contributed to *Candida* research over the years. We would like to acknowledge the numerous contributions by women scientists that we were not able to recognize in this review due to space limitations, language barriers, and inability to identify the authors, full name or sex. Here, we review our understanding of *C. albicans* morphogenesis, drug resistance, polymicrobial interactions, in vivo pathogenesis, and host-immune responses, highlighting the contributions of women scientists.

2.3 *C. albicans* Morphogenesis

One of the most distinguishing features of *C. albicans* is its ability to undergo morphogenetic transitions, from oval single-celled yeasts to morphologies such as elongated, multi-cellular filaments, enlarged chlamydospores and yeast- like cells such as opaque, gray, and gastrointestinally-induced transition (GUT) cells[255]. These transitions are part of an arsenal of *C. albicans* virulence traits that it exploits during infections to colonize, disseminate, evade the immune system, invade organs, and cause systemic damage, as these morphogenetic states

impart distinct advantages to *C. albicans* in different host niches and infection states[255]. Additionally, early observations of growth of *C. albicans* (then referred to as *Monilia albicans*) in various morphogenetic states were exploited as a diagnostic tool, as it was a trait that was not conserved in related *Candida* species or more distantly related ascomycete fungi. One of the trailblazing medical mycologists, Benham, reported three morphogenetic characteristics distinctive of *C. albicans*: the growth of mycelium or large masses of hyphal and pseudohyphal cells surrounding the fungal colony on solid medium, budding cells from the septa of hyphal cells, and large chlamydospores[253,256]. Together, this illuminates the utility and importance of morphogenetic transitions, especially chlamydospore production and the yeast-to-hyphal transition, which we will focus on further.

The formation of chlamydospores was long considered to be the most reliable diagnostic test for distinguishing *C. albicans* clinical samples from other non-pathogenic species[253]. Chlamydospores are large, thick-walled *C. albicans* cells often observed at the end of filaments. Early work by the groups of Benham, Taschdjian, Stein, Carter, Grant, and others characterized the growth medium and conditions to induce chlamydospore production[263], demonstrating the influence of carbon source, oxygen levels, inoculation size, age of cells, detergents, and alterations in temperature and pH[263]. Chlamydospore formation is correlated with conditions that favor filamentous growth, which Hayes identified isa result of altered distribution of complex polysaccharides and lipids through the cell wall during filamentation that accumulate to produce a thick, dense cell wall[263]. Biochemical and enzymatic studies from Jansons were critical in understanding the structure of *C. albicans* chlamydospores, containing a complex cell wall composed of an outer cell wall of mostly β- 1,3-glucan and a dense proteinaceous cell wall layer, sur- rounding a core with high lipid and RNA content[264,265]. Subsequent electron microscopy studies from Miller and colleagues demonstrated that ultrastructural changes occur within chlamydospores, coinciding in a dramatic reduction in metabolic activity[266,267]. Many questions remain about the biological function of chlamydospores and their structure, and it remains controversial whether these cells have a spore-like function[268]. Without an understanding of their function, it remains unknown why chlamydospores are specific to *C. albicans* and *Candida dubliniensis* and not shared among related *Candida* species[268], although this specificity proved useful as a diagnostic tool to identify *C. albicans*.

The most well-characterized *C. albicans* morphological transition is the yeast-to-hyphal transition. Taschdjian and colleagues were among the first scientists to observe that *C. albicans* induces filamentation within 90 min of being exposed to human or animal serum at 37°C, facilitating the development of a simple and rapid diagnostic test in serum[267]. It is now understood that *C. albicans* transitions from ovoid budding yeasts to elongated filamentous forms, including hyphal and the intermediary pseudohyphal forms, in response to many host-relevant environmental signals including exposure to serum, elevated temperature, nutrient limitation, embedded conditions, and alterations in pH[269]. The yeast-to-hyphal transition can also be induced by the misregulation of morphogenetic regulators through genetic or genotoxic manipulation. Studies from Pomés, Gil, and Nomela utilized UV irradiation to generate *C. albicans* mutants that were filamentous in the absence of an inducing cue, indicating the misregulation of an unknown morphogenetic regulator[270,271].

Though *C. albicans* filamentation has been studied for over 60 years, the complex regulatory circuitry underpinning morphogenesis in response to diverse cues is still being explored. Many groups, including Sundstrom, Hogan, and colleagues, have established that the cyclic AMP-protein kinase A (cAMP-PKA) pathway is a critical signaling hub for the induction of filamentous growth in response to diverse cues[272–276]. Shapiro, Cowen, and colleagues identified that the essential molecular chaperone, Hsp90, represses morphogenetic signaling through the cAMP-PKA pathway[277]. Bachewich and colleagues identified that depletion of critical cell cycle regulators or pharmacological inhibition of the cell cycle induces *C. albicans* filamentation, demonstrating a clear regulatory role of the cell cycle on morphogenesis[278,279]. Substantial work by Liu and colleagues helped map many of the signaling transduction pathways, including mitogen- activated protein kinases, cyclin-dependent kinases, and transcription factors, required for filamentation in response to different cues[280–284]. Blankenship's group revealed that the genetic requirements for filamentation in response to diverse inducing cues are mostly affected by the state of the medium and identified a core transcriptional program associated with, but not required for, filamentation[285]. The expansion of *C. albicans* genetic mutant libraries and the use of high- throughput systematic genetic screens, such as those performed by O'Meara, Veri, Cowen and colleagues[278], are expanding our capacity to unveil the complex and interconnected pathways regulating morphogenesis.

In contrast to chlamydospores, the biological importance of *C. albicans* filamentation in virulence has been well explored. Early clinical work found that yeast and filament forms were often observed in clinical samples, including studies of *C. albicans* in newborns by Taschdjian[286]. This work showed that mostly yeast were observed in the pre-clinical oral smears and the detection of hyphae coincided with the onset of clinical thrush, as hyphae invaded the oral epithelium[286]. Early work from scientists such as Young was instrumental in understanding that *C. albicans* yeast cells rapidly convert to filamentous forms when injected intraperitoneally into mice and while the yeast disseminated through the bloodstream, the filaments were observed to invade the pancreas with hyphae penetrating the tissues[287]. Young also observed that the yeast cells, but not the larger filaments, could be phagocytosed by immune cells[287]. Findings from Lo and colleagues observed that a *C. albicans* mutant deficient in filamentation was avirulent in a mouse model of infection[13]. Work from Bendel and Wells demonstrated that a constitutively filamentous strain, incapable of growing as yeast, was deficient in dissemination and was avirulent in oral and intravenous mouse models of infection[288]. These findings were expanded upon by many groups, including work from Noble and colleagues, establishing the current paradigm that the majority of mutants that are blocked in the morphogenetic transition are avirulent in mice[289], as both forms play critical and distinct roles in infection[289].

Morphogenesis also has a profound effect on *C. albicans* virulence by influencing the formation of treatment-resistant biofilms on indwelling medical devices such as catheters and pacemakers[51]. Work from Douglas was foundational in establishing the first methods to grow and monitor *C. albicans* biofilms, identifying that while yeast cells attach to a surface, biofilms develop into a dense network of yeast, hyphae, and pseudohyphae surrounded by an extracellular matrix[289–291]. *C. albicans* morphogenesis is required for the formation and persistence of biofilms, as the yeast and hyphae form distinct biofilm layers necessary for adherent, properly formed biofilms[292]. Douglas' group also performed foundational work establishing that *C. albicans* biofilms are multi-drug-resistant[293,294] .Nobile and colleagues established many factors required for proper *C. albicans* biofilm formation, including adhesins, hyphal wall proteins, and the transcription factor Bcr1[295–298], many of which also play roles in hyphal development. Nobile's work illuminated the master circuit transcriptionally regulating biofilm formation through the connected efforts of six transcription factors[299]. In addition to the threats posed by the drug-resistant biofilms, Uppuluri established that yeast cells that disperse from biofilms and

disseminate through the bloodstream are more adherent, have enhanced filamentation and biofilm formation, and have increased pathogenicity compared to planktonic yeast cells[300–302]. *C. albicans* biofilms pose a major impediment to the treatment of infections, as well as providing a source for dangerous, subsequent infections.

2.4 *C. albicans* Treatment and Drug Resistance

There are a limited number of classes of antifungals available in the clinic to treat life-threatening *Candida* infections. The first of these classes, the polyenes, were developed in the 1950s, and Hazen and Brown discovered and purified the first member of the polyene macrolide group in 1950 and named it Fungicidin (now nystatin)[303]. This was the first antifungal agent approved for use in humans. They demonstrated its effectiveness against *C. albicans* both in vitro and in vivo[304,305]. Silva-Hutner, referred to by some as the "matriarch of mycology," also contributed to the development and characterization of nystatin[306]. Currently, nystatin is not indicated for systemic use, though is still used topically to treat oral candidiasis[307]. The most common member of the polyene class of antifungals is amphotericin B, which is currently used for the treatment of candidiasis, though its use is limited by host toxicity[307]. Halde contributed to some of the early characterization of amphotericin B in mice and in humans[308]. The mechanism of action of the polyenes was initially poorly understood. Early work by Sokol-Anderson identified a role for oxidative damage in mediating *C. albicans* lethality[309] and identified an association between resistance to amphotericin B and oxidant stress[310]. More recent work has revealed that amphotericin B acts as a "sterol sponge," extracting the critical sterol, ergosterol, from fungal membranes[118]. Thankfully however, fungal resistance to the polyene class of antifungals remains rare. Important work by the Lindquist group used whole genome sequencing and laboratory-evolved strains to determine that the acquisition of resistance-conferring mutations results in a large fitness cost[119]. Thus, while fungal resistance to amphotericin B remains rare, the use of this antifungal is generally reserved as an alternative therapy for invasive candidiasis due to its toxic effects on the host[307].

The most commonly used antifungal agents in the clinic belong to the class of azole antifungals. The azoles were first introduced in the 1980s, and they function by inhibiting synthesis of ergosterol in fungal cell membranes, thus disrupting the fungal cell membrane [313,314]. Most first-generation azoles were limited to topical use and suffered from bioavailability challenges. These have been largely replaced with triazoles, of which fluconazole is the first-line

agent[307,312]. While the triazoles can be used systemically, are orally bioavailable, and have an improved safety profile, the acquisition of resistance to this fungistatic agent is of major concern[315]. A common mechanism of resistance involves mutations in the fungal gene *ERG11*, which encodes the enzyme in the ergosterol biosynthetic cascade targeted by azoles. Work by Kelly and others have demonstrated that mutations in *C. albicans ERG11* result in reduced azole binding to the enzyme, thus inhibiting its antifungal activity[313–315], and work by Flowers has contributed to the characterization of *ERG11* mutations in *C. albicans* clinical isolates[108]. Furthermore, Flowers established that mutations in a key regulator of ergosterol biosynthesis, *UPC2*, contribute to fluconazole resistance in the clinic[109]. Overexpression of drug efflux pumps, such as the ABC transporters Cdr1 and Cdr2, is another common mechanism by which *Candida* species gain resistance to azoles. Coste and others identified Tac1 as a transcriptional regulator of *CRD1* and *CDR2*[316] and subsequently identified hyperactive *TAC1* alleles that confer azole resistance[111,317]. Overexpression of Mdr1, a member of the major facilitator family of drug efflux pumps, also contributes to *C. albicans* fluconazole resistance, as first confirmed by Wirsching[318].

In addition to these specific mechanisms conferring azole resistance, stress response pathways play a key role in modulating azole resistance in *Candida* species. Important work by Cowen and Lindquist identified the molecular chaperone Hsp90 as a potentiator of the evolution of antifungal drug resistance[319] and found that inhibition of *C. albicans* Hsp90 impairs azole resistance in vivo[320]. Regulators downstream of Hsp90 that mediate azole resistance include the protein phosphatase calcineurin, and work by Singh, Cowen, and others established calcineurin as the first client protein of Hsp90 in *C. albicans*[319,321,322], and Cruz demonstrated that inhibition of calcineurin decreases azole tolerance[323]. Furthermore, Hsp90 regulates circuitry involving the protein kinase C (PKC) mitogen-activated protein kinase pathway to respond to cell wall stress, as shown by LaFayette[324]. Together this work reveals inhibition of Hsp90 and downstream stress response regulators as a strategy by which to block the emergence of azole resistance and enhance azole efficacy.

C. albicans is also known for its remarkable genomic plasticity, which contributes to its genetic diversity. Rustchenko's group first reported that *C. albicans* fluconazole resistance can be dependent on chromosomal nondisjunction[325] and had made previous observations connecting *C. albicans* chromosomal copy number alteration to regulation of gene expression[326]. The Selmecki, Forche, and Berman team made further important connections between aneuploidies

and azole resistance. They found aneuploidies of multiple chromosomes (most commonly, trisomy of chromosome 5) and the presence of an isochromosome composed of the two left arms of chromosome 5 (i(5L)) were associated with azole resistance[327]. Further work by this group determined that the major mechanism by which i(5L) confers resistance in vivo is by amplifying *ERG11*, encoding the drug target, and *TAC1*, encoding a transcription factor that regulates efflux pump expression[328]. More recently, work by the Selmecki group has identified long repeat sequences as drivers of *C. albicans* genome instability and has provided detailed mechanistic insight, highlighting how the remarkable genomic plasticity of this fungus contributes to its evolution of antifungal resistance[329,330].

The newest class of antifungal approved for the treatment of invasive fungal infections is the echinocandins, with caspofungin being approved by the Food and Drug Administration (FDA) in 2001[331]. This semi-synthetic compound shows an excellent safety profile and is the first-line antifungal used for the treatment of invasive candidiasis[307]. Poor oral bioavailability, however, limits the usage of this antifungal class to intravenous administration. Echinocandins impair fungal cell wall synthesis by binding to a subunit of 1,3-β-D-glucan synthase, encoded by *C. albicans FSK1*. *Candida* acquires resistance to this class of antifungals primarily through mutations in hot-spot regions of the drug target[332]. Recent work by the Rustchenko group observed that *C. albicans FKS2* and *FKS3* have a role in modulating *FKS1* expression and that their deletion alters echinocandin resistance[332].

As with the azoles, multiple mediators of fungal stress responses have important roles in modulating echinocandin- induced stress. In addition to modulating azole-induced stress, Singh, Cowen, and others identified Hsp90 as an important mediator of stress induced by echinocandins, in which depletion of Hsp90 reduced echinocandin resistance in *C. albicans* clinical isolates[322]. As with the azoles, calcineurin is a key Hsp90 client protein that mediates echinocandin resistance[322]. Additional Hsp90 client proteins involved in mediating cell wall stress are those belonging to the protein kinase C (PKC) cell wall integrity pathway, as shown by work in the Cowen group[324,333,334]. Pathways governing cell wall synthesis are also key mediators of echinocandin-induced stress. Blankenship identified a network of protein kinases governing cell wall integrity and biogenesis[335]. Walker, Munro, and others have also made important contributions to our understanding of cell wall biosynthesis and regulation. Cell wall stress results in the compensatory upregulation of chitin synthesis in many species of *Candida*, which

is mediated by PKC, HOG, and calcineurin signaling pathways[129,130,153]. Thus, women have made important contributions to our understanding of response pathways mediating antifungal-induced stress, giving further insight into strategies that can be used to combat resistance to available antifungals.

2.5 Polymicrobial Interactions

C. albicans interacts with bacteria that co-colonize similar niches in the host. These fungal-bacterial interactions are diverse in their nature; some bacteria provide a protective effect to the host by antagonizing the pathogenicity of *C. albicans* or preventing fungal overgrowth through competition for resources. Other bacteria can work alongside *C. albicans* to cause life-threatening polymicrobial infections. The importance of fungal-bacterial interactions was first realized following the widespread use of antibacterial antibiotics. An early example is aureomycin, first isolated in 1948; many patients who underwent aureomycin treatment later suffered from acute inflammation of different areas of the body, which was originally attributed to a decrease in bacterial abundance. Work from Schnall indicated that *C. albicans* could be isolated from many of these patients and may therefore be the causative agent of inflammatory infections following antibiotic treatment. Furthermore, it was shown that aureomycin stimulates the growth of *C. albicans*[337]. This phenomenon was further investigated by Sharp, who demonstrated an increase in *C. albicans* colonization in patients following oxytetracycline treatment, but not sulfadiazine[338]; this highlighted that specific bacteria may limit *C. albicans* growth. This study also indicated that *C. albicans* can colonize multiple body sites commensally, as the fungus was isolated from sputum, throat swabs, and rectal swabs of patients with no clinical indications of disease. Jarvis and Johnston further demonstrated an increase in oral *C. albicans* colonization in diabetic and leukemia patients, as well as those receiving antibiotics[336].

The life-threatening nature of polymicrobial infections was reported by Dyess, who found that polymicrobial blood infections are more fatal than bacteremia or candidemia alone[337]. *Staphylococcus* and *Pseudomonas* are the bacterial genera most commonly isolated from bloodstream infections with *C. albicans*, and investigating the mechanisms behind fungal-bacterial interactions has remained an important topic of research to the present day. Neely developed a mouse model to study co-infection with *Pseudomonas aeruginosa* and *C. albicans*, which resulted in significantly higher mortality rates than monoinfection[337]. This group identified a *P. aeruginosa* proteolytic enzyme that significantly contributed to increased mortality during

co-infections. In the years since, several *P. aeruginosa* secreted compounds have been identified and characterized based on their effect on *C. albicans*[338]. Work from Hogan revealed that *P. aeruginosa* attaches to and kills the filamentous form of *C. albicans* and identified a *P. aeruginosa* quorum-sensing molecule that inhibits *Candida* filamentation[338]. Morales then determined the killing mechanism behind a *P. aeruginosa* toxin with antifungal properties[339]. Recently, *Enterococcus faecalis* peptides were also shown to inhibit *C. albicans* filamentation; Graham also demonstrated that this peptide can inhibit virulence[340].

Douglas, who did extensive work describing *C. albicans* biofilms, was the first to describe mixed species biofilms between *Staphylococcus epidermidis* and *C. albicans* on medical implant devices[340]. The polymicrobial biofilm was found to provide some protection to both microbes against antibiotic and antifungal treatments. In more recent years, the interplay between the pathogen *Staphylococcus aureus* and *C. albicans* has been investigated by Noverr, who first characterized mixed biofilms between them[341]. Similar to *C. albicans* and *S. epidermidis* mixed biofilms, formation of a polymicrobial biofilm with *S. aureus* provides the bacteria with increased resistance to the antibacterial vancomycin[341].

As both *C. albicans* and *Lactobacillus* spp. are prominent colonizers of body sites including the mouth and vaginal tract, the influence of these two microbes on one another has been investigated for decades. Young and colleagues demonstrated that *C. albicans* growth is delayed in the presence of *Lactobacillus acidophilus* and that direct addition of lactic acid delays *Candida* growth[342]. This group utilized vitamin-deficient conditions to show that *C. albicans* can support the growth of *L. acidophilus*, and imaging of mixed colonies revealed that *L. acidophilus* adheres to *Candida* cells. This work was expanded upon by a group including Hodges, Tribby, and Studell, who similarly manipulated nutritional parameters to test the ability of several *Lactobacillus* spp. to grow in the presence of and antagonize the growth of *C. albicans*[343]. Strus used vaginal lactobacilli isolates to demonstrate that hydrogen peroxide production by *Lactobacillus* spp. is partially responsible for the growth inhibition of *C. albicans*[344].

These are only a small number of defined interactions between *C. albicans* and bacteria, and many more interactions are under current investigation. Recent work from Valentine indicates that members of the genus *Bacteroides*, many of which have considerable polysaccharide-degrading abilities, can digest *Candida* cell wall components as a carbon source[345]. Eckstein demonstrated co-localization of *C. albicans* and *Bacteroides*

thetaiotaomicron to the gastrointestinal tract outer mucus layer during colonization[346]. As our understanding of microbial ecology grows, this early work on polymicrobial interactions will serve as a strong foundation for future research.

2.6 In Vivo Pathogenesis Models

Pirofski and Casadevall developed the damage-response framework, which posits that disease comes from damage and that this damage can come from either the microbe or the host immune response[346–348]. To understand the host, researchers turned to animal models of candidiasis, which allow for study of both the microbe in a complex environment and the host response to the microbe. In the 1950s, Berg and colleagues helped establish mouse models of infection, including intraperitoneal, subcutaneous, cerebral, and intracardiac infections[349]. Additional models for examining disseminated candidiasis and fungal virulence have been developed, including an embryonated egg model from Jacobsen[350], a zebrafish model described by Brothers [351,352], and a wax worm model from Fuchs[353]. While all of these models have utility for studying infections, the mouse model is the standard for the field for examining virulence of different fungal mutant strains due to ease and cost and the availability of knockout strains.

Many of these models focus on disseminated candidiasis, but *C. albicans* also causes oral thrush and vulvovaginal candidiasis, in addition to being a commensal gastrointestinal colonizer. To examine these different modes of interaction with the host, additional animal models were needed. Yano helped develop the vaginal model of *C. albicans* vulvovaginal candidiasis that mimics human infection[354,355]. The oropharyngeal models of *C. albicans* described by Solis[356,357] and Conti[358] use immunocompromisation with corticosteroids to model the thrush observed in many HIV/AIDS patients. Denture models are also used for examining oral infections in rats [359] and in mice[360]. For gastrointestinal colonization, many models use antibiotic treatment to establish robust colonization. Wells and colleagues showed colonization throughout the gastrointestinal tract and the presence of both yeast and hyphal forms of *C. albicans* in the cecal contents[361]. The team of Witchley, Pennumetcha, and Noble recently used fluorescence in situ hybridization to show these morphologies during infection and localization in the mucosal layer[362,363].

Gnotobiotic animal models provide a useful model to study *Candida*-host interactions without the need to treat with antibiotics to establish fungal colonization and without the influence of resident microbes; as noted above, *Candida* has a variety of interactions with

bacteria that alter the fungus as well as host outcomes. For studying colonization, Kumamoto first established the gnotobiotic piglet model[364].Westwater used a gnotobiotic mouse model to investigate the differential pathogenicity of *C. albicans* and the related species, *Candida glabrata*[365–367]. Importantly, without the interference of the resident microbiota, *C. albicans* behaves differently in the gastrointestinal tract of gnotobiotic mice. Böhm demonstrated that in gnotobiotic mice, *C. albicans* preferentially exists in the yeast form, unlike in conventional, antibiotic-treated mice, where *C. albicans* displays a heterogeneous mixture of yeast and filaments[368]. The germ-free status can also be combined with immunocompromisation. Immunocompromised individuals represent one of the most at-risk populations for candidiasis. Cantorna utilized germ-free mice with immunodeficiencies to demonstrate differing levels of lethality of mucosal candidiasis in immunodeficient models and establish an animal model that is naturally susceptible to endogenous mucosal and systemic candidiasis[369]. Additionally, Cantorna determined that gastrointestinal colonization with *C. albicans* is not sufficient to confer susceptibility to vaginal candidiasis, even in immunodeficient mice[370].

2.7 Host Immune Responses

The innate immune system is the first line of defense against invasive candidiasis. In 1969, Stanley and Hurley showed that macrophages readily phagocytose *C. albicans* and that the fungi undergo a morphogenetic shift from yeast to hyphae, with eventual macrophage cell death[371]. Recent work from Hise, Wellington, and Uwamahoro demonstrated that the macrophage cell death is mediated through the NLRP3 inflammasome and pyroptosis[372–374]. The genetic determinants regulating fungal activation of the NLRP3 inflammasome are still being defined, but a recent screen from O'Meara identified multiple cell wall components as major contributors[374]; and Kaspar identified a role for the fungal secreted peptide toxin candidalysin[375]. Hise's lab went on to show that the NLRC4 inflammasome is specifically required for defense against *C. albicans* oral infection[376]. Additionally, Gringhuis showed that *C. albicans* can induce a non-canonical caspase-8 inflammasom[377].

The innate immune cells recognize *C. albicans* through conserved pathogen-associated molecular patterns, especially β-glucan[378]. The pattern recognition receptor Dectin-1 plays a key role in recognizing *C. albicans* and enabling phagocytosis by macrophages, though interestingly, its role during systemic candidiasis depends on the fungal and host genetic backgrounds[379]. This was highlighted in joint publications from Saijo and Taylor; Saijo showed that wild-type and

dectin-1-knockout mice were equally susceptible to *C. albicans* infection[90], and Taylor showed increased susceptibility of the dectin-1 knockout mice[379]. On the fungal side, there has been extensive research on fungal genes and environmental cues that influence *C. albicans* β-glucan shielding from recognition, with a resulting decrease in virulence, including work from Galán-Díez[380] ,Klippel[380], Ene[381], Davis[382], Bain[381], Ballou[382], and Childers[383], among others. In addition to β-glucan, various other *C. albicans* cell wall components can be recognized by additional pattern recognition receptors (PRRs); Heinsbroek showed that macrophage C-type lectin receptors (CLRs) coordinate with complement receptors and mannose receptors when phagocytosing *C. albicans*[383], and Villamon showed that MyD88, the toll-like receptor (TLR) adaptor protein, is required for immunity to *C. albicans* and production of proinflammatory cytokines in response to infection[384].

Other cell wall components have also been identified as important antigens[385]. These differences in cell wall composition may underlie some of the variation in virulence observed by the Goldberg lab, who demonstrated differences in cell wall between virulent and avirulent strains[386]. Domer also showed that cell wall mannoproteins can stimulate CD8+ T cells and that this may be through IL-12p40, a subunit of IL-23[387]. Conti and Farah showed that IL-12p40 knockout mice are highly susceptible to oral candidiasis[358,388], and recent work from the LeibundGut-Landmann lab showed that IL-23 is critical for anti-*Candida* defense[389]. The Gaffen and LeibundGut-Landmann labs have also spearheaded the analyses of the IL-17 cytokine and Th17 cells in the response to *Candida*. These Th17 cells are the major determinant of mucosal adaptive immunity to *C. albicans* infections at oral and vaginal sites[55,390]. Zelante in the Romani lab showed that IL-17 may directly bind *C. albicans* to induce autophagy, thus inhibiting its growth and pathogenesis[391].

Analysis of the host has also identified pathways that are important for control of fungal infections. Devesty[392], Carrow[393], and more recent works by Tuite and Radovanovic identified genetic loci underlying differences in susceptibility to candidiasis of different inbred mouse backgrounds[394–396]. Choi investigated human loci associated with candidiasis in leukemia patients and identified an association with variants in IL-4[397]. Puel identified many human genetic loci that are associated with susceptibility to candidiasis, with errors in IL-17 immunity resulting in chronic mucocutaneous candidiasis[57,398,399]. This complements the work from the Gaffen lab on IL-17and immunity to mucosal candidiasis[55,358] Additionally, the Puel lab

identified Card9 deficiencies that are associated with increased *C. albicans* disease[400]. Altogether, these findings illustrate that both fungal factors and variation in host immune responses play key roles in mediating susceptibility to candidiasis.

An ongoing challenge is the development of a vaccine against fungal infections. Friedman performed some of the earliest work on immunization of mice against *C. albicans* and showed some protection when mice were vaccinated with sonicated killed yeast[401]. She also trained Domer, whose group investigated immune defenses against *Candida* for many years; their work demonstrated that a combination of antibody, cell-mediated immunity, and innate defenses are required for defense against systemic candidiasis[402–404]. One of the earliest protective antibodies against *C. albicans* was against Hsp90, in work from Matthews and colleagues, who used a monoclonal antibody against CaHsp90 to prophylactically protect against systemic *C. albicans* infection[405]. Moragues identified roles for anti- Candida mannoprotein antibodies in preventing adherence and filamentation, in addition to direct cidal activity[406]. Excitingly, work from Uppuluri and colleagues has shown the efficacy of an anti-Als3p antibody against recurrent vulvovaginal candidiasis[407]. This is the only *C. albicans* vaccine that has undergone phase III clinical trials.

2.8 Conclusions

This review represents an opportunity to recognize and celebrate the many contributions to *C. albicans* research made by women who helped establish and shape the field of medical mycology. While exploring primary literature relating to *C. albicans*, we were pleasantly surprised to learn that many foundational aspects of *C. albicans* biology that remain heavily investigated to this day were first described by women. The works collected represent nearly a century of *Candida* research by women. It is our intention for this review to serve as a basic introduction to *C. albicans* while also ensuring that the significant contributions from these women are not overlooked as the field expands upon their work. We have focused on five major topics, but women also helped discover other diverse and important aspects of *C. albicans* biology. For example, Hull and Magee helped decipher *C. albicans* mating[408,409], Slutsky and Anderson in the Soll lab investigated white-opaque switching[410,411], Hickman and Berman described the first *C. albicans* haploid strain[412], and Magee helped map *C. albicans* chromosomal structure[413]. More recently, women have played important roles in identifying and characterizing the emerging species, *Candida auris*. Chowdhary, Litvintseva, and Cuomo have played key roles

in tracking the emergence of this fungus around the globe, sequencing its genome, mapping its patterns of antifungal drug resistance, and tracing its evolutionary origins[114,116,414,415].

While this review focused on the contributions made by women mycologists, we do not want to minimize the instrumental work done by other groups of scientists, including individuals who are part of other underrepresented groups like the Black, Indigenous, People of Color, disabled, or LGBTQ2S+ communities, as well as people in the intersections of these groups. We acknowledge their contributions to the field, which we hope will be the focus of future reviews.

Chapter 3 *Candida albicans* Selection for Human Commensalism Results in Substantial Within-Host Diversity Without Decreasing Fitness for Invasive Disease

The contents of this chapter have been published in *PLOS Biology*[416] as: Anderson FM, Visser ND, Amses KR, Hodgins-Davis A, Weber AM, Metzner KM, McFadden MJ, Mills RE, O'Meara MJ, James TY, O'Meara TR, ***Candida albicans* Selection for Human Commensalism Results in Substantial Within-Host Diversity Without Decreasing Fitness for Invasive Disease**; *PLOS Biology* 2023. Noelle Visser and Katura Metzner assisted with strain collection and archival. Noelle Visser and Andrea Hodgins-Davis assisted with growth curves and initial phenotyping. Kevin Amses and Timothy James assisted with phylogenetic analysis. Alexandra Weber and Ryan Mills assisted with genome assembly. Matthew O'Meara assisted with UMAP plots. Teresa O'Meara assisted with project development, writing, and editing.

3.1 Abstract

Candida albicans is a frequent colonizer of human mucosal surfaces as well as an opportunistic pathogen. *C. albicans* is remarkably versatile in its ability to colonize diverse host sites with differences in oxygen and nutrient availability, pH, immune responses, and resident microbes, among other cues. It is unclear how the genetic background of a commensal colonizing population can influence the shift to pathogenicity. Therefore, we examined 910 commensal isolates from 35 healthy donors to identify host niche-specific adaptations. We demonstrate that healthy people are reservoirs for genotypically and phenotypically diverse *C. albicans* strains. Using limited diversity exploitation, we identified a single nucleotide change in the uncharacterized *ZMS1* transcription factor that was sufficient to drive hyper invasion into agar. We found that SC5314 was significantly different from the majority of both commensal and bloodstream isolates in its ability to induce host cell death. However, our commensal strains retained the capacity to cause disease in the *Galleria* model of systemic infection, including outcompeting the SC5314 reference strain during systemic competition assays. This study provides a global view of commensal strain variation and within- host strain diversity of *C.*

albicans and suggests that selection for commensalism in humans does not result in a fitness cost for invasive disease.

3.2 Introduction

Candida albicans is a common colonizer of humans, with between 20% and 80% of the world's population estimated to be asymptomatically colonized at any given time[417,418], although this depends on many factors, including host health status and diet[7,8,419]. Colonization occurs at multiple body sites including the mouth, skin, GI tract, and vaginal tract[255,420]. These sites present a wide range of physiological stresses to colonizing fungi, including variation in pH, temperature, and oxygen levels, as well as nutrient limitation and host responses[255,421–423]. *C. albicans*-host interactions are generally commensal, but *C. albicans* can also act as an opportunistic pathogen, resulting in an estimated 400,000 serious bloodstream infections per year[70,424,425]. Additionally, *C. albicans* can cause more minor mucosal infections, including oral and vaginal thrush and skin infections[425]. As a consequence *C. albicans* represents the second most common human fungal pathogen and the most common source of healthcare-associated fungal infections[426].

While host immune status is known to be an important predictor of disease outcomes, whether genetic variation between *C. albicans* strains also contributes to differences in virulence remains an open question. In the model yeast *Saccharomyces cerevisiae*, there is extensive variability in genotype and phenotype among different isolates that has been linked to the ability of *S. cerevisiae* to adapt to a wide range of environmental conditions[427,428]. Recent work has highlighted intraspecies variation in important aspects of *C. albicans* biology[426]. There are currently 17 clades of *C. albicans*, which were initially defined through multilocus sequence typing (MLST)[429–431]. More recently, genome sequencing has resolved finer population structure in the group[429]. Genetic epidemiology studies suggest that the major clades of *C. albicans* may differ in how frequently they are isolated from bloodstream infections or asymptomatic colonization[432], with 5 clades accounting for the majority of clinical isolates[72,227,247,410,429–432]. These clinical isolates have demonstrated significant variation in murine models of systemic infection, biofilm formation, cell wall remodeling, secretion of toxins and proteolytic enzymes, and morphological plasticity[72,227,247,410,432–435]. However, our primary understanding of the genotype–phenotype relationship in *C. albicans* results from analyses of a relatively limited set of pathogenic clinical isolates and their laboratory derivatives, with the majority of the work

performed in the SC5314 genetic background. Detailed analysis of the genetic determinants of biofilm regulation between 5 different strains, each representing a different clade of *C. albicans*, have highlighted that circuit diversification is widespread between strains[234,362,364,433–436], adding complexity to our understanding of *C. albicans* biology.

Recent work suggests that *C. albicans* experiences fitness tradeoffs between invasive and colonizing growth, with selection for commensal behavior during colonization[234,362,364,436–439]. In serial passage experiments or competitive fitness experiments in the gut, mutations in key transcription factors controlling hyphal formation, *EFG1* and *FLO8*, resulted in increased fitness in the gut and decreased fitness in systemic models of infection[234,362,364,436–438]. In oral candidiasis, trisomic strains have been identified with a commensal phenotype[440]. Additionally, the 529L strain of *C. albicans* causes less damage and inflammation during oropharyngeal candidiasis[441] and persists at a higher fungal burden in both the mouth and the gut[234,235,433]. These potentially divergent selection pressures imply that commensal *C. albicans* strains can differ from isolates that cause invasive disease, but the genetic determinants underlying this difference have not been defined.

Here, we demonstrate that healthy people are reservoirs for genotypically and phenotypically diverse *C. albicans* strains that retain their capacity to cause disease. Our results indicate that individuals can be colonized by strains from multiple clades and that these commensal isolates have extensive variation in growth, stress response, biofilm formation, and interaction with macrophages, but this variation was not explainable by sample origin site. We found that although the commensal isolates had a reduced capacity to cause macrophage cell death, the majority of the strains showed increased competitive fitness in invertebrate models of systemic candidiasis compared with the reference SC5314 strain and retained their capacity to cause disease during monotypic infections. Together, these data suggest that the selective pressures experienced by *C. albicans* during commensal colonization do not necessarily result in decreased pathogenic potential.

3.3 Results

3.3.1 Phenotypic characterization of commensal *C. albicans* strains

We sourced *C. albicans* from oral and fecal samples from undergraduate student donors, using these as a representative sample of colonizing *C. albicans* strains from healthy individuals. In

this population of students, 29% (29/98) were positive for oral *Candida* colonization and 10% (10/98) were positive for fecal colonization, including 4 students who exhibited both oral and fecal colonization (Fig. 3-1A). From each host and site, we collected every individual colony present on the BD ChromAgar plates and confirmed species identity through ITS amplicon sequencing. Overall, we obtained 910 *C. albicans* isolates (fecal: n = 84 colonies, oral: n = 826 colonies) (Fig 3-1B).

We then performed growth assays on all 910 isolates and the SC5314 reference strain in rich medium (yeast peptone) with dextrose, galactose, or glycerol as the carbon source. We observed primarily unimodal distributions with a long tail of slow-growing strains for both exponential growth (μ max) and saturating density (K) in rich media (Fig 3-1C). Although the 5 slowest-growing isolates were all obtained from oral samples, we did not observe a significant difference in growth rate between oral and fecal samples (Fig 3-2A), and overall, the growth rates between the different carbon sources were not correlated (Fig 3-2B).

As filamentation has been tightly associated with virulence, and because previous work in murine models has suggested that gut adapted strains may lose their ability to filament[234,235,436], we examined each isolate in the collection for their ability to form hyphae using 10% serum and febrile temperatures as 2 inducing cues. Additionally, we examined the morphology of each strain under the non-inducing condition of yeast extract peptone dextrose (YPD) at 30°C to identify constitutive filamentation, as has been observed from isolates collected from sputum samples from cystic fibrosis patients[442]. We observed that while none of the strains were constitutively filamentous, several strains aggregated at YPD 30°C (Fig 3-1D; represented by 882–46). These aggregative isolates were more likely to reach a lower carrying capacity; however, it is possible that the aggregation interfered with the accuracy of the OD reads.

All strains were able to filament in response to the standard laboratory inducing conditions of serum and high temperature, albeit with some variation in the number of hyphal cells, shape, and aggregation of the cells (Fig 3-1D). Under hyphal-inducing conditions, the aggregating strains formed filaments while the mother yeast cells remained connected, resulting

in a star-like pattern. Some isolates showed different filamentation patterns under the different

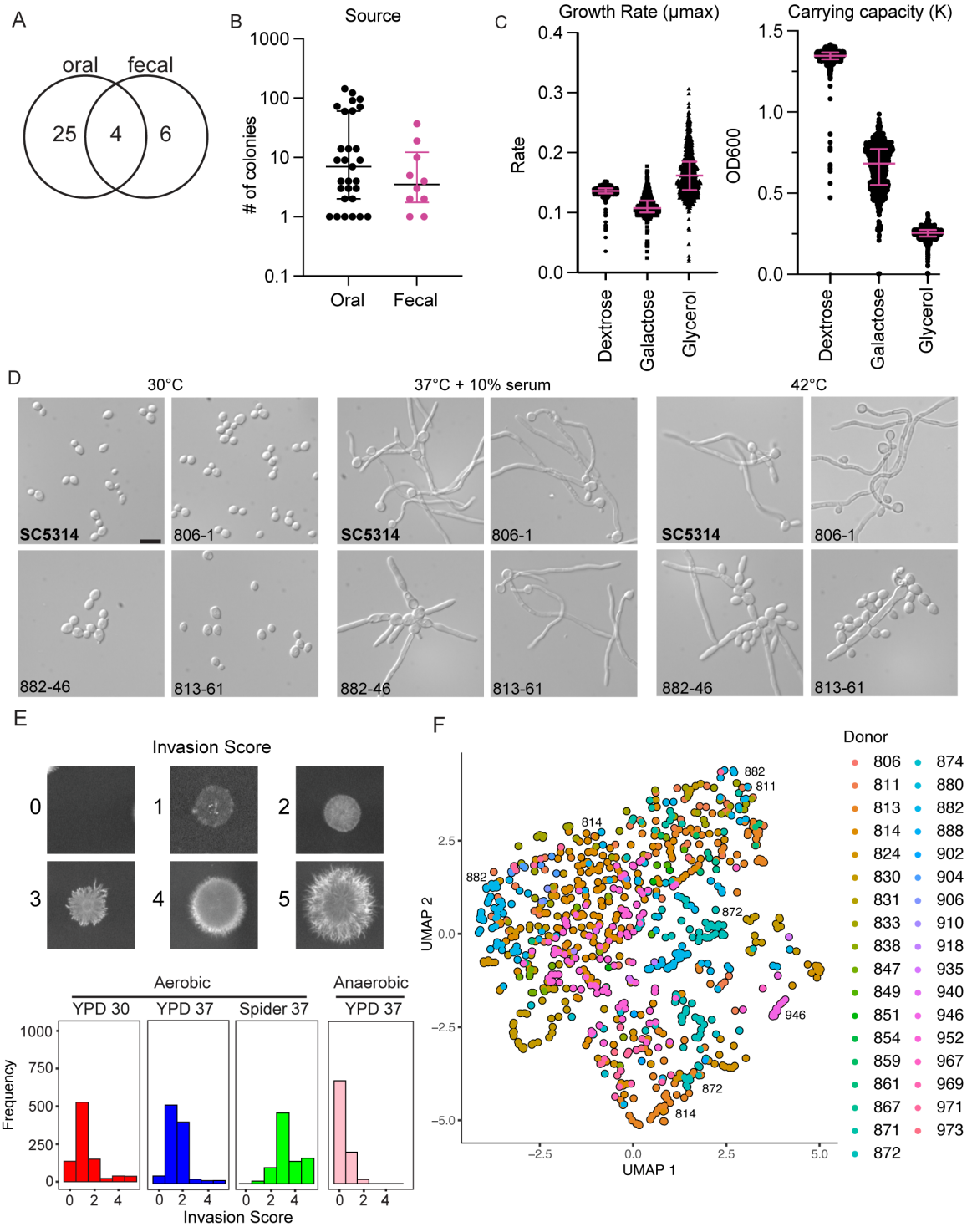


Figure 3-1: Characterization of isolates from healthy donors reveals extensive phenotypic heterogeneity.

(A) The number of healthy donors from whom *C. albicans* colonies were obtained by isolation site with 4 donors exhibiting both oral and fecal colonization. **(B)** Number of *C. albicans* colonies isolated per donor from each sample

site. Error bars represent median and interquartile range in number of colonies from each positive individual donor. Significance determined by Wilcoxon rank sum test. **(C)** Strains varied in maximum growth rate and carrying capacity in response to different carbon sources. Growth curves were performed on each isolate under 3 carbon sources at 30°C for 24 h for dextrose and 48 h for glycerol and galactose in biological duplicate. Rate and carrying capacity were determined using the GrowthcurveR analysis package. Error bars represent median and interquartile range of the growth parameter. **(D)** All strains retained the capacity to filament in liquid inducing cues, but some demonstrated altered morphology and aggregation. Strains were incubated in the indicated conditions and imaged at 40× magnification. Scale = 10 μM. **(E)** Strains varied in their capacity to invade into solid agar. Colonies were incubated on the indicated conditions for 5 days before gentle washing and imaging for invasion. **(F)** UMAP plot for strain phenotypic similarity. All growth conditions and invasion phenotypes were nonlinearly projected into 2D space and colored by donor.

inducing conditions. For example, isolate 813–61 formed filaments that resembled those of SC5314 under 37°C + 10% serum, but under the 42°C inducing cue, this isolate formed fewer filaments with many yeast cells aggregating around the filament. The ability of all our commensal isolates to form filaments may be consistent with the hypothesis that interaction with bacteria in the gut maintains selection for the hyphal program[235,436]. Although there were isolates, such as 813–61, that showed more of a mixture of yeast and hyphae than the SC5314 parent that are potentially consistent with the yeast-locked phenotypes observed in Tso and colleagues (2018)[235,437], the majority of our commensal strains retained full capacity to filament in our in vitro assays. This may suggest that the antibiotic or germ-free mouse models are not fully recapitulating important features of *C. albicans*–human interactions.

Filamentation programs under solid and liquid growth can involve distinct genetic programs[235,439], and the human host can present a variety of substrates for *C. albicans* to utilize. Therefore, we also tested each isolate for its capacity to invade into solid agar media under multiple conditions: YPD agar at 37°C under anaerobic conditions as a minimal inducing cue, YPD agar at 30°C as the baseline condition, YPD agar at 37°C as an intermediate inducing condition, and Spider agar at 37°C as a strong inducing condition (Fig 3-1D). As expected for a strong inducing cue, the highest degree of invasive growth was observed on Spider agar at 37°C[235,440]. Interestingly, although all strains showed the ability to form hyphae under liquid culture conditions, many strains failed to invade into solid agar, giving scores of 0 or 1 under multiple conditions (Fig 3-1E). We also observed substantial phenotypic heterogeneity among strains isolated from the same host, including in strains isolated from the same site, consistent with each individual being colonized by multiple, phenotypically distinct, strains of *C. albicans.*

To examine the relationship between the strains, observed phenotypes, and donors, we generated a uniform manifold approximation projection (UMAP) embedding, which will plot

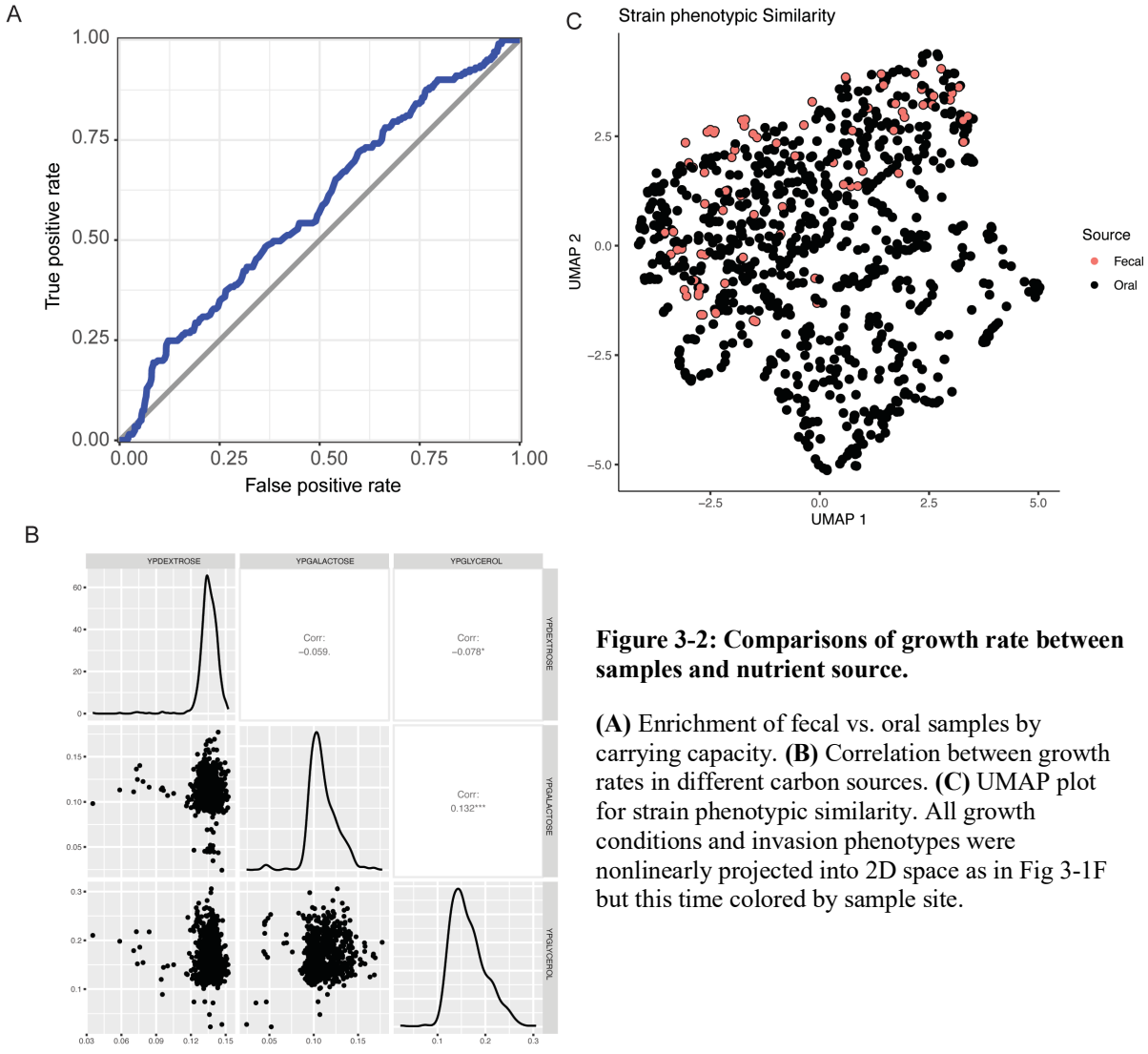


Figure 3-2: Comparisons of growth rate between samples and nutrient source.

(A) Enrichment of fecal vs. oral samples by carrying capacity. **(B)** Correlation between growth rates in different carbon sources. **(C)** UMAP plot for strain phenotypic similarity. All growth conditions and invasion phenotypes were nonlinearly projected into 2D space as in Fig 3-1F but this time colored by sample site.

strains with similar phenotypes closer together and strains with dissimilar phenotypes farther apart based on the Euclidean metric (Fig 3-1F). Using this projection, we saw significant overlap in strain phenotypes from many donors, although there were some donors that had strains that clustered away from others, such as donor 946.

Additionally, some donors had 2 separate clusters of strains, such as those from donor 814, 872, and 882. We also observed that some strains from multiple donors clustered together in this projection, including the aggregating strains from donors 811 and 882. However, we did not observe clustering based on sample origin site (Fig 3-2C). Together, these experiments demonstrate a large variation in phenotypes between commensal isolates, even among traits, such as filamentation and invasion, that are often correlated with virulence.

3.3.2 Genomic variability

Due to the extensive variation in observed phenotypes among the isolates, we next wanted to characterize the genomic variability in these strains, at both a sequence and structural variation level. To carry out these analyses, we selected a set of 45 commensal isolates, hereafter referred to as the "condensed set". Isolates were chosen for inclusion in the condensed set where we had matched pairs from oral and fecal isolates from the same donor or isolates from the same donor that exhibited multiple phenotypes based on growth, filamentation, or invasion. For these analyses, we compared each isolate to the SC5314 reference strain. We also included the human isolate, CHN1, which has been previously phenotypically and genotypically characterized as a bona fide commensal and is able to stably colonize the murine gastrointestinal tract for long periods of time, in contrast to SC5314[235,443].

Previous descriptions of population genomic variation in *C. albicans* have largely relied on short-read sequencing approaches, which are limited in their ability to resolve structural variation between strains. Therefore, we performed whole-genome sequencing on all 45 commensal strains, SC5314, and CHN1 using the Transposase Enzyme Linked Long-read Sequencing (TELL-Seq) method for library preparation[444]. This approach uses barcode linked-reads to produce synthetic long reads with Illumina quality sequence, thus allowing us to capture both single-nucleotide variants (SNVs) and structural variants.

To identify SNVs and compare our strains to the existing set of sequenced *C. albicans* isolates, we collected 388 previously published *C. albicans* genomes and, after filtering, we mapped them, and our 45 newly generated genomes, to the SC5314 reference genome with BWA-MEM[445]. We called variants using GATK HaplotypeCaller and after filtering, we obtained final set of 112,136 high-quality SNVs across 431 remaining samples. Of these, 90,675 (80.86%) were represented in at least 1 member of our set of newly sequenced strains. The population diversity captured in this analysis was consistent with the largest previous analysis of *C. albicans* genomic variation, which called 589,255 SNPs from 182 genomes[221,226,443]. Although our final SNV set was significantly smaller than that identified in past work, our filtering criteria were significantly more stringent and robust for inferring population level patterns.

We then wanted to place our newly sequenced isolates in the phylogenetic context of previous work on *C. albicans* strains[221,226,446]. To remove redundancy and focus on natural *C. albicans* diversification, we removed samples corresponding to resequenced strains (e.g.,

multiple SC5314 samples present in full data set) and those sequenced as part of experimental evolution studies (i.e.,[234,329,447]). Following removal of these samples, we were left with 324 sample SNV profiles, which were then used to cluster the samples into a dendrogram of relationships. Despite the reduced size of our data set, our SNV-based clustering recovers all major accepted clades of *C. albicans* (Fig 3-3)[221,429–432]. The fact that > 80% of the 112,136 high-

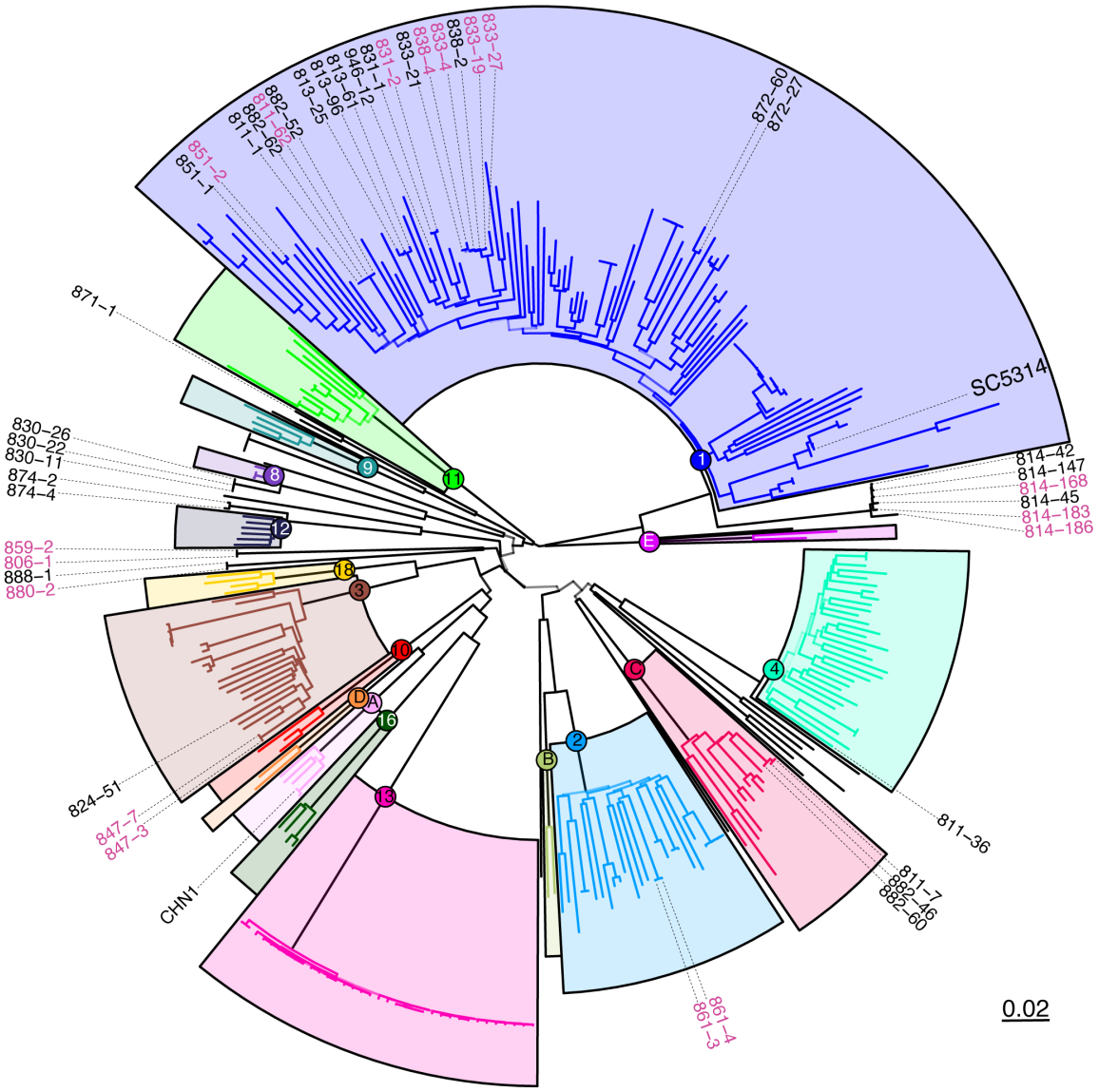


Figure 3-3: The newly sequenced *C. albicans* commensal isolates include representatives from multiple clades.

A maximum likelihood tree showing the phylogenetic relationships between the 324 isolates analyzed via (neighbor joining). Previous clusters from Ropars *et al.*, 2018 are highlighted with colored boxes. Isolates in black text are oral samples and isolates in pink text are fecal samples. Bootstrap values represented by backbone transparency. See Fig 3-4 for additional information on bootstrap values.

quality SNVs we identified are represented in the genome sequences of the 45 new *C. albicans* isolates we sequenced, in addition to their clustering near 8 major clades, asserts the high degree of diversity captured in our study of commensal *C. albicans* strains actively colonizing humans. In line with past work and underpinning the validity of our SNV-based clustering, we did not collect isolates from clades of *C. albicans* known to exhibit a high degree of geographic specificity (e.g., Clade 13) (Fig 3-3)[447].

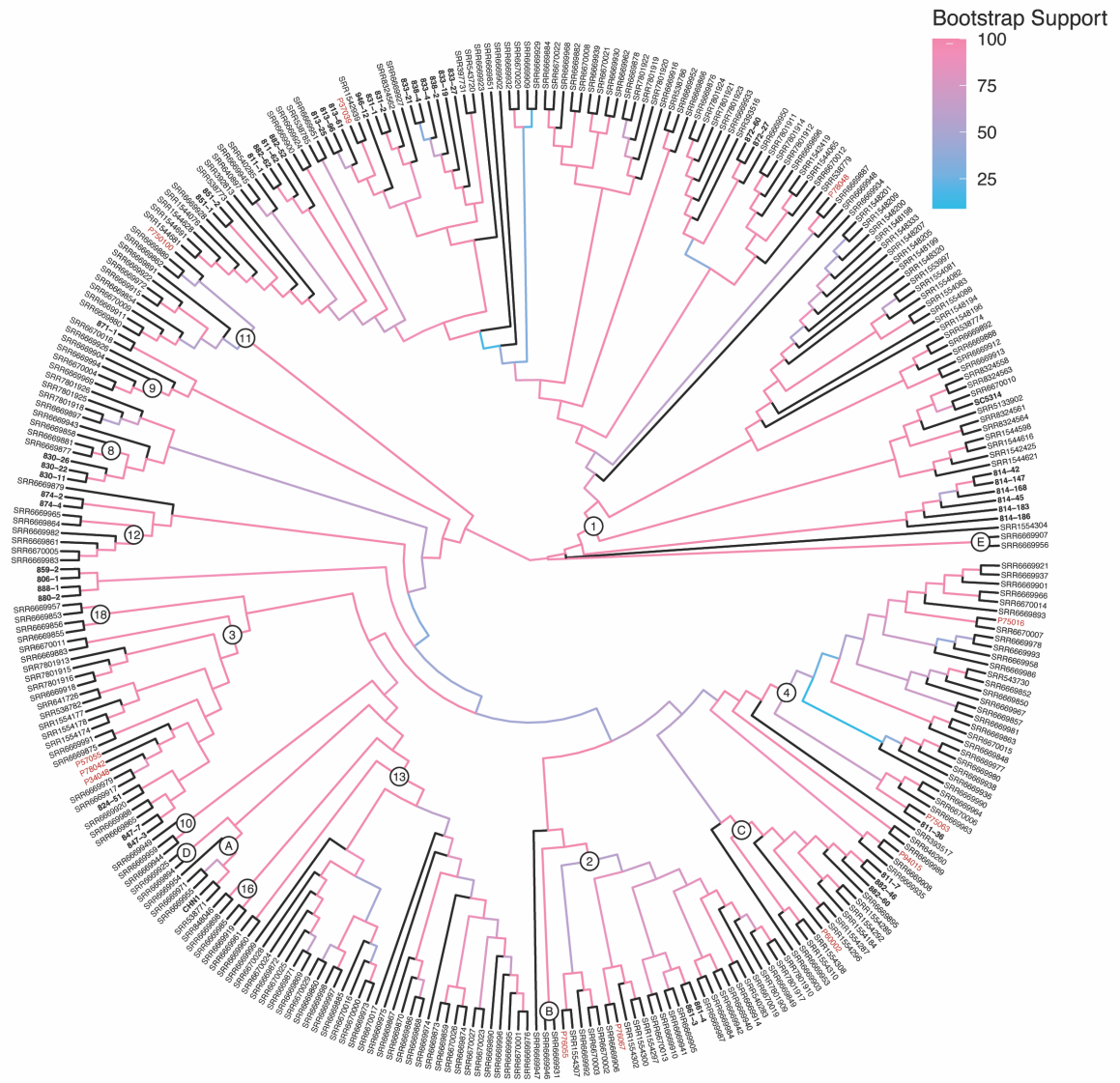


Figure 3-4: Cladogram of the SNP tree (branch lengths all equal to 1) with the backbone colored by bootstrap support values.

One hundred bootstrap replicates were generated by randomly sampling rows from the SNP table with replacement to yield a table with the same dimensions as the original SNP table. Distance matrices and neighboring-joining trees were generated for bootstrap replicates identically to the original SNP table. Bootstrap support values were computed based on the bootstrap replicate trees and annotated onto the original SNP tree with IQTree2. Bloodstream isolates used in Fig 3-7 are indicated with red text.

The majority of the new isolates (26/45) belonged to Clade 1, of which the reference strain SC5314 is also a member. We identified cases where isolates from the same donor clustered tightly together, such as donor 814, whose 6 strains included in the condensed set clustered in Clade 1. Consistent with previous reports on microevolution in the host[448], we observed primarily SNVs and short-tract loss of heterozygosity between these 6 isolates, perhaps consistent with clonal expansion and diversification during colonization. In the 4 donors colonized at both the oral and fecal sites (811, 814, 831, and 851), both oral and fecal isolates were closely genetically related. However, we also identified donors with colonizing strains from multiple clades, such as donor 882, whose 4 strains came from Clade 1 and Clade C, or donor 811, whose 4 strains came from Clade 1, Clade C, and Clade 4 (Fig 3-3). Interestingly, some isolates from multiple donors clustered within one another, such as those the donor pairs 838 & 833 and 882 & 811, potentially indicating transmission events between individuals, due to the phylogenetic closeness of the strains. Together, this suggests that variation in an individual's colonizing *C. albicans* strains may come from both within-host diversification and between-host transmission.

To characterize genomic variation at a structural level, we performed pulsed-field gel electrophoresis to separate the chromosomes of our condensed set of commensal *C. albicans* isolates, including SC5314 as a reference (Figs 3-5A and 3-6A). The commensal *C. albicans* strains show between 7 and 10 chromosome bands, ranging from approximately 0.8 MB to approximately 3.2 MB in size[449,450]. We observed many size differences in chromosomes, especially among the smaller chromosomes (corresponding with Chr 5, 6, and 7 in SC5314), but we also observed size variation in large chromosomes at approximately ~ 1 MB, ~1.5 MB, and ~2 MB, potentially indicating variation in Chrs 2, 4, and R. Size variation of larger chromosomes may be mostly associated with allelic expansion or contraction of the rDNA repeat array on ChrR.

When comparing the chromosomal structural variations to our SNV tree, we identified several unique patterns and observed that a phylogenetic ordering of the isolates did not encompass the structural variation. For example, a subset of isolates within Clade 1 from donors 833 and 838 all contained an additional band below Chr 4, with the exception of isolate 833–19, despite being within the same phylogenetic cluster based on SNV analyses (Fig 3-5A). We also observed clade-level variation in karyotypes: Isolate 871–1 was the only strain in the condensed

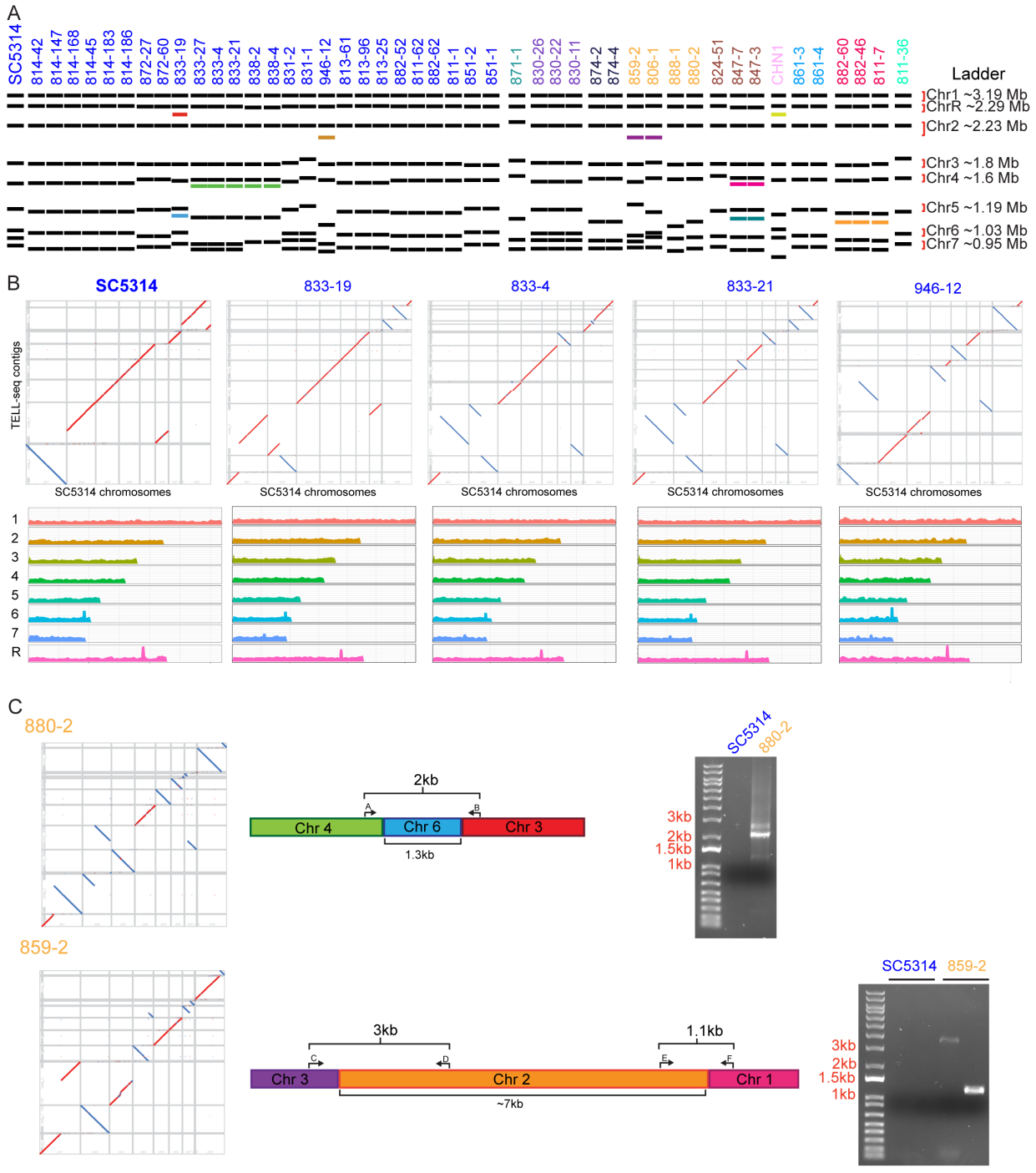


Figure 3-5: *C. albicans* commensal isolates display extensive structural variation.

(A) CHEF karyotyping gels show alterations in chromosome size and number between *C. albicans* isolates. Isolate labels were colored based on the nearest defined cluster from Fig 3-4 and ordered based on phylogeny. Unique band sizes are indicated with the colored bands. Gel images in Fig 3-6. **(B)** Above: Dot plots showing synteny alignments between new isolates and SC5314. Below: Coverage maps in 5 kb sliding windows when aligned to the SC5314 reference genome. **(C)** Isolates 880–2 and 859–2 chromosomal fusion events chosen for PCR validation. Bands corresponding with fusion events were not present in SC5314.

set from Clade 9, and this strain showed unique banding patterns at Chrs 2, 3, and 4. The 3 strains from Clade C, which originated from donors 882 and 811, all contained a band between Chrs 5 and 6. Finally, the 2 closely related strains, 859–2 and 806–1, both contained a band between Chrs 2 and 3 (Fig 3-5A). The observed altered band sizes could represent either loss of genome content or chromosomal fusion events. An advantage of our TELL-seq–based platform was the opportunity to resolve the differences between the SNV-level analysis and the structural variants that we identified through the CHEF gels. We used the synthetic long-reads to assemble contigs for each strain, using Universal Sequencing's TELL-seq pipelines: Tell-Read and Tell-Link (Fig 3-5B). We could observe variation in copy number across the chromosomes (Figs 3-5B and 3-6B), as well as potential inversions, duplications, or deletions (Fig 3-6C)[451]. We also see some peaks in copy number that are associated with MRS and rDNA sequences that were not resolved in our mapping. However, there may be some additional technical limitations of the TELL-seq approach, as we identified some inversions, duplications, and deletions in the resequenced SC5314 (Fig 3-6C). Therefore, we focused on those that were unique to the commensal isolates.

Notably, we were able to identify structural rearrangements and putative chromosome fusions that occurred in a set of the commensal isolates (Fig 3-5C) and used PCR to test for the presence of the fusion event. In strain 880–2, we observed a fusion event between chromosomes 3 and 4, connected by a 1.3 kb intervening sequence (Fig 3-5C). This intervening sequence had 94% sequence identity to an intergenic sub-telomeric region of chromosome 6. To determine whether this was a true event or a sequencing artifact, we designed primers to span the junction and performed PCR to amplify the fusion (Fig 3-5C). Using this approach, we observed that in strain 880–2, there is a bona fide structural rearrangement that links chromosomes 3 and 4. In strain 859–2, we observed a fusion event between chromosomes 1 and 3, connected by an approximately 7 kb intervening sequence with no obvious sequence identity to the SC5314 reference strain, but instead had 99.76% sequence identity to a region on chromosome 2 from *C. albicans* strain TIMM 1768, a highly virulent strain originally isolated from the feces of a candidiasis patient[450] (Fig 3-5C). TIMM 1768 is closely related to CHN1, a member of Clade A[452]. We were again able to use PCR to span both junctions observed the presence of the fusion

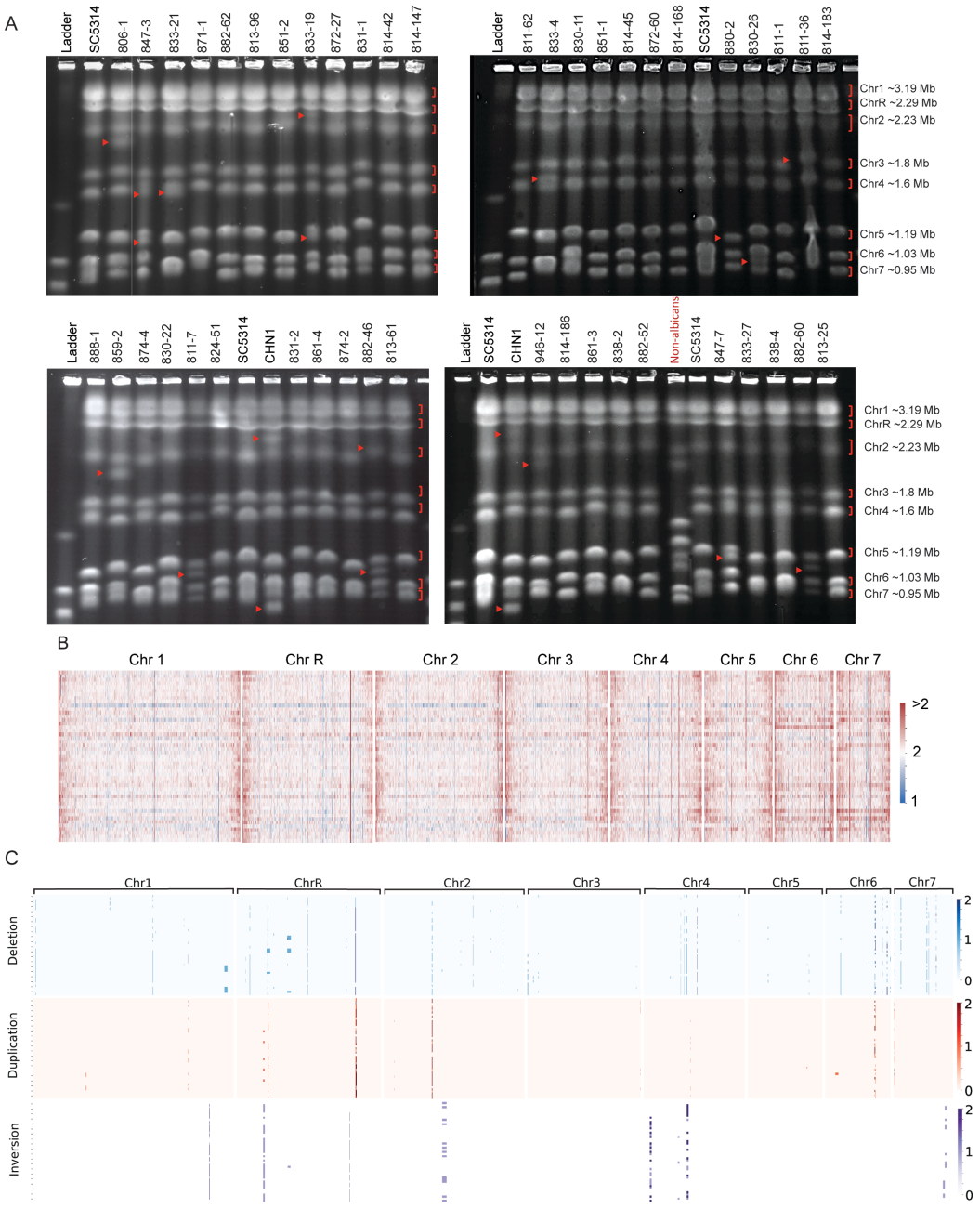


Figure 3-6: Structural variation.

(A) CHEF karyotype gels were performed on the condensed set of *C. albicans* isolates and visualized using ethidium bromide staining. Red arrows indicate large chromosome banding patterns that differ from SC5314. Chromosome 5 showed especially extensive variability in size between isolates. **(B)** Heatmaps of read coverage across the condensed set of isolates for each chromosome. Each column represents a 500 bp bin of the reference genome and each row is a condensed set isolate, with SC5314 represented by the top row. The rows are ordered, top to bottom, in the phylogenetic order used in Fig 3-5. Values greater than 1 (red) suggest potential duplications while values less than 1 (blue) suggest potential deletions. **(C)** Heatmaps of Lumpy Structural variation calls for the condensed set of isolates. Each column represents a 500 bp bin of the reference genome and each row of the heat map for a given variant class is an isolate from the condensed set. The value for each bin indicates the number of SV calls overlapping the 500 bp window.

between chromosomes 1, 2, and 3 (Fig 3-5C). This fusion event may correspond to the additional chromosomal band between chromosomes 2 and 3 that we observed in the karyotype for this strain. Importantly, neither of these fusion events were present in the SC5314 reference strain, indicating that the fusions were unique to the specific isolate (Fig 3-5C). These structural variations were not captured in the SNV analysis and may play important roles in gene regulation or phenotypic variation between the strains.

3.3.3 Deep phenotyping of commensal isolates

The set of isolates for sequencing were initially chosen based on variation in growth rate in rich medium and alterations in invasion into agar. However, we hypothesized that we may identify site-specific adaptations, as host sites commonly colonized by *C. albicans* vary dramatically in environmental cues. Additionally, we hypothesized we may identify phenotypes associated with specific *C. albicans* clades, as we were able to identify structural variants shared between closely related isolates. To test this, we performed a set of growth analyses under multiple environmental conditions, including pH stresses, nutrient limitation, cell wall stressors, and antifungal drugs (Fig 3-7A). These analyses produced a dense array of quantitative phenotypic information for each strain.

From these data, we identified 3 strains, 882–60, 882–46, and 811–7, that consistently reached a lower carrying capacity than the wild type under multiple conditions; this is consistent with the aggregative phenotype exhibited by these isolates at 30°C (Fig 3-1D). These strains all belonged to Clade C and were closely related, despite arising from 2 donors (Fig 3-7A). Growth rates in the nutrient limitation conditions were generally correlated with each other. However, we did not observe a correlation between body site and growth rate, even in response to cues that would appear to be specific for a particular body site, such as anaerobic growth. Across the commensal isolates, we noted the most variation in growth in response to caffeine and the antifungals fluconazole and rapamycin. In addition to growth, we measured each of the strains for their ability to form biofilms on plastic surfaces[453]. Although we observed variation between the strains, there was no correlation between isolation site or clade with the propensity of isolates to form biofilms (Fig 3-8).

Our dense array of phenotypic data across 45 *C. albicans* isolates and 8 clades reveal that commensal isolates largely retain the plasticity to grow efficiently under diverse environmental

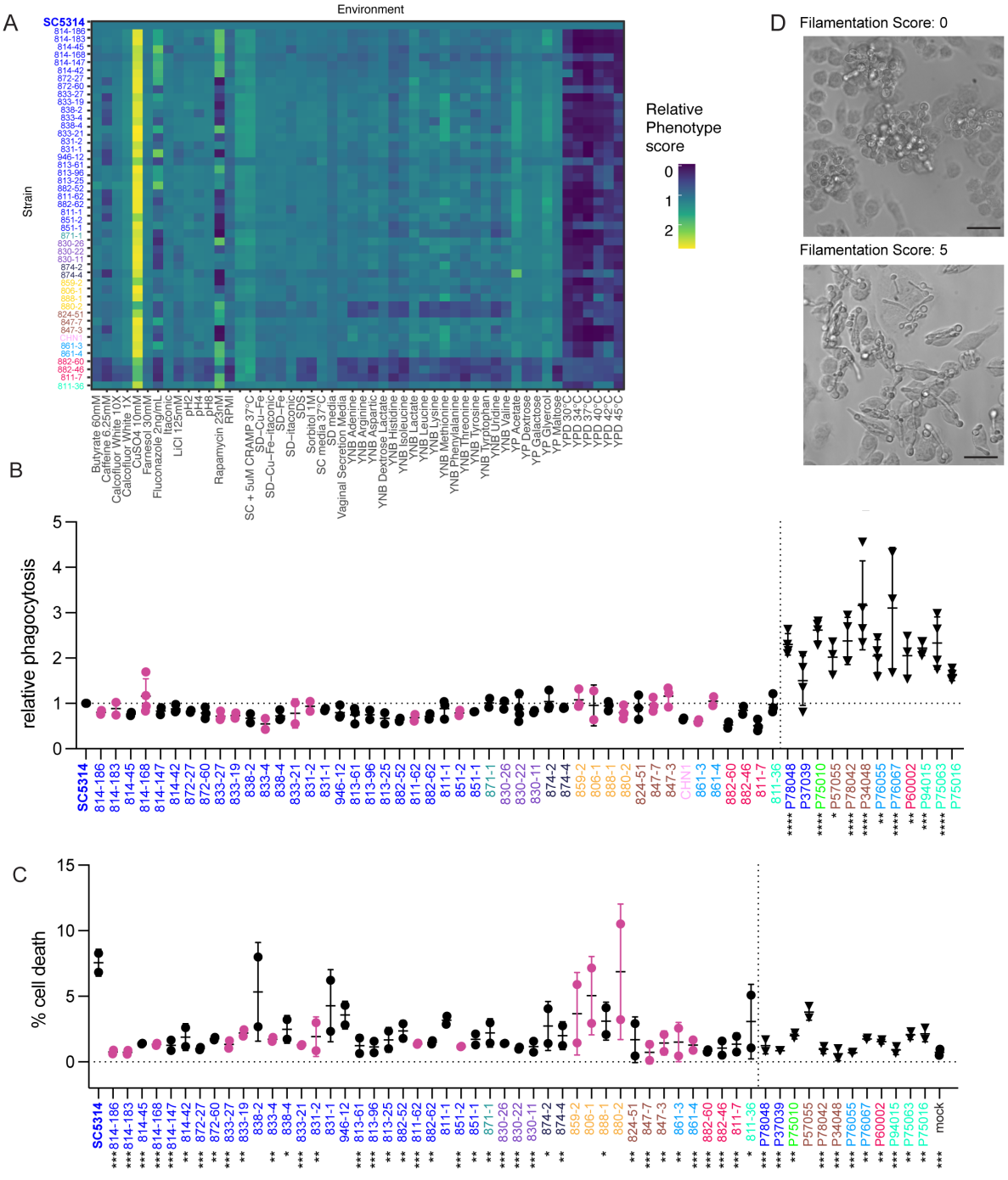


Figure 3-7: Deep phenotyping reveals heterogeneity in *in vitro* and host phenotypes.

(A) Growth curve analysis under multiple environmental conditions. Carrying capacity (K) was normalized to SC5314 and the fold-change plotted by heatmap. Aggregating strains (882–60, 882–46, and 811–7) demonstrate a consistently lower carrying capacity. **(B)** Macrophage phagocytosis rates of commensal isolates relative to SC5314. Black data points indicate an oral isolate and pink data points indicate a fecal isolate. Triangles represent bloodstream isolates. **(C)** Macrophage cell death rates. **(D)** Representative images of isolates following 4 h macrophage infection. Representative filamentation score of 0 (top). Representative filamentation score of 5 (bottom) and 20× magnification. Scale = 50 µM. For phagocytosis and cell death rates, significant differences from SC5314 were determined by one-way ANOVA, with Dunnett's multiple correction testing.

cues, even those not immediately relevant to their colonizing site, as we did not observe growth enrichment in cues specific to isolation sites.

A major stress condition and environmental factor impacting *C. albicans* in the host is the immune response. Therefore, we moved from pure growth assays to measuring host–microbe interactions, using macrophages as representative phagocytes. We first hypothesized that the oral strains may show decreased recognition by macrophages, as persistent oral isolates were recently shown to result in reduced immune recognition and inflammation in both an OPC model of infection and in cell culture[454]. We tested this by measuring phagocytosis of each strain by immortalized bone marrow-derived macrophages and determining the ratio of internalized to external cells by differential staining and microscopy (Fig 3-7B)[455]. Although most isolates were not significantly different from the SC5314 reference, the isolates generally had a lower phagocytic rate than SC5314. Additionally, there was no correlation between sample origin site or clade with phagocytosis rate.

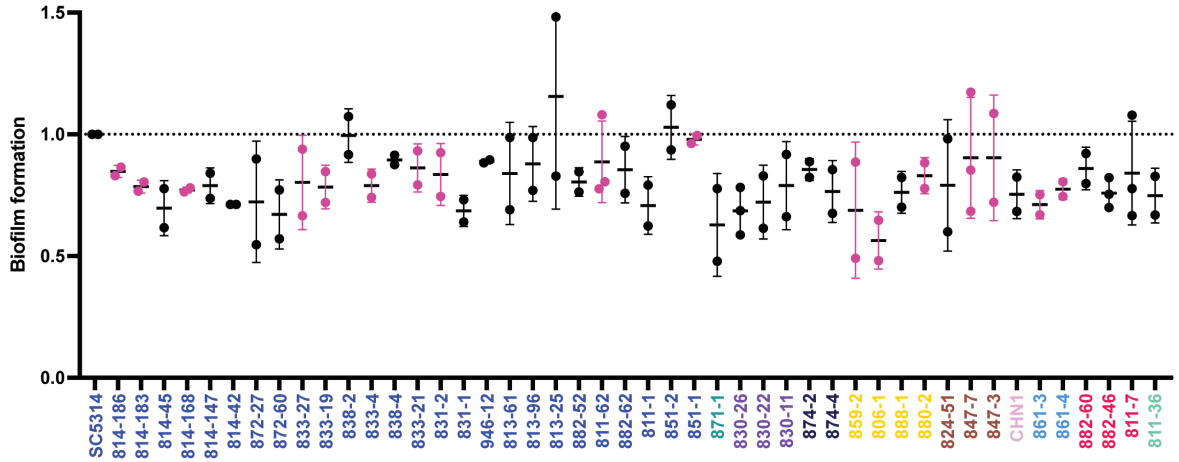


Figure 3-8: Biofilm formation.

Each condensed set isolate was tested for its ability to form a biofilm on a plastic surface. Isolate labels were colored based on the nearest defined cluster from Fig 3-3 and ordered based on phylogeny. Black data points indicate an oral isolate and pink data points indicate a fecal isolate. Significance from SC5314 determined by one-way ANOVA with Dunnett's multiple correction testing.

As phagocytosis was not a major differentiating factor between strains, we then wanted to examine whether the strains would induce different levels of macrophage cell death. We primed bone marrow-derived macrophage for 2 h with LPS before infecting with each of our isolates for 4 h. Following infection, we stained the cells with propidium iodide (PI) as a measure of cell death (Fig 3-7C). Strikingly, many of the commensal isolates induced less cell death than SC5314. Our results are consistent with previous reports that commensal oral isolates of *C.*

albicans are characterized by a reduced capacity to damage host cells[228,449]. To test whether this increased killing capacity of SC5314 was shared with other bloodstream isolates, we measured the phagocytosis and cell death rates for 12 bloodstream isolates originally described in Hirakawa and colleagues (2015)[228,450]. These results indicated a higher rate of phagocytosis for the bloodstream isolates (Fig 3-7B). However, for most of the bloodstream isolates, we also observed decreased capacity for macrophage killing (Fig 3-7C). The bloodstream isolate P94015, which was identified by Hirakawa and colleagues as having a loss of function of the transcription factor EFG1, behaved similarly to the other bloodstream isolates in these assays, despite having a decrease in virulence in their animal model[228,452]. These results indicate that the ability to kill host cells is not conserved across bloodstream isolates.

Recently, we showed that *C. albicans* mutants that filament in serum are not always filamentous within macrophages[228,453]. As filamentation is linked, but not required, for inflammasome activation within host phagocytes[228,456], and clinical isolates show variability in induction of host inflammatory responses[457], we examined the morphology of the commensal isolates after incubation for 4 h with macrophages. We observed considerable variation in the extent of filamentation among the natural isolates (Fig 3-7D), including strains that completely failed to filament and those that filamented more than the SC5314 reference strain. The aggregative strains, 882–60, 882–46, and 811–7 failed to filament during incubation with macrophages. Notably, the extent of filamentation did not correlate with colony morphology or invasion on agar, with many strains showing invasion into agar but no filamentation inside the macrophage, and vice versa (Fig 3-9). Additionally, oral and fecal isolates both demonstrated defects in filamentation in macrophages, and filamentation in macrophages was not predictive of the phagocytic rate or cell death rate.

Using individual phenotypic measures, we were unable to identify associations between strains based on body site or donor. However, it is possible that the combined phenotypic and genotypic profile would identify clusters of strains with similar distinct phenotypes or reveal connections between isolates. Therefore, we turned to UMAP embedding, which will plot strains with similar phenotypes closer together and strains with dissimilar phenotypes farther apart based on the cosign metric. We did not observe any obvious clusters that segregated by isolation site, clade, or participant (Fig 3-10). In sum, all of the commensal isolates showed extensive

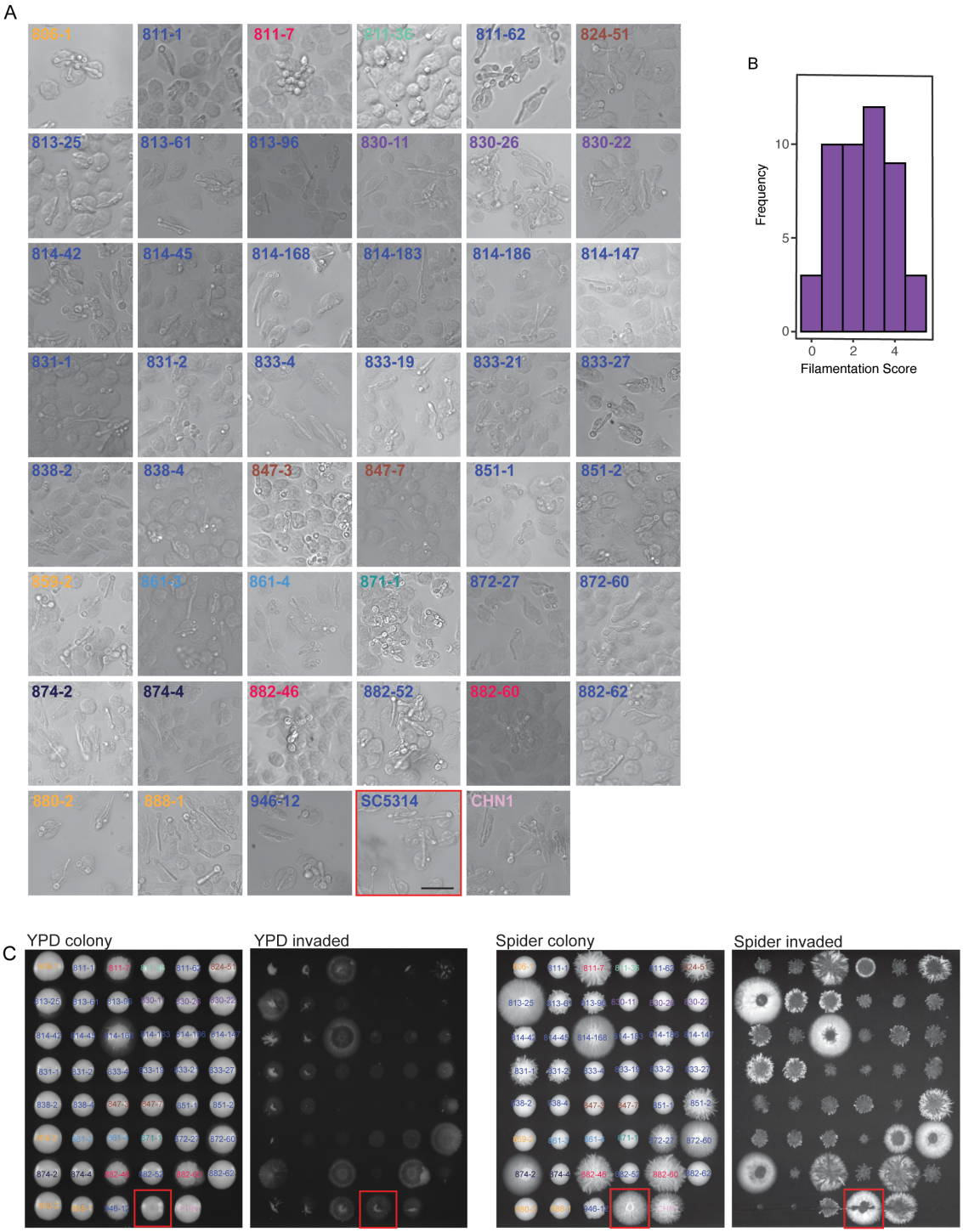


Figure 3-9: Comparison between filamentation in macrophages and agar invasion.

(A) Images of *C. albicans* condensed set isolates after growth in macrophages for 4 h. *C. albicans* were stained with calcofluor white. Images taken using DIC and DAPI channels at 20× magnification. Scale = 50 µM. **(B)** Histogram of the distribution of macrophage filamentation scores of the condensed set. **(C)** Colony morphology and agar invasion for *C. albicans* condensed set isolates on YPD agar at 30°C and Spider agar at 37°C after 5 days.

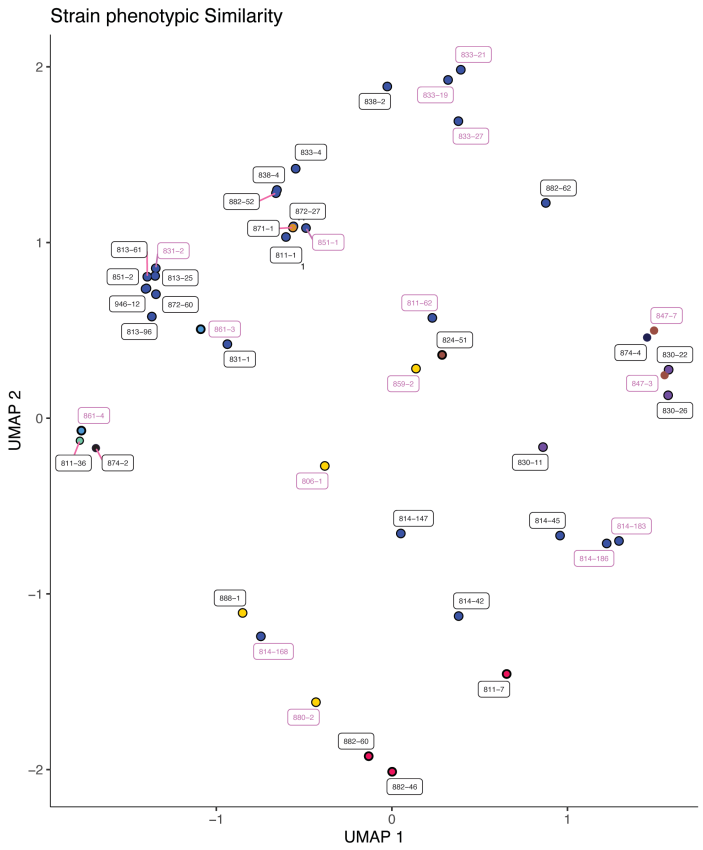


Figure 3-10: UMAP embedding.

Nonlinear embedding dimensionality reduction was performed on the phenotypic data on the condensed set of isolates using UMAP. Clusters did not segregate by sample site, donor, or clade. Clade information is indicated by color. Pink or black outlines indicate fecal of oral isolate, respectively.

phenotypic variation, but this was not dependent on the body site or participant from which they were collected.

3.3.4 Limited diversity exploitation

Genome-wide association studies have been a powerful tool for identifying the genetic basis of variation in phenotypes of interest in humans and other recombining species. However, the generally clonal and asexual reproduction of *C. albicans* creates a population structure that confounds traditional GWAS methods. By sampling multiple isolates from each individual, we were able to obtain phenotypically diverse strains with a limited set of unique SNPs between isolates, allowing us to identify causative variants associated with a particular phenotype.

We focused on the 6 strains from donor 814 included in the condensed set, which clustered tightly in Clade 1; we hypothesized this would allow us to identify causative variants associated with particular phenotypes that were divergent between strains. Our agar invasion analysis revealed that isolate 814–168 demonstrated hyper invasion into Spider agar at 37°C, whereas the other 5 isolates from the condensed set were less invasive (Fig 3-11A). Moreover, from this donor's 163 total isolates (144 oral isolates and 19 fecal isolates), only this single isolate exhibited the hyper invasive phenotype into Spider agar at 37°C (Fig 3-11B); this phenotype was the motivation for initially including this strain in the condensed set.

Variant analysis identified 12 genes with unique SNVs in the 814–168 strain compared with the other 5 sequenced 814 strains, including a heterozygous adenine to thymine SNV in the

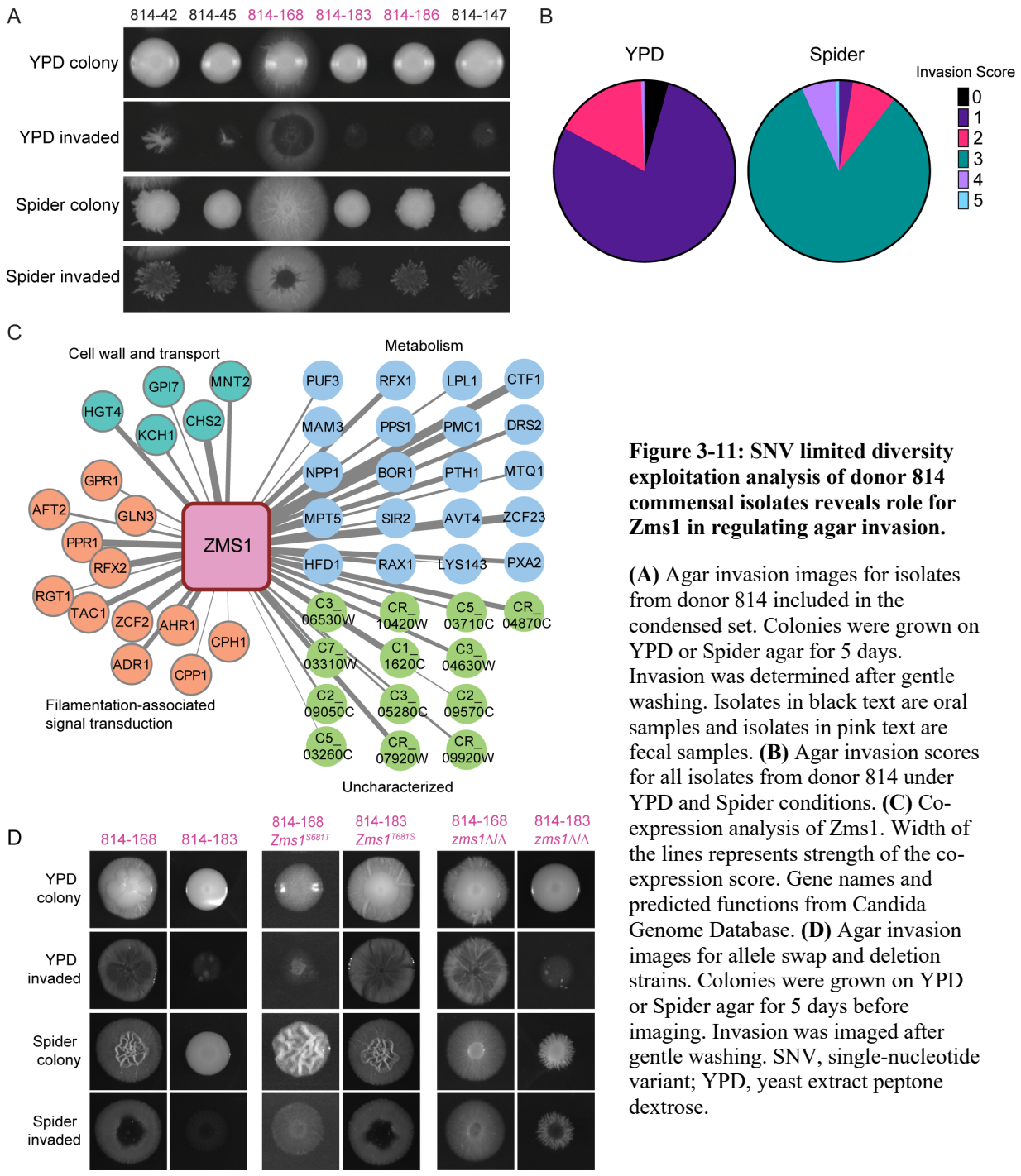


Figure 3-11: SNV limited diversity exploitation analysis of donor 814 commensal isolates reveals role for Zms1 in regulating agar invasion.

(A) Agar invasion images for isolates from donor 814 included in the condensed set. Colonies were grown on YPD or Spider agar for 5 days. Invasion was determined after gentle washing. Isolates in black text are oral samples and isolates in pink text are fecal samples. **(B)** Agar invasion scores for all isolates from donor 814 under YPD and Spider conditions. **(C)** Co-expression analysis of Zms1. Width of the lines represents strength of the co-expression score. Gene names and predicted functions from Candida Genome Database. **(D)** Agar invasion images for allele swap and deletion strains. Colonies were grown on YPD or Spider agar for 5 days before imaging. Invasion was imaged after gentle washing. SNV, single-nucleotide variant; YPD, yeast extract peptone dextrose.

transcription factor Zms1, resulting in a change in amino acid 681 from a threonine to a serine. Moreover, co-expression analysis[458] of ZMS1 revealed that it is highly correlated with genes involved in regulating the yeast-to-hyphal morphogenic transition (Fig 3-11C). To test whether this SNV can drive invasion, we generated complementation plasmids encoding each of the alleles from the 2 strain backgrounds and performed allele swap experiments between the high

and low invasion strains. In the minimally invasive 814–183 background, replacing 1 copy of the endogenous ZMS1 allele with the ZMS1-T681S allele was sufficient to drive hyper invasion into both YPD and Spider agar (Fig 3-11D). Similarly, replacing the invasive ZMS1 allele with the ZMS1-S681T allele was sufficient to reduce invasion into both YPD and Spider agar (Fig 3-11D).

Previous work on the function of Zms1 via deletion mutant analysis had not revealed a phenotype[226,456,457]; however, this was in the SC5314 genetic background and the impact of a specific transcription factor on a given phenotype can vary depending on the strain[226,459,460]. Therefore, we deleted *ZMS1* from both 814 backgrounds and tested the strains for invasion and filamentation. On YPD agar, as before, deletion of *ZMS1* in both genetic backgrounds had minimal effects, with the mutant strains behaving similarly to their parent strains (Fig 3-11D). However, on Spider agar, *ZMS1* deletion changed the colony morphology from wrinkly to smooth in the 814–168 background, although it did not decrease overall invasion. In contrast, deletion of *ZMS1* increased invasion in the otherwise minimally invasive 814–183 background, highlighting the differential impact of *ZMS1* mutation in the different genetic backgrounds (Fig 3-11D). Our results demonstrate that a single SNV changing amino acid 681 to a serine is a dominant negative allele that is sufficient to drive a hyphal invasion program into Spider agar. We also identified natural variation that was distinct from deletion phenotypes. This approach, which we have termed "limited diversity exploitation," highlights how deep phenotypic analysis of a limited set of natural isolates from a single host can be exploited to identify causative variants and identify new functions for under-characterized genes.

3.3.5 Virulence

We next examined the fitness and virulence of the commensal isolates relative to the SC5314 reference strain; we hypothesized that the commensal isolates would have decreased virulence compared to SC5314, a clinical isolate. To test this, we turned to the *Galleria mellonella* model of systemic infection as this insect model is significantly correlated with the murine systemic infection model[461]. We first examined competitive fitness by infecting with a 1:1 mixture of fluorescently marked SC5314 and each sequenced commensal isolate[459,460]. After 3 days, the worms were homogenized and CFUs were plated to determine the competitive index, calculated as the log2 ratio of fluorescent to nonfluorescent colonies[462,463]. When comparing the marked and unmarked SC5314 strains, we obtained a competitive index of 0, indicating that both strains are

equally fit and that the fluorescence does not impose a fitness cost. In contrast, most commensal strains had a competitive index > 2, suggesting that these strains have a competitive advantage over SC5314, even during systemic infection (Fig 3-12A). Notably, the 3 strains previously identified from Clade C, 882–60, 882–46, and 811–7, consistently demonstrated a competitive index of less than 0, indicating these strains are less fit than SC5314 in this model of infection. This is consistent with the aggregation exhibited by these strains in many growth conditions (Fig 3-7A).

The striking increased competitive fitness of the other isolates motivated us to test whether this increased ratio was correlated with increased disease. Here, we examined the

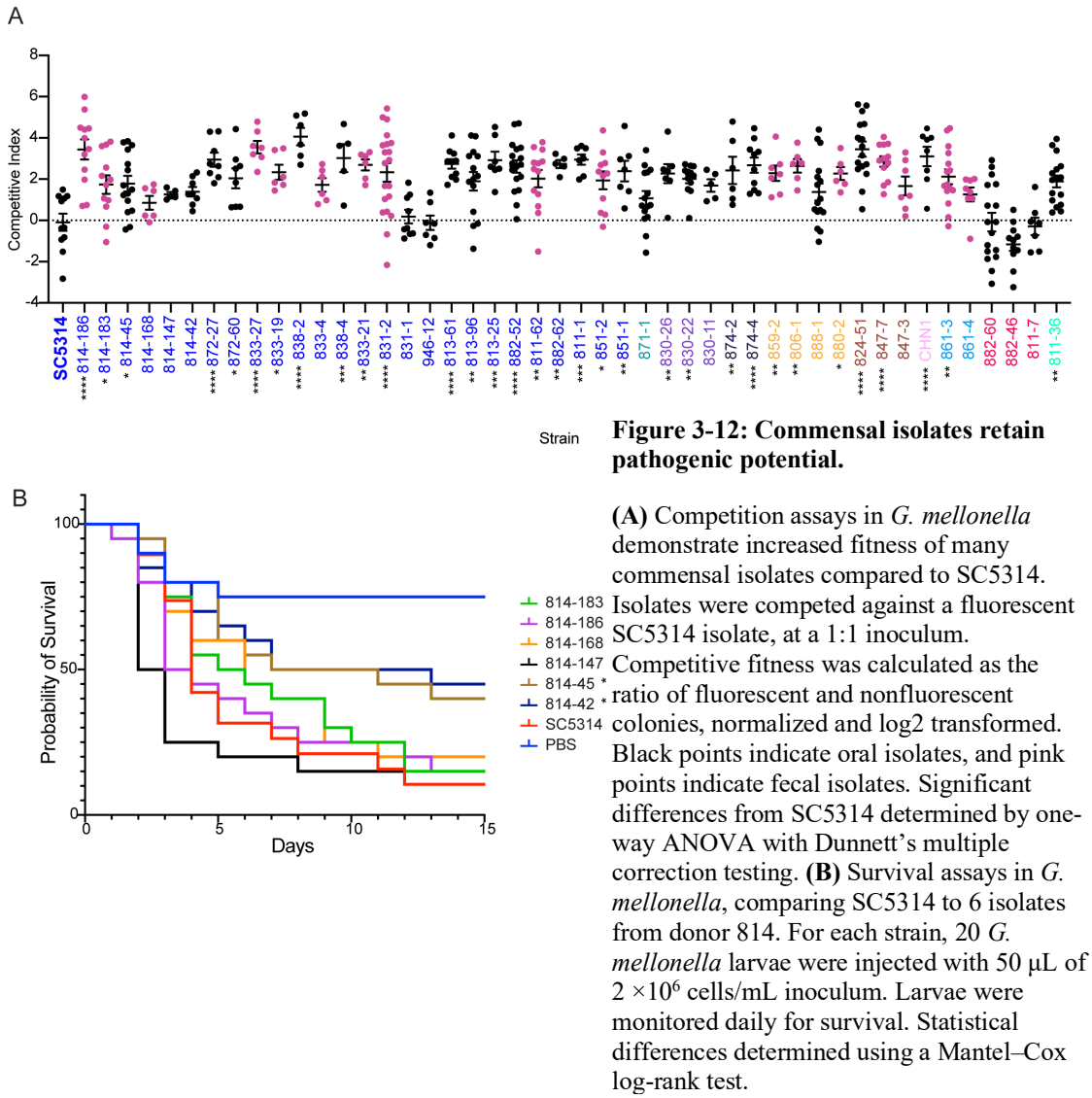


Figure 3-12: Commensal isolates retain pathogenic potential.

(A) Competition assays in *G. mellonella* demonstrate increased fitness of many commensal isolates compared to SC5314. Isolates were competed against a fluorescent SC5314 isolate, at a 1:1 inoculum. Competitive fitness was calculated as the ratio of fluorescent and nonfluorescent colonies, normalized and log2 transformed. Black points indicate oral isolates, and pink points indicate fecal isolates. Significant differences from SC5314 determined by one-way ANOVA with Dunnett's multiple correction testing. **(B)** Survival assays in *G. mellonella*, comparing SC5314 to 6 isolates from donor 814. For each strain, 20 *G. mellonella* larvae were injected with 50 µL of 2 $\times 10^6$ cells/mL inoculum. Larvae were monitored daily for survival. Statistical differences determined using a Mantel–Cox log-rank test.

survival of *G. mellonella* after performing monotypic infections. We started by using the 6

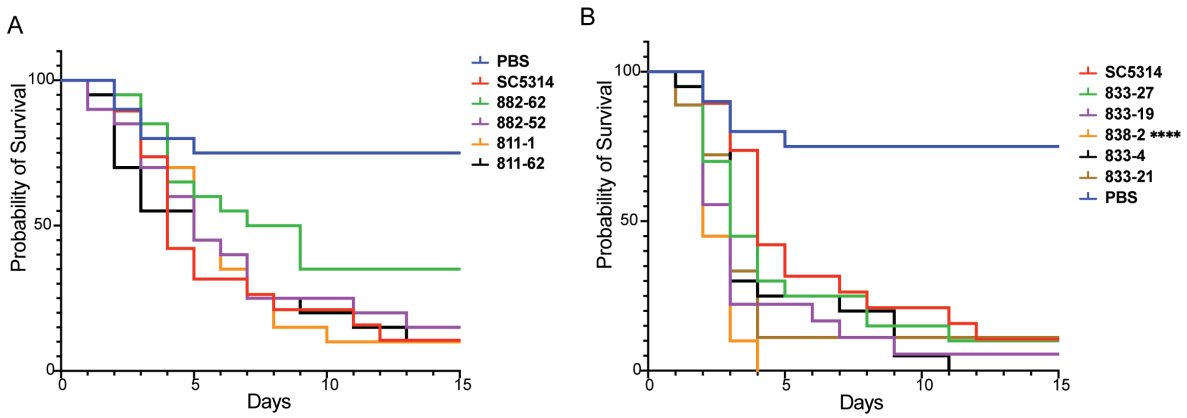


Figure 3-13: Virulence in *G. mellonella*.

(A) Survival assays in *G. mellonella*, comparing SC5314 to 4 isolates from donors 882 and 811. **(B)** Survival assays in *G. mellonella*, comparing SC5314 to 5 isolates from donors 833 and 838. For each strain, 20 *G. mellonella* larvae were injected with 50 µL of 2 $\times 10^6$ cells/mL inoculum. Larvae were monitored daily for survival. Statistical differences were determined using a Mantel–Cox log-rank test.

isolates from donor 814 to test the hypothesis that increased invasion is associated with increased disease. Three of the 6 isolates from 814 had increased competitive fitness compared to SC5314. However, the majority of the strains from donor 814 were not significantly different from the SC5314 reference strain ($p > 0.05$, log-rank test), including the hyper-invasive 814–168 isolate (Fig 3-12B). Isolates 814–42 and 814–45 had a slight defect in virulence ($p < 0.05$ log-rank test). We additionally tested 2 other clusters of strains for their ability to cause systemic disease in the insect model. However, the human commensal isolates were again not significantly decreased in virulence from the SC5314 reference strain (Fig 3-13), despite the increased ability of the SC5314 strain to cause host immune cell death (Fig 3-7C). Together, this suggests that there is not a consistent selection for avirulent behavior in the commensal human isolates in this model of systemic infection. Although we observed wide variation in in vitro host response phenotypes, the isolates generally retained their pathogenic potential, indicating that our in vitro assays may not capture the complex stresses experienced during whole-organism infections.

3.4 Conclusions

Intraspecies analyses of microbial strains can allow for the identification of variants that are associated with specific clinical outcomes, as demonstrated widely in bacterial virulence[464,465] and recently in the human fungal pathogen *Cryptococcus neoformans*[437,463]. Understanding the differences between strains can allow for insights into mechanisms of colonization and pathogenesis[440,466]. However, assessing the underlying genetic variation responsible for

differences in virulence in *C. albicans* is challenging in the absence of clear candidate genes because *C. albicans* is a primarily clonal yeast that does not generally undergo meiosis[466,467]. Additionally, the genetic basis underlying the ability of commensal strains of *C. albicans* to transition to pathogenic behavior is not well defined. Moreover, *C. albicans* exhibits high rates of structural mutation and ploidy variation[440,468] as well as high heterozygosity[431]. Previous descriptions of population genomic variation in *C. albicans* have largely relied on short-read sequencing[465,466] or molecular typing methods[467,468] at relatively few loci to define genetic variation in the species. Here, we have greatly expanded the number of available long-read genomes for *C. albicans* and have generated a catalog of structural variants that was largely absent from previous descriptions of natural diversity. We were able to leverage clonal variation within a single donor to identify variation within a host, potentially including variation that arose during colonization. Overall, we performed a systematic phenotypic analysis of commensal isolates from healthy donors, thus allowing us to examine *C. albicans* genotypic and phenotypic diversity.

Strikingly, we observed higher competitive fitness of the commensal strains during systemic competition assays, and when we tested 15 isolates for their ability to cause disease, we saw similar kinetics of mortality. This suggests that our commensal strains generally maintained their capacity to cause disease in our *Galleria* model of infection, despite SC5314 being able to cause more cell death in a macrophage model of infection for all but 7 commensal isolates. Importantly, other bloodstream isolates were also unable to cause host cell death. Additionally, our commensal strains were still able to filament in response to the inducing cues of 10% serum or high temperature, in contrast to work demonstrating that strains passaged through the mammalian gut resulted in a decrease in systemic virulence and defects during in vitro filamentation assays[438]. Potentially, the *Galleria* model does not recapitulate the disease process that would be caused by these isolates in a mammalian host. Although we observed significant variation in the ability of strains to invade into agar, recent intravital imaging approaches suggest that filamentation in response to serum matched that seen in vivo more than filamentation in response to solid Spider agar[469,470] although this may not recapitulate the environment seen in the gut. Potentially, the selective pressures that occur during mouse models of colonization may not recapitulate the selection that occurs during human colonization.

Although we were not able to associate a particular phenotype with increased systemic disease, we observed extensive phenotypic and genotypic variation between the commensal isolates. This variability is also consistent with recent work from clinical, disease-associated strains[458]. Moreover, our commensal strains were able to proliferate in a range of different environmental conditions, and we did not observe significant differences in phenotypes between isolates obtained from oral or fecal sites, except for a slight increase in invasion into Spider medium for oral samples. This work highlights the striking ability of *C. albicans* to adapt to a wide range of environmental conditions and indicates that colonization at a specific body site does not necessarily predict pathogenic potential.

Previous work has suggested that the *C. albicans* population within a given individual is clonal[80,236,461,471,472] and that the fungus is acquired during birth as a part of the normal microbiota[443]. In these studies, samples often came from patients with active disease; this may suggest that there is selection for the ability to cause disease, resulting in repeated isolation of representative samples of a clonal population. In contrast, we identified disparate individuals that appeared to be colonized by strains that were nearly identical, suggesting that there was some transmission between individuals. Whether these transmission events allow for long-term colonization, and how they affect the initial *C. albicans* colonizing strains, is still not fully understood. An important limitation of our study is that the undergraduate student donors were anonymous; therefore, we are unable to provide specific demographic information including age, sex, immune status, and recent antibiotic use that may allow us to expand our conclusions.

We also observed diversification within hosts, with multiple instances of closely related strains showing variation in phenotypes, such as invasion into agar. In one representative example, we were able to use comparative genome analysis coupled with co-expression, which we term “limited diversity exploitation,” to identify a candidate transcription factor that regulates invasion. Previous work on a *ZMS1* knockout strain of *C. albicans* did not show any differences in phenotype compared with the parent strain[471]. However, we observed that a single amino acid substitution in the predicted fungal transcription factor regulatory middle homology region was sufficient to drive hyper-invasive growth. Moreover, this phenotype was distinct from the deletion phenotypes in these 2 genetic backgrounds, again contrasting with the SC5314 reference strain. It is likely that populations of colonizing *C. albicans* will vary in other important clinically relevant traits, including filamentation in macrophages or intrinsic drug tolerance and

resistance, and our results suggest that studying more than a single representative isolate gives opportunities to discover new biology.

3.5 Methods

3.5.1 Human subjects and sample collection

Study volunteers were recruited through the Authentic Research Sections of the introductory biology laboratory course at the University of Michigan (BIO173). All participants provided written, informed consent for sample collection as well as isolation and characterization of microbes from feces. This study was approved by the Institutional Review Board of the University of Michigan Medical School (HUM00094242 and HUM00118951) and was conducted in compliance with the Helsinki Declaration.

Oral samples were obtained by self-administered cotton swabbing, and fecal samples were collected and diluted in PBS+DMSO before plating; in each case, BD ChromAgar was used to identify *C. albicans* colonies. Individual *C. albicans* colonies were picked from all plates with a toothpick into 100 μL of YPD in a 96-well plate. The cultures were then inoculated onto BD ChromAgar to differentiate between yeast species and ITS regions were amplified to confirm *C. albicans* strains. The *C. albicans* colonies were individually inoculated into fresh 96-well plate in YPD and after 24 h of incubation at 30°C, 50% glycerol was added to generate the stock plates. For each oral sample, individual *C. albicans* colonies were picked from the ChromAgar plates and incubated overnight in 100 μL of YPD in a 96-well plate. After 24 h incubation at 30°C, 50% glycerol was added to the 96 wells to generate the stock plates. All strains were maintained in −80°C cryoculture.

3.5.2 Reference strains

SC5314 reference strain was obtained from the gene replacement and conditional expression (GRACE) library[473]. CHN1 human isolate was obtained from the Huffnagle laboratory group[472].

3.5.3 Media and culture conditions

Media for growth curves is described in Table 3-1.

3.5.4 Growth curve analysis

Overnight cultures of each *C. albicans* isolate were grown in 200 μL of YPD in 96-well plates at 30°C, then subcultured into fresh media using a sterile pinner. Growth curves were performed on

a BioTek 800 TS Absorbance Reader in the indicated conditions for 24 h, without shaking. For the glycerol and galactose growth curves, the strains were incubated for 48 h due to the slower growth. Maximum growth rate and carrying capacity were determined using the GrowthcurveR analysis package[474]. A minimum of 2 biological replicates were performed per isolate per growth condition. All media are listed in Table 3-1.

3.5.5 Filamentation analysis

Overnight cultures of each *C. albicans* isolate were grown in 100 µL of YPD in 96-well plates at 30°C, then subcultured into 100 µL of YPD at either 30°C or 42°C for 3 h. After 3 h, the plates were imaged on an Olympus IX80 microscope at 20× magnification. To test the response to serum, overnight cultures were subcultured into 5 mL of YPD with 10% serum and rotated in a 37°C incubator for 3 h before vortexing and imaging on glass slides at 20× magnification.

3.5.6 Agar invasion analysis

Isolates were taken from frozen glycerol stocks, incubated overnight in yeast extract peptone dextrose (YPD) in 96-well plates and inoculated onto solid YPD and Spider media using a 96-pin replicator tool (Singer Instruments). Plates were then incubated at the indicated temperature and oxygen conditions for 5 to 7 days. Colonies on plates were first imaged on a Biorad Gel Doc XR. Colonies were then gently washed off with deionized water. Plates were imaged again to capture invasion images. The invasiveness of each isolate was determined through a rubric scale of 0 to 5, as indicated in Fig 3-1. A 0 indicates no invasion, 1 to 2 indicates minimal invasion, a 3 indicates distinct circular hyphal invasion, while a 4 indicates an even larger circular hyphal invasion. A 5 indicates the most aggressive invasion, with a “halo” of more hyphae surrounding the initial growth. A minimum of 3 biological replicates was performed for each isolate and the median score was determined.

3.5.7 High molecular weight genomic DNA extraction and sequencing

Genomic DNA was extracted from the 45 commensal isolates, SC5314, and CHN1. High molecular weight (> 20 kb fragment) genomic DNA was prepared using the Qiagen MagAttract HMW DNA Kit (Qiagen 67563), following the manufacturer’s protocol, with minor modification. Fungal cell walls were first digested using Zymolyase (Zymo E1005) before DNA extraction. TELL-seq[471] libraries were prepared at the University of Michigan Advanced

Genomics facility. Libraries were sequenced on an Illumina NovaSeq SP 300 cycle flow cell. All sequences are uploaded to NCBI SRA at PRJNA875200.

3.5.8 Sequence variation analysis

To identify SNVs across all published isolates of *C. albicans* and the newly sequenced commensal isolates, we mapped 435 read libraries to the SC5314 reference genome with BWA-MEM[234,329,447]. We used various samtools utilities to convert alignment files, remove PCRduplicates, and assign read groups[473]. Variants were called with GATK HaplotypeCaller and individual sample GVCFs were combined with GATK CombineGVCFs. Finally, we genotyped our combined GVCF across samples and loci with GATK GenotypeGVCFs[475]. GATK identified 851,355 total variable loci. Of the 741,027 diallelic loci, GATK identified 60,626 indel-derived alleles (8.18%) and 680,401 SNV alleles (91.82%). To refine our raw variant set to only include high-confidence SNVs, we removed low-quality variant calls at the (i) individual genotype call; (ii) whole locus; and (iii) whole sample levels. First, we removed individual sample genotype calls if their genotype quality (i.e., GQ) was < 0.99 (out of 1.0) or the results of the map quality rank sum test (i.e., MQRS) differed from 0.0 (i.e., the perfect score). Second, we removed all variant calls with more than 1 alternative allele (i.e., not diallelic), an alternate allele longer than 1 nucleotide (i.e., indels), or with > 5% missing genotype calls across samples. Finally, we removed entire samples from the combined VCF if their genotype calls across all loci were more than 90% missing, which resulted in the removal of 3 entire samples: SRR6669899, SRR6669970, and SRR1103579. Filtering our variant set in this way yielded a final set of 112,136 high-quality SNVs across 431 remaining samples. Of these, 90,675 (80.86%) were represented in at least 1 member of our set of newly sequenced strains. To remove redundancy and focus on natural *C. albicans* diversification, we removed additional samples corresponding to resequenced strains (e.g., multiple SC5314 samples present in full data set) and those sequenced as part of experimental evolution studies (i.e.,[474]). Following removal of these samples, we were left with 324 sample SNV profiles (280 published and 44 new genome strains). To generate an input matrix for distance calculation and NJ clustering, we coded genotypes as homozygous for the reference allele I, heterozygous (H), homozygous for the alternative allele (A), or missing (N). Raw distance between 2 sample genotypes at a particular locus (i.e, GT_i and GT_j) were calculated as 0.5 per alternative allele, with respect to the SC5314 reference such that D(H, A) = 0.5, D(R, A) = 1.0, etc. Missing genotypes (i.e., coded as N) were

ignored. Using these raw distances, we calculated the pairwise distance between all sample pairs across all 112,136 loci according to the generalized distance function for sampIe *i* and sampIe *j*.

$$D_{ij} = \frac{1}{nS - Ps - nN} \sum_{x=1}^{nSNPs} D(GT_{ix}, GT_{jx})$$

Where *nSNPs* is the total number of high-quality SNPs in our data set (i.e., 112,136), *nN* is the number of uncalled genotypes between each pair (i.e., coded as N), GT_{ix} is the genotype of sample *i* at locus *x*, and GT_{jx} is genotype of sample *j* at locus *x*. The resulting distance matrix was clustered with the *nj* function in phytools in R[476]. We visualized the resulting tree structure and associated data with ggtree in R[477–479].

3.5.9 Bootstrapping

One hundred bootstrap replicates were generated by randomly sampling rows from the SNP table with replacement to yield a table with the same dimensions as the original SNP table. Distance matrices and neighboring-joining trees were generated for bootstrap replicates identically to the original SNP table. Bootstrap support values were computed based on the bootstrap replicate trees and annotated onto the original SNP tree with IQTree2.

3.5.10 Structural variant analysis from TELL-seq

To identify structural variation genome wide in the condensed set of *C. albicans* isolates, we mapped the read libraries to the SC5314 reference genome with BWA-MEM[477]. We visualized the read depth across the genome by breaking the reference genome into 500 bp bins. Each read was assigned to a single bin based on the first coordinate in the reference genome to which the read aligned. The read counts were normalized across the samples by the average read coverage for each sample. The value for each bin ($v_{b,s}$) for each sample was calculated using the following formula:

$$v_{b,s} = \frac{bin\ read\ count * read\ length}{bin\ size * sample\ coverage}$$

Additionally, we performed structural variant calling using lumpy-sv[480] and genotyping with svtyper[481] using smoove (version 0.2.5). We visualized the variant calls by breaking the reference genome into 500 bp bins and identified the number of variant calls of a give type that overlapped with each bin.

To identify potential translocations from the TELL-seq data, we used the Tell-Link pipeline to assemble the read libraries into contigs and aligned the assembled contigs to the

SC5314 reference genome using MiniMap2[482]. We identified candidate junctions where consecutive aligned segments longer than 10,000 bp on the same contig aligned to different chromosomes. To experimentally validate the predicted junctions, we designed primers from uniquely mapped contig segments on either side of the junction, i.e., one from each of the 2 chromosomes predicted to be joined together. Primers were selected from the 500 bp directly upstream and downstream from the predicted junction location unless the junction was directly flanked by non-uniquely mapping segments in which case, the 500 bp of the closest uniquely mapping segments were used. Oligonucleotides are in Table 3-3.

3.5.11 CHEF gel electrophoresis

Agarose plugs for CHEF gel electrophoresis were prepared as in Selmecki 2005[482]. Electrophoresis was performed as in Chibana[483], with minor modifications to improve chromosome separation. Plugs were run on 0.9% megabase agarose (Biorad 1613108), with run conditions of 60 to 300 s, 4.5 V/cm, 120 angle for 36 h, followed by 720 to 900 s, 2.0 V/cm, 106 for 24 h. Sizes were determined based on approximations from Selmecki and a CHEF DNASize Marker, 0.2–2.2 Mb, *S. cerevisiae* Ladder (Biorad 1703605).

3.5.12 Biofilm formation

Biofilm formation was assessed as previously described[477] Briefly, overnights of *C. albicans* isolates were incubated and diluted to 0.5 OD_{600}. In a 96-well plate, isolates were added to 200 µL of RPMI media, covered with a Breathe-Easy film, and incubated at 37°C shaking at 250 rpm. After 90 min, RPMI media was removed and wells were washed once with 200 µL of 1× PBS and 200 µL of fresh RPMI media was added. Plates were covered in a Breathe-Easy film and left to incubate at 37°C with shaking at 250 rpm for 24 h before a final read on the plate reader at OD_{600}.

3.5.13 Mammalian cell culture

J2-iBMDM cells were isolated from the bone marrows of C57BL/6J mice and differentiated in BMDM medium (50% DMEM, 2 mM l-glutamine, 1 mM sodium pyruvate, 30% L929-conditioned medium, 20% heat-inactivated fetal bovine serum [FBS; Invitrogen], 55 µM 2-mercaptoethanol, and Pen/Strep), then immortalized using Cre-J2 viral supernatants.

3.5.14 Phagocytosis

Phagocytosis assays were performed as previously described[479]. Briefly, iBMDM macrophages were prepared for infection in RPMI media containing 3% FBS, diluted to 3× 10^6 cells/ mL and incubated overnight at 100 µL/well in a 96-well plate. Overnight cultures of *C. albicans* isolates were incubated and diluted to 4× 10^6 cells/mL into RPMI media with 3% FBS and used to infect macrophages. Inoculated plates were centrifuged for 1 min at 1,000 rpm to synchronize. After 30 min, media was removed, and cells were fixed with 4% paraformaldehyde (PFA) for 10 min. The cells were washed 3 times in 1× PBS. Cells were then stained with 50 µL of FITC-Concanavalin (5 µg/mL Sigma-Aldrich C7642) at room temperature, rocking for 30 min, wrapped in foil. The plates were then washed 3× with 100 µL of 1× PBS, and then 50 µL of 0.05% Triton-X100 was added to permeabilize the cells. Cells were then washed 3× with 1× PBS and a final stain of 50 µL of calcofluor white (100 µg/mL, Sigma-Aldrich C7642) was added to cells to incubate for 10 min. The cells were then washed 3× with 100 µL of 1× PBS and then maintained in 100 µL of 1× PBS at 4°C before imaging on the microscope at 20× magnification using the DIC, FITC, and DAPI channels. Images were analyzed with a CellProfiler pipeline to determine the percentage of internalized *Candida*. The total number of *Candida* was determined through calcofluor white staining. Next, the number of external *Candida* was determined through FITC-ConA staining. (1 –external cells)/total cells = % of internalized *Candida*.

3.5.15 Macrophage filamentation assay

To assess filamentation of isolates in macrophages, iBMDM macrophages were prepared for infection in RPMI media containing 3% FBS, diluted to 3× 10^6 cells/mL and incubated overnight at 100 µL/well in a 96-well plate. Overnights of *C. albicans* isolates were incubated and diluted to 4× 10^6 cells/mL into RPMI media with 3% FBS and used to infect macrophages at an MOI of approximately 1:1. The inoculated plate was centrifuged for 1 min at 1,000 rpm to synchronize phagocytosis. After 2 h, the media was removed, and cells were fixed with 4% PFA for 10 min, permeabilized with 0.05% Triton-X100, and stained with 50 µL of calcofluor white (100 ug/mL, Sigma-Aldrich C7642) before imaging at 40× magnification using the DIC and DAPI channels. The extent of filamentation for each isolate was scored on a rubric from 0 to 5. A score of 0 indicates an isolate that exhibited only yeast morphology with no filamentation during macrophage infection. A score of 1 indicates an isolate that remains primarily in the yeast form, with some hyphae or pseudohyphae, while a score of 2 indicates an isolate that remains primarily

in the yeast form, with more hyphae and pseudohyphae present than a score of 1. A score of 3 indicates an isolate that had approximately equal numbers of yeast and true hyphae. A score of 4 indicates an isolate with more true hyphae than yeast during infection, and a score of 5 indicates an isolate in which the majority of cells formed hyphae with very few yeast remaining. A minimum of 3 biological replicates was performed for each isolate and the median score was determined.

3.5.16 Cell death assay

To assess macrophage cell death, J2-iBMDM macrophages were prepared for infection in RPMI media containing 3% FBS, diluted to 4×10^5 cells/mL and incubated overnight at 100 µL/well in a 96-well plate. Macrophages were primed with 200 ng/mL LPS in RPMI media with 3% FBS for 2 h. Overnights of *C. albicans* isolates were incubated and diluted to 5×10^5 cells/mL into RPMI media with 3% FBS and used to infect macrophages at an MOI of approximately 1:1. The plate was centrifuged for 1 min at 1,000 rpm to synchronize phagocytosis. After 4 h, the media was removed and cells were stained with Hoechst (20 µM, Cayman Chemical 33342) to mark nuclei and propidium iodide (1 µg/mL, Acros Organics 440300250) to mark cell death. Plates were then imaged on an Cellomics ArrayScanVTI Objective Module at 20× with at least 5 images taken per well. Images were analyzed with a CellProfiler pipeline (available by request) to determine the percent of dead macrophages. Macrophages were identified through Hoescht nuclear staining to determine the total number of cells in each field of view. Next, cell death events were determined based on propidium iodide staining. (# of propidium iodide events)/(# of total cells) = % of dead macrophages.

3.5.17 ZMS1 strain construction

To make the *ZMS1* allele swap strains, we used the NEBuilder HiFi assembly kit to clone the endogenous *ZMS1S681T* allele from the 814–183 strain background and the *ZMS1T681S* allele from the 814–168 strain background into the pUC19 cloning vector, along with the nourseothricin resistance cassette, to generate plasmids pTO274 and pTO192. *ZMS1* and 500 bp of putative terminator was amplified using oTO771+oTO734. NAT was amplified using oTO18+ oTO735. pUC19 was amplified using oTO590 + oTO591. The plasmids were Sanger sequenced to confirm the presence of the specific ZMS1 allele and the absence of additional mutations using oTO736. These plasmids were transformed into the 814–168 and 814–183 strain

backgrounds using a transient CRISPR approach[484]. NAT-resistant transformants were tested for the presence of specific *ZMS1* alleles by Sanger sequencing using oTO736. To generate the deletion strains, the *ZMS1::NAT* cassette was amplified from the NAT flipper plasmid [483] using primers oTO1215 and oTO1216, and transformed into the 814–168 and 814–183 strain backgrounds using a transient CRISPR approach[484]. Integration was tested using oTO5 and oTO1218 and loss of the wild-type *ZMS1* gene was tested using oTO736 and oTO1218. Plasmids used in this study are listed in Table 3-2 and oligonucleotides are listed in Table 3-3.

3.5.18 *Galleria mellonella* infections

Each isolate was examined for competitive fitness in a one-to-one ratio with a fluorescent wild-type SC5314 *C. albicans* strain in *G. mellonella* larvae. Infections were performed as previously described[485]. Briefly, *G. mellonella* larvae were purchased from speedyworm.com and maintained in sawdust at room temperature. Overnights were prepared for each isolate and wild-type strain in YPD at 30°C, with rotation. To measure competitive fitness, a 1:1 ratio of fluorescent wild type to unlabeled isolate was prepared in 1× PBS at 5×10^5 cells/mL. 10 larvae/strain were randomly chosen and infected via the last right proleg with 50 µL of the 1:1 inoculum using an exel veterinary U-40 diabetic syringe (0.5CC × 29G × ½). After injection, larvae were maintained at room temperature for 3 days before harvesting using a Benchmark D1000 homogenizer. Larvae were homogenized in 0.5 mL of 1× PBS, diluted 1:10 in PBS, and plated onto YPD plates containing gentamicin, ampicillin, and ciprofloxacin. Plates were left at 30°C for 48 h before imaging on a Typhoon FLA 9500 biomolecular Imager. The ratio of fluorescent to unmarked strains was compared with the inoculum to determine competitive index. To measure virulence, 20 *G. mellonella* larvae/strain were infected with 50 µL of 2×10^6 cells/mL inoculum using an exel veterinary U-40 diabetic syringe (0.5CC × 29G × ½). After injection, larvae were maintained at room temperature and monitored daily for survival. Virulence was analyzed using Kaplan–Meier survival curves in GraphPad Prism (version 9).

Media	Recipe
YPD	Yeast extract (BD), peptone (BD), 2% dextrose (Fisher
Butyrate 60 mM	YPD + 60 mM butyrate (Fisher Scientific)
Caffeine 6.25 mM	YPD + 6.25 mM caffeine (Millipore Sigma
Calcofluor White 10X	CFW 20 uM in YPD
Calcofluor White 1X	CFW 2uM in YPD
$CuSO_4$ 10 mM	10 mM $CuSO_4$ in YPD
Farnesol 30 mM	30 mM farnesol in YPD
Fluconazole 2 ng/mL	2 ng/mL fluconazole in YPD
Itaconic 100 mM	100 mM itaconic acid in YPD
LiCl 125 mM	125 mM LiCl in YPD
YNB Lactate	2% lactate in YNB
YNB Dextrose Lactate	2% lactate + 2% dextrose in YNB
pH2	YPD + added HEPES (1.785 g) titrated appropriately with HCl & OH
pH4	YPD + added HEPES (1.785 g) titrated appropriately with HCl & OH
pH8	YPD + added HEPES (1.785 g) titrated appropriately with HCl & OH
Rapamycin 23 nM	23 nM rapamycin (Cayman Chemical) in YPD
Rapamycin 35 nM	25 nM rapamycin (Cayman Chemical) in YPD
RPMI	RPMI-1640 Medium, catalog #R6504-1L
Synthetic Complete (SC) media	YNB 6.7 g/L + all amino acids + 2% glucose
SC + 5 uM CRAMP	SC media + 5 uM CRAMP (Anaspec)
SC + 10 uM CRAMP	SC media + 10 uM CRAMP (Anaspec)
Synthetic Defined (SD) media	1.71 YNB no ammonium sulfate (BD) + 5g ammonium sulfate + 20 g dextrose
SD-Cu-Fe	YNB-$CuSO_4$-$FeCl_3$ (Sunrise science products)
SD-Cu-Fe Itaconic	100 mM itaconic acid in YNB-$CuSO_4$-$FeCl_3$
SD-Fe	YNB-$CuSO_4$-$FeCl_3$ with $CuSO_4$
SD Itaconic	100 mM itaconic acid in YNB
SDS	0.05% SDS in YPD
Sorbitol	1M sorbitol in YPD
Vaginal Secretion Media (VSM)	58 mM NaCl, 18 mM KOH, 2 mM $Ca(OH)_2$, 1.75 mM glycerol, 6.7 mM urea, 33 mM glucose in YNB, buffered to pH 2
YP Acetate	2% acetate (10g in 50 mL of sterile water) added to 450 mL of YP broth

YP Galactose	2% galactose (10g in 50 mL of sterile water) added to 450 mL of YP broth
YP Glycerol	2% acetate (20 mL of 50% glycerol)) added to 450 mL of YP broth
YP Maltose	2% maltose (10g in 50 mL of sterile water) added to 450 mL of YP broth
YNB adenine	YNB + adenine
YNB arginine	YNB + arginine
YNB aspartic acid	YNB + aspartic acid
YNB histidine	YNB + histidine
YNB isoleucine	YNB + isoleucine
YNB leucine	YNB + leucine
YNB lysine	YNB + lysine
YNB methionine	YNB + methionine
YNB phenylalanine	YNB + phenylalanine
YNB threonine	YNB + threonine
YNB tryptophan	YNB + tryptophan
YNB tyrosine	YNB + tyrosine
YNB uridine	YNB + uridine
YNB valine	YNB + valine

Table 3-1: Growth media used in this chapter.

Name	Description	Source
pUC19	*ampR*	[486]
pLC49	*FLP-NAT, natR, ampR*	[320]
pLC963	*CaCas9, sgRNA, ampR*	[171,487–490]
pTO192	*ZMS1-T681S, natR, ampR*	This study
pTO274	*ZMS1-S681T, natR, ampR*	This study

Table 3-2: Plasmids used in this chapter.

Name	Sequence	Use
oTO771	GAATTCGAGCTCGGTACCgATGAATAT GCAACCATCAG	Generation of pTO192 and pTO274
oTO734	catggtcatagctgtttcctgCGAATATTGGATTTTATTGATTG	
oTO735	GTCGACTCTAGAGGATCCCgtaaaacgacggccag	
oTO18	CAGGAAACAGCTATGAC	
oTO590	ggatcctctagagtcgac	
oTO591	ggtaccgagctcgaattc	
oTO1215	TTTCCTCCCCATATTGAAACCATATTCAAGA CATTTACAGggaaacagctatgaccatg	Amplification of NAT cassette
oTO1216	ATATCATCATAAAGCATTCTATAAGCTTGGTCAT TCAATCCCAAgtaaaacgacggccag	
oTO6	gactgtcaaggagggtattc	Amplification of guide RNA
oTO7	CCGCaagtgattagacttag	
oTO8	gaataccacttgtttaccgg	
oTO9	GGTGGCGGCAAAACTAATTC	
oTO1213	gacttgcgtaaactatttttaatttgTCAGTTTCAGTAAACTCACC	
oTO1214	cttgctatttctagctctaaaacGGTGAGTTTACTGAAACTGA	
oTO1218	TTCTGGTAATGCTGATGGTG	Check for NAT integration
oTO736	TGCTATTGGTGCATTGTATG	Check for NAT integration & loss of gene; validate specific ZMS1 allele
oTO5	CAGCACCTCTTTCTCTGG	Check for loss of gene
oTO1184	CGTTTGTGTCAGGGAAATAC	Validate Chr3-4 fusion in 880-2
oTO1186	TCCGCCTTTTCTACTCACCC	
oTO1193	GGAAATAATCTCAATGTCGC	Validate Chr3-2 fusion in 859-2
oTO1195	CAAACTCTACTAACAAAGCC	
oTO1204	AACCACTGTCCCACCATACG	Validate Chr2-1 fusion in 859-2
oTO1207	TAAGAAGTCGGAATAGTAGC	

Table 3-3: Oligonucleotides used in this chapter.

Chapter 4 *Candida* albicans Remodels its Cell Wall in Response to Bacteria, Impacting Immune Recognition and Antifungal Sensitivity

Jing Liang from the Michigan Medicine Microscopy Core assisted with transmission electron microscopy sample preparation. Jaidyn Bryant and Shannon Esher Righi assisted with the HEK-Blue reporter cell assay. Kyla Ost assisted with IgA binding assay, germ-free mouse colonization, and staining of intestinal contents. Kalpana Singh and Tuo Wang assisted with solid-state NMR analysis. Joseph Krampen and Marcy Balunas assisted with bioassay-guided fractionation.

4.1 Abstract

The fungus *Candida albicans* commensally colonizes mucosal surfaces in healthy individuals but can cause both superficial mucosal and life-threatening disseminated infections. The balance between commensalism and pathogenicity is complex and depends on host and fungal genetic background, the host environment, and fungal interactions with local microbes. The major interaction interface of *C. albicans* with the host is its multilayered cell wall, which is dynamic and highly responsive to the surrounding environment. Therefore, factors that influence the fungal cell wall will directly impact *C. albicans*-host interactions. Here, we demonstrate that multiple physiologically relevant gastrointestinal bacteria influence fungal cell wall composition during co-culture with *C. albicans.* Using *Escherichia coli* as a model, we determined that bacterial-induced fungal cell wall remodeling occurs rapidly and is mediated by a secreted bacterial metabolite. Fungal mutant analysis revealed that the high osmolarity glycerol (HOG) pathway, which is critical for responding to environmental stresses, has an important role in regulating this cell wall remodeling phenotype. Importantly, bacterial-mediated fungal cell wall remodeling alters *C. albicans* susceptibility to antifungals and both innate and adaptive immune responses. Furthermore, we observed that *E. coli* influences the fungal cell wall composition *in vivo*. Overall, this work comprehensively characterizes an interaction between *C. albicans* and

common gastrointestinal bacteria, with important implications for fungal biology and host interactions.

4.2 Introduction

Candida albicans can exist as a commensal member of the mucosal microbiota, but also has the capacity to cause a range of disease, from superficial mucosal infections to life-threatening disseminated infections[132,491]. The balance between commensalism and pathogenicity is complex and multifactorial, depending on the genetic backgrounds of both host and fungus, host immune status, and fungal interactions with the local microbiota[88,491]. *C. albicans* is highly adaptable to different host micro-environments and responds to changing environmental conditions by making a morphological transition, altering its metabolism, or remodeling its multilayered cell wall[88,492].

As the main interface between *C. albicans* and the surrounding environment, the fungal cell wall is critical for providing structural integrity, sensing and responding to environmental stress, and mediating interactions between the fungus and host cells. Due to this crucial role, the fungal cell wall is highly responsive to changes in environmental conditions, including nutrient source, oxygen content, metal availability, pH, and temperature[96–98,134–136,492]. Such changes induce fungal cell wall remodeling, which has downstream consequences on antifungal sensitivity, tolerance to stress, and importantly, recognition by host immune cells. The inner layer of the fungal cell wall is composed of chitin and β-glucan that provide structure, while the outer cell wall layer is made up of branching mannan fibrils that are covalently linked to cell wall proteins[491,492]. β-1,3-glucan is the major immunostimulatory ligand that is recognized by the C-type lectin receptor (CLR), Dectin-1, to mediate recognition and phagocytosis by innate immune cells[88,493]. To evade immune detection, *C. albicans* reduces cell surface exposure of β-1,3-glucan by using the outer mannan layer as a physical shield or by deploying glucanases to shave off exposed β-1,3-glucan[493,494]. It is critical to understand the diverse environmental signals that trigger fungal cell wall remodeling, due to the important downstream implications for immune recognition, antifungal resistance, stress responses, and overall fungal virulence.

Bacteria have profound impacts on fungal biology, colonization, and virulence, both *in vitro* and *in vivo*. Several studies have identified fungal-bacterial interactions that influence *C. albicans* biology by inhibiting filamentation, inhibiting growth, or directly killing fungal cells[23,27,143,171,172,199,339,343,494,495]. Experimental evolution of *C. albicans* SC5314 through the

murine gastrointestinal tract consistently produced yeast-locked strains with higher competitive fitness and decreased virulence, but this outcome only occurred in mice maintained on antibiotics[149,496,497]. Furthermore, *C. albicans* exists primarily in the yeast form during gastrointestinal colonization of germ-free mice, but displays a mixture of yeast and hyphal morphologies during colonization of conventionally raised, antibiotic-treated mice[494,495]. In contrast, human commensal *C. albicans* isolates retain the capacity to filament and cause disease[416]. Therefore, the human gastrointestinal tract does not consistently select for yeast-locked and avirulent isolates, implying that an intact microbiota is important for applying selective pressure on *C. albicans*.

Despite the rich body of literature investigating fungal-bacterial interactions, the interplay between bacteria and the fungal cell wall has only recently begun to be explored. *Bacteroides* species, which are abundant in the human gut, are experts at glycan degradation, and recent work has shown that some members of this genus can degrade purified fungal cell wall components, including mannan and β-1,6-glucan[143,498]. However, it is unclear if these bacteria can digest fungal glycans directly from the fungal cell wall and how this would impact fungal biology. Recent work has shown evidence that co-incubation with live bacteria or bacterial supernatants can change fungal cell wall composition, although the exact mechanistic details and consequences on other aspects of fungal biology have not been determined[149,499,500].

Our work seeks to comprehensively characterize how bacteria influence fungal cell wall composition and define the downstream implications of this co-colonization on the host. We demonstrate that bacterial species have varying abilities to induce fungal cell wall remodeling, and *E. coli* has the most significant impact on *C. albicans* cell wall composition. A secreted bacterial metabolite is responsible for inducing the remodeling phenotype, and a central stress pathway in *C. albicans* is required for the full remodeling response. Critically, we observed that bacterial-mediated fungal cell wall remodeling alters antifungal susceptibility to caspofungin and both innate and adaptive immune responses to *C. albicans*. These results underscore the importance of investigating fungal-bacterial interactions and how they may alter fungal virulence and disease outcomes.

4.3 Results

4.3.1 *Candida albicans* undergoes global cell wall remodeling during co-culture with *Escherichia coli*

To investigate the impact of common gastrointestinal-colonizing bacteria on the *Candida albicans* cell wall, we first developed an *in vitro* co-culture model that would allow for microscopic analysis of the fungal cell wall. We grew *C. albicans* (SC5314) for 24 hours in rich media, Yeast Peptone Dextrose (YPD), in monoculture or co-culture with *Escherichia coli* (MC1061). The standard growth conditions for *C. albicans*, YPD media at 30°C, also allows for growth of *E. coli* (Fig 4-1). Although we observed a decrease in *C. albicans* growth rate during co-culture with *E. coli*, fungal cells remained viable following 24 hours of co-culture, based on propidium iodide staining (Fig 4-2).

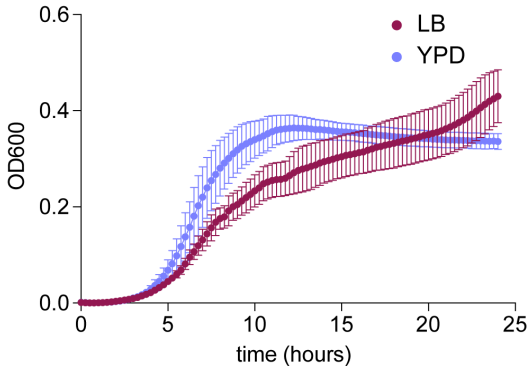


Figure 4-1:*E. coli* grows under co-culture conditions.

Growth curves of *E. coli* grown in LB or YPD for 24 hours at 30°C.

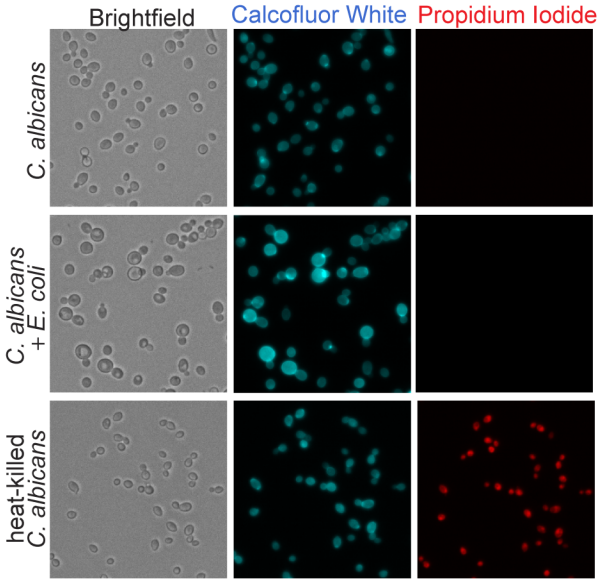


Figure 4-2: *C. albicans* cells are viable after 24 hours of co-culture with *E. coli*.

Brightfield and fluorescent microscopy of *C. albicans* alone (top), *C. albicans* + *E. coli* (middle), or heat-killed *C. albicans* (bottom). Cells were stained with calcofluor white to mark total cells and propidium iodide to mark dead cells. 40x magnification.

After establishing our co-culture protocol, we turned to Transmission Electron Microscopy (TEM) as a method to visualize changes in the overall cell wall architecture following co-culture with *E. coli.* We collected fungal cells after 24 hours of co-culture and used TEM after pressure freezing-freeze substitution to preserve ultra-fine structures. We found that mannan fibrils were significantly longer when *C. albicans* was grown with *E. coli* (Fig 4-3A-B). This TEM preparation did not consistently preserve the integrity of the inner cell wall layer, precluding our ability to measure its thickness (Fig 4-4). Therefore, we used a combination of fluorescent microscopy and flow cytometry to visualize and quantify components of both the

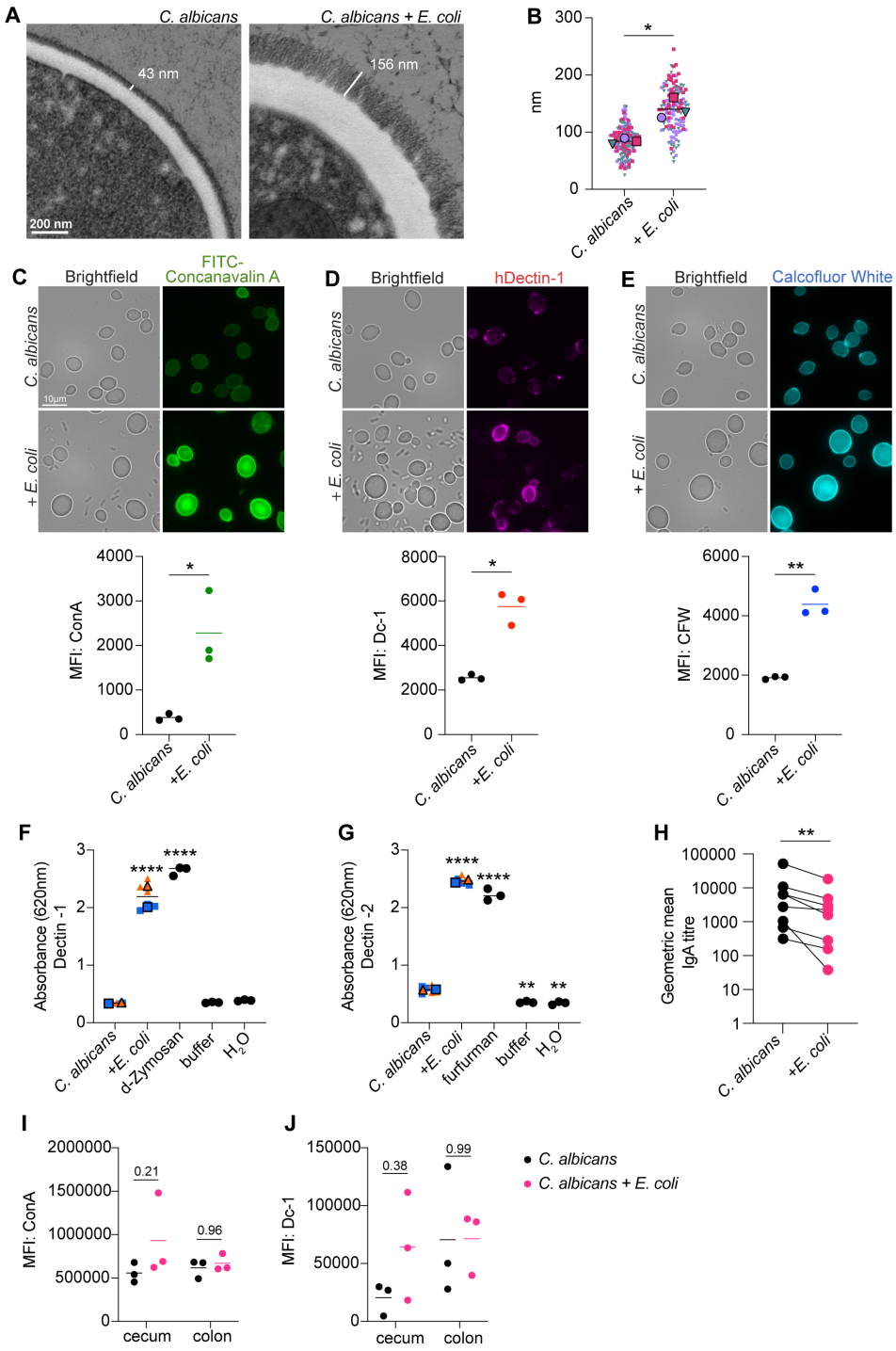


Figure 4-3: *Candida albicans* undergoes cell wall remodeling during co-culture with *Escherichia coli* with an impact on immune recognition.

(A) Representative transmission electron micrographs (TEMs) of *C. albicans* grown for 24 hours in monoculture (left) or co-culture with *E. coli* (right). White bars mark the outer mannan layer. 10,000x magnification. **(B)** Quantification of mannan fibril length from TEMs across 3 biological replicates. Large, outlined symbols represent the average of each biological replicate while the smaller symbols represent technical replicates. Significance determined by paired t-test on biological replicates.

inner and outer cell wall. We stained cells with FITC-Concanavalin A (ConA) for mannan (Fig 4-3C), hDectin-1a for exposed β-1,3-glucan (Fig 4-3D), and Calcofluor White (CFW) for chitin (Fig 4-3E). Fluorescence microscopy and flow cytometric quantification corroborated the TEM data and indicated that *C. albicans* co-cultured with *E. coli* had increased levels of cell wall mannan (Fig 4-3C). The co-cultured cells were visibility brighter by fluorescence microscopy (Fig 4-3C). *C. albicans* co-cultured with *E. coli* had overall more β-1,3-glucan exposure

(**C, D, E)** Determination of *C. albicans* cell wall mannan **(C)**, exposed β-1,3-glucan **(D)**, and chitin **(E)** following 24-hour co-culture with *E. coli*. Representative brightfield and fluorescent microscopy images (top). 100x magnification. Flow cytometric quantification of cell wall component (bottom). Cell wall mannan stained with FITC-Concanavalin A (ConA), exposed β-1,3-glucan stained with hDectin-1a and anti-IgG antibody conjugated with Alexa Fluor 647 (Dc-1), chitin stained with Calcofluor White (CFW). Gating strategy is illustrated in SFig 4A. Significance determined by paired t-test. MFI = mean fluorescence intensity. (**F, G)** Engagement of Dectin-1 **(F)** or Dectin-2 **(G)** with *C. albicans* grown in monoculture or co-culture with *E. coli*. D-Zymosan and furfurman represent positive controls for each receptor. Large, outlined symbols represent the average of each biological replicate while the smaller symbols represent technical replicates. Significance determined by one-way ANOVA with Dunnett's multiple comparison test. (**H)** Human fecal IgA binding to *C. albicans* grown in monoculture or co-culture with *E. coli.* Significance determined by Wilcoxon test. (**I, J)** Flow cytometric quantification of cell wall mannan **(I)** or exposed β-1,3-glucan **(J)** from the colon or cecum of germ-free mice colonized with *C. albicans* or *C. albicans* and *E. coli*.

than monocultured *C. albicans,* although we saw heterogeneity in this phenotype, as evident by the wide histogram and fluorescent microscopy (Fig 4-3D). Cell wall chitin content was also increased in the co-culture condition (Fig 4-3E). Notably, during co-culture with *E. coli*, some *C. albicans* cells appeared larger and more uniformly round, and this increased cell size was apparent when comparing forward scatter of monocultured and co-cultured cells (Fig 4-5B). In staining for cell wall chitin, we noted a trend that the larger *C. albicans* cells in the co-culture condition were brighter than the smaller cells. We investigated the relationship between cell size and cell wall contents and found a positive relationship between cell size and cell wall chitin content in monocultured and co-cultured cells (Fig 4-6C). We did not observe a relationship between cell size and cell wall mannan or β-1,3-glucan exposure (Fig4-6A-B). Monocultured *C. albicans* cells exhibited increased chitin and β-1,3-glucan exposure primarily at bud scars, which has been previously reported[501,502]. Overall, our combination of TEM, fluorescence microscopy,

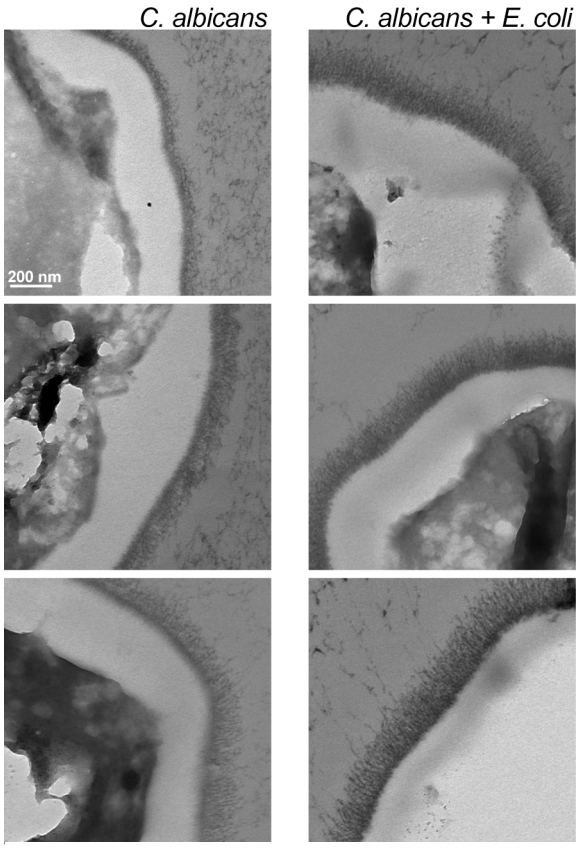


Figure 4-4 ：TEM preparation did not preserve the inner fungal cell wall.

Representative transmission electron micrographs depicting distorted inner cell walls of *C. albicans* grown alone (left) or in co-culture with *E. coli* (right).

and flow cytometry indicate that during co-culture with *E. coli* under rich media conditions, *C. albicans* undergoes cell wall remodeling, resulting in increased levels of cell wall mannan, chitin, and β-1-3-glucan exposure.

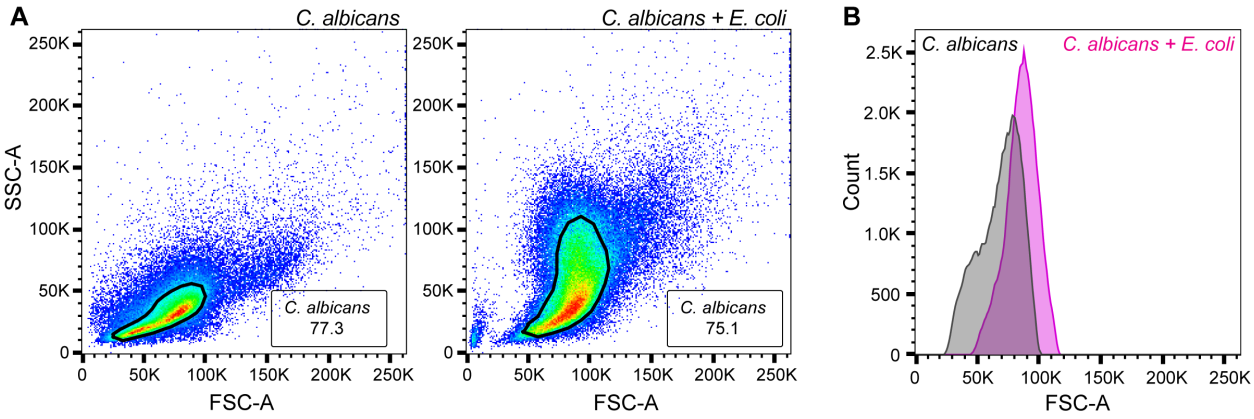


Figure 4-5: Flow cytometry gating strategy and comparison of cell size.

(A) Fungal cells were gated based on forward and side scatter to capture only fungal cells. Similar gating was performed on *C. albicans* in monoculture (left) or in co-culture with *E. coli* (right). **(B)** Forward scatter histogram depicting differences in cell size when *C. albicans* is grown in monoculture (grey) or in co-culture with *E. coli* (pink).

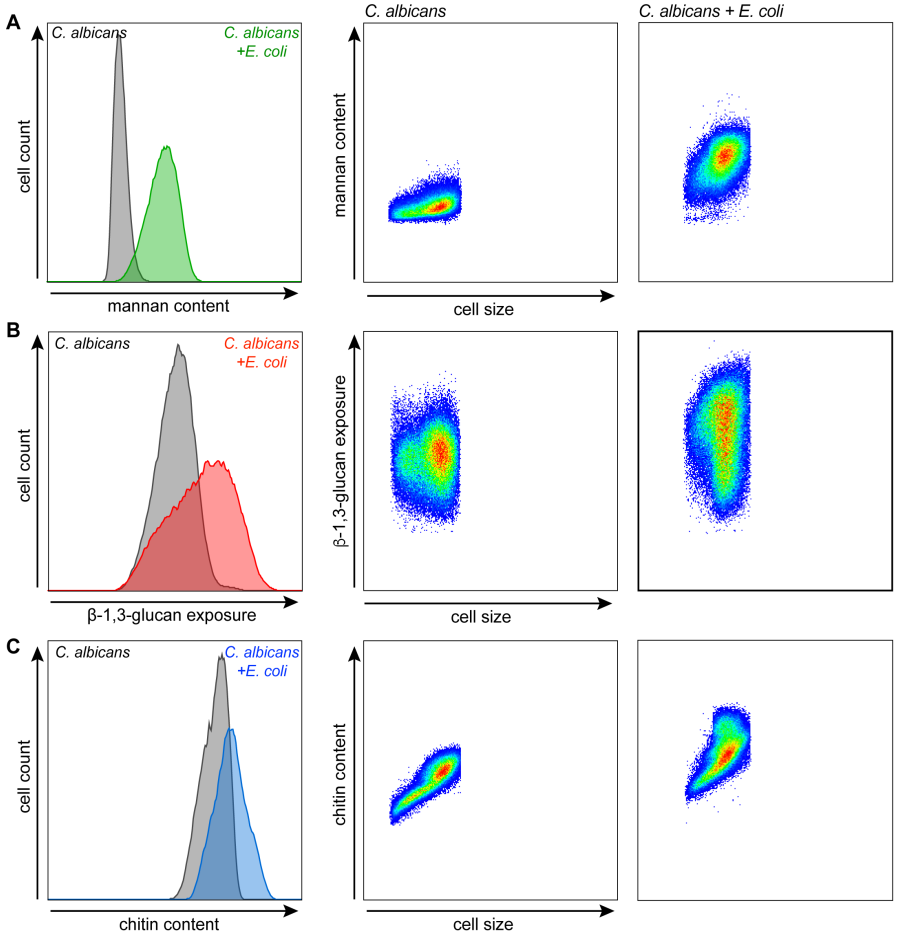


Figure 4-6: Relationship between cell size and cell wall contents.

(A, B, C) Representative histogram of cell wall staining (left) for mannan **(A)**, exposed β-1,3-glucan **(B)**, or chitin **(C)**. Gray peaks represent *C. albicans* grown in mono-culture. Flow cytometric dot plots comparing cell size with cell wall components during *C. albicans* monoculture or co-culture with *E. coli* (right).

4.3.2 *E. coli*-induced fungal cell wall remodeling impacts innate and adaptive immune responses and is relevant *in vivo*

We were particularly interested in understanding how bacterial-mediated fungal cell wall remodeling would impact innate immune recognition of *C. albicans*. Due to the observed increase in β-1,3-glucan exposure (Fig 4-3D), we hypothesized that fungal cells co-cultured with *E. coli* would have higher engagement with Dectin-1 compared to monocultured cells. To test this, we used HEK-blue reporter cell lines expressing a single CLR that drives the expression of SEAP for a colorimetric report of CLR agonism. Using these reporter cells, we focused on the CLRs Dectin-1, which recognizes β-1,3-glucan, and Dectin-2, which recognizes α-mannans[503]. Our results indicated that co-culture with *E. coli* leads to increased engagement of *C. albicans* with both Dectin-1 and Dectin-2 (Fig 4-3F-G). These results are consistent with the increase in cell wall mannan and exposure of β-1,3-glucan observed following co-culture with *E. coli* (Fig 4-3A-D).

Beyond the clear role for the innate immune response, there is an increasing appreciation for the role of the adaptive immune responses in controlling gut commensal fungi. Intestinal IgA antibodies preferentially target *C. albicans* in the hyphal form, and this targeting promotes the competitive fitness of *C. albicans* and helps maintain homeostasis [502,503]. Although we did not see an increase in hyphal formation during *in vitro* co-culture, we hypothesized that the altered cell wall may also impact IgA targeting. Using human fecal wash, we quantified IgA binding to *C. albicans* grown in monoculture or in co-culture with *E. coli*. Our results indicated that co-culture with *E. coli* led to decreased IgA binding (Fig 4-3H, Fig 4-7). Together, this suggests that bacteria influence both innate and adaptive immune responses to *C. albicans,* with a potential impact on the inflammatory capacity of the fungus.

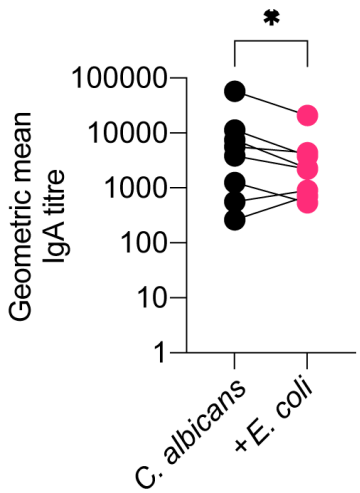


Figure 4-7: Human fecal IgA binding to *C. albicans* grown in monoculture or co-culture with *E. coli*.

Significance determined by Wilcoxon test.

Next, to determine if *E. coli* could induce fungal cell wall remodeling *in vivo*, we colonized germ-free mice with *C. albicans* alone or *C. albicans* and *E. coli.* After one week of colonization, the mice were sacrificed and we collected cecum and colon contents and stained them for cell wall mannan and β-1,3-glucan exposure. We observed a trend of increased

mannan content and β-1,3-glucan exposure in the cecum of mice colonized with both *C. albicans* and *E. coli* (Fig 4-3I). In contrast, there was little difference in cell wall staining from colon contents (Fig 4-3J). These results indicate that bacteria may influence *C. albicans* cell wall composition *in vivo*, but this influence is also dependent on other environmental cues that occur in the host.

4.3.3 Solid-State NMR analysis of the fungal cell wall

As cell wall mannan is involved in reducing exposure of β-1,3-glucan, we were somewhat surprised to see increased β-1,3-glucan exposure alongside increased mannan content[504,505]. Therefore, we turned to solid state NMR spectroscopy to characterize the molecular architecture of the *C. albicans* cell wall during monoculture or co-culture with *E. coli*[506–508]. This method has recently been applied to a variety of pathogenic fungal species to detail their atomic-level changes in cell wall structure using living cells[509,510]. We probed the rigid core of the fungal cell wall using 1D cross polarization (CP) and 2D ^{13}C-^{13}C CORD experimental schemes and this analysis revealed it was composed of β-1,3-glucan, chitin, and β-1,6-glucan, as expected (Fig 4-8A-B)[511–513]. Importantly, we confirmed that there were no carbohydrate signals from *E. coli* in the rigid phase (Fig 4-9A). When *C. albicans* was co-cultured with *E. coli*, we observed a decrease in β-1,3-glucan content and an increase in mannan content, whereas we observed minor changes in the chitin content (Fig 4-8D). Interestingly, co-culture with *E. coli* shifted some mannan polymers from the mobile phase to the rigid phase, while no mannan was present in the rigid phase during monoculture (Fig 4-8B-C). We probed the mobile domain of the cell wall using ^{13}C DP refocused J-INADEQUATE spectra, mostly including molecules forming the dynamic matrix and the surface layer, including β-1,3-linkages (B) in the mainchain, β-1,3,6-linkages (B^{Br}) at branching points, and β-1,6-linkages (H) in the side chains (Fig 4-8E-F). While we did detect *E. coli* carbohydrate signals in the mobile phase, these did not correspond to the carbohydrate signals from *C. albicans* (Fig 4-9B). Instead, they were predominantly attributed to β -1,3-linked muramic acid, a key component of peptidoglycan (Fig 4-9B). In the mobile phase, we observed signals from α-1,2- and α-1,6-linked mannose residues ($Mn^{1,2}$ and $Mn^{1,6}$) in the mannan fibrils, as well as weak signals from galactose (Gal) residues (Fig 4-8E). Our compositional analysis revealed a decrease in β-1,3-glucan and β-1,6-glucan content and an increase in mannan content following co-culture with *E. coli* (Fig 4-8G). Additionally, the β-1,3-glucan from co-culture with *E. coli* contained less branching than β-1,3-glucan from monoculture

(Fig 4-8E). We did not observe significant changes in galactose contents between conditions (Fig 4-8G). This detailed characterization of the fungal cell wall provides deeper insight into how *E.*

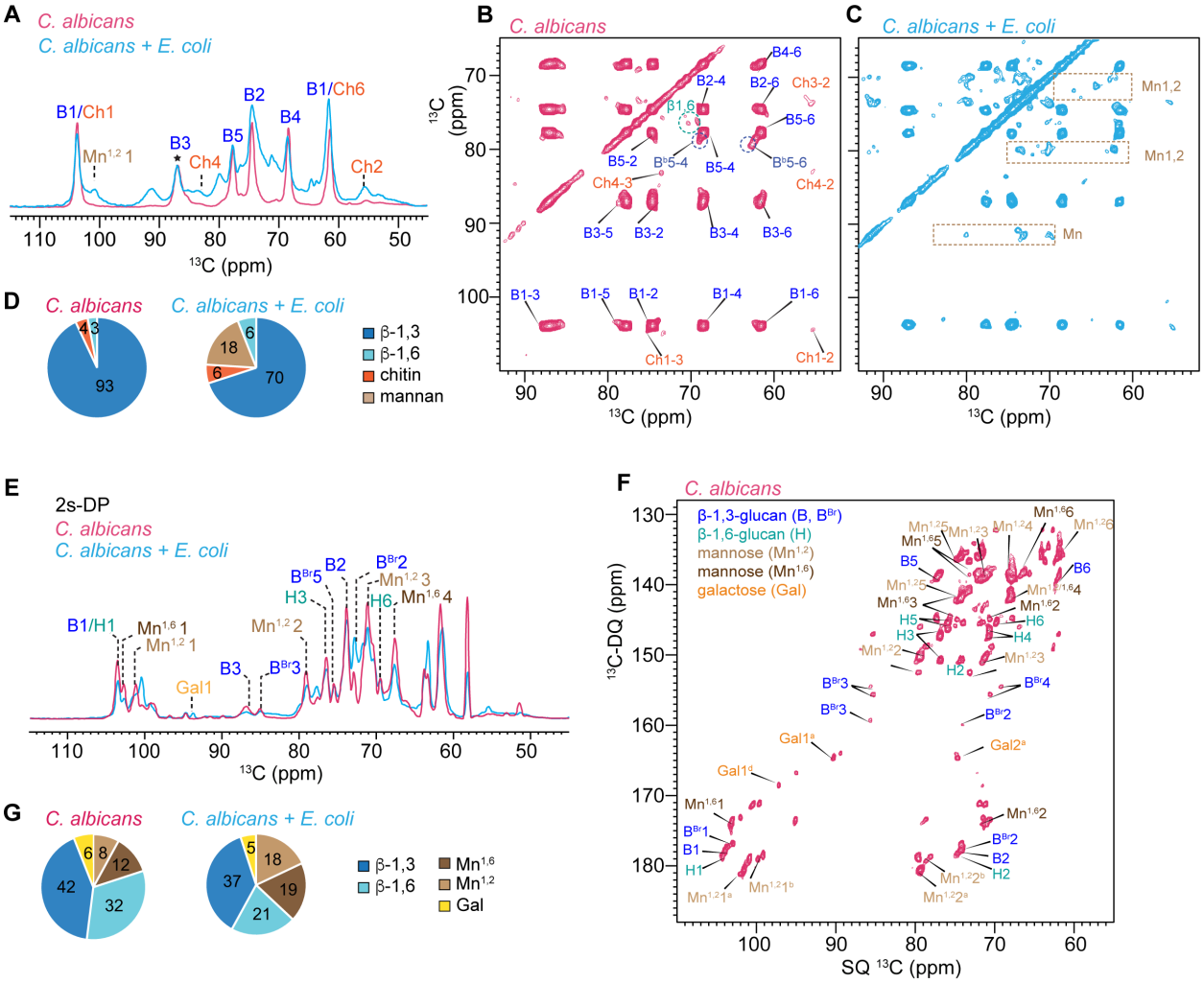


Figure 4-8: Composition of rigid and mobile polysaccharides probed by high-resolution ssNMR.

(A) Overlay of cross-polarization (CP) spectra representing rigid glucans for *C. albicans* in pink and *C. albicans* + *E. coli* in blue. Spectra were normalized by β -1,3 glucan B3 (86 ppm) peak, indicated at the star. **(B)** The 2D ^{13}C-^{13}C CORD correlation spectrum displays the spatial arrangement of cross-linkages among β-1,3-glucan, β-1,6-glucan, and chitin in the rigid cell wall of *C. albicans.* **(C)** The 2D ^{13}C-^{13}C CORD correlation spectrum displays the spatial arrangement of cross-linkages among β-1,3-glucan, β-1,6-glucan, and chitin and the dominance of mannan signals in the rigid cell wall of *C. albicans* + *E. coli*. **(D)** The molar composition of the rigid components as determined by analyzing peak volumes in the 2D ^{13}C-^{13}C CORD spectra. Glucan types and their corresponding carbon signals are abbreviated and color-coded as follows: β-1,3-glucan (B, blue), Chitin (Ch, orange) and Mannan (Mn, light brown). **(E)** Overlay of 2 s direct polarization (DP) spectra representing mobile glucans for *C. albicans* in pink and *C. albicans* + *E. coli* in blue. **(F)** 2D ^{13}C-^{13}C through-bond INADEQUATE spectrum of *C. albicans*, with assignments linking monomers to spectral peaks. **(G)** The molar composition of these mobile components was determined by analyzing peak volumes in the 2D ^{13}C-^{13}C INADEQUATE spectra.

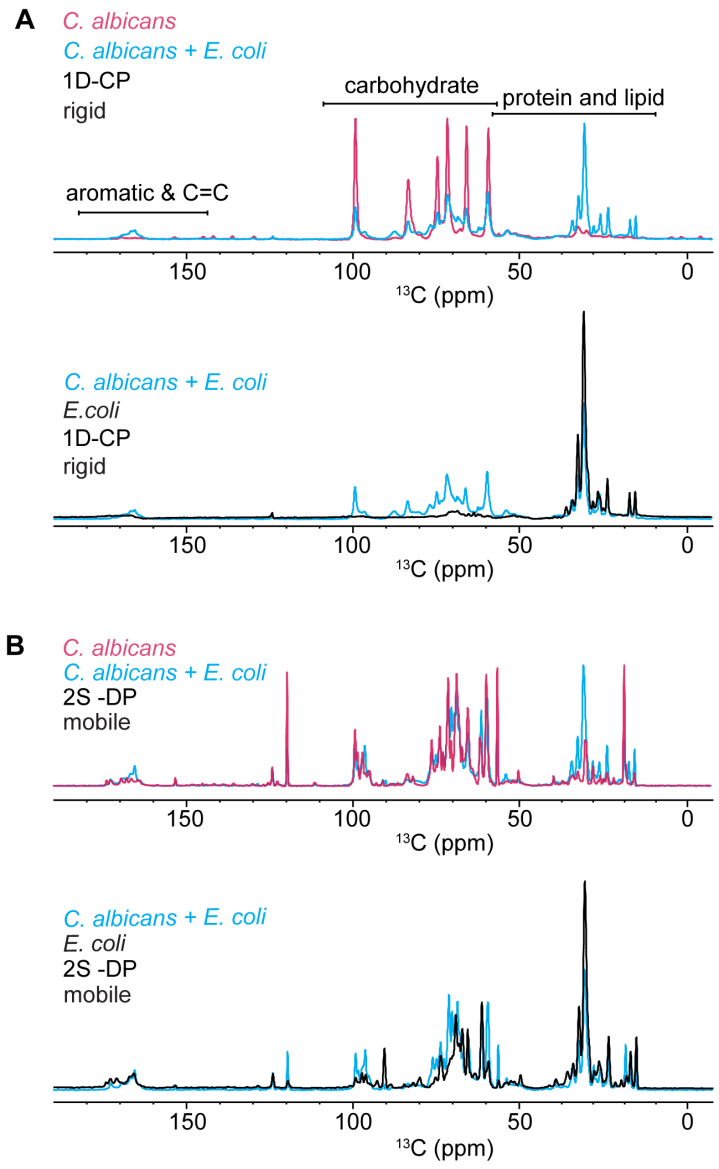


Figure 4-9: Representative dynamic gradients of polysaccharides in the cell wall.

(A) Cross polarization (CP) spectra representing rigid components. (**B)** 2 s direct polarization (DP) spectra representing mobile components.

coli co-culture influences the total amount, flexibility, and branching of cell wall polysaccharides and can explain how we obtained both more mannan and higher Dectin-1 engagement.

4.3.4 Fungal cell wall remodeling in response to bacteria is broadly conserved

Although the laboratory reference strain, SC5314, has been used in the majority of studies, *C. albicans* isolates display remarkable diversity in their growth rates, filamentation profiles, and interactions with host cells, among other phenotypes[221,226,227,247,416,432,433]. Therefore, we reasoned that different genetic backgrounds of *C. albicans* may have different responses to bacterial co-culture. To test this, we performed *E. coli* co-cultures with *C. albicans* isolates from commensal colonization or bloodstream infections and used flow cytometry to quantitatively measure cell wall mannan content as a readout for cell wall remodeling[226,416]. We found that regardless of genetic clade or sample origin, all tested *C. albicans* isolates underwent cell wall remodeling following co-culture with *E. coli* (Fig 4-10A). Therefore, cell wall remodeling during bacterial co-culture is a conserved response across these *C. albicans* isolates that is not dependent on sample origin site or genetic background. We also assayed additional strains of *E. coli* for their ability to induce cell wall remodeling. We used two common laboratory strains, MC1061 and MG1655, and two

previously characterized uropathogenic isolates, CFT073 and UTI89 [512]. We observed that all tested strains of *E. coli* induced fungal cell wall remodeling resulting in increased mannan (Fig 4-10B). Therefore, this interaction between *C. albicans* and *E. coli* is not restricted to fungal or bacterial laboratory strains.

Next, we wanted to determine if *E. coli* induces cell wall remodeling in other *Candida* species. Therefore, we performed 24-hour *E. coli* co-culture with *Candida dubliniensis, Candida tropicalis, Candida parapsilosis, Candida auris,* and *Candida glabrata*. These *Candida* species had wide variation in their initial mannan content, with *C. dubliniensis* having more mannan than *C. albicans* while the rest of the species had less (Fig 4-11) There was an overall trend towards increased cell wall mannan when these *Candida* species were co-cultured with *E. coli* (Fig 4-10C). Co-culture with *E. coli* induced a similar magnitude of cell wall remodeling in *C. dubliniensis* and *C. glabrata* as was observed in *C. albicans*, although remodeling in *C. dubliniensis* did not reach statistical significance (Fig 4-10C). Meanwhile, *C. parapsilosis* displayed more cell wall remodeling than *C. albicans*, while *C. tropicalis* and *C. auris* displayed less cell wall remodeling (Fig 4-10C). This indicates that *E. coli* can induce cell wall remodeling in multiple

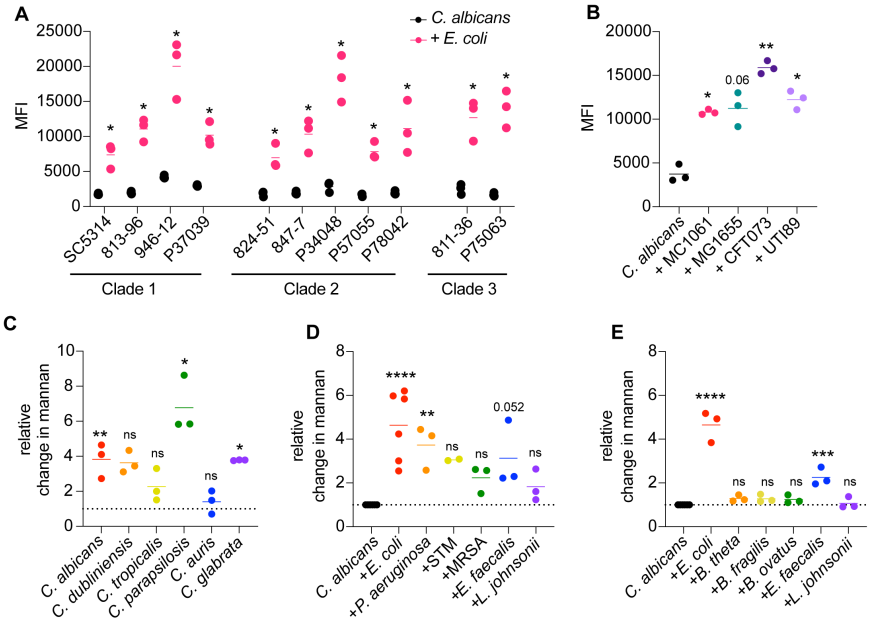


Figure 4-10: Cell wall remodeling in response to bacteria is broadly conserved.

(A) Flow cytometric quantification of cell wall mannan content of the indicated *C. albicans* isolates in monoculture or co-culture with *E. coli* after 24 hours. Significance determined by paired t-tests of each isolate during monoculture vs co-culture. **(B)** Flow cytometric quantification of cell wall mannan content of *C. albicans* SC5314 following 24 hours of co-culture with the indicated *E. coli* strains. Significance determined by one-way ANOVA with Dunnett's multiple comparison test. **(C)** Relative change in cell wall mannan content of the indicated *Candida* species after 24 hours of co-culture with *E. coli.* Significance determined by paired t-tests of each *Candida* species during monoculture or co-culture with *E. coli*. **(D, E)** Relative change in cell wall mannan content of *C. albicans* following 24 hours of aerobic **(D)** or anaerobic **(E)** bacterial co-culture. Significance determined by one-way ANOVA with Dunnett's multiple comparison test.

Candida species, but the mechanism in each species is not known.

Finally, we sought to determine if fungal cell wall remodeling in response to bacteria was specific to the interaction between *C. albicans* and *E. coli* or if it could be more widely attributed to additional bacteria species. We selected a panel of bacteria that colonize similar niches as *C. albicans* and have previously reported interactions with *C. albicans*. We performed fungal-bacterial co-cultures to test for their ability to induce fungal cell remodeling. Under aerobic conditions at 30°C, we observed a consistent trend of cell wall remodeling when *C. albicans* was co-cultured with bacteria, although the magnitude of remodeling varied between the bacterial species (Fig 4-10D). *E. coli* and *Pseudomonas aeruginosa* induced the most significant cell wall remodeling response (Fig 4-10D). The other tested species, *Staphylococcus aureus* (MRSA), *Salmonella enterica* serovar Typhimurium (STM), *Enterococcus faecalis*, and *Lactobacillus johnsonii*, induced a weaker remodeling response that did not reach statistical significance (Fig 3D). Of the additional bacteria tested, only co-culture with *P. aeruginosa* resulted in increased cell size, similar to *E. coli* (Fig 4-12A).

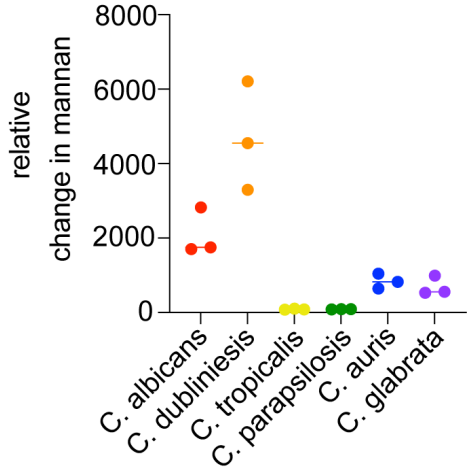


Figure 4-11: Cell wall mannan content of different *Candida* species.

Flow cytometric quantification of cell wall mannan for the indicated *Candida* species.

As *C. albicans* colonizes body sites with low oxygen levels, and hypoxia is a known cue for cell wall remodeling, we also performed anaerobic co-cultures between *C. albicans* and a set of strict and facultative anaerobes[514]. We tested the ability of three *Bacteroides* species, *B. thetaiotaomicron*, *B. fragilis*, and *B. ovatus* to induce fungal cell wall remodeling. Some *Bacteroides* species, including *B. thetaiotaomicron* and *B. fragilis*, can use purified yeast mannan as a sole carbon source[513]. As this ability is not widely reported in other bacterial species, we reasoned we might see a distinct cell wall mannan phenotype following co-culture of *C. albicans* with mannan degraders. However, co-culture with each of the three tested *Bacteroides* species, regardless of their ability to degrade fungal mannan, resulted in a consistent, but slight increase

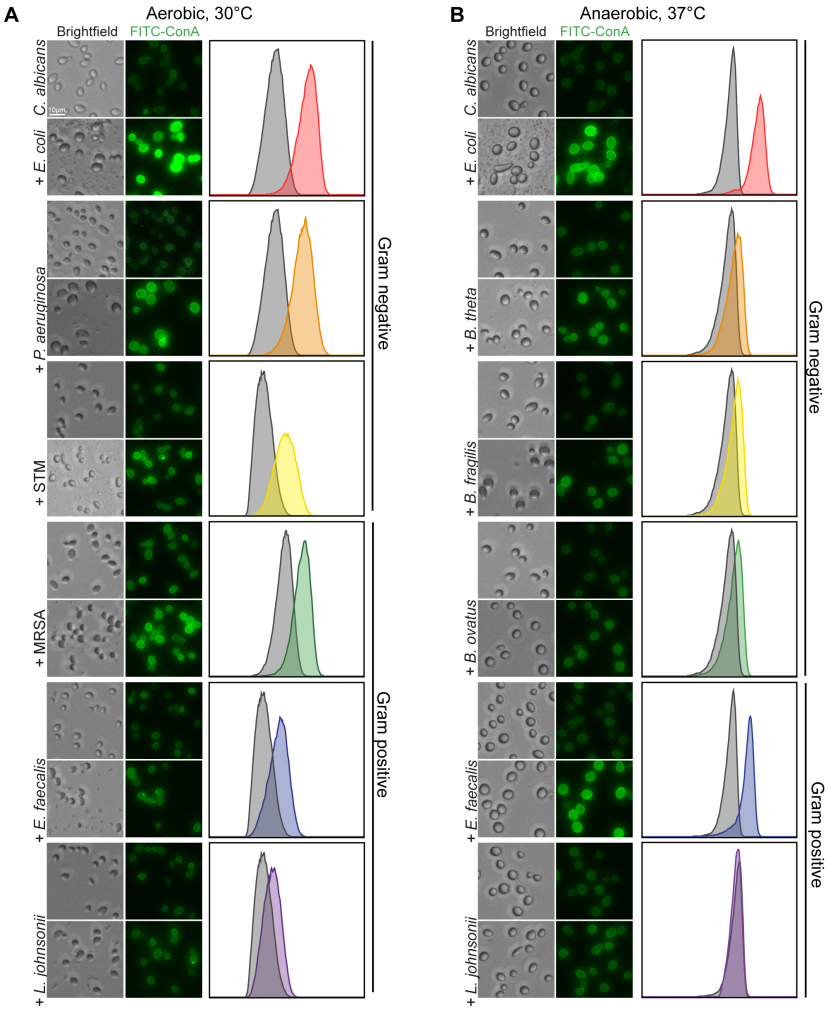


Figure 4-12: Cell wall mannan during bacterial co-culture

(B, C) Representative brightfield and fluorescent microscopy images (left) and mannan histograms (right) of *C. albicans* grown alone or with indicated bacterial species under aerobic **(A)** or anaerobic **(B)** conditions. 40X magnification.

in cell wall mannan and not a reduction as might be expected if *B. thetaiotaomicron* or *B. fragilis* were consuming fungal mannan (Fig 4-10E). We assayed the ability of facultative anaerobes, *E. coli, E. faecalis,* and *L. johnsonii* to induce fungal cell wall remodeling under anaerobic conditions. Under anaerobic conditions, *E. coli* induced the most significant amount of cell wall remodeling, followed by *E. faecalis* (Fig 4-10E). *L. johnsonii* failed to induce remodeling under anaerobic conditions (Fig 4-10E). Additionally, the increased cell size observed following aerobic co-culture with *E. coli* did not occur under anaerobic conditions (Fig 4-12B). Therefore, multiple bacteria that *C. albicans* is likely to encounter during human colonization can influence cell wall composition to varying degrees. Among the bacteria tested, co-culture with *E. coli* resulted in the most consistent and significant fungal cell wall remodeling phenotype. These results emphasize that bacterial-mediated cell wall remodeling can be induced by multiple bacterial species and is not limited to *E. coli*.

4.3.5 The HOG pathway is required for fungal cell wall remodeling in response to bacterial co-culture

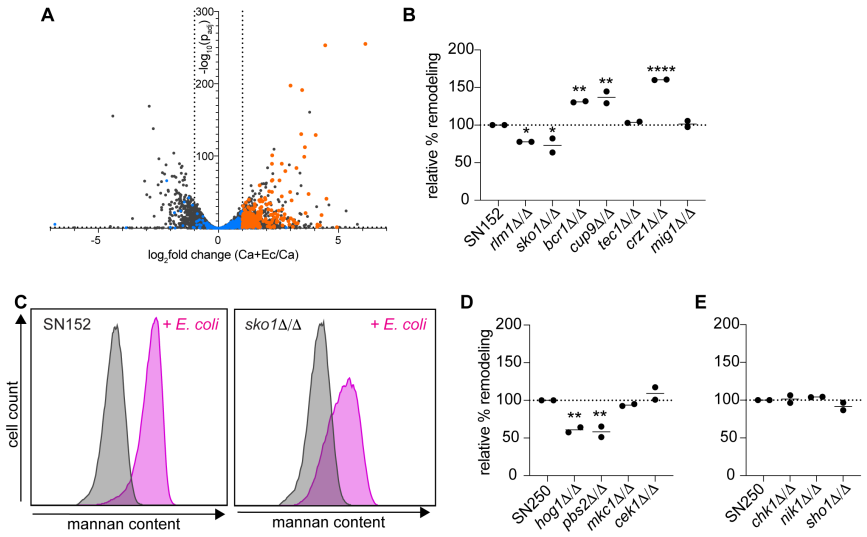


Figure 4-13: Mutants in the high osmolarity glycerol cascade are defective at remodeling in response to *E. coli* co-culture.

(A) Volcano plot of *C. albicans* differentially expressed genes during co-culture with *E. coli* compared to monoculture 6 hours after the initiation of co-culture. Dotted lines represent significance thresholds. Colored points are genes with GO term annotations of 'carbohydrate transport' in the Candida Genome Database. Orange plots are significantly upregulated and blue dots are not. (**B)** Relative amount of remodeling, based on change in cell wall mannan content, following 24 hours of co-culture with *E. coli* for each indicated mutant strain from the Homann collection. Set relative to cell wall remodeling of parental strain, SN152. Each point is an average of two biological replicates of one independent deletion clone. (**C)** Flow cytometric histograms representing cell wall mannan content of SN152 (left) or *sko1*Δ/Δ (right) during monoculture (grey) or *E. coli* co-culture (pink). (**D, E)** Relative amount of remodeling, based on change in cell wall mannan content, following 24 hours of co-culture with *E. coli* for each indicated mutant strain from the Noble collection. Set relative to cell wall remodeling of parental strain, SN250. Each point is an average of two biological replicates of an independent deletion clone. Significance of **(B, D, E)** determined by one-way ANOVA with Dunnett's multiple comparison test.

To determine what transcriptional changes occur during bacterial co-culture, we performed RNA sequencing on *C. albicans* grown for 6 hours in monoculture or co-culture with *E. coli*. In response to co-culture with *E. coli*, 672 *C. albicans* transcripts were significantly upregulated and 321 were significantly downregulated (Fig 4-13A). Of the upregulated transcripts, we saw a significant signature of alternate carbon utilization, indicating that *C. albicans* undergoes a global metabolic shift during co-culture with *E. coli.* Key genes involved in the glyoxylate cycle (*ICL1, MLS1*), beta-oxidation (*FOX3, PXP2*), gluconeogenesis (*PCK1*, *FBP1*), and galactose utilization (*GAL1, GAL10)* were highly upregulated during co-culture with *E. coli*. We also noted upregulation of several sugar transporters and genes involved in the biosynthesis and transport of arginine. Transcripts that were significantly downregulated in response to *E. coli* largely included genes involved in DNA replication and cell cycle. This signature is consistent with decreased growth rate observed when *C. albicans* is grown with *E. coli*.

To understand what fungal signaling pathways are involved in the cell wall remodeling response to *E. coli*, we leveraged existing mutant libraries and selected transcription factor

mutants with known roles in cell wall remodeling pathways or regulation of alternate carbon metabolism[514]. For each mutant, we compared the magnitude of cell wall remodeling during co-culture with *E. coli* to that of the corresponding wildtype strain. From our mutant analysis, we found that *bcr1*Δ/Δ, *cup9*Δ/Δ, and *crz1*Δ/Δ were hyper-responsive to co-culture with *E. coli*, indicating that they are repressors of this response (Fig 4-13B). However, *rlm1*Δ/Δ and *sko1*Δ/Δ had a reduced capacity to remodel during co-culture with *E. coli*, indicating that they are positive regulators of bacterial-mediated fungal cell wall remodeling (Fig 4-13B). The reduced capacity of *sko1*Δ/Δ to remodel was also apparent based on its mannan histograms, which had more overlap between conditions than that of the parental SN152 strain (Fig 4-13C). After identifying transcription factors required for the full remodeling phenotype, we wanted to determine which signaling pathways were responsible for transcription factor activation. The fungal cell wall remodeling response is regulated by cell wall integrity (CWI) and stress responsive pathways that have extensive crosstalk with one another to coordinate cell wall remodeling in response to changing environmental stresses, as cell wall composition and susceptibility to stressors are intrinsically linked. Many of these relevant pathways are controlled by mitogen-activated protein kinase (MAPK) cascades; therefore, we chose representative MAPKs from three signaling pathways with well-established roles in the regulation of cell wall remodeling. We found that *mkc1*Δ/Δ, from the PKC pathway, and *cek1*Δ/Δ, from the Cek1-mediated pathway, had a normal remodeling response (Fig 4-13D). Representative kinases from the high osmolarity glycerol (HOG) pathway, *hog1*Δ/Δ and *pbs2*Δ/Δ, had a reduced capacity to remodel in response to *E. coli* co-culture, similar to *sko1*Δ/Δ and *rlm1*Δ/Δ (Fig 4-13D). Therefore, the HOG cascade is required for fungal cell wall remodeling during co-culture with *E. coli*. Finally, we sought to identify the upstream sensor responsible for activating the HOG cascade. *C. albicans* has three histidine kinases (HKs) that canonically feed into the HOG cascade. From the existing deletion mutant collections, we tested the involvement of two of these HKs, Nik1 and Chk1, in response to *E. coli* co-culture. We also tested the involvement of Sho1, an adaptor protein with a minor role in activating *C. albicans* Hog1 in response to osmotic and oxidative stress[127,513]. We found that *nik1*Δ/Δ, *chk1*Δ/Δ, and *sho1*Δ/Δ had a normal remodeling phenotype, indicating that they are not responsible for activating the HOG cascade in response to *E. coli* co-culture (Fig 4-13E). Activation of the HOG pathway in response to bacterial co-culture may be redundant, occur through the Sln1 kinase, or through a non-canonical signaling branch.

4.3.6 Bacterial-induced fungal cell wall remodeling is mediated by a secreted metabolite

In addition to defining the fungal signaling pathways involved in bacterial-mediated cell wall remodeling, we wanted to understand the mechanism by which *E. coli* induces this unique phenotype. To achieve this, we first measured *C. albicans* mannan content for the first 6 hours of co-culture with *E. coli* to understand the temporal dynamics of our phenotype. Fungal cell wall remodeling occurred rapidly, and the mannan content differed significantly between the conditions by 3 hours (Fig 4-14A). To determine if *E.*

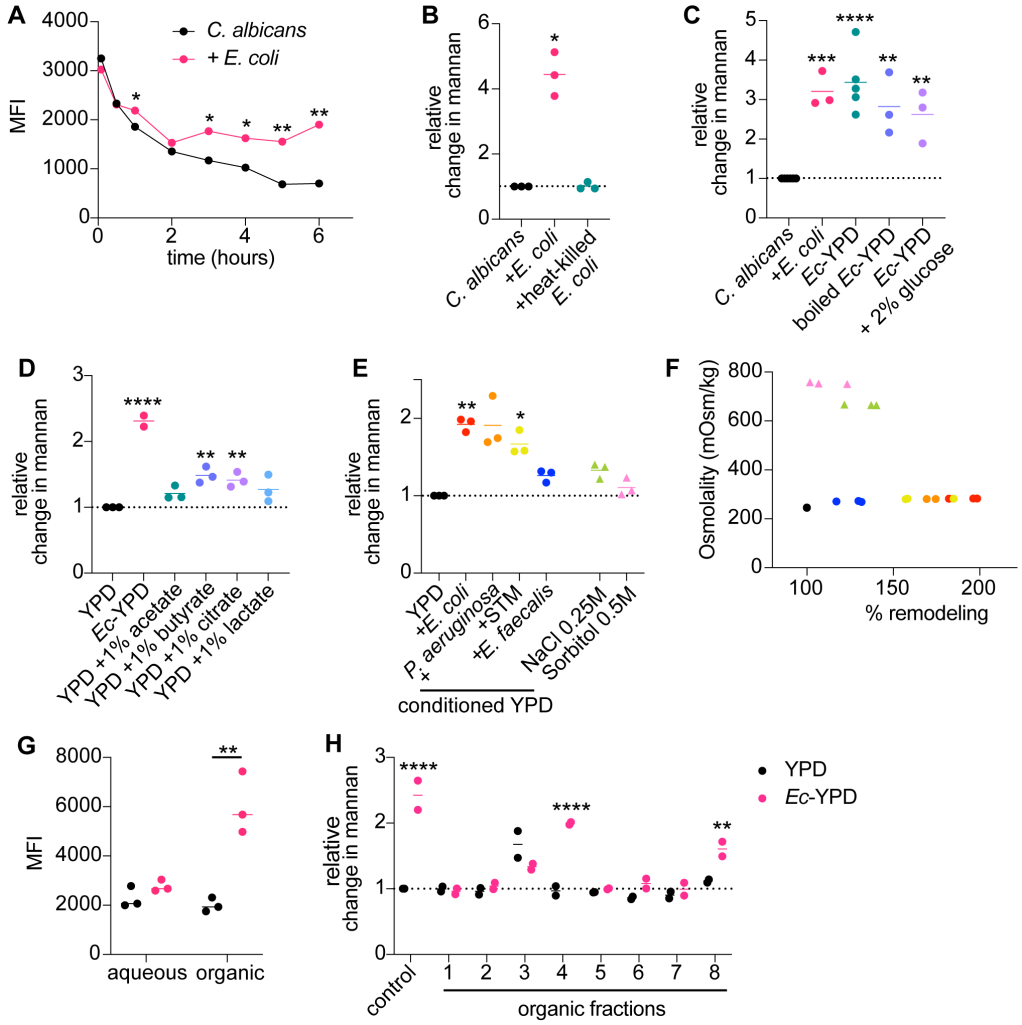


Figure 4-14: *E. coli*-induced fungal cell wall remodeling is mediated by a secreted metabolite.

(A) Flow cytometric quantification of cell wall mannan content over a 6-hour time course of *C. albicans* grown alone or in co-culture with *E. coli*. *C. albicans* was grown to mid-log phase before the addition of YPD media with or without *E. coli*. Significance determined by paired t-tests at each time point. **(B)** Relative change in cell wall mannan content of *C. albicans* grown alone or co-cultured with live or heat-killed *E. coli* for 24 hours. **(C, D, E)** Relative change in cell wall mannan content of *C. albicans* grown in the indicated conditions for 6 hours. Significance of **(B, C, D, E)** determined by one-way ANOVA with Dunnett's multiple comparison test. **(F)** Linear regression comparing relative magnitude of remodeling content and osmolality of media from previous panel. **(G)** Flow cytometric quantification of *C. albicans* cell wall mannan content after 6 hours of growth in YPD with 50 mg/mL of aqueous and organic extracts from YPD or *Ec*-YPD. **(H)** Relative change in cell wall mannan content for *C. albicans* grown in organic fractions of YPD or *Ec*-YPD for 6 hours. Set relative to YPD control. Concentrations of organic fractions listed in Table 4-1. Significance of **(G, H)** determined by two-way ANOVA with Sidak's multiple comparison test.

Fraction	YPD	*Ec*-YPD
1	10 mg/mL	10 mg/mL
2	10 mg/mL	10 mg/mL
3	10 mg/mL	10 mg/mL
4	2 mg/mL	10 mg/mL
5	2 mg/mL	2 mg/mL
6	10 mg/mL	0.5 mg/mL
7	0.5 mg/mL	2 mg/mL
8	0.5 mg/mL	0.5 mg/mL

Table 4-1: Tested concentrations of organic fractions from Fig 4-14H

coli must be alive to induce cell wall remodeling, *E. coli* was heat-killed at 65°C for 30 minutes prior to the initiation of co-cultures. *C. albicans* co-cultured for 24 hours in the presence of heat-killed *E. coli* did not undergo cell wall remodeling, indicating that *E. coli* must be live and metabolically active to induce fungal cell wall remodeling (Fig 4-14B), and suggests that it is not peptidoglycan from *E. coli* driving this remodeling[127,515]. To determine if a secreted factor is responsible for the induction of fungal cell wall remodeling, we grew *E. coli* overnight in YPD before bacterial cells were removed by filtration to create *E. coli*-conditioned YPD (*Ec*-YPD). We found that 6 hours of growth in *Ec*-YPD was sufficient to induce cell wall remodeling to the same degree as co-culture with live *E. coli* (Fig 4-14C). This phenotype remained when *Ec*-YPD was heated to 60°C for 30 minutes to inactivate proteins, indicating that a secreted, non-proteinaceous factor mediates the induction of cell wall remodeling (Fig 4-14C). We observed a reduced growth rate when *C. albicans* was grown in *Ec*-YPD, consistent with results from live co-culture and RNAseq data (Fig 4-15). We also considered that nutrient deprivation could be triggering fungal cell wall remodeling and therefore supplemented Ec-YPD with 2% glucose, to to ensure *C. albicans* had sufficient access to its preferred carbon source. The cell wall remodeling response was conserved following growth in *Ec*-YPD + 2% glucose, indicating that nutrient competition is not responsible for the cell wall remodeling phenotype (Fig 4-14C).

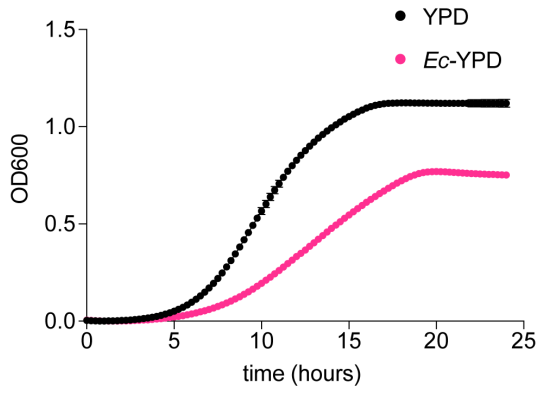


Figure 4-15: *E. coli*-conditioned YPD delays growth of *C. albicans*.

Growth curve of *C. albicans* grown in YPD or *Ec*-YPD for 24 hours.

As bacteria secrete metabolic byproducts, including short chain fatty acids (SCFAs), that influence the *C. albicans* cell wall, and as our RNAseq experiment identified a global metabolic remodeling signature during *E. coli* co-culture, we considered that changes in the available carbon sources could be involved in the remodeling

phenotype[516]. We tested if the addition of certain organic acids, including the common SCFAs acetate and butyrate, was sufficient to induce fungal cell wall remodeling. Organic acids are byproducts of bacterial metabolism, are present in the gastrointestinal tract, and some have been shown to impact *C. albicans* cell wall composition[517]. We added 1% w/v of acetate, butyrate, citrate, or lactate to YPD and compared cell wall mannan content following growth in these conditions to *Ec*-YPD. None of the added organic acids induced fungal cell wall remodeling to the same magnitude as *Ec*-YPD (Fig 4-14D). Therefore, the organic acids tested here are not drivers of bacterial-mediated cell wall remodeling.

Due to the involvement of the HOG pathway in the response to fungal cell wall remodeling (Fig 4-13D), we wanted to determine if our cell wall remodeling phenotype was driven by osmotic stress. Exposure to 1M NaCl has previously been shown to induce short-term changes in cell wall architecture, but the impact of prolonged growth under osmotic stress on the cell wall has not been described[492]. We measured cell wall mannan content after 6 hours of growth in conditioned YPD from bacteria we have previously shown to induce remodeling (Fig 4-10D). Consistent with our results from live bacterial co-culture, we observed a trend of increased cell wall mannan during growth in conditioned YPD from *E. coli, P. aeruginosa,* STM, and *E. faecalis* (Fig 4-14E). We compared these conditions to two known osmotic stresses, NaCl (0.25M) and sorbitol (0.5M) and found that growth in NaCl induced a similar level of remodeling as growth in *E. faecalis* conditioned media (Fig 4-14E). We measured the osmolality of these media conditions with an osmometer and performed a linear regression comparing the magnitude of cell wall remodeling under these conditions to the osmolality of each media condition (Fig 4-14F). We found no relationship between osmolality and extent of cell wall remodeling, indicating that despite the involvement of the HOG cascade, osmotic stress is not driving bacterial-mediated cell wall remodeling.

From our data, we thus hypothesized that a secreted bacterial metabolite was responsible for inducing *C. albicans* cell wall remodeling. To test this hypothesis, we turned to the discovery-based approach of bioassay-guided fractionation. YPD and *Ec*-YPD were separated into aqueous and organic extracts. These extracts were added back to fresh YPD media at 50 mg/mL, and we measured *C. albicans* mannan content after 6 hours of growth. We found that no remodeling occurred following growth in the aqueous extract of *Ec*-YPD, but we did observe remodeling following growth in the organic extract of *Ec*-YPD (Fig 4-14G). Next, the organic

extracts from YPD and *Ec*-YPD were further fractionated using a methanol solvent gradient. We observed that fractions 4 and 8 induced cell wall remodeling (Fig 4-14H). In the future, these active fractions will be analyzed via liquid chromatography-mass spectrometry (LC-MS) to identify metabolite candidates that may induce fungal cell wall remodeling.

4.3.7 Bacterial-mediated fungal cell wall remodeling modulates antifungal resistance

As the three main available classes of antifungals function through targeting the cell wall or cell membrane components, we sought to determine if bacterial-induced cell wall remodeling could modulate antifungal drug resistance. To this end, we determined the minimum inhibitory concentration (MICs) for amphotericin B, caspofungin, and fluconazole, in both YPD and *Ec*-YPD. We found that growth in *Ec*-YPD led to a slight increase in sensitivity to amphotericin and a slight increase in resistance to fluconazole (Fig 4-16A-B). These alterations were subtle, but reproducible (Fig 4-16A-B). Most strikingly, we found a significant increase in resistance to caspofungin when *C. albicans* was grown in *Ec*-YPD (Fig 4-16A-B). The observed increased resistance to caspofungin is in agreement with work showing that increased cell wall chitin levels

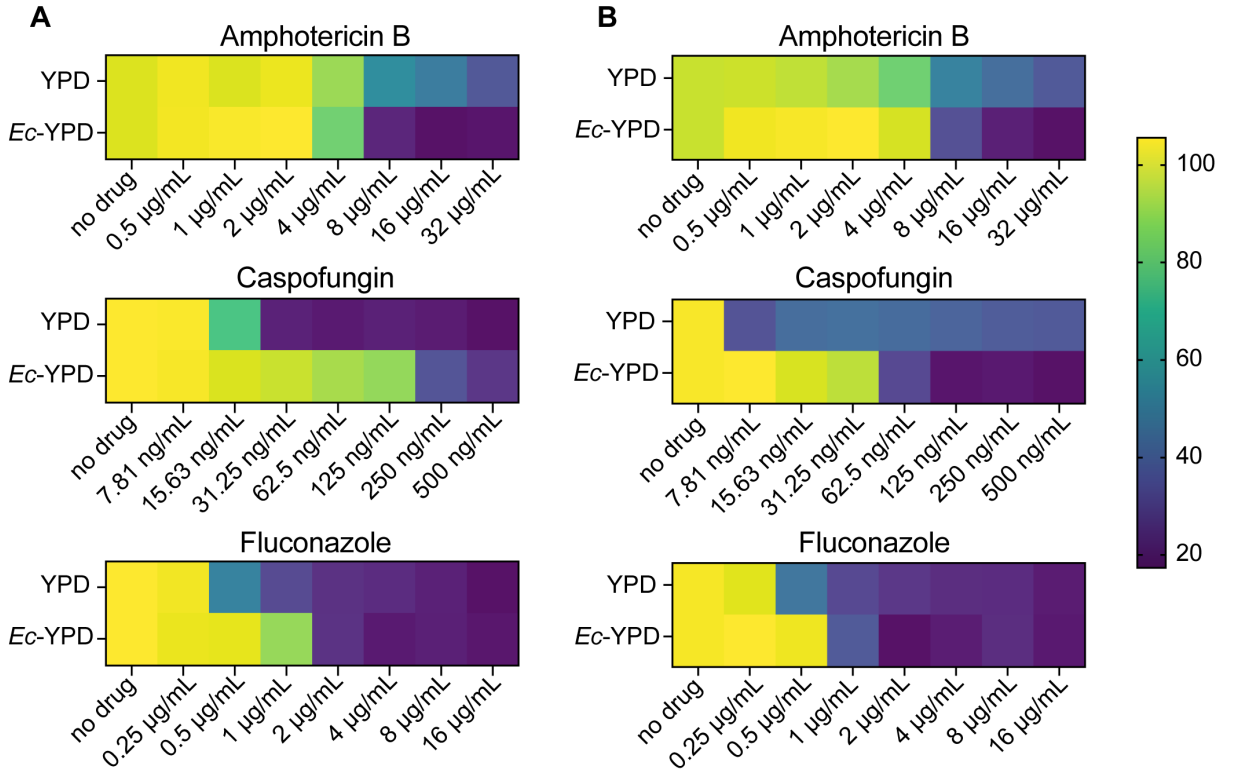


Figure 4-16: Bacterial-induced fungal cell wall remodeling alters antifungal resistance.

(A, B) Minimum inhibitory concentration (MIC) assay for *C. albicans* grown in YPD or *Ec*-YPD and treated with increasing concentrations of amphotericin B, caspofungin, and fluconazole, 2 biological replicates **(A, B)**, each row is the average of two technical replicates.

correlate with increased echinocandin resistance[158,518,519]. This highlights how interactions with bacteria may alter the efficacy of antifungal treatment *in vivo*.

4.4 Discussion

The fungal cell wall is a dynamic and essential organelle that protects structure, protects the cell from external stresses, and mediates interactions with host immune cells. As a result of its important roles, the fungal cell wall is highly responsive to changes in environmental conditions. Here, we have demonstrated that *C. albicans* undergoes cell wall remodeling following co-culture with *E. coli* that increases cell wall mannan and chitin content as well as increasing the exposure of the major immunostimulatory ligand, β-1,3-glucan. Solid-state NMR analysis of the rigid and mobile phases of the fungal cell wall revealed changes in cell wall content, polymer flexibility, and branching. These significant changes in the cell wall composition resulted in altered antifungal susceptibility, increased recognition by innate PRRs, and decreased binding of human IgA. Furthermore, we demonstrated that bacterial-mediated fungal cell wall remodeling is relevant *in vivo*. We found that fungal cell wall remodeling is broadly conserved amongst *Candida* and bacterial species. Through mutant analysis we identified that the HOG cascade in *C. albicans* is required for the full remodeling response and demonstrated that *C. albicans* undergoes a global metabolic shift during co-culture with *E. coli*. Finally, we determined that bacterial-mediated fungal cell wall remodeling is mediated by a secreted metabolite and used the untargeted approach of bioassay-guided fractionation to begin identifying the causative metabolite. Overall, our work reveals that bacteria influence the *C. albicans* cell wall with implication for immune recognition and antifungal resistance.

This work adds to existing knowledge of environmental cues that trigger cell wall remodeling in *C. albicans* and alter exposure of the major fungal PAMP, β-1,3-glucan[96–98,134–136,492]. A potential limitation of our work was that we primarily focused on growth under rich media conditions and in the absence of other host-associated cues that are known to influence fungal morphology and cell wall composition. In the future, it will be important to characterize how the presence of multiple cell wall remodeling cues impacts the fungal cell wall and how these cues are prioritized. For example, hypoxia, which triggers β-glucan masking, was shown to be the dominant cue over exposure to CO_2, a cue that induces unmasking of β-glucan[520]. Understanding how combinations of known cell wall remodeling cues impact cell wall composition and other important aspects of fungal biology and how response to these cues differ

in vitro and *in vivo* will be important topics of future research. In line with this idea, there is a growing appreciation that host-associated cues have profound impacts on fungal biology and that these effects are often not accounted for during *in vitro* research. Recent work demonstrated that host-relevant concentrations of CO_2 enhances resistance to echinocandins, emphasizing that antifungal susceptibility testing in a laboratory environment can preclude identification of antifungal resistance[509]. Studies have also demonstrated that the presence or absence of gastrointestinal bacteria in murine models can influence fungal evolution, colonization, and virulence[521]. Overall, these results highlight the importance of conducting research in conditions that most closely mimic relevant *in vivo* conditions for the greatest interpretability of data in relation to human colonization and disease.

We identified that the transcription factors, Rlm1 and Sko1, as well as the central kinases of the HOG cascade, Hog1 and Pbs2, were required for the full remodeling phenotype. Deletion of these regulators resulted in a 25-40% decrease in the magnitude of remodeling but did not abolish the phenotype. Cell wall remodeling is complexly regulated and frequently involves crosstalk and coordination between multiple signaling pathways and the molecular response to different environmental stimuli is unique[522]. Therefore, it is highly probable that additional signaling pathways are involved in regulating bacterial-mediated fungal cell wall remodeling. As we were unable to identify an upstream sensor involved in initiating the signaling cascade, the HOG cascade could be activated through crosstalk with an additional pathway.

Curiously, our cell wall staining and flow cytometric analysis of the cell wall revealed that both mannan content and β-1,3-glucan exposure were increased during *E. coli* co-culture. This observation is at odds with the model that cell wall mannan masks β-1,3-glucan from detection by immune cells[523]. When we analyzed the cell wall in more depth through SS-NMR, we discovered that *E. coli* co-culture led to an increase in cell wall mannan but a reduction in total β-glucan. Additionally, co-culture with *E. coli* changes the physical properties of these polysaccharides. Some mannan polymers from *E. coli* co-culture had shifted from the mobile phase to the rigid phase and β-glucan from *E. coli* co-culture was more linear. Therefore, the relationship between the total amount of cell wall polysaccharides and immunogenic exposure of β-1,3-glucan is not necessarily straightforward. Our detailed analysis of the fungal cell wall using multiple, parallel methods underscores the complexity of this organelle and suggests that

properties including polymer length and branching, flexibility, porosity are important determinants of how the cell wall is recognized by immune cells.

Given the importance of the fungal cell wall in *C. albicans* biology, exploring the impacts of the microbiome will be critical for understanding the physiology of *C. albicans* during colonization. We have identified a broadly conserved response to co-culture and inter-microbial interactions. From our work, we propose that adding complexity to the current *in vitro* models of *C. albicans* will allow us to make better predictions about the impact of certain perturbations on crucial virulence traits such as antifungal resistance or immune recognition.

4.5 Methods

4.5.1 Strains and culture conditions

The fungal strains used in this study are listed in Table 4-2. *C. albicans* strains were grown in liquid YPD (1% yeast extract, 2% bacto-peptone, 2% glucose) media at 30°C. The bacterial strains used in this study are listed in Table 4-3. *E. coli*, *P. aeruginosa*, and STM were grown in liquid LB media at 37°C. MRSA was grown in liquid TSB media at 37°C. *E. faecalis* and *L. johnsonii* were grown in liquid MRS media at 37°C. *Bacteroides* species were grown in TYG media at 37°C in an anaerobic chamber. All strains were maintained at -80C cryoculture in 50% glycerol.

4.5.2 Fungal-bacterial co-culture

Overnight cultures of *C. albicans* were diluted in YPD to an OD_{600} of 0.1 in YPD. Overnight cultures of bacteria were washed with water to remove bacterial media, then diluted to an OD_{600} of 0.5 in YPD. 1mL of the *C. albicans* dilution was added to each well of a 6- or 12-well plate. 1mL of fresh YPD or 1mL of the bacterial dilution was added to the *C. albicans* dilution. Co-cultures were conducted at 30°C in aerobic conditions or at 37°C in an anaerobic chamber. Cells were collected after 24 hours, unless otherwise indicated. The cell suspensions were collected in 1.5mL microcentrifuge tubes and centrifuged at 13,000 rpm for 1 minute to pellet cells. The supernatant was removed and cells were fixed with 1mL of 4% paraformaldehyde (PFA) for 10 minutes at room temperature. The cells were centrifuged again and PFA was removed. The cells were washed with 1mL of PBS 3 times. Cells were resuspended in 1mL of PBS and stored at -20°C.

4.5.3 Transmission electron microscopy

Co-cultures were performed as described above, and fresh cells (not fixed) were provided to the Michigan Microscopy Core for preparation. Samples were mixed 1:1 with YPD media and 1% ultra-low gelling temperature agarose for a final concentration of 0.5% agarose. These suspensions were frozen with a Lecia EM ICE high pressure freezer and stored in liquid nitrogen. Frozen samples were removed from liquid nitrogen and freeze substituted in a solution containing 2% OsO_4, 0.1% uranyl acetate, and 5% H_2O in a Lecia AFS-2. Freeze substitution was carried out at the following temperature schedule: keep samples at -90°C for 24 hours, raise temperature to -60°C in 15 hours (2°C/hour), keep samples at -60°C for 24 hours, raise temperature to -30°C in 15 hours (2°C/hour), keep samples at -30°C for 24 hours, raise temperature to 4°C at 3°C/hour, raise temperature to 25°C in 30 minutes, keep samples at 25°C for 1 hour. After freeze substitution, samples were washed with acetone 3 times then infiltrated with Epon resin/acetone gradient solutions at the following schedule: samples infiltrated with 1:5 solution for 3 hours, 1:2 solution for 4 hours, 1:1 solution overnight, 2:1 solution for 8 hours, 5:1 solution overnight, and pure resin for 24 hours. Samples were embedded in fresh resin and cured at 60°C for 48 hours. Cured samples were cut into 70 nm sections and mounted on Formvar/carbon copper grids for imaging. Samples were imaged using a JEOL JEM 1400 Plus Transmission Electron Microscope. ImageJ software was used to determine the length of mannan fibrils. For each image, the scale was set using the embedded scale bar. For each cell, 3 measurements were taken for mannan fibril length, and these measurements were averaged for final fibril length. A minimum of 35 cells were measured for each replicate.

4.5.4 Flow cytometric quantification of cell wall components

Cells from co-culture experiments were thawed and transferred to a new microcentrifuge tube for staining. To quantify mannan content, cells were stained with 5 μg/mL of FITC-Concanavalin A (MilliporeSigma, C7642) for 30 minutes. To quantify exposed β-1,3-glucan, cells were blocked with 3% bovine serum albumin & 5% normal goat serum (Invitrogen, 10000C) for 30 minutes. After blocking, cells were stained with 15 ug/mL of hDectin-1a (InvivoGen, fc-hec1a-2) for 1 hour. Cells were washed twice with PBS before secondary staining with 4 mg/mL of goat raised anti-human IgG antibody conjugated with Alexa Fluor 647 (Invitrogen A-21445) for 30 minutes. To quantify chitin content, cells were stained with 0.1 g/L of Calcofluor White (MilliporeSigma, 18909-100ML-F) for 10 minutes. Following staining, cells were washed with 500uL PBS three

times and resuspended in 500uL PBS. Samples were analyzed on a LSRFortessa Flow Cytometer (BD Bioscience, NJ, USA) using BD FACSDiva Software. 100,000 events were recorded for each sample. FlowJo software was used to gate for fungal cells as shown in Fig 4-5 and to determine the mean fluorescence intensity (MFI).

4.5.5 Fluorescence microscopy

Cells were stained as described above. Microscopy was performed on a Biotek Lionheart FX automated microscope using 100X oil objective or 40X air objective. The FITC imaging filter cube was used to visualize mannan, the DAPI imaging filter cube was used to visualize chitin, and the CY5 imaging filter cube was used to visualize exposed β-1,3-glucan.

4.5.6 HEK-blue reporter cells

HEK-Blue mDectin-1b, mDectin-2, and control Null1-v cells were purchased from Invivogen and cultured in DMEM with 100 U/mL Pen/Strep, 2 mM L-glut, 10% heat-inactivated fetal bovine serum, and 100 ug/mL Normocin. The following selective antibiotics were used for each cell line: mDectin-1b, 1 ug/mL puromycin, 1x HEK-Blue CLR Selection; mDectin-2, 1 ug/mL puromycin, 1x HEK-Blue CLR Selection, 30 ug/mL blasticidin; Null1-v, 100 ug/mL zeocin. For in vitro reporter cell assays, formaldehyde fixed *C. albicans* strain SC5314 alone and with *E. coli* were co-cultured with 5.04x10 4 HEK-Blue cells at an MOI of 2 (based on *C. albicans*) in 96-well plates in HEK-Blue Detection medium. Control agonists were included for each cell line. Depleted zymosan (100 ug/mL) was used as a positive control for mDectin-1b, furfurman (1000 ug/mL) was used as a positive control for mDectin-2, and trehalose-6,6-dibehenate (TDB) (100 ug/mL) was employed as a negative control for both cell lines. All three control agonists were plated with the Null1-v cells. The co-cultures were incubated for 20 hours at 37°C in 5% CO_2, followed by quantification of secreted embryonic alkaline phosphatase (SEAP) by measuring absorbance at 620 nm.

4.5.7 Quantification of IgA binding

To quantify IgA binding to monocultured or co-cultured *C. albicans*, 500 µL–1 mL of fecal or intestinal homogenate was filtered through a 40-µm or 70-µm filter into a 50-mL conical tube. Filters were rinsed with 10 mL cold PBS, filters were discarded and then samples were spun at 4,000 rpm for 5 min. Supernatants were discarded, and pellets were resuspended in 10 mL PBS and spun at 4,000 rpm for 5 min. Supernatants were discarded and pellets were resuspended in

the residual PBS by vortexing. Subsequently, 10 µL of each sample was pipetted into a 96-well V-bottom plate. A well was prepared for an unstained control and IgA isotype control. Then, 200 µL of 10% FBS (v/v) in PBS was added to each sample and incubated on ice for 10 min. Samples were spun down at 3,000 rpm for 5 min, and the samples were stained with 100 µL 1:250 anti mouse IgA PE (eBioscience clone mA-6E1) and 5 µg/mL calcofluor white (CFW) (Sigma-Aldrich) in column buffer (PBS supplemented with 10mM HEPES (Corning) 2 mM EDTA (Corning), and 0.5% (v/v) FBS (Gibco BRL)). The isotype control sample was similarly stained, but with 1:500 rat IgG1 K isotype control PE. Samples were analyzed on the BD LSR Fortessa and data analyzed by FlowJo.

4.5.8 Germ free mouse colonization

5-week-old GF C57Bl/6 mice were gavaged with 10^6 *C. albicans* (SC5314) or 10^6 *C. albicans* with $5x10^8$ *E. coli*. Mice were euthanized 7 days post-colonization, and colon and cecal contents were harvested. Animal experiments were approved by the institutional Animal Care and Use Committee at the University of Colorado AMC protocol #01221. The University of Colorado AMC is AAALAC accredited, and its facilities meet and adhere to the standards in "Guide for the Care and Use".

4.5.9 Staining intestinal contents

Intestinal contents were homogenized in sterile PBS to a concentration of 100 mg/ml. 20 µL were washed twice with 150 µL PBS with 1% BSA and 5mM EDTA. Samples were then stained with 25 µg/mL ConA AF674, 2 µg/mL CFW, and 1:500 dilution of anti-Candida FITC (Meridian) for 20 min. Cells were washed twice with 150 µL PBS 1% BSA 5mM EDTA and analyzed on a CytoFLEX S Flow cytometer. Contents were separately stained with FcDectin-1. For this panel, 20 µL contents were blocked for 30 minutes in 5% normal goat serum (Invitrogen, 10000C) in PBS 1% BSA 5mM EDTA, then stained with 15 µg/mL hDectin-1a (InvivoGen, Fc-hec1a-2) for 1 hour. Samples washed twice with PBS 1% BSA 5mM EDTA and then stained with 4 mg/mL anti-human IgG AF 674, 2 µg/mL CFW, and 1:500 anti-Candida FITC (Meridian) for 20 minutes. Cells were washed twice with PBS 1% BSA 5mM EDTA and analyzed on CytoFLEX S Flow cytometer.

4.5.10 Solid-state NMR

1D and 2D high-resolution solid-state NMR experiments were conducted on a Bruker Advance NEO 800 MHz (18.8 Tesla) spectrometer at MSU Max T. Roger NMR facility. The experiments were conducted using a 3.2 mm triple-resonance HCN probe under 15 kHz magic-angle spinning (MAS) at 280 K. The ^{13}C chemical shifts were externally referred to adamantane CH_2 signal at 38.48 ppm on the TMS scale. The magic angle was calibrated using KBr. Typical ^{1}H radiofrequency field strengths 50-83 kHz and 50-62.5 kHz for ^{13}C. The initial magnetization for the experiment was created using ^{1}H-^{13}C cross-polarization that preferentially detects rigid molecules. Typically, 1 ms Hartmann-Hahn contact was used for CP. The 2D refocused J-INADEQUATE experiment [520] was integrated with either direct polarization (DP) and short recycle delays of 2 s for the selective detection of mobile components. A 2D ^{13}C-^{13}C correlation experiment was also measured using the CORD [521] scheme with a 53-ms recoupling period. The composition of rigid and mobile components was determined by analyzing peak volumes in 2D CORD and DP refocused J-INADEQUATE spectra, respectively. To minimize uncertainties from spectral crowding, only well-resolved signals were considered for the compositional analysis.

4.5.11 RNA extraction

RNA extraction was performed using a formamide extraction method[458]. Briefly, cells were grown in monoculture or in co-culture with *E. coli* in YPD at 30°C for 6 hours before being harvested by centrifugation and all media was removed. Dry cell pellets were frozen on dry ice and stored at -80 °C before processing. To extract RNA, cell pellets were thawed at room temperature and resuspended in 100 µL FE Buffer (98% formamide, 0.01M EDTA). 50 µL of 500 µm RNAse-free glass beads was added to this suspension and the mixture was homogenized for 30 sec 3 times using a BioSpec Mini-Beadbeater-16 (Biospec Products Inc., Bartlesville, OK, USA). The resulting cell lysate was clarified by centrifugation to remove cell debris. The supernatant was collected as the crude RNA extract. The crude extract was purified using a Qiagen RNeasy mini kit (ref 74104, Qiagen) according to the manufacturer's instructions. Samples were DNAse treated with Invitrogen DNAse (RNAse free) (Qiagen, cat no. 79254). The integrity and purity of the extracted RNA was confirmed via Nanodrop and agarose gel electrophoresis using the bleach gel method prior to downstream applications[458].

4.5.12 *E. coli*-conditioned YPD

E. coli was grown for 18 hours in YPD media at 37°C with rocking. Cells were harvested by centrifugation at 4000 rpm for 5 minutes for small quantities (5 mL) or at 10,000xg for 10 minutes for large quantities (500 mL). The supernatant was collected and passed through a 0.2 μm filter to remove any remaining cells. The solution was used immediately or aliquoted and stored at -20°C to be used within 2 weeks.

4.5.13 Determination of media osmolality

Conditioned YPD media from *P. aeruginosa,* STM, and *E. faecalis* was prepared as described above. The osmolality of blank YPD media, bacteria-conditioned YPD media, and YPD media with the addition of 0.25M NaCl or 0.5M sorbitol were measured using a Fiske Model 210 Micro-Osmometer.

4.5.14 Bioassay-guided fractionation

Three rounds of sequential ethyl acetate extractions were performed on 500 mL of unconditioned YPD media and 500 mL of *E. coli* conditioned YPD media. The 500 mL unconditioned and conditioned media were first sonicated for 5 minutes and then poured into separatory funnels where 1:1 volume of ethyl acetate was added and mixed with the media with gently inverting for about 1 minute. After 15 minutes of incubation at room temperature, the aqueous bottom layer and organic top layer were collected. The aqueous layer was added back to the separatory funnel and extracted with ethyl acetate two more times.

After three rounds of ethyl acetate extractions, the aqueous and organic extracts were dried in 1L round glass flasks using a rotovap. The organic extract was then resuspended in 100% LCMS grade methanol and moved to a 20 mL glass vial, and the aqueous component was resuspended in 100% LCMS grade water and moved to a 20 mL glass vials. A Biotage V10 evaporator was used to perform the final drying step on the extracts in their 20 mL vials.

Over 100 mg of organic extract from the unconditioned media and *E. coli* conditioned media were added to a Biotage Sfar C18 D column (Part No. FSUD-0401-0006) connected to a Biotage Selekt for fractionation. The organic extracts were fractionated into eight fractions based on a 0-100% Methanol solvent gradient in which 2 column volumes (18mL total) were collected per fraction: fraction #1 is 0-20% methanol, fraction #2 is 20-30% methanol, fraction #3 is 30-40% methanol, fraction #4 is 40-50% methanol, fraction #5 is 50-60% methanol, fraction #6 is

60-70% methanol, fraction #7 is 70-90% methanol, and fraction #8 is 90-100% methanol. Fractions were collected and dried with a Biotage V10.

4.5.15 MIC assays

Antifungal susceptibility testing was evaluated by broth microdilution MIC assay in flat-bottom 96-well plates as previously described[522]. Assays were performed in a total volume of 200 uL per well, with 2-fold dilutions of each drug in YPD or *Ec*-YPD. Plates were incubated for 24 hours at 30°C before OD_{600} values were determined on a BioTek 800 TS Absorbance Reader. Each condition was tested in biological and technical duplicates. Growth was normalized to the no drug control.

Name	Species	Alias	Source
CaTO1	*C. albicans*	SC5314	wildtype
CaTO167	*C. albicans*	813-61	416
CaTO168	*C. albicans*	946-12	416
CaTO392	*C. albicans*	P37039	458
CaTO93	*C. albicans*	811-36	416
CaTO387	*C. albicans*	P75063	492
CaTO165	*C. albicans*	824-51	416
CaTO174	*C. albicans*	847-7	416
CaTO378	*C. albicans*	P34048	463,464,493
CaTO386	*C. albicans*	P57055	496
CaTO390	*C. albicans*	P78042	497
CaTO146	*C. albicans*	SN152	500
CaTO640	*C. albicans*	rlm1Δ/Δ	501
CaTO641	*C. albicans*	rlm1Δ/Δ	502
CaTO642	*C. albicans*	sko1Δ/Δ	503
CaTO643	*C. albicans*	sko1Δ/Δ	505
CaTO620	*C. albicans*	bcr1Δ/Δ	506
CaTO621	*C. albicans*	bcr1Δ/Δ	507
CaTO622	*C. albicans*	cup9Δ/Δ	509
CaTO623	*C. albicans*	cup9Δ/Δ	510
CaTO626	*C. albicans*	tec1Δ/Δ	512
CaTO627	*C. albicans*	tec1Δ/Δ	480,481,510
CaTO634	*C. albicans*	crz1Δ/Δ	514
CaTO635	*C. albicans*	crz1Δ/Δ	516
CaTO636	*C. albicans*	mig1Δ/Δ	519
CaTO637	*C. albicans*	mig1Δ/Δ	520
CaTO119	*C. albicans*	SN250	521
CaTO657	*C. albicans*	hog1Δ/Δ	522
CaTO658	*C. albicans*	hog1Δ/Δ	491,492,521
CaTO661	*C. albicans*	pbs2Δ/Δ	492,493,522
CaTO662	*C. albicans*	pbs2Δ/Δ	523
CaTO659	*C. albicans*	mkc1Δ/Δ	525
CaTO660	*C. albicans*	mkc1Δ/Δ	344,493
CaTO685	*C. albicans*	cek1Δ/Δ	494,495,524
CaTO686	*C. albicans*	cek1Δ/Δ	496,497,526
CaTO741	*C. albicans*	chk1Δ/Δ	344,498
CaTO742	*C. albicans*	chk1Δ/Δ	513
CaTO743	*C. albicans*	nik1Δ/Δ	344,496
CaTO744	*C. albicans*	nik1Δ/Δ	344,498
CaTO687	*C. albicans*	sho1Δ/Δ	524
CaTO688	*C. albicans*	sho1Δ/Δ	515
CaTO204	*C. auris*	AR386	415,525
CaTO205	*C. dubliniensis*	Wü284	526
CaTO206	*C. glabrata*	Vaginal isolate	sent by Shannon Esher Righi

CaTO208	*C. parapsilosis*	ATCC 90018	sent by Shannon Esher Righi
CaTO209	*C. tropcalis*	ATCC 44508	sent by Shannon Esher Righi

Table 4-2: Fungal strains used in this chapter.

Name	Species	Alias
pTO217	*Escherichia coli*	MC1061
pTO353	*Escherichia coli*	MG1655
pTO354	*Escherichia coli*	CFT073
pTO355	*Escherichia coli*	UTI89
pTO218	*Pseudomonas aeruginosa*	PAK
pTO132	*Bacteroides thetaiotaomicron*	VPI-5482
pTO237	*Bacteroides fragilis*	VPI 2553
pTO238	*Bacteroides ovatus*	NCTC 11153
pTO317	*Enterococcus faecalis*	NCTC 775
pTO138	*Lactobacillus johnsonii*	MR-1

Table 4-3: Bacterial strains used in this chapter.

Chapter 5 Discussion

5.1 Overview

The goal of this work was to expand the current knowledge of *C. albicans* biology, with an emphasis on leveraging natural diversity and considering relevant host factors. I believe that careful consideration and incorporation of host factors and environmental pressures has the power to strengthen the interpretability of experimental results. First, as the majority of *C. albicans* research has been performed in the reference strain SC5314, I collected over 900 commensal *C. albicans* isolates from healthy donors to describe within-host diversity and identify potential adaptations that promote commensalism. Additionally, as both bacterial interactions and cell wall composition have profound impacts on fungal biology and virulence, I explored the intersection of these ideas to comprehensively characterize how bacteria alter the fungal cell wall and the downstream implications on antifungal sensitivity and immune recognition.

In Chapter 3, I collected commensal *C. albicans* isolates from healthy donors as a source of natural genetic and phenotypic diversity. My analysis of these isolates indicated that hosts can be simultaneously colonized by multiple, genetically distinct strains of *C. albicans*. We did not identify any genetic or phenotypic separation between oral and fecal isolates, emphasizing the versatility of *C. albicans* to colonize diverse niches. Importantly, we demonstrate that these commensal isolates retain their pathogenic potential, suggesting that commensal and clinical isolates of *C. albicans* are not distinct populations. We also leveraged genetically related isolates with divergent phenotypes to identify a causative mutation, highlighting the power of natural isolates in uncovering new facets of *C. albicans* biology.

In Chapter 4, I demonstrate that co-culture with bacteria induces fungal cell wall remodeling in *C. albicans*. This response was broadly conserved across different genetic backgrounds of *C. albicans* and *E. coli*, as well as multiple *Candida* and bacterial species, emphasizing the relevance of this interaction. Bacterial-induced fungal cell wall remodeling altered *C. albicans* antifungal sensitivity, recognition by innate immune receptors, and intestinal

IgA binding. Critically, I demonstrate that the addition of a single bacterial species to *in vivo* gastrointestinal colonization had the power to influence the fungal cell wall in the cecum.

5.2 Unanswered questions and future directions

5.2.1 Demographic information and longitudinal sampling

An important knowledge gap in the field that should be further explored is to correlate *C. albicans* colonization with demographic information, especially in regards to commensal colonization. Our donors in Chapter 3 were entirely anonymous, but ideally, we would have collected demographic information to broaden our conclusions. We would have liked to know our donor's age, sex, immune status, diet, and any recent antibiotic usage. As only 36% (35/98) of the donors were colonized with *C. albicans*, we could assess whether any particular host demographic information was associated with *C. albicans* colonization. For example, based on the mouse data, we might expect donors who had recently been treated with antibiotics to be more likely to be colonized with *C. albicans*. Although demographic information would be useful, determining correlations would still be difficult due to the number of variables that come into play.

We sampled donors for *C. albicans* colonization at only one time point, but longitudinal sampling could inform us about the stability of *C. albicans* carriage over time. For example, donors 882 and 811 were each colonized by multiple isolates that belonged to at least three distinct genetic clades. Longitudinal sampling across several months or years could inform us if distinct isolates can coexist long-term in a host or if some of these isolates might be transient colonizers and a dominant isolate would emerge. Additionally, in donor 814, we identified an isolate that displayed hyper-invasion into solid agar, which we could attribute to a single nucleotide polymorphism in Zms1. This hyper-invasive phenotype was only observed in one of this donor's 163 isolates. Although this isolate did not exhibit differences in competitive fitness or virulence in our *Galleria mellonella* models compared to its related isolates, longitudinal sampling could inform us if this phenotype conferred a fitness advantage or disadvantage for long-term colonization.

5.2.2 Limited diversity exploitation

It is common in the field to collect one representative colony of *C. albicans* when sampling from a donor; however, this approach assumes that hosts are colonized by only one strain of *C.*

albicans at a time. Therefore, when sampling for commensal *C. albicans* isolates, we intentionally collected every colony from each donor's sample in order to capture the breadth of diversity in a host. This approach allowed us to demonstrate that hosts can be simultaneously colonized by multiple, genetically distinct lineages of *C. albicans*. Another strength of our approach was that it provided us with many closely related isolates that displayed phenotypic variation but contained a limited number of single nucleotide polymorphisms. Therefore, we leveraged comparative genomics to identify causative variants in an approach we termed "limited diversity exploitation". This approach, coupled with longitudinal sampling, could be used to track *in vivo* evolution under different conditions. For example, the development of antifungal resistance during treatment could be monitored. In earlier time points following the initiation of antifungal treatment, many mutations that confer antifungal resistance or tolerance are likely to emerge but not all of these mutations will persist. Tracking the emergence and persistence of resistance-conferring mutations could provide important insights into how *C. albicans* adapts during antifungal treatment.

5.2.3 Potential transmission events

It is generally believed that the *C. albicans* population within a single host is clonal and that colonization is acquired during birth[441]. For these reasons, *C. albicans* is not thought to be commonly transmitted between hosts, like many pathogens are. Whole-genome sequencing of the condensed set of commensal isolates revealed that donors 882 and 811 had two instances, in two different genetic clades, of isolates that were nearly genetically identical. We believe this could indicate a transmission event between these individuals. We noted similar trends with other pairs of donors, where isolates collected from separate donors were closely related, such as in the case of isolates 859-2 and 806-1 or isolates 888-1 or 880-2. We hypothesize that donors with very closely related isolates may spend significant amounts of time together or even live together; however, we do not have the data to currently draw these conclusions.

In the future, the possibility of transmission between individuals could be investigated directly. For example, in the case of college students sharing a dorm room, unconnected individuals could be sampled for *C. albicans* before moving in together and throughout their time as roommates. If this kind of sampling could be performed on a large scale, it could inform us about how frequent or prevalent transmission of *C. albicans* is between cohabitating individuals. Transmission of diverse *C. albicans* isolates between individuals could be a

contributing factor to development of and susceptibility to disease that has not been fully explored.

5.2.4 Investigating *ROB1* in commensal isolates

As addressed in the introduction, the reference strain SC5314 is an outlier in its ability to robustly filament and form biofilms, and these distinct phenotypes were attributed to a rare *ROB1* allele that is not present in 224 other sequences strains [525]. Similarly, nearly all of our commensal isolates had a reduced capacity to form biofilms when compared to SC5314. In the future, we would like to determine if any of our 42 sequenced commensal isolates harbor the SC5314-derived *ROB1* allele, to add to the field's understanding of how unique this allele is amongst *C. albicans*. Importantly, the phenotypic effects of the SC5314-derived *ROB1* allele are dependent on the strain background and experimental conditions [496,497,527]. Therefore, introducing this allele into our commensal isolates could provide further insight into how genetic variation and circuit diversification influence the important phenotypes of filamentation and biofilm formation.

5.2.5 The role of *Bacteroides* in fungal cell wall remodeling

In Chapter 4, we investigated if gastrointestinal bacteria could influence the *C. albicans* cell wall composition. This project was initially based on series of papers demonstrating that *Bacteroides* species, including *Bacteroides thetaiotaomicron*, could degrade purified fungal cell wall polysaccharides, including mannan from *C. albicans*[526,527]. This work prompted us to investigate if *B. thetaiotaomicron* could degrade mannan from live *C. albicans*; therefore, we co-cultured these microbes in anaerobically and measured cell wall mannan following 24 hours of co-culture. To our surprise, we observed increased cell wall mannan content following co-culture, based on transmission electron microscopy and flow cytometry (Fig 5-1A-C). Based on this data, we hypothesized that if *B. thetaiotaomicron* was degrading mannan directly from the fungal cell wall, the increase in mannan we observed could be due to *C. albicans* upregulating mannan production as a compensatory mechanism. To test this, we obtained several *B. thetaiotaomicron* mutants that were missing individual enzymes or entire loci dedicated to degrading fungal mannan, including one strain that was missing all four polysaccharide utilization loci involved in mannan degradation. When we co-cultured *C. albicans* with these mutants, we consistently observed an increase in cell wall mannan, regardless of the bacteria's ability to degrade fungal

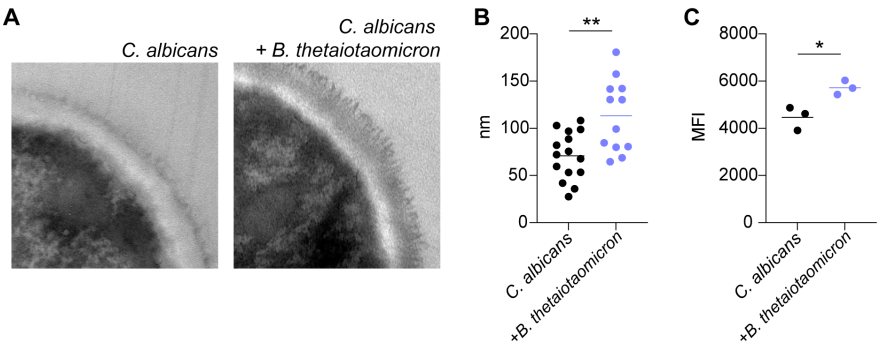


Figure 5-1: *C. albicans* displays increased mannan content following co-culture with *B. thetaiotaomicron.*

(A) Representative transmission electron micrographs of *C. albicans* grown for 24 hours in monoculture (left) or co-culture with *B. thetaiotaomicron* (right). 10,000x magnification. **(B)** Quantification of mannan fibrils lengths from TEMs. Significance determined by unpaired t-test. **(C)** Flow cytometric quantification of cel wall mannan content for *C. albicans* grown in monoculture or co-culture with *B. thetaiotaomicron*. Significance determined by paired t-test.

mannan (Fig 5-2). Based on these results, we concluded that mannan degradation was not related to the change in cell wall mannan content. We tested additional bacteria for their ability to influence the *C. albicans* cell wall and ultimately determined that *Bacteroides* species induced a comparatively weak cell wall remodeling response. Although we did not observe *B. thetaiotaomicron*-mediated mannan degradation in our system, work from other groups suggest that *Bacteroides* species can indeed degrade mannan from both live and dead *Candida* cells, although this has not been investigated in great mechanistic detail[528,529]. Importantly, these studies performed fungal-bacterial co-cultures under different media conditions from our study and from each other. This emphasizes that environmental conditions will have profound impacts on experimental results and should be carefully accounted for. Additionally, treating *C. albicans* with either murine colonic extracts or supernatants from *B. thetaiotaomicron* resulted in decreased mannan content, evident by fluorescent microscopy, flow cytometric quantification, and TEM images[529]. Finally, the localization of *C. albicans* in the murine gut is different when it is the sole colonizer than when *B. thetaiotaomicron* is also present. When both microbes are present, *B. thetaiotaomicron* promotes the formation of a robust mucus layer where *C. albicans* and *B. thetaiotaomicron* localize in close

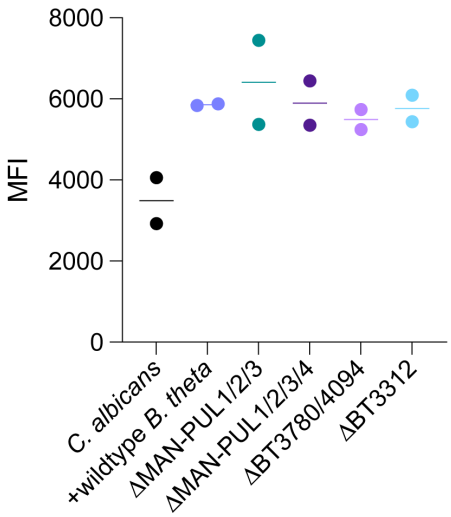


Figure 5-2: *B. thetaiotaomicron* mutants induce fungal cell wall remodeling, regardless of mannan-degradation abilities.

Flow cytometric quantification of *C. albicans* grown in monoculture or in co-culture with the indicates *B. thetaiotaomicron* mutants.

association, increasing the relevancy of potential *in vivo* interactions[528]. Altogether, these studies support the likelihood that *B. thetaiotaomicron* can degrade fungal mannan directly from an intact *C. albicans* cell wall and more research should be conducted to explore this interaction and the potential implications for both fungal and bacterial biology.

To further investigate interactions between these microbes, I would grow *B. thetaiotaomicron* in minimal media supplemented with purified fungal mannan, dead *C. albicans* cells, or live *C. albicans* cells. Over a time course, I would measure the bacterial growth rate in each of these conditions to determine when *B. thetaiotaomicron* can use fungal mannan to support its growth and if any of these conditions resulted in better growth efficiency. I would simultaneously quantify *C. albicans* cell wall mannan content with flow cytometry. If *B. thetaiotaomicron* was degrading fungal mannan from dead *C. albicans* cells, I would expect to observe a decrease in cell wall mannan that corresponds with the bacterial growth rate. I would compare the change in cell wall mannan content between dead and live *C. albicans* cells to determine if *C. albicans* alters its cell wall composition in response to degradation by *B. thetaiotaomicron*. In these experiments, *B. thetaiotaomicron* mutants deficient in mannan degradation could be used as a negative control. Next, I could supplement minimal media with different carbon sources to determine which carbon sources *B. thetaiotaomicron* would prioritize over fungal mannan. I would also determine if *E. coli*-mediated fungal cell wall remodeling, which results in increased mannan content, could better support *B. thetaiotaomicron* growth due to the increased mannan content. Finally, I would colonize mice with *C. albicans* alone or *C. albicans* and *B. thetaiotaomicron* to determine how *B. thetaiotaomicron* influences the fungal cell wall in the context of gastrointestinal colonization.

5.2.6 Bacterial-mediated fungal cell wall remodeling in the context of gastrointestinal colonization

There is a lack of understanding in the field of how different compositions of the bacterial microbiota influence the cell wall and the resulting immune response to *C. albicans* in the gastrointestinal tract. We demonstrated that the addition of *E. coli* to mice colonized with *C. albicans* influenced fungal cell wall composition and this influence differed based on the gastrointestinal compartment. In the future, we would like to more thoroughly characterize how bacteria influence the *C. albicans* cell wall during gastrointestinal colonization. For example, we demonstrated that bacteria have varying abilities to induce fungal cell wall remodeling;

therefore, we could hypothesize that different microbiota compositions would have different influences on the *C. albicans* cell wall during gastrointestinal colonization. To test this, we would begin by testing the contributions of individual bacteria, like we did with *E. coli*. After we determined how individual bacterial species influence the fungal cell wall during gastrointestinal colonization, we could begin increasing the complexity of the microbiota by introducing more bacterial species, one at a time. Introducing additional bacterial species individually would allow us to understand their relative contributions and determine if any species has a more substantial effect on the fungal cell wall. This should be coupled with quantifying the abundance of bacteria during gastrointestinal colonization; it might also be interesting to collect tissue and perform fluorescence *in situ* hybridization to consider how the spatial arrangements of *C. albicans* and bacterial species impacts their role in altering the fungal cell wall. In addition to measuring changes to the fungal cell wall *in vivo*, we could simultaneously test how these combinations of bacterial species influence the fungal cell wall in an *in vitro* co-culture system, to understand how host-intrinsic factors play a role in altering the fungal cell wall. Finally, it will be important to determine how these changes in the fungal cell wall alter the immune response to *C. albicans.* These experiments would allow us a deeper understanding of how bacterial-induced fungal cell wall remodeling is relevant during gastrointestinal colonization and how different microbiota compositions influence the fungal cell wall and the resulting immune response.

5.3 Future perspectives: incorporating host-relevant conditions and considering limitations of current models

It is becoming increasingly clear that the conditions under which experiments are conducted will have drastic impacts on the results and subsequent interpretation. This is especially relevant as we know *C. albicans* actively remodels its cell wall in response to different environment conditions, and the fungal cell wall has critical roles in antifungal sensitivity and immune recognition. For an example in my own work, as discussed above, in my co-culture system, I observed an increase in *C. albicans* cell wall mannan following co-culture with *B. thetaiotaomicron*, whereas other research groups investigating these microbes under alternate environment conditions demonstrated a decrease in cell wall mannan content[530]. In a similar vein, divergent cell wall remodeling in response to lactate was attributed to different sources of water between locations[531]. Additionally, characterizing antifungal resistance-conferring mutations in clinical isolates allows for novel mechanisms of resistance to be uncovered,

emphasizing that the selective pressures experienced in the host environment are distinct from those experienced in a laboratory setting[532]. In a particularly striking recent example, one research group demonstrated that host-relevant concentrations of CO_2 enhanced resistance to caspofungin, negatively impacting treatment efficacy [44,45,102–104,503,533]. Critically, strains that displayed resistance to caspofungin under host-relevant CO_2 concentrations remained susceptible in air, potentially implying that the current standards of susceptibility testing could be underestimating the true burden of antifungal resistance[528]. These results demonstrate that host-relevant conditions can greatly impact antifungal sensitivity and the development of resistance and further emphasizes the importance of conducting research with the relevant host environment in mind. Therefore, in order for our experimental results to have the most interpretability in relation to human colonization and disease, we must refine our models and make every effort to accurately replicate the host environment. This is especially true for *in vivo* models, which are intended to be interpretable in the context of human colonization and disease.

My work demonstrates that the addition of even a single bacteria *in vivo* can influence the *C. albicans* cell wall composition. Historically, the impact of bacteria, or the lack of bacteria, on fungal biology *in vivo* has been underappreciated and not always accounted for. As mice are not naturally colonized by *C. albicans*, adult mice are resistant to gastrointestinal colonization with SC5314; however, stable *C. albicans* gastrointestinal colonization can be established in mice which lack a robust gastrointestinal bacterial community. This can be achieved through antibiotic treatment or the use of germ-free or neonatal mice[527]. Although humans frequently receive antibiotic treatment and this represents an important risk factor for developing invasive infection, no one will ever be colonized by *C. albicans* in the absence of other microbes.

The presence or absence of bacteria when measuring fitness during gastrointestinal colonization can significantly impact conclusions. One experimental evolution study serially passaged *C. albicans* SC5314 through the murine gut in neonatal mice maintained either on antibiotics or control water[234]. Strains that were defective in filamentation, avirulent, and were hyperfit for gastrointestinal colonization were consistently produced only in the mice maintained on antibiotics[234]. These results imply that in the murine gut, the presence of an intact bacterial microbiota applies selective pressure on *C. albicans* to maintain morphogenesis and virulence programs. Several studies have similarly demonstrated that the yeast form of *C. albicans* is better suited for gastrointestinal colonization, however these results were also achieved in antibiotic-

treated or germ-free mice[529,530]. Indeed, yeast-locked strains of *C. albicans* only outcompete filamentation-competent strains when bacterial communities are depleted through antibiotic treatment. When fungal colonization is established through dietary intervention, a method that broadly preserves the native microbiota, yeast-locked strains are greatly outcompeted by the wildtype strain[528,529]. Of course, the results presented in this dissertation demonstrate that commensal isolates from healthy donors consistently retain the capacity to filament in response to standard laboratory inducing cues and retain their pathogenic potential. Together, this emphasizes that *in vivo* experimental results obtained when bacteria are severely depleted or absent entirely may not be reliable or interpretable in the context of human colonization and disease.

Importantly, the experiments described above used the standard reference isolate, SC5314. I have described how SC5314 is not an ideal representative of *C. albicans* as a species and how leveraging the natural diversity of commensal and clinical isolates allows us to gain new knowledge about fungal biology. In line with this, not all *C. albicans* isolates require antibiotic treatment to establish stable murine gastrointestinal colonization. CHN1, a lung isolate from clade A and 529L, an oral isolate from clade 16 are able to stably colonize the murine gastrointestinal tract without antibiotic intervention[235]. This difference was attributed to differential sensitivity to the antimicrobial peptide, CRAMP [531]. Identifying additional *C. albicans* isolates that can stably colonize the murine gastrointestinal tract without antibiotic intervention would increase the interpretability of *in vivo* results, as the impacts of a robust microbiota would be inherently accounted for. Natural commensal and clinical isolates of *C. albicans*, particularly ones derived from fecal samples, would be a strong starting place for identifying appropriate isolates.

The most frequently employed murine model of systemic candidiasis is induced by intravenous inoculation[532]. This method is technically straightforward and allows for high reproducibility. However, there are two critical flaws in this method that negatively impacts the interpretability of results in the context of human infection[533]. First, this method bypasses the requirement for *C. albicans* to translocate across mucosal barriers as an initial step in establishing disseminated infection. This precludes our ability to investigate host and fungal factors that prevent or promote translocation. Additionally, intravenous injection and gastrointestinal translocation demonstrate distinct routes of dissemination. In the intravenous

injection models, the kidneys are the main target, whereas during translocation, dissemination to the liver is more prominent[44,45,102–104,503,534]. Secondly, in the intravenous model of infection, the murine host is immunologically naïve to *C. albicans* and therefore does not have any trained innate immunity or adaptive immunity towards the pathogen[44,45,102–104,502,533]. Again, this is not an accurate reflection of how invasive infection arises in hospitalized patients, where an existing mucosal colonizing population is believed to be the primary source of disseminated candidiasis[70]. Therefore, intravenous injections do not account for innate and adaptive immune protection against systemic infections that develop as a result of commensal colonization prior to invasive infections.

Although we cannot solve all of the discrepancies between our *in vivo* models and the reality of human colonization and disease, we must at the very least be aware of the shortcomings of each model and take them into careful consideration when interpreting results. Leveraging the power of natural *C. albicans* isolates and considering the contributions of bacteria are two ways to increase the relevancy and interpretability of experimental results.

Bibliography

1. Nash, A. K. *et al.* The gut mycobiome of the Human Microbiome Project healthy cohort. *Microbiome* **5**, 153 (2017).
2. Delavy, M. *et al.* Unveiling Candida albicans intestinal carriage in healthy volunteers: the role of micro- and mycobiota, diet, host genetics and immune response. *Gut Microbes* **15**, 2287618 (2023).
3. Bougnoux, M.-E. *et al.* Multilocus sequence typing reveals intrafamilial transmission and microevolutions of Candida albicans isolates from the human digestive tract. *J. Clin. Microbiol.* **44**, 1810–1820 (2006).
4. Mukherjee, P. K. *et al.* Oral mycobiome analysis of HIV-infected patients: identification of Pichia as an antagonist of opportunistic fungi. *PLoS Pathog.* **10**, e1003996 (2014).
5. Xu, J. *et al.* Species and genotypic diversities and similarities of pathogenic yeasts colonizing women. *J. Clin. Microbiol.* **37**, 3835–3843 (1999).
6. Angebault, C. *et al.* Candida albicans is not always the preferential yeast colonizing humans: a study in Wayampi Amerindians. *J. Infect. Dis.* **208**, 1705–1716 (2013).
7. Gunsalus, K. T. W., Tornberg-Belanger, S. N., Matthan, N. R., Lichtenstein, A. H. & Kumamoto, C. A. Manipulation of host diet to reduce gastrointestinal colonization by the opportunistic pathogen Candida albicans. *mSphere* **1**, (2016).
8. Hoffmann, C. *et al.* Archaea and fungi of the human gut microbiome: correlations with diet and bacterial residents. *PLoS One* **8**, e66019 (2013).
9. Salmanton-García, J. *et al.* Attributable mortality of candidemia - Results from the ECMM Candida III multinational European Observational Cohort Study. *J. Infect.* **89**, 106229 (2024).
10. Pfaller, M. A. & Diekema, D. J. Epidemiology of invasive candidiasis: a persistent public health problem. *Clin. Microbiol. Rev.* **20**, 133–163 (2007).
11. World Health Organization. *WHO Fungal Priority Pathogens List Guide Research, Development Public Health Action*. (World Health Organization, Geneva, 2022).

12. Taschdjian, C. L., Burchall, J. J. & Kozinn, P. J. Rapid identification of Candida albicans by filamentation on serum and serum substitutes. *AMA J. Dis. Child.* **99**, 212–215 (1960).
13. Lo, H. J. *et al.* Nonfilamentous C. albicans mutants are avirulent. *Cell* **90**, 939–949 (1997).
14. Saville, S. P., Lazzell, A. L., Monteagudo, C. & Lopez-Ribot, J. L. Engineered control of cell morphology in vivo reveals distinct roles for yeast and filamentous forms of Candida albicans during infection. *Eukaryot. Cell* **2**, 1053–1060 (2003).
15. Noble, S. M., French, S., Kohn, L. A., Chen, V. & Johnson, A. D. Systematic screens of a Candida albicans homozygous deletion library decouple morphogenetic switching and pathogenicity. *Nat. Genet.* **42**, 590–598 (2010).
16. Braun, B. R., Head, W. S., Wang, M. X. & Johnson, A. D. Identification and characterization of TUP1-regulated genes in Candida albicans. *Genetics* **156**, 31–44 (2000).
17. Dunker, C. *et al.* Rapid proliferation due to better metabolic adaptation results in full virulence of a filament-deficient Candida albicans strain. *Nat. Commun.* **12**, 3899 (2021).
18. O'Meara, T. R. *et al.* High-Throughput Screening Identifies Genes Required for Candida albicans Induction of Macrophage Pyroptosis. *MBio* **9**, (2018).
19. O'Meara, T. R. *et al.* Global analysis of fungal morphology exposes mechanisms of host cell escape. *Nat. Commun.* **6**, 6741 (2015).
20. Wellington, M., Koselny, K. & Krysan, D. J. Candida albicans morphogenesis is not required for macrophage interleukin 1β production. *MBio* **4**, e00433-12 (2012).
21. Chow, E. W. L., Pang, L. M. & Wang, Y. From Jekyll to Hyde: The Yeast-Hyphal Transition of Candida albicans. *Pathogens* **10**, 859 (2021).
22. Takagi, J. *et al.* Mucin O-glycans are natural inhibitors of Candida albicans pathogenicity. *Nat. Chem. Biol.* 1–12 (2022).
23. Hogan, D. A., Vik, A. & Kolter, R. A Pseudomonas aeruginosa quorum-sensing molecule influences Candida albicans morphology. *Mol. Microbiol.* **54**, 1212–1223 (2004).
24. Kebaara, B. W. *et al.* Candida albicans Tup1 is involved in farnesol-mediated inhibition of filamentous-growth induction. *Eukaryot. Cell* **7**, 980–987 (2008).
25. Hornby, J. M. *et al.* Quorum sensing in the dimorphic fungus Candida albicans is mediated by farnesol. *Appl. Environ. Microbiol.* **67**, 2982–2992 (2001).

26. Cruz, M. R., Graham, C. E., Gagliano, B. C., Lorenz, M. C. & Garsin, D. A. Enterococcus faecalis inhibits hyphal morphogenesis and virulence of Candida albicans. *Infect. Immun.* **81**, 189–200 (2013).
27. MacAlpine, J. *et al.* A small molecule produced by Lactobacillus species blocks Candida albicans filamentation by inhibiting a DYRK1-family kinase. *Nat. Commun.* **12**, 6151 (2021).
28. Chen, H., Zhou, X., Ren, B. & Cheng, L. The regulation of hyphae growth in Candida albicans. *Virulence* **11**, 337–348 (2020).
29. Villa, S. *et al.* Transcriptional control of hyphal morphogenesis in Candida albicans. *FEMS Yeast Res.* **20**, (2020).
30. Glazier, V. E. EFG1, Everyone's Favorite Gene in Candida albicans: A Comprehensive Literature Review. *Front. Cell. Infect. Microbiol.* **12**, 855229 (2022).
31. Heilmann, C. J. *et al.* Hyphal induction in the human fungal pathogen Candida albicans reveals a characteristic wall protein profile. *Microbiology* **157**, 2297–2307 (2011).
32. Mukaremera, L., Lee, K. K., Mora-Montes, H. M. & Gow, N. A. R. Candida albicans Yeast, Pseudohyphal, and Hyphal Morphogenesis Differentially Affects Immune Recognition. *Front. Immunol.* **8**, 629 (2017).
33. Nantel, A. *et al.* Transcription profiling of Candida albicans cells undergoing the yeast-to-hyphal transition. *Mol. Biol. Cell* **13**, 3452–3465 (2002).
34. Lane, S., Birse, C., Zhou, S., Matson, R. & Liu, H. DNA array studies demonstrate convergent regulation of virulence factors by Cph1, Cph2, and Efg1 in Candida albicans. *J. Biol. Chem.* **276**, 48988–48996 (2001).
35. Kadosh, D. & Johnson, A. D. Induction of the Candida albicans filamentous growth program by relief of transcriptional repression: a genome-wide analysis. *Mol. Biol. Cell* **16**, 2903–2912 (2005).
36. Véronique, L., Véronique, A., Guillaume, C., Jean-Michel, C. & Françoise, A. Candida albicans cells exhibit media specific proteomic profiles during induction of filamentation. *BMC Microbiol.* **24**, 500 (2024).
37. Martínez-López, R. *et al.* Candida albicans Hyphal Extracellular Vesicles Are Different from Yeast Ones, Carrying an Active Proteasome Complex and Showing a Different Role in Host Immune Response. *Microbiol Spectr* e0069822 (2022).

38. Lowman, D. W. *et al.* Novel structural features in Candida albicans hyphal glucan provide a basis for differential innate immune recognition of hyphae versus yeast. *J. Biol. Chem.* **289**, 3432–3443 (2014).
39. Shibata, N., Suzuki, A., Kobayashi, H. & Okawa, Y. Chemical structure of the cell-wall mannan of Candida albicans serotype A and its difference in yeast and hyphal forms. *Biochem. J* **404**, 365–372 (2007).
40. Pérez, J. C. Candida albicans dwelling in the mammalian gut. *Curr. Opin. Microbiol.* **52**, 41–46 (2019).
41. Mishra, A. A. & Koh, A. Y. The microbial and host factors that govern Candida gastrointestinal colonization and dissemination. *Curr. Opin. Microbiol.* **63**, 29–35 (2021).
42. Markey, L. *et al.* Pre-colonization with the commensal fungus Candida albicans reduces murine susceptibility to Clostridium difficile infection. *Gut Microbes* **9**, 497–509 (2018).
43. Uppuluri, P. *et al.* The Hyr1 protein from the fungus Candida albicans is a cross kingdom immunotherapeutic target for Acinetobacter bacterial infection. *PLoS Pathog.* **14**, e1007056 (2018).
44. Quintin, J. *et al.* Candida albicans infection affords protection against reinfection via functional reprogramming of monocytes. *Cell Host Microbe* **12**, 223–232 (2012).
45. Saeed, S. *et al.* Epigenetic programming of monocyte-to-macrophage differentiation and trained innate immunity. *Science* **345**, 1251086 (2014).
46. Shao, T.-Y. *et al.* Commensal Candida albicans Positively Calibrates Systemic Th17 Immunological Responses. *Cell Host Microbe* **25**, 404-417.e6 (2019).
47. Richardson, J. P. *et al.* Candidalysins Are a New Family of Cytolytic Fungal Peptide Toxins. *MBio* e0351021 (2022).
48. Naglik, J. R., Gaffen, S. L. & Hube, B. Candidalysin: discovery and function in Candida albicans infections. *Curr. Opin. Microbiol.* **52**, 100–109 (2019).
49. Moyes, D. L. *et al.* Candidalysin is a fungal peptide toxin critical for mucosal infection. *Nature* **532**, 64–68 (2016).
50. Gulati, M. & Nobile, C. J. Candida albicans biofilms: development, regulation, and molecular mechanisms. *Microbes Infect.* **18**, 310–321 (2016).
51. Nobile, C. J. & Mitchell, A. P. Genetics and genomics of Candida albicans biofilm formation. *Cell. Microbiol.* **8**, 1382–1391 (2006).

52. Nobile, C. J. & Johnson, A. D. Candida albicans Biofilms and Human Disease. *Annu. Rev. Microbiol.* **69**, 71–92 (2015).
53. Tsui, C., Kong, E. F. & Jabra-Rizk, M. A. Pathogenesis of Candida albicans biofilm. *Pathog. Dis.* **74**, ftw018 (2016).
54. Puel, A. *et al.* Inborn errors of human IL-17 immunity underlie chronic mucocutaneous candidiasis. *Curr. Opin. Allergy Clin. Immunol.* **12**, 616–622 (2012).
55. Hernández-Santos, N. & Gaffen, S. L. Th17 cells in immunity to Candida albicans. *Cell Host Microbe* **11**, 425–435 (2012).
56. Gaffen, S. L., Hernández-Santos, N. & Peterson, A. C. IL-17 signaling in host defense against Candida albicans. *Immunol. Res.* **50**, 181–187 (2011).
57. Li, J., Casanova, J.-L. & Puel, A. Mucocutaneous IL-17 immunity in mice and humans: host defense vs. excessive inflammation. *Mucosal Immunol.* **11**, 581–589 (2018).
58. Ferwerda, B. *et al.* Human dectin-1 deficiency and mucocutaneous fungal infections. *N. Engl. J. Med.* **361**, 1760–1767 (2009).
59. van de Veerdonk, F. L. *et al.* STAT1 mutations in autosomal dominant chronic mucocutaneous candidiasis. *N. Engl. J. Med.* **365**, 54–61 (2011).
60. Liu, L. *et al.* Gain-of-function human STAT1 mutations impair IL-17 immunity and underlie chronic mucocutaneous candidiasis. *J. Exp. Med.* **208**, 1635–1648 (2011).
61. Glocker, E.-O. *et al.* A homozygous CARD9 mutation in a family with susceptibility to fungal infections. *N. Engl. J. Med.* **361**, 1727–1735 (2009).
62. Mengesha, B. G. & Conti, H. R. The role of IL-17 in protection against mucosal Candida infections. *J. Fungi (Basel)* **3**, (2017).
63. Strollo, S., Lionakis, M. S., Adjemian, J., Steiner, C. A. & Prevots, D. R. Epidemiology of hospitalizations associated with invasive candidiasis, United States, 2002-20121. *Emerg. Infect. Dis.* **23**, 7–13 (2016).
64. Wisplinghoff, H. *et al.* Nosocomial bloodstream infections in US hospitals: analysis of 24,179 cases from a prospective nationwide surveillance study. *Clin. Infect. Dis.* **39**, 309–317 (2004).
65. Wisplinghoff, H. *et al.* Nosocomial bloodstream infections due to Candida spp. in the USA: species distribution, clinical features and antifungal susceptibilities. *Int. J. Antimicrob. Agents* **43**, 78–81 (2014).

66. Enoch, D. A., Yang, H., Aliyu, S. H. & Micallef, C. The changing epidemiology of invasive fungal infections. *Methods Mol. Biol.* **1508**, 17–65 (2017).
67. Marco, F. *et al.* Elucidating the origins of nosocomial infections with Candida albicans by DNA fingerprinting with the complex probe Ca3. *J. Clin. Microbiol.* **37**, 2817–2828 (1999).
68. Nucci, M. & Anaissie, E. Revisiting the source of candidemia: skin or gut? *Clin. Infect. Dis.* **33**, 1959–1967 (2001).
69. Miranda, L. N. *et al.* Candida colonisation as a source for candidaemia. *J. Hosp. Infect.* **72**, 9–16 (2009).
70. Zhai, B. *et al.* High-resolution mycobiota analysis reveals dynamic intestinal translocation preceding invasive candidiasis. *Nat. Med.* **26**, 59–64 (2020).
71. Das, I., Nightingale, P., Patel, M. & Jumaa, P. Epidemiology, clinical characteristics, and outcome of candidemia: experience in a tertiary referral center in the UK. *Int. J. Infect. Dis.* **15**, e759-63 (2011).
72. Pappas, P. G., Lionakis, M. S., Arendrup, M. C., Ostrosky-Zeichner, L. & Kullberg, B. J. Invasive candidiasis. *Nat Rev Dis Primers* **4**, 18026 (2018).
73. Yapar, N. Epidemiology and risk factors for invasive candidiasis. *Ther. Clin. Risk Manag.* **10**, 95–105 (2014).
74. Kullberg, B. J. & Arendrup, M. C. Invasive candidiasis. *N. Engl. J. Med.* **373**, 1445–1456 (2015).
75. McCarty, T. P. & Pappas, P. G. Invasive candidiasis. *Infect. Dis. Clin. North Am.* **30**, 103–124 (2016).
76. Navarro-Arias, M. J. *et al.* Differential recognition of Candida tropicalis, Candida guilliermondii, Candida krusei, and Candida auris by human innate immune cells. *Infect. Drug Resist.* **12**, 783–794 (2019).
77. Munro, C. A. *et al.* Chs1 of Candida albicans is an essential chitin synthase required for synthesis of the septum and for cell integrity: CaChs1p is essential for growth and septum formation. *Mol. Microbiol.* **39**, 1414–1426 (2001).
78. Lenardon, M. D., Sood, P., Dorfmueller, H. C., Brown, A. J. P. & Gow, N. A. R. Scalar nanostructure of the Candida albicans cell wall; a molecular, cellular and ultrastructural analysis and interpretation. *Cell Surf* **6**, 100047 (2020).

79. Kitamura, A. *et al.* Effect of beta-1,6-glucan inhibitors on the invasion process of Candida albicans: potential mechanism of their in vivo efficacy. *Antimicrob. Agents Chemother.* **53**, 3963–3971 (2009).
80. Roemer, T. *et al.* Large-scale essential gene identification in Candida albicans and applications to antifungal drug discovery. *Molecular Microbiology* vol. 50 167–181 Preprint at https://doi.org/10.1046/j.1365-2958.2003.03697.x (2003).
81. Douglas, C. M. *et al.* Identification of the FKS1 gene of Candida albicans as the essential target of 1,3-beta-D-glucan synthase inhibitors. *Antimicrob. Agents Chemother.* **41**, 2471–2479 (1997).
82. Bates, S. *et al.* Role of the Candida albicans MNN1 gene family in cell wall structure and virulence. *BMC Res. Notes* **6**, 294 (2013).
83. Munro, C. A. *et al.* Mnt1p and Mnt2p of Candida albicans are partially redundant alpha-1,2-mannosyltransferases that participate in O-linked mannosylation and are required for adhesion and virulence. *J. Biol. Chem.* **280**, 1051–1060 (2005).
84. Bates, S. *et al.* Outer chain N-glycans are required for cell wall integrity and virulence of Candida albicans. *J. Biol. Chem.* **281**, 90–98 (2006).
85. Mille, C. *et al.* Inactivation of CaMIT1 inhibits Candida albicans phospholipomannan beta-mannosylation, reduces virulence, and alters cell wall protein beta-mannosylation. *J. Biol. Chem.* **279**, 47952–47960 (2004).
86. Pardini, G. *et al.* The CRH family coding for cell wall glycosylphosphatidylinositol proteins with a predicted transglycosidase domain affects cell wall organization and virulence of Candida albicans. *J. Biol. Chem.* **281**, 40399–40411 (2006).
87. Herrero, A. B. *et al.* KRE5 gene null mutant strains of Candida albicans are avirulent and have altered cell wall composition and hypha formation properties. *Eukaryot. Cell* **3**, 1423–1432 (2004).
88. Taylor, P. R. *et al.* Dectin-1 is required for beta-glucan recognition and control of fungal infection. *Nat. Immunol.* **8**, 31–38 (2007).
89. Vautier, S. *et al.* Dectin-1 is not required for controlling Candida albicans colonization of the gastrointestinal tract. *Infect. Immun.* **80**, 4216–4222 (2012).
90. Saijo, S. *et al.* Dectin-1 is required for host defense against Pneumocystis carinii but not against Candida albicans. *Nat. Immunol.* **8**, 39–46 (2007).

91. Rosentul, D. C. *et al.* Genetic variation in the dectin-1/CARD9 recognition pathway and susceptibility to candidemia. *J. Infect. Dis.* **204**, 1138–1145 (2011).
92. Pyz, E., Marshall, A. S. J., Gordon, S. & Brown, G. D. C-type lectin-like receptors on myeloid cells. *Ann. Med.* **38**, 242–251 (2006).
93. Rao, R. *et al.* Interleukin 17-producing γδT cells promote hepatic regeneration in mice. *Gastroenterology* **147**, 473–84.e2 (2014).
94. Taylor, P. R. *et al.* The beta-glucan receptor, dectin-1, is predominantly expressed on the surface of cells of the monocyte/macrophage and neutrophil lineages. *J. Immunol.* **169**, 3876–3882 (2002).
95. Pradhan, A. *et al.* Non-canonical signalling mediates changes in fungal cell wall PAMPs that drive immune evasion. *Nat. Commun.* **10**, 5315 (2019).
96. Ballou, E. R. *et al.* Lactate signalling regulates fungal β-glucan masking and immune evasion. *Nat Microbiol* **2**, 16238 (2016).
97. Sherrington, S. L. *et al.* Adaptation of Candida albicans to environmental pH induces cell wall remodelling and enhances innate immune recognition. *PLoS Pathog.* **13**, e1006403 (2017).
98. Tripathi, A., Liverani, E., Tsygankov, A. Y. & Puri, S. Iron alters the cell wall composition and intracellular lactate to affect Candida albicans susceptibility to antifungals and host immune response. *J. Biol. Chem.* **295**, 10032–10044 (2020).
99. Galán-Díez, M. *et al.* Candida albicans beta-glucan exposure is controlled by the fungal CEK1-mediated mitogen-activated protein kinase pathway that modulates immune responses triggered through dectin-1. *Infect. Immun.* **78**, 1426–1436 (2010).
100. Herre, J. *et al.* Dectin-1 uses novel mechanisms for yeast phagocytosis in macrophages. *Blood* **104**, 4038–4045 (2004).
101. Miramón, P., Kasper, L. & Hube, B. Thriving within the host: Candida spp. interactions with phagocytic cells. *Med. Microbiol. Immunol.* **202**, 183–195 (2013).
102. Mata-Martínez, P., Bergón-Gutiérrez, M. & Del Fresno, C. Dectin-1 Signaling Update: New Perspectives for Trained Immunity. *Front. Immunol.* **13**, 812148 (2022).
103. Drummond, R. A. *et al.* CD4(+) T-cell survival in the GI tract requires dectin-1 during fungal infection. *Mucosal Immunol.* **9**, 492–502 (2016).

104. Gringhuis, S. I. *et al.* Fungal sensing by dectin-1 directs the non-pathogenic polarization of TH17 cells through balanced type I IFN responses in human DCs. *Nat. Immunol.* 1–14 (2022).
105. Akins, R. A. An update on antifungal targets and mechanisms of resistance in Candida albicans. *Med. Mycol.* **43**, 285–318 (2005).
106. Eliaš, D., Tóth Hervay, N. & Gbelská, Y. Ergosterol biosynthesis and regulation impact the antifungal resistance and virulence of Candida spp. *Stresses* **4**, 641–662 (2024).
107. Nishimoto, A. T., Sharma, C. & Rogers, P. D. Molecular and genetic basis of azole antifungal resistance in the opportunistic pathogenic fungus Candida albicans. *J. Antimicrob. Chemother.* **75**, 257–270 (2020).
108. Flowers, S. A., Colón, B., Whaley, S. G., Schuler, M. A. & Rogers, P. D. Contribution of clinically derived mutations in ERG11 to azole resistance in Candida albicans. *Antimicrob. Agents Chemother.* **59**, 450–460 (2015).
109. Flowers, S. A. *et al.* Gain-of-function mutations in UPC2 are a frequent cause of ERG11 upregulation in azole-resistant clinical isolates of Candida albicans. *Eukaryot. Cell* **11**, 1289–1299 (2012).
110. Shi, H., Zhang, Y., Zhang, M., Chang, W. & Lou, H. Molecular mechanisms of azole resistance in four clinical Candida albicans isolates. *Microb. Drug Resist.* **27**, 1641–1651 (2021).
111. Coste, A. *et al.* Genotypic evolution of azole resistance mechanisms in sequential Candida albicans isolates. *Eukaryot. Cell* **6**, 1889–1904 (2007).
112. Espinel-Ingroff, A. *et al.* Multilaboratory study of epidemiological cutoff values for detection of resistance in eight Candida species to fluconazole, posaconazole, and voriconazole. *Antimicrob. Agents Chemother.* **58**, 2006–2012 (2014).
113. Whaley, S. G. *et al.* Azole antifungal resistance in Candida albicans and emerging non-albicans Candida species. *Front. Microbiol.* **7**, 2173 (2016).
114. Chow, N. A. *et al.* Tracing the evolutionary history and global expansion of Candida auris using population genomic analyses. *MBio* **11**, (2020).
115. Rybak, J. M., Cuomo, C. A. & Rogers, P. D. The molecular and genetic basis of antifungal resistance in the emerging fungal pathogen Candida auris. *Curr. Opin. Microbiol.* **70**, 102208 (2022).

116. Chowdhary, A. *et al.* A multicentre study of antifungal susceptibility patterns among 350 Candida auris isolates (2009-17) in India: role of the ERG11 and FKS1 genes in azole and echinocandin resistance. *J. Antimicrob. Chemother.* **73**, 891–899 (2018).
117. Dutcher, J. D. The discovery and development of amphotericin B. *Dis. Chest* **54**, Suppl 1:296-8 (1968).
118. Anderson, T. M. *et al.* Amphotericin forms an extramembranous and fungicidal sterol sponge. *Nat. Chem. Biol.* **10**, 400–406 (2014).
119. Vincent, B. M., Lancaster, A. K., Scherz-Shouval, R., Whitesell, L. & Lindquist, S. Fitness trade-offs restrict the evolution of resistance to amphotericin B. *PLoS Biol.* **11**, e1001692 (2013).
120. Baginski, M., Resat, H. & Borowski, E. Comparative molecular dynamics simulations of amphotericin B-cholesterol/ergosterol membrane channels. *Biochim. Biophys. Acta* **1567**, 63–78 (2002).
121. Kamiński, D. M. Recent progress in the study of the interactions of amphotericin B with cholesterol and ergosterol in lipid environments. *Eur. Biophys. J.* **43**, 453–467 (2014).
122. Park, S. *et al.* Specific substitutions in the echinocandin target Fks1p account for reduced susceptibility of rare laboratory and clinical Candida sp. isolates. *Antimicrob. Agents Chemother.* **49**, 3264–3273 (2005).
123. Balashov, S. V., Park, S. & Perlin, D. S. Assessing resistance to the echinocandin antifungal drug caspofungin in Candida albicans by profiling mutations in FKS1. *Antimicrob. Agents Chemother.* **50**, 2058–2063 (2006).
124. Hori, Y. & Shibuya, K. Role of FKS gene in the susceptibility of pathogenic fungi to echinocandins. *Med. Mycol. J.* **59**, E31–E40 (2018).
125. Yang, F. *et al.* Tolerance to caspofungin in Candida albicans is associated with at least three distinctive mechanisms that govern expression of FKS genes and cell wall remodeling. *Antimicrob. Agents Chemother.* **61**, (2017).
126. Husain, F., Yadav, A., Sah, S. K., Hayes, J. J. & Rustchenko, E. Candida albicans strains adapted to caspofungin due to aneuploidy become highly tolerant under continued drug pressure. *Microorganisms* **11**, 23 (2022).
127. Plaine, A. *et al.* Functional analysis of Candida albicans GPI-anchored proteins: roles in cell wall integrity and caspofungin sensitivity. *Fungal Genet. Biol.* **45**, 1404–1414 (2008).

128. Sah, S. K., Yadav, A., Kruppa, M. D. & Rustchenko, E. Identification of 10 genes on Candida albicans chromosome 5 that control surface exposure of the immunogenic cell wall epitope β-glucan and cell wall remodeling in caspofungin-adapted mutants. *Microbiol Spectr* e0329523 (2023).
129. Walker, L. A. *et al.* Stimulation of chitin synthesis rescues Candida albicans from echinocandins. *PLoS Pathog.* **4**, e1000040 (2008).
130. Walker, L. A., Gow, N. A. R. & Munro, C. A. Elevated chitin content reduces the susceptibility of Candida species to caspofungin. *Antimicrob. Agents Chemother.* **57**, 146–154 (2013).
131. Pappas, P. G. *et al.* Clinical practice guideline for the management of candidiasis: 2016 update by the infectious diseases society of America. *Clin. Infect. Dis.* **62**, e1-50 (2016).
132. Brown, A. J. P., Brown, G. D., Netea, M. G. & Gow, N. A. R. Metabolism impacts upon Candida immunogenicity and pathogenicity at multiple levels. *Trends Microbiol.* **22**, 614–622 (2014).
133. Chen, T., Wagner, A. S. & Reynolds, T. B. When Is It Appropriate to Take Off the Mask? Signaling Pathways That Regulate ß(1,3)-Glucan Exposure in Candida albicans. *Frontiers in Fungal Biology* **3**, (2022).
134. Pradhan, A. *et al.* Hypoxia Promotes Immune Evasion by Triggering β-Glucan Masking on the Candida albicans Cell Surface via Mitochondrial and cAMP-Protein Kinase A Signaling. *MBio* **9**, (2018).
135. Ene, I. V. *et al.* Host carbon sources modulate cell wall architecture, drug resistance and virulence in a fungal pathogen. *Cell. Microbiol.* **14**, 1319–1335 (2012).
136. Cottier, F. *et al.* Remasking of Candida albicans β-Glucan in Response to Environmental pH Is Regulated by Quorum Sensing. *MBio* **10**, (2019).
137. Ma, Q. *et al.* Impact of secreted glucanases upon the cell surface and fitness of Candida albicans during colonisation and infection. *Cell Surf* **11**, 100128 (2024).
138. Tsai, P.-W., Yang, C.-Y., Chang, H.-T. & Lan, C.-Y. Human Antimicrobial Peptide LL-37 Inhibits Adhesion of Candida albicans by Interacting with Yeast Cell-Wall Carbohydrates. *PLoS ONE* vol. 6 e17755 Preprint at https://doi.org/10.1371/journal.pone.0017755 (2011).

139. Chang, H.-T. *et al.* LL37 and hBD-3 elevate the β-1,3-exoglucanase activity of Candida albicans Xog1p, resulting in reduced fungal adhesion to plastic. *Biochem. J* **441**, 963–970 (2012).
140. Ene, I. V. *et al.* Carbon source-induced reprogramming of the cell wall proteome and secretome modulates the adherence and drug resistance of the fungal pathogen Candida albicans. *Proteomics* **12**, 3164–3179 (2012).
141. Lowman, D. W. *et al.* Mannan structural complexity is decreased when Candida albicans is cultivated in blood or serum at physiological temperature. *Carbohydr. Res.* **346**, 2752–2759 (2011).
142. Graus, M. S. *et al.* Mannan Molecular Substructures Control Nanoscale Glucan Exposure in Candida. *Cell Rep.* **24**, 2432-2442.e5 (2018).
143. Avelar, G. M. *et al.* Impact of changes at the Candida albicans cell surface upon immunogenicity and colonisation in the gastrointestinal tract. *The Cell Surface* **8**, 100084 (2022).
144. Yang, M. *et al.* Control of β-glucan exposure by the endo-1,3-glucanase Eng1 in Candida albicans modulates virulence. *PLoS Pathog.* **18**, e1010192 (2022).
145. Yadav, B. *et al.* Differences in fungal immune recognition by monocytes and macrophages: N-mannan can be a shield or activator of immune recognition. *Cell Surf.* **6**, 100042 (2020).
146. Hall, R. A. *et al.* The Mnn2 mannosyltransferase family modulates mannoprotein fibril length, immune recognition and virulence of Candida albicans. *PLoS Pathog.* **9**, e1003276 (2013).
147. Bain, J. M. *et al.* Candida albicans hypha formation and mannan masking of β-glucan inhibit macrophage phagosome maturation. *mBio* **5**, e01874 (2014).
148. Childers, D. S. *et al.* Epitope Shaving Promotes Fungal Immune Evasion. *MBio* **11**, (2020).
149. de Assis, L. J. *et al.* Nature of β-1,3-Glucan-Exposing Features on Candida albicans Cell Wall and Their Modulation. *MBio* e0260522 (2022).
150. Naseem, S., Min, K., Spitzer, D., Gardin, J. & Konopka, J. B. Regulation of hyphal growth and N-acetylglucosamine catabolism by two transcription factors in Candida albicans. *Genetics* **206**, 299–314 (2017).

151. Huang, G., Huang, Q., Wei, Y., Wang, Y. & Du, H. Multiple roles and diverse regulation of the Ras/cAMP/protein kinase A pathway in Candida albicans: Ras/cAMP/PKA pathway in C. albicans. *Mol. Microbiol.* **111**, 6–16 (2019).
152. Wagner, A. S., Lumsdaine, S. W., Mangrum, M. M. & Reynolds, T. B. Caspofungin-induced β(1,3)-glucan exposure in Candida albicans is driven by increased chitin levels. *MBio* **14**, e0007423 (2023).
153. Munro, C. A. *et al.* The PKC, HOG and Ca2+ signalling pathways co-ordinately regulate chitin synthesis in Candida albicans. *Mol. Microbiol.* **63**, 1399–1413 (2007).
154. Wagner, A. S. *et al.* Cek1 regulates ß(1,3)-glucan exposure through calcineurin effectors in Candida albicans. *PLoS Genet.* **18**, e1010405 (2022).
155. Rauceo, J. M. *et al.* Regulation of the Candida albicans cell wall damage response by transcription factor Sko1 and PAS kinase Psk1. *Mol. Biol. Cell* **19**, 2741–2751 (2008).
156. Bruno, V. M. *et al.* Control of the C. albicans cell wall damage response by transcriptional regulator Cas5. *PLoS Pathog.* **2**, e21 (2006).
157. Heredia, M. Y. *et al.* An expanded cell wall damage signaling network is comprised of the transcription factors Rlm1 and Sko1 in Candida albicans. *PLoS Genet.* **16**, e1008908 (2020).
158. Heredia, M. Y., Gunasekaran, D., Ikeh, M. A. C., Nobile, C. J. & Rauceo, J. M. Transcriptional regulation of the caspofungin-induced cell wall damage response in Candida albicans. *Curr. Genet.* **66**, 1059–1068 (2020).
159. Xie, J. L. *et al.* The Candida albicans transcription factor Cas5 couples stress responses, drug resistance and cell cycle regulation. *Nat. Commun.* **8**, 499 (2017).
160. Proft, M. *et al.* Regulation of the Sko1 transcriptional repressor by the Hog1 MAP kinase in response to osmotic stress. *EMBO J.* **20**, 1123–1133 (2001).
161. Pittet, D., Li, N., Woolson, R. F. & Wenzel, R. P. Microbiological factors influencing the outcome of nosocomial bloodstream infections: a 6-year validated, population-based model. *Clin. Infect. Dis.* **24**, 1068–1078 (1997).
162. Pavlaki, M. *et al.* Polymicrobial bloodstream infections: Epidemiology and impact on mortality. *J. Glob. Antimicrob. Resist.* **1**, 207–212 (2013).

163. Hou, J. *et al.* Epidemiology, clinical characteristics, risk factors, and outcomes of candidemia in a large tertiary teaching hospital in western China: A retrospective 5-year study from 2016 to 2020. *Antibiotics (Basel)* **11**, 788 (2022).
164. Cheng, Y.-R. *et al.* Risk factors for candidemia-related mortality at a medical center in central Taiwan. *J. Microbiol. Immunol. Infect.* **39**, 155–161 (2006).
165. Thomas-Rüddel, D. O., Schlattmann, P., Pletz, M., Kurzai, O. & Bloos, F. Risk factors for invasive Candida infection in critically ill patients: A systematic review and meta-analysis. *Chest* **161**, 345–355 (2022).
166. Seelig, M. S. The role of antibiotics in the pathogenesis of Candidainfections. *Am. J. Med.* **40**, 887–917 (1966).
167. Seelig, M. S. Mechanisms by which antibiotics increase the incidence and severity of candidiasis and alter the immunological defenses. *Bacteriol. Rev.* **30**, 442–459 (1966).
168. Delavy, M. *et al.* A clinical study provides the first direct evidence that interindividual variations in fecal β-lactamase activity affect the gut mycobiota dynamics in response to β-lactam antibiotics. *MBio* **13**, e0288022 (2022).
169. Seelbinder, B. *et al.* Antibiotics create a shift from mutualism to competition in human gut communities with a longer-lasting impact on fungi than bacteria. *Microbiome* **8**, 133 (2020).
170. Ventin-Holmberg, R. *et al.* The effect of antibiotics on the infant gut fungal Microbiota. *J. Fungi (Basel)* **8**, 328 (2022).
171. Fan, D. *et al.* Activation of HIF-1α and LL-37 by commensal bacteria inhibits Candida albicans colonization. *Nat. Med.* **21**, 808–814 (2015).
172. Guinan, J., Wang, S., Hazbun, T. R., Yadav, H. & Thangamani, S. Antibiotic-induced decreases in the levels of microbial-derived short-chain fatty acids correlate with increased gastrointestinal colonization of Candida albicans. *Sci. Rep.* **9**, 8872 (2019).
173. Gutierrez, D. *et al.* Antibiotic-induced gut metabolome and microbiome alterations increase the susceptibility to Candida albicans colonization in the gastrointestinal tract. *FEMS Microbiol. Ecol.* **96**, (2020).
174. Savage, H. P. *et al.* Epithelial hypoxia maintains colonization resistance against Candida albicans. *Cell Host Microbe* (2024) doi:10.1016/j.chom.2024.05.008.

175. Tan, C. T., Xu, X., Qiao, Y. & Wang, Y. A peptidoglycan storm caused by β-lactam antibiotic's action on host microbiota drives Candida albicans infection. *Nat. Commun.* **12**, 1–13 (2021).
176. Erb Downward, J. R., Falkowski, N. R., Mason, K. L., Muraglia, R. & Huffnagle, G. B. Modulation of Post-Antibiotic Bacterial Community Reassembly and Host Response by Candida albicans. *Sci. Rep.* **3**, 1–11 (2013).
177. Mason, K. L. *et al.* Interplay between the gastric bacterial microbiota and Candida albicans during postantibiotic recolonization and gastritis. *Infect. Immun.* **80**, 150–158 (2012).
178. Mason, K. L. *et al.* Candida albicans and bacterial microbiota interactions in the cecum during recolonization following broad-spectrum antibiotic therapy. *Infect. Immun.* **80**, 3371–3380 (2012).
179. Montravers, P. *et al.* Candida as a risk factor for mortality in peritonitis. *Crit. Care Med.* **34**, 646–652 (2006).
180. Klotz, S. A., Chasin, B. S., Powell, B., Gaur, N. K. & Lipke, P. N. Polymicrobial bloodstream infections involving Candida species: analysis of patients and review of the literature. *Diagn. Microbiol. Infect. Dis.* **59**, 401–406 (2007).
181. Zhong, L. *et al.* Clinical characteristics, risk factors and outcomes of mixed Candida albicans/bacterial bloodstream infections. *BMC Infect. Dis.* **20**, 810 (2020).
182. Hughes, M. G. *et al.* Comparison of fungal and nonfungal infections in a broad-based surgical patient population. *Surg. Infect. (Larchmt)* **6**, 55–64 (2005).
183. Dyess, D. L., Garrison, R. N. & Fry, D. E. Candida sepsis. Implications of polymicrobial blood-borne infection. *Arch. Surg.* **120**, 345–348 (1985).
184. Zhong, L. *et al.* Incidence, clinical characteristics, risk factors and outcomes of patients with mixed Candida/bacterial bloodstream infections: a retrospective study. *Ann. Clin. Microbiol. Antimicrob.* **21**, 45 (2022).
185. Peters, B. M. & Noverr, M. C. Candida albicans-Staphylococcus aureus polymicrobial peritonitis modulates host innate immunity. *Infect. Immun.* **81**, 2178–2189 (2013).
186. Nash, E. E., Peters, B. M., Palmer, G. E., Fidel, P. L. & Noverr, M. C. Morphogenesis is not required for Candida albicans-Staphylococcus aureus intra-abdominal infection-mediated dissemination and lethal sepsis. *Infect. Immun.* **82**, 3426–3435 (2014).

187. Peters, B. M. *et al.* Staphylococcus aureus adherence to Candida albicans hyphae is mediated by the hyphal adhesin Als3p. *Microbiology* **158**, 2975–2986 (2012).
188. Hernandez-Cuellar, E. *et al.* Characterization of Candida albicans and Staphylococcus aureus polymicrobial biofilm on different surfaces. *Rev. Iberoam. Micol.* **39**, 36–43 (2022).
189. Baxter, K. J., Sargison, F. A., Fitzgerald, J. R., McConnell, G. & Hoskisson, P. A. Time-lapse mesoscopy of Candida albicans and Staphylococcus aureus dual-species biofilms reveals a structural role for the hyphae of C. albicans in biofilm formation. *Microbiology* **170**, (2024).
190. Harriott, M. M. & Noverr, M. C. Candida albicans and Staphylococcus aureus form polymicrobial biofilms: effects on antimicrobial resistance. *Antimicrob. Agents Chemother.* **53**, 3914–3922 (2009).
191. Kong, E. F. *et al.* Commensal Protection of Staphylococcus aureus against Antimicrobials by Candida albicans Biofilm Matrix. *MBio* **7**, (2016).
192. Rossoni, R. D. *et al.* Clinical strains of Lactobacillus reduce the filamentation of Candida albicans and protect Galleria mellonella against experimental candidiasis. *Folia Microbiol.* **63**, 307–314 (2018).
193. Wang, S. *et al.* Antimicrobial Compounds Produced by Vaginal Lactobacillus crispatus Are Able to Strongly Inhibit Candida albicans Growth, Hyphal Formation and Regulate Virulence-related Gene Expressions. *Front. Microbiol.* **8**, 564 (2017).
194. Allonsius, C. N. *et al.* Inhibition of Candida albicans morphogenesis by chitinase from Lactobacillus rhamnosus GG. *Sci. Rep.* **9**, 2900 (2019).
195. Santos, R. B. *et al.* Lactobacillus species increase the survival of Galleria mellonella infected with Candida albicans and non-albicans Candida clinical isolates. *Med. Mycol.* **57**, 391–394 (2019).
196. Hogan, D. A. & Kolter, R. Pseudomonas-Candida interactions: an ecological role for virulence factors. *Science* **296**, 2229–2232 (2002).
197. Bandara, H. M. H. N., K Cheung, B. P., Watt, R. M., Jin, L. J. & Samaranayake, L. P. Pseudomonas aeruginosa lipopolysaccharide inhibits Candida albicans hyphae formation and alters gene expression during biofilm development. *Mol. Oral Microbiol.* **28**, 54–69 (2013).

198. Brand, A., Barnes, J. D., Mackenzie, K. S., Odds, F. C. & Gow, N. A. R. Cell wall glycans and soluble factors determine the interactions between the hyphae of Candida albicans and Pseudomonas aeruginosa. *FEMS Microbiol. Lett.* **287**, 48–55 (2008).
199. Morales, D. K. *et al.* Antifungal mechanisms by which a novel Pseudomonas aeruginosa phenazine toxin kills Candida albicans in biofilms. *Mol. Microbiol.* **78**, 1379–1392 (2010).
200. Morales, D. K. *et al.* Control of Candida albicans metabolism and biofilm formation by Pseudomonas aeruginosa phenazines. *MBio* **4**, e00526-12 (2013).
201. Bergeron, A. C. *et al.* Candida albicans and Pseudomonas aeruginosa Interact To Enhance Virulence of Mucosal Infection in Transparent Zebrafish. *Infect. Immun.* **85**, (2017).
202. Neely, A. N., Law, E. J. & Holder, I. A. Increased susceptibility to lethal Candida infections in burned mice preinfected with Pseudomonas aeruginosa or pretreated with proteolytic enzymes. *Infect. Immun.* **52**, 200–204 (1986).
203. Mortimer, R. K. & Johnston, J. R. Genealogy of principal strains of the yeast genetic stock center. *Genetics* **113**, 35–43 (1986).
204. Peter, J. *et al.* Genome evolution across 1,011 Saccharomyces cerevisiae isolates. *Nature* **556**, 339–344 (2018).
205. Warringer, J. *et al.* Trait variation in yeast is defined by population history. *PLoS Genet.* **7**, e1002111 (2011).
206. Klockgether, J. *et al.* Genome diversity of Pseudomonas aeruginosa PAO1 laboratory strains. *J. Bacteriol.* **192**, 1113–1121 (2010).
207. Bradley, M. D., Neu, D., Bahar, F. & Welch, R. D. Inter-laboratory evolution of a model organism and its epistatic effects on mutagenesis screens. *Sci. Rep.* **6**, 38001 (2016).
208. Nahku, R. *et al.* Stock culture heterogeneity rather than new mutational variation complicates short-term cell physiology studies of Escherichia coli K-12 MG1655 in continuous culture. *Microbiology* **157**, 2604–2610 (2011).
209. Arras, S. D. M. *et al.* Convergent microevolution of Cryptococcus neoformans hypervirulence in the laboratory and the clinic. *Sci. Rep.* **7**, 17918 (2017).
210. Catoiu, E. A., Phaneuf, P., Monk, J. & Palsson, B. O. Whole-genome sequences from wild-type and laboratory-evolved strains define the alleleome and establish its hallmarks. *Proc. Natl. Acad. Sci. U. S. A.* **120**, e2218835120 (2023).

211. Rousset, F. *et al.* The impact of genetic diversity on gene essentiality within the Escherichia coli species. *Nat. Microbiol.* **6**, 301–312 (2021).
212. Dowell, R. D. *et al.* Genotype to phenotype: a complex problem. *Science* **328**, 469 (2010).
213. Galardini, M. *et al.* The impact of the genetic background on gene deletion phenotypes in Saccharomyces cerevisiae. *Mol. Syst. Biol.* **15**, e8831 (2019).
214. Martínez-Carranza, E. *et al.* Variability of bacterial essential genes among closely related bacteria: The case of Escherichia coli. *Front. Microbiol.* **9**, 1059 (2018).
215. Lofgren, L. A., Ross, B. S., Cramer, R. A. & Stajich, J. E. The pan-genome of Aspergillus fumigatus provides a high-resolution view of its population structure revealing high levels of lineage-specific diversity driven by recombination. *PLoS Biol.* **20**, e3001890 (2022).
216. Hale, J. J. *et al.* Genome-scale analysis of interactions between genetic perturbations and natural variation. *Nat. Commun.* **15**, 4234 (2024).
217. Jones, T. *et al.* The diploid genome sequence of Candida albicans. *Proc. Natl. Acad. Sci. U. S. A.* **101**, 7329–7334 (2004).
218. Odds, F. C., Brown, A. J. P. & Gow, N. A. R. Candida albicans genome sequence: a platform for genomics in the absence of genetics. *Genome Biol.* **5**, 230 (2004).
219. Maestrone, G. & Semar, R. Establishment and treatment of cutaneous Candida albicans infection in the rabbit. *Naturwissenschaften* **55**, 87–88 (1968).
220. Lindemann-Perez, E. & Perez, J. C. Candida albicans natural diversity: a resource to dissect fungal commensalism and pathogenesis. *Curr. Opin. Microbiol.* **80**, 102493 (2024).
221. Ropars, J. *et al.* Gene flow contributes to diversification of the major fungal pathogen Candida albicans. *Nat. Commun.* **9**, 1–10 (2018).
222. Odds, F. C. *et al.* Molecular phylogenetics of Candida albicans. *Eukaryot. Cell* **6**, 1041–1052 (2007).
223. Bougnoux, M.-E. *et al.* Multilocus sequence typing of Candida albicans: strategies, data exchange and applications. *Infect. Genet. Evol.* **4**, 243–252 (2004).
224. Tavanti, A. *et al.* Population structure and properties of Candida albicans, as determined by multilocus sequence typing. *J. Clin. Microbiol.* **43**, 5601–5613 (2005).
225. McManus, B. A. & Coleman, D. C. Molecular epidemiology, phylogeny and evolution of Candida albicans. *Infect. Genet. Evol.* **21**, 166–178 (2014).

226. Hirakawa, M. P. *et al.* Genetic and phenotypic intra-species variation in Candida albicans. *Genome Res.* **25**, 413–425 (2015).
227. Huang, M. Y., Woolford, C. A., May, G., McManus, C. J. & Mitchell, A. P. Circuit diversification in a biofilm regulatory network. *PLoS Pathog.* **15**, e1007787 (2019).
228. Shankar, M., Lo, T. L. & Traven, A. Natural variation in clinical isolates of Candida albicans modulates neutrophil responses. *mSphere* **5**, (2020).
229. Xiong, L., Goerlich, K., Do, E. & Mitchell, A. P. Strain variation in the Candida albicans iron limitation response. *mSphere* e0037224 (2024).
230. Wang, J. M. *et al.* Intraspecies Transcriptional Profiling Reveals Key Regulators of Candida albicans Pathogenic Traits. *MBio* **12**, (2021).
231. Wakade, R. S., Wellington, M. & Krysan, D. J. The role of the C. albicans transcriptional repressor NRG1 during filamentation and disseminated candidiasis is strain dependent. *mSphere* e0078523 (2024).
232. Wickramasinghe, D. N. *et al.* Variations in candidalysin amino acid sequence influence toxicity and host responses. *MBio* e0335123 (2024).
233. Liu, J. *et al.* A variant ECE1 allele contributes to reduced pathogenicity of Candida albicans during vulvovaginal candidiasis. *PLoS Pathog.* **17**, e1009884 (2021).
234. Tso, G. H. W. *et al.* Experimental evolution of a fungal pathogen into a gut symbiont. *Science* **362**, 589–595 (2018).
235. McDonough, L. D. *et al.* Candida albicans Isolates 529L and CHN1 Exhibit Stable Colonization of the Murine Gastrointestinal Tract. *MBio* e0287821 (2021).
236. Ford, C. B. *et al.* The evolution of drug resistance in clinical isolates of Candida albicans. *Elife* **4**, e00662 (2015).
237. Muzafar, S. *et al.* Identification of Genomewide Alternative Splicing Events in Sequential, Isogenic Clinical Isolates of Candida albicans Reveals a Novel Mechanism of Drug Resistance and Tolerance to Cellular Stresses. *mSphere* **5**, (2020).
238. Khalaf, R. A., Fattouh, N., Medvecky, M. & Hrabak, J. Whole genome sequencing of a clinical drug resistant Candida albicans isolate reveals known and novel mutations in genes involved in resistance acquisition mechanisms. *J. Med. Microbiol.* **70**, (2021).
239. Spettel, K. *et al.* Analysis of antifungal resistance genes in Candida albicans and Candida glabrata using next generation sequencing. *PLoS One* **14**, e0210397 (2019).

240. Eddouzi, J. *et al.* Molecular mechanisms of drug resistance in clinical Candida species isolated from Tunisian hospitals. *Antimicrob. Agents Chemother.* **57**, 3182–3193 (2013).
241. Dhamgaye, S. *et al.* RNA sequencing revealed novel actors of the acquisition of drug resistance in Candida albicans. *BMC Genomics* **13**, 396 (2012).
242. Oliveira Carvalho, V., Okay, T. S., Melhem, M. S. C., Walderez Szeszs, M. & del Negro, G. M. B. The new mutation L321F in Candida albicans ERG11 gene may be associated with fluconazole resistance. *Rev. Iberoam. Micol.* **30**, 209–212 (2013).
243. Schikora-Tamarit, M. À. & Gabaldón, T. Recent gene selection and drug resistance underscore clinical adaptation across Candida species. *Nat Microbiol* **9**, 284–307 (2024).
244. Chen, S.-H. *et al.* Identification of Y118 amino acid residue in Candida albicans sterol 14alpha-demethylase associated with the enzyme activity and selective antifungal activity of azole analogues. *Biol. Pharm. Bull.* **30**, 1246–1253 (2007).
245. Morio, F., Loge, C., Besse, B., Hennequin, C. & Le Pape, P. Screening for amino acid substitutions in the Candida albicans Erg11 protein of azole-susceptible and azole-resistant clinical isolates: new substitutions and a review of the literature. *Diagn. Microbiol. Infect. Dis.* **66**, 373–384 (2010).
246. Morschhäuser, J. The genetic basis of fluconazole resistance development in Candida albicans. *Biochim. Biophys. Acta* **1587**, 240–248 (2002).
247. Dunn, M. J., Fillinger, R. J., Anderson, L. M. & Anderson, M. Z. Automated quantification of Candida albicans biofilm-related phenotypes reveals additive contributions to biofilm production. *NPJ Biofilms Microbiomes* **6**, 36 (2020).
248. Glazier, V. E. *et al.* The Candida albicans reference strain SC5314 contains a rare, dominant allele of the transcription factor Rob1 that modulates filamentation, biofilm formation, and oral commensalism. *MBio* e0152123 (2023).
249. Lohse, M. B., Ziv, N. & Johnson, A. D. Variation in transcription regulator expression underlies differences in white-opaque switching between the SC5314 reference strain and the majority of Candida albicans clinical isolates. *Genetics* (2023) doi:10.1093/genetics/iyad162.
250. Brandquist, N. D. *et al.* Significant variation of filamentation phenotypes in clinical Candida albicans strains. *Front. Cell. Infect. Microbiol.* **13**, 1207083 (2023).

251. Anderson, F. M., Polvi, E. J., Veri, A. O. & O'Meara, T. R. Germination of a Field: Women in Candida albicans Research. *Current Clinical Microbiology Reports* **8**, 139–151 (2021).
252. De schimmelgeslachten Monilia, Oidium, Oospora en Torula. *Gedrukt bij Edauw & Johannissen* (1923).
253. Benham, R. W. Certain monilias parasitic on man: Their identification by morphology and by agglutination. *J. Infect. Dis.* **49**, 183–215 (1931).
254. Brown, G. D. *et al.* Hidden killers: Human fungal infections. *Sci. Transl. Med.* **4**, 165rv13-165rv13 (2012).
255. Noble, S. M., Gianetti, B. A. & Witchley, J. N. Candida albicans cell-type switching and functional plasticity in the mammalian host. *Nat. Rev. Microbiol.* **15**, 96–108 (2017).
256. Benham, R. W. Species of Candida most frequently isolated from man: methods and criteria for their identification. *J. Chronic Dis.* **5**, 460–472 (1957).
257. Pollack, J. D. & Benham, R. W. The chlamydospores of Candida albicans: comparison of three media for their induction. *J. Lab. Clin. Med.* **50**, 313–317 (1957).
258. Taschdjian, C. L. A simply prepared identification medium for Candida albicans. *Mycologia* (1953).
259. Taschdjian, C. L. Routine identification of candida albicans: Current methods and a new medium. *Mycologia* **49**, 332 (1957).
260. Stein, E. Comparison of chlamydospore production on new mediums. *Am. J. Clin. Pathol.* **26**, 1231–1233 (1956).
261. Reid, J. D., Jones, M. M. & Carter, E. B. A simple, clear medium for demonstration of chlamydospores of Candida albicans. *Am. J. Clin. Pathol.* **23**, 938–941 (1953).
262. Gordon, M. A., Bradley, E. G. & Grant, V. Q. The influence of different types of corn meal agar upon chlamydospore production by Candida albicans. *J. Lab. Clin. Med.* **40**, 316–320 (1952).
263. Hayes, A. B. Chlamydospore production in candida albicans. *Mycopathologia* **29**, 87–96 (1966).
264. Jansons, V. K. & Nickerson, W. J. Chemical composition of chlamydospores of Candida albicans. *J. Bacteriol.* **104**, 922–932 (1970).
265. Jansons, V. K. & Nickerson, W. J. Induction, morphogenesis, and germination of the chlamydospore of Candida albicans. *J. Bacteriol.* **104**, 910–921 (1970).

266. Miller, S. E., Spurlock, B. O. & Michaels, G. E. Electron microscopy of young Candida albicans chlamydospores. *J. Bacteriol.* **119**, 992–999 (1974).
267. Miller, S. E. & Finnerty, W. R. Age-related physiological studies comparing Candida albicans chlamydospores to yeasts. *Can. J. Microbiol.* **25**, 765–772 (1979).
268. Staib, P. & Morschhäuser, J. Chlamydospore formation in Candida albicans and Candida dubliniensis--an enigmatic developmental programme. *Mycoses* **50**, 1–12 (2007).
269. Shapiro, R. S., Robbins, N. & Cowen, L. E. Regulatory circuitry governing fungal development, drug resistance, and disease. *Microbiol. Mol. Biol. Rev.* **75**, 213–267 (2011).
270. Pomés, R., Gil, C. & Nombela, C. Genetic analysis of Candida albicans morphological mutants. *J. Gen. Microbiol.* **131**, 2107–2113 (1985).
271. Gil, C., Pomés, R. & Nombela, C. Isolation and characterization of Candida albicans morphological mutants derepressed for the formation of filamentous hypha-type structures. *J. Bacteriol.* **172**, 2384–2391 (1990).
272. Hogan, D. A. & Sundstrom, P. The Ras/cAMP/PKA signaling pathway and virulence in Candida albicans. *Future Microbiol.* **4**, 1263–1270 (2009).
273. Bahn, Y.-S., Staab, J. & Sundstrom, P. Increased high-affinity phosphodiesterase PDE2 gene expression in germ tubes counteracts CAP1-dependent synthesis of cyclic AMP, limits hypha production and promotes virulence of Candida albicans. *Mol. Microbiol.* **50**, 391–409 (2003).
274. Bahn, Y.-S. *et al.* Genome-wide transcriptional profiling of the cyclic AMP-dependent signaling pathway during morphogenic transitions of Candida albicans. *Eukaryot. Cell* **6**, 2376–2390 (2007).
275. Piispanen, A. E., Grahl, N., Hollomon, J. M. & Hogan, D. A. Regulated proteolysis of Candida albicans Ras1 is involved in morphogenesis and quorum sensing regulation. *Mol. Microbiol.* **89**, 166–178 (2013).
276. Piispanen, A. E. *et al.* Roles of Ras1 membrane localization during Candida albicans hyphal growth and farnesol response. *Eukaryot. Cell* **10**, 1473–1484 (2011).
277. Shapiro, R. S. *et al.* Hsp90 orchestrates temperature-dependent Candida albicans morphogenesis via Ras1-PKA signaling. *Curr. Biol.* **19**, 621–629 (2009).

278. Bachewich, C., Thomas, D. Y. & Whiteway, M. Depletion of a polo-like kinase in Candida albicans activates cyclase-dependent hyphal-like growth. *Mol. Biol. Cell* **14**, 2163–2180 (2003).
279. Bachewich, C., Nantel, A. & Whiteway, M. Cell cycle arrest during S or M phase generates polarized growth via distinct signals in Candida albicans. *Mol. Microbiol.* **57**, 942–959 (2005).
280. Liu, H., Köhler, J. & Fink, G. R. Suppression of hyphal formation in Candida albicans by mutation of a STE12 homolog. *Science* **266**, 1723–1726 (1994).
281. Chen, J. *et al.* Crk1, a novel Cdc2-related protein kinase, is required for hyphal development and virulence in Candida albicans. *Mol. Cell. Biol.* **20**, 8696–8708 (2000).
282. Cao, F. *et al.* The Flo8 transcription factor is essential for hyphal development and virulence in Candida albicans. *Mol. Biol. Cell* **17**, 295–307 (2006).
283. Wang, A., Raniga, P. P., Lane, S., Lu, Y. & Liu, H. Hyphal chain formation in Candida albicans: Cdc28-Hgc1 phosphorylation of Efg1 represses cell separation genes. *Mol. Cell. Biol.* **29**, 4406–4416 (2009).
284. Unoje, O., Yang, M., Lu, Y., Su, C. & Liu, H. Linking Sfl1 Regulation of Hyphal Development to Stress Response Kinases in Candida albicans. *mSphere* **5**, (2020).
285. Azadmanesh, J., Gowen, A. M., Creger, P. E., Schafer, N. D. & Blankenship, J. R. Filamentation Involves Two Overlapping, but Distinct, Programs of Filamentation in the Pathogenic Fungus Candida albicans. *G3* **7**, 3797–3808 (2017).
286. Taschdjian, C. L. & Kozinn, P. J. Laboratory and clinical studies on candidiasis in the newborn infant. *J. Pediatr.* **50**, 426–433 (1957).
287. Young, G. The process of invasion and the persistence of Candida albicans injected intraperitoneally into mice. *J. Infect. Dis.* **102**, 114–120 (1958).
288. Bendel, C. M., Hess, D. J., Garni, R. M., Henry-Stanley, M. & Wells, C. L. Comparative virulence of Candida albicans yeast and filamentous forms in orally and intravenously inoculated mice. *Crit. Care Med.* **31**, 501–507 (2003).
289. Hawser, S. P. & Douglas, L. J. Biofilm formation by Candida species on the surface of catheter materials in vitro. *Infect. Immun.* **62**, 915–921 (1994).
290. Hawser, S. P., Baillie, G. S. & Douglas, L. J. Production of extracellular matrix by Candida albicans biofilms. *J. Med. Microbiol.* **47**, 253–256 (1998).

291. McCourtie, J. & Douglas, L. J. Extracellular polymer of Candida albicans: isolation, analysis and role in adhesion. *J. Gen. Microbiol.* **131**, 495–503 (1985).
292. Baillie, G. S. & Douglas, L. J. Role of dimorphism in the development of Candida albicans biofilms. *J. Med. Microbiol.* **48**, 671–679 (1999).
293. Hawser, S. P. & Douglas, L. J. Resistance of Candida albicans biofilms to antifungal agents in vitro. *Antimicrob. Agents Chemother.* **39**, 2128–2131 (1995).
294. Al-Fattani, M. A. & Douglas, L. J. Penetration of Candida biofilms by antifungal agents. *Antimicrob. Agents Chemother.* **48**, 3291–3297 (2004).
295. Nobile, C. J. *et al.* Critical role of Bcr1-dependent adhesins in C. albicans biofilm formation in vitro and in vivo. *PLoS Pathog.* **2**, e63 (2006).
296. Nobile, C. J. & Mitchell, A. P. Regulation of cell-surface genes and biofilm formation by the C. albicans transcription factor Bcr1p. *Curr. Biol.* **15**, 1150–1155 (2005).
297. Nobile, C. J., Nett, J. E., Andes, D. R. & Mitchell, A. P. Function of Candida albicans adhesin Hwp1 in biofilm formation. *Eukaryot. Cell* **5**, 1604–1610 (2006).
298. Nobile, C. J. *et al.* Complementary adhesin function in C. albicans biofilm formation. *Curr. Biol.* **18**, 1017–1024 (2008).
299. Nobile, C. J. *et al.* A recently evolved transcriptional network controls biofilm development in Candida albicans. *Cell* **148**, 126–138 (2012).
300. Uppuluri, P. *et al.* Candida albicans dispersed cells are developmentally distinct from biofilm and planktonic cells. *MBio* **9**, (2018).
301. Uppuluri, P. *et al.* The transcriptional regulator Nrg1p controls Candida albicans biofilm formation and dispersion. *Eukaryot. Cell* **9**, 1531–1537 (2010).
302. Uppuluri, P. *et al.* Dispersion as an important step in the Candida albicans biofilm developmental cycle. *PLoS Pathog.* **6**, e1000828 (2010).
303. Hazen, E. L. & Brown, R. Two antifungal agents produced by a soil actinomycete. *Science* **112**, 423 (1950).
304. Hazen, E. L. & Brown, R. Fungicidin, an antibiotic produced by a soil actinomycete. *Proc. Soc. Exp. Biol. Med.* **76**, 93–97 (1951).
305. Brown, R., Hazen, E. L. & Mason, A. Effect of fungicidin (nystatin) in mice injected with lethal mixtures of aureomycin and Candida albicans. *Science* **117**, 609–610 (1953).

306. Nishioka, Y. & Silva-Hutner, M. Dimorphism, sensitivity to nystatin and acriflavin uptake in a strain ofCandida albicansgrown with glutamate as sole nitrogen and carbon source. *Med. Mycol.* **12**, 295–301 (1974).
307. Pappas, P. G. *et al.* Executive summary: Clinical practice guideline for the management of candidiasis: 2016 update by the infectious diseases society of America. *Clin. Infect. Dis.* **62**, 409–417 (2016).
308. Halde, C., Newcomer, V. D., Wright, E. T. & Sternberg, T. H. An evaluation of amphotericin B in vitro and in vivo in mice against Coccidioides immitis and Candida albicans, and preliminary observations concerning the administration of amphotericin B to man. *J. Invest. Dermatol.* **28**, 217–31; discussion, 231–2 (1957).
309. Sokol-Anderson, M. L., Brajtburg, J. & Medoff, G. Amphotericin B-induced oxidative damage and killing of Candida albicans. *J. Infect. Dis.* **154**, 76–83 (1986).
310. Sokol-Anderson, M. *et al.* Role of cell defense against oxidative damage in the resistance of Candida albicans to the killing effect of amphotericin B. *Antimicrob. Agents Chemother.* **32**, 702–705 (1988).
311. Lee, Y., Puumala, E., Robbins, N. & Cowen, L. E. Antifungal Drug Resistance: Molecular Mechanisms in Candida albicans and Beyond. *Chem. Rev.* **121**, 3390–3411 (2021).
312. Maertens, J. A. History of the development of azole derivatives. *Clin. Microbiol. Infect.* **10**, 1–10 (2004).
313. Warrilow, A. G. S. *et al.* S279 point mutations in Candida albicans Sterol 14-α demethylase (CYP51) reduce in vitro inhibition by fluconazole. *Antimicrob. Agents Chemother.* **56**, 2099–2107 (2012).
314. Kelly, S. L., Lamb, D. C. & Kelly, D. E. Y132H substitution inCandida albicanssterol 14Î±-demethylase confers fluconazole resistance by preventing binding to haem. *FEMS Microbiol. Lett.* **180**, 171–175 (1999).
315. Kelly, S. L., Lamb, D. C., Loeffler, J., Einsele, H. & Kelly, D. E. The G464S amino acid substitution in Candida albicans sterol 14alpha-demethylase causes fluconazole resistance in the clinic through reduced affinity. *Biochem. Biophys. Res. Commun.* **262**, 174–179 (1999).

316. Coste, A. T., Karababa, M., Ischer, F., Bille, J. & Sanglard, D. TAC1 , transcriptional activator of CDR genes, is a new transcription factor involved in the regulation of Candida albicans ABC transporters CDR1 and CDR2. *Eukaryot. Cell* **3**, 1639–1652 (2004).
317. Coste, A. *et al.* A mutation in Tac1p, a transcription factor regulating CDR1 and CDR2, is coupled with loss of heterozygosity at chromosome 5 to mediate antifungal resistance in Candida albicans. *Genetics* **172**, 2139–2156 (2006).
318. Wirsching, S., Michel, S. & Morschhäuser, J. Targeted gene disruption in Candida albicans wild-type strains: the role of the MDR1 gene in fluconazole resistance of clinical Candida albicans isolates. *Mol. Microbiol.* **36**, 856–865 (2000).
319. Cowen, L. E. & Lindquist, S. Hsp90 potentiates the rapid evolution of new traits: drug resistance in diverse fungi. *Science* **309**, 2185–2189 (2005).
320. Cowen, L. E. *et al.* Harnessing Hsp90 function as a powerful, broadly effective therapeutic strategy for fungal infectious disease. *Proc. Natl. Acad. Sci. U. S. A.* **106**, 2818–2823 (2009).
321. Cowen, L. E., Carpenter, A. E., Matangkasombut, O., Fink, G. R. & Lindquist, S. Genetic architecture of Hsp90-dependent drug resistance. *Eukaryot. Cell* **5**, 2184–2188 (2006).
322. Singh, S. D. *et al.* Hsp90 governs echinocandin resistance in the pathogenic yeast Candida albicans via calcineurin. *PLoS Pathog.* **5**, e1000532 (2009).
323. Cruz, M. C. *et al.* Calcineurin is essential for survival during membrane stress in Candida albicans. *EMBO J.* **21**, 546–559 (2002).
324. LaFayette, S. L. *et al.* PKC signaling regulates drug resistance of the fungal pathogen Candida albicans via circuitry comprised of Mkc1, calcineurin, and Hsp90. *PLoS Pathog.* **6**, e1001069 (2010).
325. Perepnikhatka, V. *et al.* Specific chromosome alterations in fluconazole-resistant mutants of Candida albicans. *J. Bacteriol.* **181**, 4041–4049 (1999).
326. Janbon, G., Sherman, F. & Rustchenko, E. Monosomy of a specific chromosome determines L-sorbose utilization: a novel regulatory mechanism in Candida albicans. *Proc. Natl. Acad. Sci. U. S. A.* **95**, 5150–5155 (1998).
327. Selmecki, A., Forche, A. & Berman, J. Aneuploidy and isochromosome formation in drug-resistant Candida albicans. *Science* **313**, 367–370 (2006).

328. Selmecki, A., Gerami-Nejad, M., Paulson, C., Forche, A. & Berman, J. An isochromosome confers drug resistance in vivo by amplification of two genes, ERG11 and TAC1. *Mol. Microbiol.* **68**, 624–641 (2008).
329. Todd, R. T., Wikoff, T. D., Forche, A. & Selmecki, A. Genome plasticity in Candida albicans is driven by long repeat sequences. *Elife* **8**, (2019).
330. Todd, R. T. & Selmecki, A. Expandable and reversible copy number amplification drives rapid adaptation to antifungal drugs. *Elife* **9**, (2020).
331. Hüttel, W. Echinocandins: structural diversity, biosynthesis, and development of antimycotics. *Appl. Microbiol. Biotechnol.* **105**, 55–66 (2021).
332. Suwunnakorn, S., Wakabayashi, H., Kordalewska, M., Perlin, D. S. & Rustchenko, E. FKS2 and FKS3 genes of opportunistic human pathogen candida albicans influence echinocandin susceptibility. *Antimicrob. Agents Chemother.* **62**, (2018).
333. Caplan, T. *et al.* Functional genomic screening reveals core modulators of echinocandin stress responses in candida albicans. *Cell Rep.* **23**, 2292–2298 (2018).
334. Diezmann, S., Michaut, M., Shapiro, R. S., Bader, G. D. & Cowen, L. E. Mapping the Hsp90 genetic interaction network in Candida albicans reveals environmental contingency and rewired circuitry. *PLoS Genet.* **8**, e1002562 (2012).
335. Blankenship, J. R., Fanning, S., Hamaker, J. J. & Mitchell, A. P. An extensive circuitry for cell wall regulation in Candida albicans. *PLoS Pathog.* **6**, e1000752 (2010).
336. Pappenfort, R. B. & Schnall, E. S. Moniliasis in patients treated with aureomycin; clinical and laboratory evidence that aureomycin stimulates the growth of Candida albicans. *AMA Arch. Intern. Med.* **88**, 729–735 (1951).
337. Sharp, J. L. The growth of Candida albicans during antibiotic therapy. *Lancet* **266**, 390–392 (1954).
338. Johnston, R. D., Chick, E. W., Johnston, N. S. & Jarvis, M. A. Asymptomatic quantitative increase of Candida albicans in the oral cavity: predisposing conditions. *South. Med. J.* **60**, 1244–1247 (1967).
339. Graham, C. E., Cruz, M. R., Garsin, D. A. & Lorenz, M. C. Enterococcus faecalis bacteriocin EntV inhibits hyphal morphogenesis, biofilm formation, and virulence of Candida albicans. *Proc. Natl. Acad. Sci. U. S. A.* **114**, 4507–4512 (2017).

340. Adam, B., Baillie, G. S. & Douglas, L. J. Mixed species biofilms of Candida albicans and Staphylococcus epidermidis. *J. Med. Microbiol.* **51**, 344–349 (2002).
341. Krasner, R. I., Young, G. & Yudkofsky, P. L. Interactions of oral strains of Candida albicans and lactobacilli. *J. Bacteriol.* **72**, 525–529 (1956).
342. Koser, S. A., Hodges, E., Tribby, I. & Stuedell, J. T. Growth of lactobacilli in association with Candida albicans. *J. Infect. Dis.* **106**, 60–68 (1960).
343. Strus, M. *et al.* The in vitro activity of vaginal Lactobacillus with probiotic properties against Candida. *Infect. Dis. Obstet. Gynecol.* **13**, 69–75 (2005).
344. Valentine, M., Benadé, E., Mouton, M., Khan, W. & Botha, A. Binary interactions between the yeast Candida albicans and two gut-associated Bacteroides species. *Microb. Pathog.* **135**, 103619 (2019).
345. Eckstein, M.-T., Moreno-Velásquez, S. D. & Pérez, J. C. Gut Bacteria Shape Intestinal Microhabitats Occupied by the Fungus Candida albicans. *Curr. Biol.* (2020) doi:10.1016/j.cub.2020.09.027.
346. Casadevall, A. & Pirofski, L.-A. What is a host? Incorporating the Microbiota into the damage-response framework. *Infect. Immun.* **83**, 2–7 (2015).
347. Casadevall, A. & Pirofski, L.-A. The damage-response framework of microbial pathogenesis. *Nat. Rev. Microbiol.* **1**, 17–24 (2003).
348. Casadevall, A. & Pirofski, L. A. Host-pathogen interactions: redefining the basic concepts of virulence and pathogenicity. *Infect. Immun.* **67**, 3703–3713 (1999).
349. Salvin, S. B., Cory, J. C. & Berg, M. K. The enhancement of the virulence of Candida albicans in mice. *J. Infect. Dis.* **90**, 177–182 (1952).
350. Jacobsen, I. D., Grosse, K. & Hube, B. Embryonated chicken eggs as alternative infection model for pathogenic fungi. *Methods Mol. Biol.* **845**, 487–496 (2012).
351. Brothers, K. M. & Wheeler, R. T. Non-invasive imaging of disseminated candidiasis in zebrafish larvae. *J. Vis. Exp.* (2012) doi:10.3791/4051.
352. Brothers, K. M., Newman, Z. R. & Wheeler, R. T. Live imaging of disseminated candidiasis in zebrafish reveals role of phagocyte oxidase in limiting filamentous growth. *Eukaryot. Cell* **10**, 932–944 (2011).
353. Fuchs, B. B., O'Brien, E., Khoury, J. B. E. & Mylonakis, E. Methods for using Galleria mellonella as a model host to study fungal pathogenesis. *Virulence* **1**, 475–482 (2010).

354. Yano, J. & Fidel, P. L., Jr. Protocols for vaginal inoculation and sample collection in the experimental mouse model of candida vaginitis. *J. Vis. Exp.* (2011) doi:10.3791/3382-v.
355. Yano, J. *et al.* Current patient perspectives of vulvovaginal candidiasis: incidence, symptoms, management and post-treatment outcomes. *BMC Womens. Health* **19**, 48 (2019).
356. Solis, N. V. & Filler, S. G. Mouse model of oropharyngeal candidiasis. *Nat. Protoc.* **7**, 637–642 (2012).
357. Conti, H. R., Huppler, A. R., Whibley, N. & Gaffen, S. L. Animal models for candidiasis. *Curr. Protoc. Immunol.* **105**, 19.6.1-19.6.17 (2014).
358. Conti, H. R. *et al.* Th17 cells and IL-17 receptor signaling are essential for mucosal host defense against oral candidiasis. *J. Exp. Med.* **206**, 299–311 (2009).
359. Nett, J. E., Marchillo, K., Spiegel, C. A. & Andes, D. R. Development and validation of an in vivo Candida albicans biofilm denture model. *Infect. Immun.* **78**, 3650–3659 (2010).
360. Johnson, C. C., Yu, A., Lee, H., Fidel, P. L., Jr & Noverr, M. C. Development of a contemporary animal model of Candida albicans-associated denture stomatitis using a novel intraoral denture system. *Infect. Immun.* **80**, 1736–1743 (2012).
361. Wiesner, S. M., Jechorek, R. P., Garni, R. M., Bendel, C. M. & Wells, C. L. Gastrointestinal colonization by candida albicans mutant strains in Antibiotic-treated mice. *Clin. Diagn. Lab. Immunol.* **8**, 192–195 (2001).
362. Witchley, J. N. *et al.* Candida albicans Morphogenesis Programs Control the Balance between Gut Commensalism and Invasive Infection. *Cell Host Microbe* **25**, 432-443.e6 (2019).
363. Witchley, J. N., Penumetcha, P. M. & Noble, S. M. Visualization of Candida albicans in the Murine Gastrointestinal Tract Using Fluorescent In Situ Hybridization. *J. Vis. Exp.* (2019) doi:10.3791/60283.
364. White, S. J. *et al.* Self-Regulation of Candida albicans Population Size during GI Colonization. *PLoS Pathog.* **3**, e184 (2007).
365. Westwater, C. *et al.* Susceptibility of gnotobiotic transgenic mice (Tgepsilon26) with combined deficiencies in natural killer cells and T cells to wild-type and hyphal signalling-defective mutants of Candida albicans. *J. Med. Microbiol.* **56**, 1138–1144 (2007).

366. Westwater, C., Schofield, D. A., Nicholas, P. J., Paulling, E. E. & Balish, E. Candida glabrata and Candida albicans; dissimilar tissue tropism and infectivity in a gnotobiotic model of mucosal candidiasis. *FEMS Immunol. Med. Microbiol.* **51**, 134–139 (2007).
367. Westwater, C. & Schofield, D. A. Laser capture microdissection of Candida albicans from host tissue. *Methods Mol. Biol.* **845**, 397–409 (2012).
368. Böhm, L. *et al.* The yeast form of the fungus Candida albicans promotes persistence in the gut of gnotobiotic mice. *PLoS Pathog.* **13**, e1006699 (2017).
369. Cantorna, M. T. & Balish, E. Mucosal and systemic candidiasis in congenitally immunodeficient mice. *Infect. Immun.* **58**, 1093–1100 (1990).
370. Cantorna, M., Mook, D. & Balish, E. Resistance of congenitally immunodeficient gnotobiotic mice to vaginal candidiasis. *Infect. Immun.* **58**, 3813–3815 (1990).
371. Stanley, V. C. & Hurley, R. The growth of Candida species in cultures of mouse peritoneal macrophages. *J. Pathol.* **97**, 357–366 (1969).
372. Wellington, M., Koselny, K., Sutterwala, F. S. & Krysan, D. J. Candida albicans triggers NLRP3-mediated pyroptosis in macrophages. *Eukaryot. Cell* **13**, 329–340 (2014).
373. Uwamahoro, N. *et al.* The pathogen Candida albicans hijacks pyroptosis for escape from macrophages. *MBio* **5**, e00003-14 (2014).
374. Hise, A. G. *et al.* An essential role for the NLRP3 inflammasome in host defense against the human fungal pathogen Candida albicans. *Cell Host Microbe* **5**, 487–497 (2009).
375. Kasper, L. *et al.* The fungal peptide toxin Candidalysin activates the NLRP3 inflammasome and causes cytolysis in mononuclear phagocytes. *Nat. Commun.* **9**, 4260 (2018).
376. Tomalka, J. *et al.* A novel role for the NLRC4 inflammasome in mucosal defenses against the fungal pathogen Candida albicans. *PLoS Pathog.* **7**, e1002379 (2011).
377. Gringhuis, S. I. *et al.* Dectin-1 is an extracellular pathogen sensor for the induction and processing of IL-1β via a noncanonical caspase-8 inflammasome. *Nat. Immunol.* **13**, 246–254 (2012).
378. Brown, G. D. *et al.* Dectin-1 Is A Major β-Glucan Receptor On Macrophages. *J. Exp. Med.* **196**, 407–412 (2002).
379. Marakalala, M. J. *et al.* Differential Adaptation of Candida albicans In Vivo Modulates Immune Recognition by Dectin-1. *PLoS Pathogens* vol. 9 e1003315 Preprint at https://doi.org/10.1371/journal.ppat.1003315 (2013).

380. Klippel, N., Cui, S., Groebe, L. & Bilitewski, U. Deletion of the Candida albicans histidine kinase gene CHK1 improves recognition by phagocytes through an increased exposure of cell wall beta-1,3-glucans. *Microbiology* **156**, 3432–3444 (2010).
381. Ene, I. V., Cheng, S.-C., Netea, M. G. & Brown, A. J. P. Growth of Candida albicans cells on the physiologically relevant carbon source lactate affects their recognition and phagocytosis by immune cells. *Infect. Immun.* **81**, 238–248 (2013).
382. Davis, S. E. *et al.* Masking of β(1-3)-glucan in the cell wall of Candida albicans from detection by innate immune cells depends on phosphatidylserine. *Infect. Immun.* **82**, 4405–4413 (2014).
383. Heinsbroek, S. E. M. *et al.* Stage-specific sampling by pattern recognition receptors during Candida albicans phagocytosis. *PLoS Pathog.* **4**, e1000218 (2008).
384. Villamón, E. *et al.* Myeloid differentiation factor 88 (MyD88) is required for murine resistance to Candida albicans and is critically involved in Candida -induced production of cytokines. *Eur. Cytokine Netw.* **15**, 263–271 (2004).
385. Casadevall, A. & Pirofski, L.-A. Immunoglobulins in defense, pathogenesis, and therapy of fungal diseases. *Cell Host Microbe* **11**, 447–456 (2012).
386. Isenberg, H. D., Allerhand, J., Berkman, J. I. & Goldberg, D. IMMUNOLOGICAL AND TOXIC DIFFERENCES BETWEEN MOUSE-VIRULENT AND MOUSE-AVIRULENT CANDIDA ALBICANS. *J. Bacteriol.* **86**, 1010–1018 (1963).
387. Wang, Y., Li, S. P., Moser, S. A., Bost, K. L. & Domer, J. E. Cytokine involvement in immunomodulatory activity affected by Candida albicans mannan. *Infect. Immun.* **66**, 1384–1391 (1998).
388. Farah, C. S., Hu, Y., Riminton, S. & Ashman, R. B. Distinct roles for interleukin-12p40 and tumour necrosis factor in resistance to oral candidiasis defined by gene-targeting. *Oral Microbiol. Immunol.* **21**, 252–255 (2006).
389. Nur, S. *et al.* IL-23 supports host defense against systemic Candida albicans infection by ensuring myeloid cell survival. *PLoS Pathog.* **15**, e1008115 (2019).
390. Gladiator, A., Wangler, N., Trautwein-Weidner, K. & LeibundGut-Landmann, S. Cutting edge: IL-17-secreting innate lymphoid cells are essential for host defense against fungal infection. *J. Immunol.* **190**, 521–525 (2013).

391. Zelante, T. *et al.* Sensing of mammalian IL-17A regulates fungal adaptation and virulence. *Nat. Commun.* **3**, 683 (2012).
392. Gale, D. & Devesty, G. Response of mice to inoculations of both Candida albicans and Escherichia coli. II. The effect of the strain of mice. *J. Infect. Dis.* **101**, 48–50 (1957).
393. Hector, R. F., Domer, J. E. & Carrow, E. W. Immune responses to Candida albicans in genetically distinct mice. *Infect. Immun.* **38**, 1020–1028 (1982).
394. Tuite, A., Elias, M., Picard, S., Mullick, A. & Gros, P. Genetic control of susceptibility to Candida albicans in susceptible A/J and resistant C57BL/6J mice. *Genes Immun.* **6**, 672–682 (2005).
395. Radovanovic, I., Mullick, A. & Gros, P. Genetic control of susceptibility to infection with Candida albicans in mice. *PLoS One* **6**, e18957 (2011).
396. Radovanovic, I. *et al.* Genetic control of susceptibility to Candida albicans in SM/J mice. *J. Immunol.* **193**, 1290–1300 (2014).
397. Choi, E. H. *et al.* Association between chronic disseminated candidiasis in adult acute leukemia and common IL4 promoter haplotypes. *J. Infect. Dis.* **187**, 1153–1156 (2003).
398. Puel, A. *et al.* Chronic mucocutaneous candidiasis in humans with inborn errors of interleukin-17 immunity. *Science* **332**, 65–68 (2011).
399. Lévy, R. *et al.* Genetic, immunological, and clinical features of patients with bacterial and fungal infections due to inherited IL-17RA deficiency. *Proc. Natl. Acad. Sci. U. S. A.* **113**, E8277–E8285 (2016).
400. Corvilain, E., Casanova, J.-L. & Puel, A. Inherited CARD9 deficiency: Invasive disease caused by Ascomycete fungi in previously healthy children and adults. *J. Clin. Immunol.* **38**, 656–693 (2018).
401. Mourad, S. & Friedman, L. Active immunization of mice against Candida albicans. *Proc. Soc. Exp. Biol. Med.* **106**, 570–572 (1961).
402. Kuruganti, U. *et al.* Nonspecific and *candida* -specific immune responses in mice suppressed by chronic administration of anti-μ. *J. Leukoc. Biol.* **44**, 422–433 (1988).
403. Lyon, F. L., Hector, R. F. & Domer, J. E. Innate and acquired immune responses against*Candida albicans*in congenic B10.D2 mice with deficiency of the C5 complement component. *Med. Mycol.* **24**, 359–367 (1986).

404. Moser, S. A. & Domer, J. E. Effects of cyclophosphamide on murine candidiasis. *Infect. Immun.* **27**, 376–386 (1980).
405. Matthews, R. C., Burnie, J. P., Howat, D., Rowland, T. & Walton, F. Autoantibody to heat-shock protein 90 can mediate protection against systemic candidosis. *Immunology* **74**, 20–24 (1991).
406. Moragues, M. D. *et al.* A monoclonal antibody directed against a Candida albicans cell wall mannoprotein exerts three anti-C. albicans activities. *Infect. Immun.* **71**, 5273–5279 (2003).
407. Uppuluri, P. *et al.* Human anti-Als3p antibodies are surrogate markers of NDV-3A vaccine efficacy against recurrent vulvovaginal candidiasis. *Front. Immunol.* **9**, (2018).
408. Hull, C. M., Raisner, R. M. & Johnson, A. D. Evidence for mating of the "asexual" yeast Candida albicans in a mammalian host. *Science* **289**, 307–310 (2000).
409. Magee, B. B. & Magee, P. T. Induction of mating in Candida albicans by construction of MTLa and MTLalpha strains. *Science* **289**, 310–313 (2000).
410. Slutsky, B. *et al.* "White-opaque transition": a second high-frequency switching system in Candida albicans. *J. Bacteriol.* **169**, 189–197 (1987).
411. Anderson, J. M. & Soll, D. R. Unique phenotype of opaque cells in the white-opaque transition of Candida albicans. *J. Bacteriol.* **169**, 5579–5588 (1987).
412. Hickman, M. A. *et al.* The "obligate diploid" Candida albicans forms mating-competent haploids. *Nature* **494**, 55–59 (2013).
413. Magee, B. B., D'Souza, T. M. & Magee, P. T. Strain and species identification by restriction fragment length polymorphisms in the ribosomal DNA repeat of Candida species. *J. Bacteriol.* **169**, 1639–1643 (1987).
414. Sharma, C., Kumar, N., Meis, J. F., Pandey, R. & Chowdhary, A. Draft genome sequence of a fluconazole-resistant candida auris strain from a candidemia patient in India. *Genome Announc.* **3**, (2015).
415. Lockhart, S. R. *et al.* Simultaneous emergence of multidrug-resistant candida auris on 3 continents confirmed by whole-genome sequencing and epidemiological analyses. *Clin. Infect. Dis.* **64**, 134–140 (2017).
416. Anderson, F. M. *et al.* Candida albicans selection for human commensalism results in substantial within-host diversity without decreasing fitness for invasive disease. *PLoS Biol.* **21**, e3001822 (2023).

417. Mukherjee, P. K. *et al.* Mycobiota in gastrointestinal diseases. *Nat. Rev. Gastroenterol. Hepatol.* **12**, 77–87 (2015).
418. Polvi, E. J., Li, X., O'Meara, T. R., Leach, M. D. & Cowen, L. E. Opportunistic yeast pathogens: reservoirs, virulence mechanisms, and therapeutic strategies. *Cell. Mol. Life Sci.* **72**, 2261–2287 (2015).
419. Li, J. *et al.* Fungi in Gastrointestinal Tracts of Human and Mice: from Community to Functions. *Microb. Ecol.* **75**, 821–829 (2018).
420. Limon, J. J., Skalski, J. H. & Underhill, D. M. Commensal Fungi in Health and Disease. *Cell Host Microbe* **22**, 156–165 (2017).
421. Alves, R. *et al.* Adapting to survive: How Candida overcomes host-imposed constraints during human colonization. *PLoS Pathog.* **16**, e1008478 (2020).
422. Ene, I. V., Brunke, S., Brown, A. J. P. & Hube, B. Metabolism in fungal pathogenesis. *Cold Spring Harb. Perspect. Med.* **4**, a019695 (2014).
423. Polke, M., Hube, B. & Jacobsen, I. D. Candida survival strategies. *Adv. Appl. Microbiol.* **91**, 139–235 (2015).
424. Yan, L., Yang, C. & Tang, J. Disruption of the intestinal mucosal barrier in Candida albicans infections. *Microbiol. Res.* **168**, 389–395 (2013).
425. Alenazy, H., Alghamdi, A., Pinto, R. & Daneman, N. Candida colonization as a predictor of invasive candidiasis in non-neutropenic ICU patients with sepsis: A systematic review and meta-analysis. *Int. J. Infect. Dis.* **102**, 357–362 (2021).
426. Magill, S. S. *et al.* Changes in prevalence of health care-associated infections in U.s. hospitals. *N. Engl. J. Med.* **379**, 1732–1744 (2018).
427. Libkind, D. *et al.* Microbe domestication and the identification of the wild genetic stock of lager-brewing yeast. *Proc. Natl. Acad. Sci. U. S. A.* **108**, 14539–14544 (2011).
428. Hittinger, C. T. Saccharomyces diversity and evolution: a budding model genus. *Trends Genet.* **29**, 309–317 (2013).
429. Soll, D. R. & Pujol, C. Candida albicans clades. *FEMS Immunol. Med. Microbiol.* **39**, 1–7 (2003).
430. Blignaut, E., Pujol, C., Lockhart, S., Joly, S. & Soll, D. R. Ca3 fingerprinting of Candida albicans isolates from human immunodeficiency virus-positive and healthy individuals reveals a new clade in South Africa. *J. Clin. Microbiol.* **40**, 826–836 (2002).

431. Odds, F. C. Molecular phylogenetics and epidemiology of Candida albicans. *Future Microbiol.* **5**, 67–79 (2010).
432. MacCallum, D. M. *et al.* Property differences among the four major Candida albicans strain clades. *Eukaryot. Cell* **8**, 373–387 (2009).
433. Li, X., Yan, Z. & Xu, J. Quantitative variation of biofilms among strains in natural populations of Candida albicans. *Microbiology* **149**, 353–362 (2003).
434. Wu, W., Lockhart, S. R., Pujol, C., Srikantha, T. & Soll, D. R. Heterozygosity of genes on the sex chromosome regulates Candida albicans virulence: Gene heterozygosity andC. albicansvirulence. *Mol. Microbiol.* **64**, 1587–1604 (2007).
435. Calderone, R. A. & Fonzi, W. A. Virulence factors of Candida albicans. *Trends Microbiol.* **9**, 327–335 (2001).
436. Pierce, J. V. & Kumamoto, C. A. Variation in Candida albicans *EFG1* expression enables host-dependent changes in colonizing fungal populations. *MBio* **3**, e00117-12 (2012).
437. Liang, S.-H. *et al.* Hemizygosity Enables a Mutational Transition Governing Fungal Virulence and Commensalism. *Cell Host Microbe* **25**, 418-431.e6 (2019).
438. Witchley, J. N., Basso, P., Brimacombe, C. A., Abon, N. V. & Noble, S. M. Recording of DNA-binding events reveals the importance of a repurposed Candida albicans regulatory network for gut commensalism. *Cell Host Microbe* **29**, 1002-1013.e9 (2021).
439. Pande, K., Chen, C. & Noble, S. M. Passage through the mammalian gut triggers a phenotypic switch that promotes Candida albicans commensalism. *Nat. Genet.* **45**, 1088–1091 (2013).
440. Forche, A. *et al.* Selection of Candida albicans trisomy during oropharyngeal infection results in a commensal-like phenotype. *PLoS Genet.* **15**, e1008137 (2019).
441. Schönherr, F. A. *et al.* The intraspecies diversity of C. albicans triggers qualitatively and temporally distinct host responses that determine the balance between commensalism and pathogenicity. *Mucosal Immunol.* **10**, 1335–1350 (2017).
442. Kim, S. H. *et al.* Global analysis of the fungal microbiome in cystic fibrosis patients reveals loss of function of the transcriptional repressor Nrg1 as a mechanism of pathogen adaptation. *PLoS Pathog.* **11**, e1005308 (2015).

443. Garg, S., Ranjan, P., Erb-Downward, J. R. & Huffnagle, G. B. High-Quality Genome Reconstruction of Candida albicans CHN1 Using Nanopore and Illumina Sequencing and Hybrid Assembly. *Microbiol Resour Announc* **10**, e0029921 (2021).
444. Chen, Z. *et al.* Ultralow-input single-tube linked-read library method enables short-read second-generation sequencing systems to routinely generate highly accurate and economical long-range sequencing information. *Genome Res.* **30**, 898–909 (2020).
445. Li, H. *et al.* 1000 Genome Project Data Processing Subgroup. 2009. The sequence alignment/map format and samtools. *Bioinformatics* **25**, 2078–2079 (2009).
446. Sitterlé, E. *et al.* Large-scale genome mining allows identification of neutral polymorphisms and novel resistance mutations in genes involved in Candida albicans resistance to azoles and echinocandins. *J. Antimicrob. Chemother.* **75**, 835–848 (2020).
447. Ene, I. V. *et al.* Global analysis of mutations driving microevolution of a heterozygous diploid fungal pathogen. *Proc. Natl. Acad. Sci. U. S. A.* **115**, E8688–E8697 (2018).
448. Pittet, D. *et al.* Contour-clamped homogeneous electric field gel electrophoresis as a powerful epidemiologic tool in yeast infections. *Am. J. Med.* **91**, 256S-263S (1991).
449. Forche, A. *et al.* Rapid Phenotypic and Genotypic Diversification After Exposure to the Oral Host Niche in Candida albicans. *Genetics* **209**, 725–741 (2018).
450. Smith, A. C. & Hickman, M. A. Host-Induced Genome Instability Rapidly Generates Phenotypic Variation across Candida albicans Strains and Ploidy States. *mSphere* **5**, (2020).
451. Panthee, S., Hamamoto, H., Ishijima, S. A., Paudel, A. & Sekimizu, K. Utilization of Hybrid Assembly Approach to Determine the Genome of an Opportunistic Pathogenic Fungus, Candida albicans TIMM 1768. *Genome Biol. Evol.* **10**, 2017–2022 (2018).
452. Gulati, M. *et al.* In Vitro Culturing and Screening of Candida albicans Biofilms. *Curr. Protoc. Microbiol.* **50**, e60 (2018).
453. Kirchner, F. R. *et al.* Persistence of Candida albicans in the oral mucosa induces a curbed inflammatory host response that is independent of immunosuppression. *Front. Immunol.* **10**, 330 (2019).
454. Santana, D. J., Anderson, F. M. & O'Meara, T. R. Monitoring Inflammasome Priming and Activation in Response to Candida albicans. *Curr. Protoc. Microbiol.* **59**, e124 (2020).
455. Lemberg, C. *et al.* Candida albicans commensalism in the oral mucosa is favoured by limited virulence and metabolic adaptation. *PLoS Pathog.* **18**, e1010012 (2022).

456. Gerwien, F. *et al.* Clinical Candida albicans vaginal isolates and a laboratory strain show divergent behaviors during macrophage interactions. *mSphere* **5**, (2020).
457. O'Meara, T. R. & O'Meara, M. J. DeORFanizing Candida albicans Genes using Coexpression. *mSphere* **6**, (2021).
458. Homann, O. R., Dea, J., Noble, S. M. & Johnson, A. D. A phenotypic profile of the Candida albicans regulatory network. *PLoS Genet.* **5**, e1000783 (2009).
459. Brennan, M., Thomas, D. Y., Whiteway, M. & Kavanagh, K. Correlation between virulence ofCandida albicansmutants in mice andGalleria mellonellalarvae. *FEMS Immunol. Med. Microbiol.* **34**, 153–157 (2002).
460. Dunn, M. J., Woodruff, A. L. & Anderson, M. Z. The Galleria mellonella waxworm infection model for disseminated candidiasis. *J. Vis. Exp.* (2018) doi:10.3791/58914.
461. Hill, J. A., O'Meara, T. R. & Cowen, L. E. Fitness trade-offs associated with the evolution of resistance to antifungal drug combinations. *Cell Rep.* **10**, 809–819 (2015).
462. Martin, R. M. & Bachman, M. A. Colonization, Infection, and the Accessory Genome of Klebsiella pneumoniae. *Front. Cell. Infect. Microbiol.* **8**, 4 (2018).
463. Allen, J. P., Snitkin, E., Pincus, N. B. & Hauser, A. R. Forest and trees: Exploring bacterial virulence with genome-wide association studies and machine learning. *Trends Microbiol.* **29**, 621–633 (2021).
464. Gerstein, A. C. *et al.* Identification of pathogen genomic differences that impact human immune response and disease during Cryptococcus neoformans infection. *MBio* **10**, (2019).
465. Beale, M. A. *et al.* Genotypic diversity is associated with clinical outcome and phenotype in cryptococcal meningitis across Southern Africa. *PLoS Negl. Trop. Dis.* **9**, e0003847 (2015).
466. Forche, A. *et al.* The parasexual cycle in Candida albicans provides an alternative pathway to meiosis for the formation of recombinant strains. *PLoS Biol.* **6**, e110 (2008).
467. Mixão, V. & Gabaldón, T. Genomic evidence for a hybrid origin of the yeast opportunistic pathogen Candida albicans. *BMC Biol.* **18**, 48 (2020).
468. Ene, I. V., Bennett, R. J. & Anderson, M. Z. Mechanisms of genome evolution in Candida albicans. *Curr. Opin. Microbiol.* **52**, 47–54 (2019).
469. Wakade, R. S., Ristow, L. C., Wellington, M. & Krysan, D. J. Intravital imaging based genetic screen reveals the transcriptional network governing Candida albicans filamentation during mammalian infection. *Elife* **12**, (2023).

470. Pujol, C. *et al.* The yeast Candida albicans has a clonal mode of reproduction in a population of infected human immunodeficiency virus-positive patients. *Proc. Natl. Acad. Sci. U. S. A.* **90**, 9456–9459 (1993).
471. Moorhouse, A. J., Rennison, C., Raza, M., Lilic, D. & Gow, N. A. R. Clonal strain persistence of Candida albicans isolates from chronic mucocutaneous candidiasis patients. *PLoS One* **11**, e0145888 (2016).
472. McManus, B. A. *et al.* Enrichment of multilocus sequence typing clade 1 with oral Candida albicans isolates in patients with untreated periodontitis. *J. Clin. Microbiol.* **50**, 3335–3344 (2012).
473. Sprouffske, K. & Wagner, A. Growthcurver: an R package for obtaining interpretable metrics from microbial growth curves. *BMC Bioinformatics* **17**, 172 (2016).
474. Van der Auwera, G. A. *et al.* From FastQ data to high confidence variant calls: the Genome Analysis Toolkit best practices pipeline. *Curr. Protoc. Bioinformatics* **43**, 11.10.1-11.10.33 (2013).
475. Revell, L. J. phytools: an R package for phylogenetic comparative biology (and other things). Methods Ecol Evol. Preprint at (2012).
476. Yu, G. Using ggtree to Visualize Data on Tree-Like Structures. *Curr. Protoc. Bioinformatics* **69**, e96 (2020).
477. Yu, G., Lam, T. T.-Y., Zhu, H. & Guan, Y. Two methods for mapping and visualizing associated data on phylogeny using ggtree. *Mol. Biol. Evol.* **35**, 3041–3043 (2018).
478. Yu, G., Smith, D. K., Zhu, H., Guan, Y. & Lam, T. T.-Y. Ggtree: An r package for visualization and annotation of phylogenetic trees with their covariates and other associated data. *Methods Ecol. Evol.* **8**, 28–36 (2017).
479. Layer, R. M., Chiang, C., Quinlan, A. R. & Hall, I. M. LUMPY: a probabilistic framework for structural variant discovery. *Genome Biol.* **15**, R84 (2014).
480. Chiang, C. *et al.* SpeedSeq: ultra-fast personal genome analysis and interpretation. *Nat. Methods* **12**, 966–968 (2015).
481. Li, H. Minimap2: pairwise alignment for nucleotide sequences. *Bioinformatics* **34**, 3094–3100 (2018).

482. Selmecki, A., Bergmann, S. & Berman, J. Comparative genome hybridization reveals widespread aneuploidy in Candida albicans laboratory strains: CGH of C. albicans laboratory strain aneuploidies. *Mol. Microbiol.* **55**, 1553–1565 (2005).
483. Chibana, H., Beckerman, J. L. & Magee, P. T. Fine-resolution physical mapping of genomic diversity in Candida albicans. *Genome Res.* **10**, 1865–1877 (2000).
484. Shen, J., Guo, W. & Köhler, J. R. CaNAT1, a heterologous dominant selectable marker for transformation of Candida albicans and other pathogenic Candida species. *Infect. Immun.* **73**, 1239–1242 (2005).
485. Norrander, J., Kempe, T. & Messing, J. Construction of improved M13 vectors using oligodeoxynucleotide-directed mutagenesis. *Gene* **26**, 101–106 (1983).
486. Veri, A. O. *et al.* Tuning Hsf1 levels drives distinct fungal morphogenetic programs with depletion impairing Hsp90 function and overexpression expanding the target space. *PLoS Genet.* **14**, e1007270 (2018).
487. Lionakis, M. S. & Netea, M. G. Candida and host determinants of susceptibility to invasive candidiasis. *PLoS Pathog.* **9**, e1003079 (2013).
488. Neville, B. A., d'Enfert, C. & Bougnoux, M.-E. Candida albicans commensalism in the gastrointestinal tract. *FEMS Yeast Res.* **15**, (2015).
489. Puel, A. Human inborn errors of immunity underlying superficial or invasive candidiasis. *Hum. Genet.* **139**, 1011–1022 (2020).
490. d'Enfert, C. *et al.* The impact of the Fungus-Host-Microbiota interplay upon Candida albicans infections: current knowledge and new perspectives. *FEMS Microbiol. Rev.* (2020) doi:10.1093/femsre/fuaa060.
491. Hall, R. A. Adapting to change: interactions of Candida albicans with its environment. *Future Microbiol.* **12**, 931–934 (2017).
492. Ene, I. V. *et al.* Cell Wall Remodeling Enzymes Modulate Fungal Cell Wall Elasticity and Osmotic Stress Resistance. *MBio* **6**, e00986 (2015).
493. Brown, G. D. & Gordon, S. Immune recognition. A new receptor for beta-glucans. *Nature* **413**, 36–37 (2001).
494. McCrory, C., Lenardon, M. & Traven, A. Bacteria-derived short-chain fatty acids as potential regulators of fungal commensalism and pathogenesis. *Trends Microbiol.* (2024) doi:10.1016/j.tim.2024.04.004.

495. Noverr, M. C. & Huffnagle, G. B. Regulation of Candida albicans morphogenesis by fatty acid metabolites. *Infect. Immun.* **72**, 6206–6210 (2004).
496. Cuskin, F. *et al.* Human gut Bacteroidetes can utilize yeast mannan through a selfish mechanism. *Nature* **517**, 165–169 (2015).
497. Temple, M. J. *et al.* A Bacteroidetes locus dedicated to fungal 1,6-β-glucan degradation: Unique substrate conformation drives specificity of the key endo-1,6-β-glucanase. *J. Biol. Chem.* **292**, 10639–10650 (2017).
498. Charlet, R., Bortolus, C., Sendid, B. & Jawhara, S. Bacteroides thetaiotaomicron and Lactobacillus johnsonii modulate intestinal inflammation and eliminate fungi via enzymatic hydrolysis of the fungal cell wall. *Sci. Rep.* **10**, 11510 (2020).
499. Gantner, B. N., Simmons, R. M. & Underhill, D. M. Dectin-1 mediates macrophage recognition of Candida albicans yeast but not filaments. *EMBO J.* **24**, 1277–1286 (2005).
500. Cabib, E. & Bowers, B. Chitin and yeast budding. *J. Biol. Chem.* **246**, 152–159 (1971).
501. McGreal, E. P. *et al.* The carbohydrate-recognition domain of Dectin-2 is a C-type lectin with specificity for high mannose. *Glycobiology* **16**, 422–430 (2006).
502. Saijo, S. *et al.* Dectin-2 recognition of alpha-mannans and induction of Th17 cell differentiation is essential for host defense against Candida albicans. *Immunity* **32**, 681–691 (2010).
503. Ost, K. S. *et al.* Adaptive immunity induces mutualism between commensal eukaryotes. *Nature* (2021) doi:10.1038/s41586-021-03722-w.
504. Chakraborty, A. *et al.* A molecular vision of fungal cell wall organization by functional genomics and solid-state NMR. *Nat. Commun.* **12**, 1–12 (2021).
505. Ghassemi, N. *et al.* Solid-state NMR investigations of extracellular matrixes and cell walls of algae, bacteria, fungi, and plants. *Chem. Rev.* **122**, 10036–10086 (2022).
506. Cheng, Q. *et al.* Molecular architecture of chitin and chitosan-dominated cell walls in zygomycetous fungal pathogens by solid-state NMR. *Nat. Commun.* **15**, 8295 (2024).
507. Dickwella Widanage, M. C. *et al.* Adaptative survival of Aspergillus fumigatus to echinocandins arises from cell wall remodeling beyond β-1,3-glucan synthesis inhibition. *Nat. Commun.* **15**, 6382 (2024).

508. Lamon, G. *et al.* Solid-state NMR molecular snapshots of Aspergillus fumigatus cell wall architecture during a conidial morphotype transition. *Proc. Natl. Acad. Sci. U. S. A.* **120**, e2212003120 (2023).

509. Hou, G., Yan, S., Trébosc, J., Amoureux, J.-P. & Polenova, T. Broadband homonuclear correlation spectroscopy driven by combined R2(n)(v) sequences under fast magic angle spinning for NMR structural analysis of organic and biological solids. *J. Magn. Reson.* **232**, 18–30 (2013).

510. Dickwella Widanage, M. C. *et al.* Unveiling cell wall structure and echinocandin response in Candida auris and Candida albicans via solid-state NMR. *bioRxiv* 2024.12.02.626508 (2024) doi:10.1101/2024.12.02.626508.

511. Blattner, F. R. *et al.* The complete genome sequence of Escherichia coli K-12. *Science* **277**, 1453–1462 (1997).

512. Mobley, H. L. *et al.* Pyelonephritogenic Escherichia coli and killing of cultured human renal proximal tubular epithelial cells: role of hemolysin in some strains. *Infect. Immun.* **58**, 1281–1289 (1990).

513. Mulvey, M. A., Schilling, J. D. & Hultgren, S. J. Establishment of a persistent Escherichia coli reservoir during the acute phase of a bladder infection. *Infect. Immun.* **69**, 4572–4579 (2001).

514. Román, E., Nombela, C. & Pla, J. The Sho1 adaptor protein links oxidative stress to morphogenesis and cell wall biosynthesis in the fungal pathogen Candida albicans. *Mol. Cell. Biol.* **25**, 10611–10627 (2005).

515. Lee, K. K. *et al.* Elevated cell wall chitin in Candida albicans confers echinocandin resistance in vivo. *Antimicrob. Agents Chemother.* **56**, 208–217 (2012).

516. Avelar, G. M. *et al.* A CO2 sensing module modulates β-1,3-glucan exposure in Candida albicans. *MBio* e0189823 (2024).

517. Zhang, M. *et al.* CO2 potentiates echinocandin efficacy during invasive candidiasis therapy via dephosphorylation of Hsp90 by Ptc2 in condensates. *Proc. Natl. Acad. Sci. U. S. A.* **122**, e2417721122 (2025).

518. Rodríguez-Peña, J. M., García, R., Nombela, C. & Arroyo, J. The high-osmolarity glycerol (HOG) and cell wall integrity (CWI) signalling pathways interplay: a yeast dialogue between MAPK routes. *Yeast* **27**, 495–502 (2010).

519. Brown, A. J. P. *et al.* Stress adaptation in a pathogenic fungus. *J. Exp. Biol.* **217**, 144–155 (2014).
520. Lesage, A., Bardet, M. & Emsley, L. Through-bond Carbon−Carbon connectivities in disordered solids by NMR. *J. Am. Chem. Soc.* **121**, 10987–10993 (1999).
521. Lee, D. W., Hong, C. P. & Kang, H. A. An effective and rapid method for RNA preparation from non-conventional yeast species. *Anal. Biochem.* **586**, 113408 (2019).
522. Aranda, P. S., LaJoie, D. M. & Jorcyk, C. L. Bleach gel: a simple agarose gel for analyzing RNA quality. *Electrophoresis* **33**, 366–369 (2012).
523. O'Meara, T. R. *et al.* Global proteomic analyses define an environmentally contingent Hsp90 interactome and reveal chaperone-dependent regulation of stress granule proteins and the R2TP complex in a fungal pathogen. *PLoS Biol.* **17**, e3000358 (2019).
524. Noble, S. M. & Johnson, A. D. Strains and strategies for large-scale gene deletion studies of the diploid human fungal pathogen Candida albicans. *Eukaryot. Cell* **4**, 298–309 (2005).
525. Lutgring, J. D. *et al.* FDA-CDC Antimicrobial Resistance Isolate Bank: A publicly available resource to support research, development, and regulatory requirements. *J. Clin. Microbiol.* **56**, (2018).
526. Morschhäuser, J., Ruhnke, M., Michel, S. & Hacker, J. Identification of CARE-2-negative Candida albicans isolates as Candida dubliniensis. *Mycoses* **42**, 29–32 (1999).
527. Cuskin, F. *et al.* The GH130 Family of Mannoside Phosphorylases Contains Glycoside Hydrolases That Target β-1,2-Mannosidic Linkages in Candida Mannan. *J. Biol. Chem.* **290**, 25023–25033 (2015).
528. Koh, A. Y. Murine models of Candida gastrointestinal colonization and dissemination. *Eukaryot. Cell* **12**, 1416–1422 (2013).
529. Liang, S.-H. *et al.* The hyphal-specific toxin candidalysin promotes fungal gut commensalism. *Nature* **627**, 620–627 (2024).
530. Yamaguchi, N. *et al.* Gastric colonization of Candida albicans differs in mice fed commercial and purified diets. *J. Nutr.* **135**, 109–115 (2005).
531. Szabo, E. K. & MacCallum, D. M. The contribution of mouse models to our understanding of systemic candidiasis: Modelling systemic Candida infection in mice. *FEMS Microbiol. Lett.* **320**, 1–8 (2011).

532. Jungnickel, B. & Jacobsen, I. D. Systemic candidiasis in mice: New insights from an old model. *Front. Fungal Biol.* **3**, 940884 (2022).
533. Koh, A. Y., Köhler, J. R., Coggshall, K. T., Van Rooijen, N. & Pier, G. B. Mucosal damage and neutropenia are required for Candida albicans dissemination. *PLoS Pathog.* **4**, e35 (2008).
534. Bacher, P. *et al.* Human Anti-fungal Th17 Immunity and Pathology Rely on Cross-Reactivity against Candida albicans. *Cell* **176**, 1340-1355.e15 (2019).